



(NASA-TN-X-69540) SATURN 1B LAUNCH  
VEHICLE FLIGHT EVALUATION REPORT-SA-207:  
SKYLAB-3 (NASA) 234 p HC \$13.75



# SATURN

**MPR-SAT-FE-73-5**

**OCTOBER 8, 1973**

N73-33821

CSSL 22C

Unclas

G3/30

19844

## SATURN 1B LAUNCH VEHICLE FLIGHT EVALUATION REPORT-SA-207 SKYLAB-3



**PREPARED BY  
SATURN FLIGHT EVALUATION WORKING GROUP**



NATIONAL AERONAUTICS AND SPACE ADMINISTRATION

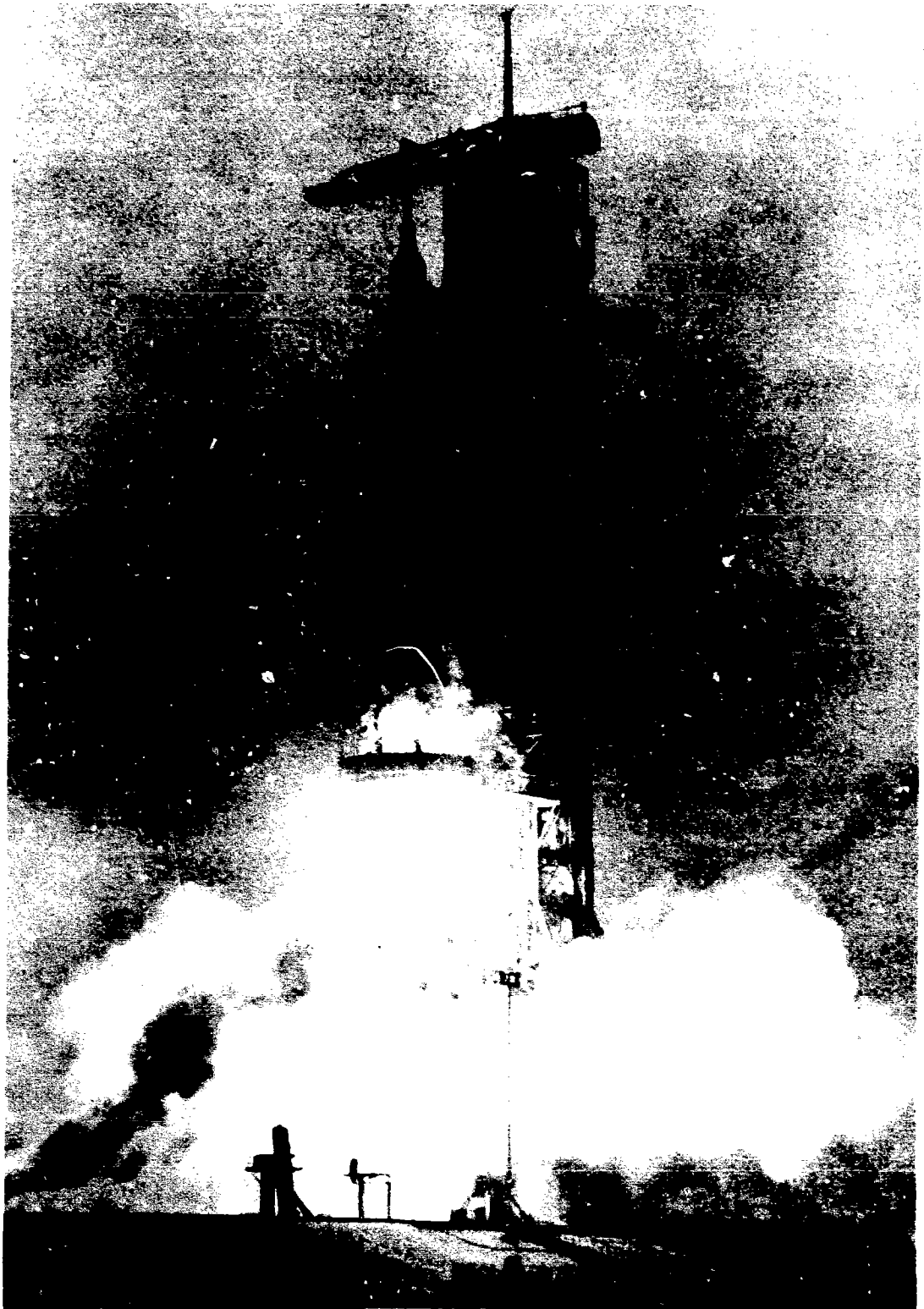
**GEORGE C. MARSHALL SPACE FLIGHT CENTER**

**MPR-SAT-FE-73-5**

**OCTOBER 8, 1973**

**SATURN IB LAUNCH VEHICLE  
FLIGHT EVALUATION  
REPORT-SA-207  
SKYLAB-3**

**PREPARED BY  
SATURN FLIGHT EVALUATION  
WORKING GROUP**



MPR-SAT-FE-73-5

SATURN IB LAUNCH VEHICLE FLIGHT EVALUATION REPORT - SA-207

SKYLAB-3

BY

Saturn Flight Evaluation Working Group

George C. Marshall Space Flight Center

ABSTRACT

The Saturn IB, SA-207 Launch Vehicle was launched on July 28, 1973, from Kennedy Space Center and placed the Command Service Module containing three crew members into an 149.87 x 226.29 km altitude earth orbit. No anomalies occurred that seriously affected the mission.

Any questions or comments pertaining to the information contained in this report should be directed to:

Director, George C. Marshall Space Flight Center  
Huntsville, Alabama 35812  
Attention: Chairman, Saturn Flight Evaluation Working  
Group, SAT-E (Phone 205-453-1030)

PRECEDING PAGE BLANK NOT FILMED

TABLE OF CONTENTS

	Page		Page
TABLE OF CONTENTS	iii	5.4 Impact	5-6
LIST OF ILLUSTRATIONS	v	SECTION 6 - S-IB PROPULSION	6-1
LIST OF TABLES	viii	6.1 Summary	6-1
ACKNOWLEDGEMENT	xi	6.2 S-IB Ignition Transient Performance	6-1
ABBREVIATIONS	xiii	6.3 S-IB Mainstage Performance	6-1
MISSION PLAN	xvii	6.4 S-IB Shutdown Transient Performance	6-6
FLIGHT SUMMARY	xix	6.5 S-IB Stage Propellant Management	6-6
MISSION OBJECTIVES ACCOMPLISHMENT	xxiii	6.6 S-IB Pressurization System	6-11
FAILURES AND ANOMALIES	xxv	6.6.1 Fuel Pressurization System	6-11
		6.6.2 LOX Pressurization System	6-11
SECTION 1 - INTRODUCTION	1-1	6.7 S-IB Pneumatic Control Pressure System	6-13
1.1 Purpose	1-1	6.8 S-IB Hydraulic System	6-13
1.2 Scope	1-1	SECTION 7 - S-IVB PROPULSION	7-1
1.3 Performance Predictions Baseline	1-1	7.1 Summary	7-1
SECTION 2 - EVENT TIMES	2-1	7.2 S-IVB Chilldown and Buildup Transient Performance	7-2
2.1 Summary of Events	2-1	7.3 S-IVB Mainstage Performance	7-2
2.2 Variable Time and Commanded Switch selector events	2-1	7.4 S-IVB Shutdown Transient Performance	7-5
SECTION 3 - LAUNCH OPERATIONS	3-1	7.5 S-IVB Stage Propellant Management	7-6
3.1 Summary	3-1	7.6 S-IVB Pressurization System	7-7
3.2 Prelaunch Milestones	3-1	7.6.1 S-IVB Fuel Pressurization System	7-7
3.3 Terminal Countdown	3-1	7.6.2 S-IVB LOX Pressurization System	7-7
3.4 Propellant Loading	3-1	7.7 S-IVB Pneumatic Control Pressure System	7-10
3.4.1 RP-1 Loading	3-1	7.8 S-IVB Auxiliary Propulsion System	7-14
3.4.2 LOX Loading	3-3	7.9 S-IVB/IU Stage Deorbit Propellant Dump	7-14
3.4.3 LH <sub>2</sub> Loading	3-6	7.10 S-IVB Orbital Coast and Safing	7-19
3.5 Ground Support Equipment	3-6	7.10.1 Fuel Tank Orbital Coast and Safing	7-19
3.5.1 Ground/Vehicle Interface	3-6	7.10.2 LOX Tank Orbital Coast and Safing	7-22
3.5.2 MSFC Furnished Ground Support Equipment	3-7	7.10.3 Cold Helium Dump	7-22
SECTION 4 - TRAJECTORY	4-1	7.10.4 Stage Pneumatic Control and Engine Control Sphere Safing	7-24
4.1 Summary	4-1		
4.2 Trajectory Evaluation	4-1		
4.2.1 Ascent Phase	4-1		
4.2.2 Parking Orbit Phase	4-10		
SECTION 5 - S-IVB/IU DEORBIT TRAJECTORY	5-1		
5.1 Summary	5-1		
5.2 Deorbit Maneuvers	5-1		
5.3 Deorbit Trajectory Evaluation	5-1		

## TABLES OF CONTENTS (CONTINUED)

	Page		Page
7.11 S-IVB Hydraulic System	7-24	SECTION 13 - VEHICLE THERMAL ENVIRONMENT	13-1
SECTION 8 - STRUCTURES	8-1	13.1 S-IB Base Heating	13-1
8.1 Summary	8-1	SECTION 14 - ENVIRONMENTAL CONTROL SYSTEMS	14-1
8.2 Total Vehicle Structures Evaluation	8-1	14.1 Summary	14-1
8.2.1 Longitudinal Loads	8-1	14.2 S-IB Environmental Control	14-1
8.2.2 Bending Moments	8-3	14.3 IU Environmental Control	14-1
8.2.3 Combined Loads	8-3	14.3.1 Thermal Conditioning System (TCS)	14-2
8.2.4 Vehicle Dynamic Characteristics	8-8	14.3.2 Gas Bearing System (GBS)	14-2
SECTION 9 - GUIDANCE AND NAVIGATION	9-1	14.3.3 Component Temperatures	14-7
9.1 Summary	9-1	SECTION 15 - DATA SYSTEMS	15-1
9.2 Guidance Comparisons	9-1	15.1 Summary	15-1
9.3 Guidance and Navigation Scheme Evaluation	9-5	15.2 Vehicle Measurement Evaluation	15-1
9.3.1 First Stage Boost	9-5	15.3 Airborne Telemetry System	15-1
9.3.2 Second Stage Boost	9-5	15.3.1 S-IVB Remote Digital Sub-Multiplexer Failure	15-6
9.3.3 Orbital Phase	9-9	15.3.2 Loss of Operational Data Display During Revolution No. 3	15-7
9.3.4 Deorbit Phase	9-9	15.4 C-Band Radar System Evaluation	15-7
9.4 Guidance and Navigation System Components	9-9	15.5 Secure Range Safety Command Systems Evaluation	15-7
9.4.1 ST-124M Stabilized Platform System	9-11	15.6 Digital Command System Evaluation	15-9
9.4.2 Guidance Computer	9-12	15.7 Ground Engineering Cameras	15-9
SECTION 10 - CONTROL AND SEPARATION	10-1	SECTION 16 - MASS CHARACTERISTICS	16-1
10.1 Summary	10-1	16.1 Summary	16-1
10.2 S-IB Control System Evaluation	10-1	16.2 Mass Evaluation	16-1
10.3 S-IVB Control System Evaluation	10-2	SECTION 17 - SPACECRAFT SUMMARY	17-1
10.3.1 S-IVB Control System Evaluation During Burn	10-2	SECTION 18 - MSFC INFLIGHT EXPERIMENT	18-1
10.3.2 S-IVB Control System Evaluation During Orbit	10-10	18.1 Summary	18-1
10.3.3 S-IVB Control System Evaluation During Deorbit	10-21	18.2 Experiment Anomaly	18-1
10.4 Instrument Unit Control Components Evaluation	10-24	18.2.1 Gas System Description	18-2
10.5 Separation	10-24	18.2.2 Gas System Performance	18-2
10.5.1 S-IB/S-IVB Separation	10-24	18.2.3 Gas Consumption	18-4
10.5.2 S-IVB/CSM Separation	10-25	APPENDIX A - ATMOSPHERE	A-1
SECTION 11- ELECTRICAL NETWORKS AND EMERGENCY DETECTION SYSTEM	11-1	APPENDIX B - SA-207 SIGNIFICANT CONFIGURATION CHANGES	B-1
11.1 Summary	11-1		
11.2 S-IB Stage Electrical System	11-1		
11.3 S-IVB Stage Electrical System	11-2		
11.4 Instrument Unit Electrical System	11-7		
11.5 Emergency Detection System	11-11		
SECTION 12 - VEHICLE PRESSURE Environment	12-1		
12.1 S-IB Base Pressure	12-1		

## LIST OF ILLUSTRATIONS

Figure		Page	Figure		Page
2-1	LVDC Clock/Ground Time Difference	2-2	7-5	S-IVB LOX Tank Ullage Pressure - Boost Phase	7-11
3-1	SA-207 Prelaunch Venting	3-4	7-6	S-IVB LOX Pump Inlet Conditions - Burn	7-12
3-2	Center LOX Tank - Outboard LOX Tank Relationship	3-5	7-7	S-IVB Cold Helium Supply History	7-13
4-1	Ascent Trajectory Position Comparison	4-3	7-8	S-IVB APS Propellant Usage	7-15
4-2	Ascent Trajectory Space-Fixed Velocity and Flight Path Angle Comparison	4-4	7-9	S-IVB Deorbit Propellant Dump and Safing Sequence	7-17
4-3	Ascent Trajectory Acceleration Comparison	4-5	7-10	S-IVB LOX Dump	7-18
4-4	Ascent Trajectory Dynamic Pressure and Mach Number Comparison	4-8	7-11	S-IVB LH <sub>2</sub> Dump	7-20
4-5	Launch Vehicle Ground Track	4-11	7-12	S-IVB LH <sub>2</sub> Ullage Pressure - Orbital Coast	7-21
5-1	S-IVB/IU Ground Track During Propellant Dump	5-2	7-13	S-IVB LOX Tank Ullage Pressure - Orbit, Dump, and Safing	7-23
5-2	S-IVB/IU Deorbit Velocity Change	5-3	7-14	S-IVB Hydraulic System - Boost	7-25
5-3	S-IVB/IU Deorbit Altitude Profile	5-5	8-1	SA-207 Longitudinal Accelerations at IU and CM During Thrust Buildup and Launch	8-2
5-4	S-IVB/IU Ground Track - Dump to Impact	5-7	8-2	SA-207 Longitudinal Acceleration at the IU and CM During S-IB Cutoff	8-2
6-1	S-IB Engines Thrust Buildup	6-3	8-3	S-IB-7 Longitudinal Load from Strain Data at Station 942	8-3
6-2	S-IB Stage Propulsion Performance	6-4	8-4	SA-207 Longitudinal Load Distribution at Time of Maximum Bending Moment and IECO	8-4
6-3	S-IB Inboard Engines Total Thrust Decay	6-7	8-5	SA-207 Resultant Bending Moment Distribution at Time of Maximum Resultant Moment	8-5
6-4	S-IB Outboard Engines Total Thrust Decay	6-8	8-6	SA-207 Pitch Bending Moment and Normal Load Factor Distributions at Time of Maximum Resultant Moment	8-6
6-5	S-IB Stage LOX Mass Above Main LOX Valve	6-10	8-7	Yaw Bending Moment Distributions at Time of Maximum Resultant Moment	8-7
6-6	S-IB Stage Fuel Mass Above Main Fuel Valve	6-10	8-8	Combined Loads Producing Minimum Safety Margins During SA-207 Flight	8-9
6-7	S-IB Fuel Tank Ullage Pressure	6-12	8-9	Minimum Factor of Safety During SA-207 S-IB Flight	8-10
6-8	S-IB Fuel Tank Helium Pressurization Sphere Pressure	6-12	8-10	Vehicle Bending Frequencies	8-11
6-9	S-IB Center LOX Tank Ullage Pressure	6-14	8-11	Vehicle Bending Amplitudes	8-12
6-10	S-IB GOX Flow Control Valve Position	6-15	8-12	Vibration Measured During First Stage Burn	8-13
6-11	S-IB Pneumatic Control Pressure	6-16	8-13	Low Frequency Vibration and Pressure Oscillations Measured During S-IVB Stage Burn	8-14
7-1	S-IVB Start Box and Run Requirements	7-3	8-14	Low Frequency Spectral Analysis of Vibration and Engine Pressures	8-15
7-2	S-IVB Steady-State Performance	7-4	8-15	S-IVB Cutoff Transients on J-2 Engine Gimbal Block, SA-207 and SA-206	8-16
7-3	S-IVB LH <sub>2</sub> Ullage Pressure - Boost Phase	7-8			
7-4	S-IVB Fuel Pump Inlet Conditions - Burn	7-9			

## LIST OF ILLUSTRATIONS (CONTINUED)

Figure		Page	Figure		Page
9-1	SA-207 Trajectory and ST-124M Platform Velocity Comparisons (OMPT Minus LVDC)	9-2	12-1	S-IB Stage Heat Shield Pressure	12-2
9-2	Roll Command During Boost	9-6	12-2	S-IB Stage Flame Shield Pressure	12-3
9-3	Pitch Command During Boost	9-7	12-3	S-IB Stage Heat Shield Loading	12-4
9-4	Yaw Command During Boost	9-8	12-4	S-IB Stage Base Drag Coefficient	12-5
9-5	Inertial Velocity Component Increments During S-IVB Thrust Decay	9-10	13-1	S-IB Stage Heat Shield Inner Region Total Heating Rate	13-2
10-1	Pitch Plane Dynamics During S-IB Burn	10-3	13-2	S-IB Stage Heat Shield Inner Region Radiation Heating Rate	13-3
10-2	Yaw Plane Dynamics During S-IB Burn	10-4	13-3	S-IB Stage Heat Shield Inner Region Gas Temperature	13-4
10-3	Roll Plane Dynamics During S-IB Burn	10-5	13-4	S-IB Stage Heat Shield Outer Region Gas Temperature	13-5
10-4	Pitch and Yaw Plane Free Stream Angle of Attack During S-IB Burn	10-6	13-5	S-IB Stage Flame Shield Total Heating Rate	13-6
10-5	Pitch Plane Dynamics - S-IVB Burn	10-8	13-6	S-IB Stage Flame Shield Gas Temperature	13-7
10-6	Yaw Plane Dynamics - S-IVB Burn	10-9	13-7	S-IB Stage Flame Shield Radiation Heating Rate	13-8
10-7	Pitch Plane Dynamics During Orbit (Sheet 1 of 4)	10-12	13-8	S-IB Stage Flame Shield Configurations	13-10
10-8	APS Activity During LH <sub>2</sub> NPV Relief Venting (Sheet 1 of 2)	10-17	13-9	Comparison of S-IB Stage Flame Shield Radiant Heating Data with Design Level	13-11
10-9	S-IVB Pitch Disturbance During Coast	10-19	13-10	Comparison of S-IB Stage Flame Shield Total Heating Data with Design Level	13-12
10-10	Comparison of Measured S-IVB Pitch Actuator Motion with Simulation Incorporating Effects of Stiction	10-20	13-11	Comparison of S-IB Stage Flame Shield Gas Temperature Data	13-13
10-11	Vehicle Dynamics During Deorbit (Sheet 1 of 2)	10-22	14-1	IU Sublimator Start Up Parameters for Initial Cycle	14-3
10-12	S-IB/S-IVB Longitudinal Acceleration During Separation	10-26	14-2	IU TCS Coolant Control Parameters	14-4
10-13	Angular Velocities During S-IB/S-IVB Separation	10-27	14-3	IU TCS Hydraulic Performance	14-5
11-1	S-IVB Stage Forward No. 1 Battery Voltage, Current, and Temperature	11-3	14-4	IU TCS GN <sub>2</sub> Sphere Pressure (D25-601)	14-6
11-2	S-IVB Stage Forward No. 2 Battery Voltage, Current, and Temperature	11-4	14-5	IU Platform Internal Gas Bearing GN <sub>2</sub> Pressures	14-7
11-3	S-IVB Stage Aft No. 1 Battery Voltage, Current, and Temperature	11-5	14-6	IU GBS GN <sub>2</sub> Sphere Pressure (D10-603)	14-8
11-4	S-IVB Stage Aft No. 2 Battery Voltage, Current, and Temperature	11-6	14-7	Selected IU Component Temperatures	14-9
11-5	IU 6D10 Battery Parameters	11-8	14-8	Selected IU Component Temperatures	14-9
11-6	IU 6D30 Battery Parameters	11-9	15-1	SA-207 Telemetry Ground Station Coverage	15-5
11-7	IU 6D40 Battery Parameters	11-10	15-2	SA-207 C-Band Acquisition and Loss Times	15-8
			18-1	P-10 Gas Supply System Schematic	18-3

## LIST OF ILLUSTRATIONS (CONTINUED)

Figure		Page
18-2	S-150 Environmental Parameter History	18-5
A-1	Surface Weather Map Approximately 49 Minutes After Launch of SA-207/SL-3	A-2
A-2	500 Millibar Map Approximately 49 Minutes After Launch of SA-207/SL-3	A-3
A-3	Scalar Wind Speed at Launch Time of SA-207/SL-3	A-6
A-4	Wind Direction at Launch Time of SA-207/SL-3	A-7
A-5	Pitch Wind Velocity Component ( $W_x$ ) at Launch Time of SA-207/SL-3	A-8
A-6	Yaw Wind Velocity Component ( $W_z$ ) at Launch Time of SA-207/SL-3	A-10
A-7	Pitch ( $S_x$ ) and Yaw ( $S_z$ ) Component Wind Shears at Launch Time of SA-207/SL-3	A-11
A-8	Relative Deviation of Temperature and Pressure from the PRA-63 Reference Atmosphere, SA-207/SL-3	A-14
A-9	Relative Deviation of Density and Absolute Deviation of the Index of Refraction from the PRA-63 Reference Atmosphere, SA-207/SL-3	A-15

## LIST OF TABLES

Table	Page	Table	Page		
1	Mission Objectives Accomplishment	9-4	SA-207 Orbital Phase Flight Program Attitude Commands	9-11	
2	Summary of Failures and Anomalies	10-1	Misalignment Summary	10-1	
2-1	Time Base Summary	2-2	10-2	Maximum Control Parameters During S-IB Burn	10-7
2-2	Significant Event Times Summary	2-3	10-3	Maximum Control Parameters During S-IVB Burn	10-10
2-3	Variable Time and Commanded Switch Selector Events	2-10	10-4	Attitude Maneuvers During Orbit	10-11
3-1	SA-207/Skylab-3 Prelaunch Milestones	3-2	11-1	S-IB Stage Battery Power Consumption	11-2
4-1	Summary of Available Tracking Data	4-2	11-2	S-IVB Stage Battery Power Consumption	11-7
4-2	Comparison of Cutoff Events	4-6	11-3	IU Battery Power Consumption	11-11
4-3	Comparison of Significant Trajectory Events	4-6	15-1	SA-207 Measurement Summary	15-2
4-4	Comparison of Separation Events	4-7	15-2	SA-207 Flight Measurements Waived Prior to Flight	15-3
4-5	Comparison of S-IB Spent Stage Impact Point	4-9	15-3	SA-207 Measurement Malfunctions	15-3
4-6	S-IB Spent Stage Impact Envelope	4-9	15-4	SA-207 Launch Vehicle Telemetry Links Performance Summary	15-4
4-7	Comparison of Orbit Insertion Conditions	4-10	15-5	SA-207 S-150 Experiment ASAP Data Dumps	15-6
5-1	S-IVB/IU Propellant Dump Velocity Changes	5-4	15-6	SA-207 IU Commands	15-10
5-2	S-IVB/IU Orbit Trajectory Components at TB5	5-4	16-1	SA-207 Total Vehicle Masses (Kilograms)	16-3
5-3	S-IVB/IU Deorbit Position at Breakup	5-6	16-2	SA-207 Total Vehicle Masses (Pounds)	16-4
5-4	SA-207 S-IVB Impact Dispersion Limits	5-6	16-3	SA-207 Upper Stages and Payload Vehicle Masses (Kilograms)	16-5
6-1	S-IB Engine Start Characteristics	6-2	16-4	SA-207 Upper Stages and Payload Vehicle Masses (Pounds)	16-6
6-2	S-IB Individual Engine Propulsion Performance	6-5	16-5	SA-207 Flight Sequence Mass Summary	16-7
6-3	S-IB Propellant Usage	6-9	16-6	SA-207 Mass Characteristics Comparison	16-9
6-4	S-IB Propellant Mass History	6-11	A-1	Surface Observations at SA-207 Launch Time	A-4
7-1	S-IVB Steady State Performance (STDV Open +60 Second Time Slice at Standard Altitude Conditions)	7-5	A-2	Systems Used to Measure Upper Air Wind Data for SA-207	A-5
7-2	S-IVB Stage Propellant Mass History	7-6	A-3	Maximum Wind Speed in High Dynamic Pressure Region for Saturn Launch Vehicles 201 Through 207	A-12
7-3	S-IVB APS Propellant Consumption	7-16	A-4	Extreme Wind Shear Values in the High Dynamic Pressure Region for Saturn Launch Vehicles 201 Through 207	A-13
9-1	SA-207 Inertial Platform Velocity Comparisons	9-3			
9-2	SA-207 Navigation Position and Velocity Comparisons (PACSS-13)	9-4			
9-3	SA-207 Boost Terminal Conditions	9-5			

## LIST OF TABLES (CONTINUED)

Table		Page
A-5	Selected Atmospheric Observations for Saturn Launch Vehicles 201 Through 207 at Kennedy Space Center, Florida	A-16
B-1	S-IB Significant Configuration Changes	B-1
B-2	S-IVB Significant Configuration Changes	B-1
B-3	IU Significant Configuration Changes	B-2

## ACKNOWLEDGEMENT

This report is published by the Saturn Flight Evaluation Working Group, composed of representatives of Marshall Space Flight Center (MSFC), Kennedy Space Center, and MSFC's prime contractors, and in cooperation with the Johnson Space Center. Significant contributions to the evaluation have been made by:

George C. Marshall Space Flight Center

Science and Engineering

Aero-Astroynamics Laboratory

Astrionics Laboratory

Computation Laboratory

Astronautics Laboratory

Saturn Program Office

John F. Kennedy Space Center

Lyndon B. Johnson Space Center

Chrysler Corporation

McDonnell Douglas Astronautics Company

International Business Machines Corporation

Rockwell International Corporation

General Electric Company

The Boeing Company

## ABBREVIATIONS

ACN	Ascension Island	ESC	Engine Start Command
AOS	Acquisition of Signal	FCC	Flight Control Computer
APS	Auxiliary Propulsion System	FM	Frequency Modulation
ARIA	Apollo Range Instrumented Aircraft	GBS	Gas Bearing System
ASAP	Auxiliary Storage and Playback	GCS	Guidance Cutoff Signal
AUX	Auxiliary	GDS	Goldstone
BDA	Bermuda	GFCV	GOX Flow Control Valve
CDDT	Countdown Demonstration Test	GN <sub>2</sub>	Gaseous Nitrogen
CG	Center of Gravity	GRR	Guidance Reference Release
CIF	Central Instrumentation Facility	HAW	Hawaii
CM	Command Module	HE	Helium
CSM	Command and Service Module	HSK	Honeysuckle
CYI	Canary Island	HZ	Hertz
DCS	Digital Command System	IBM	International Business Machines
EBW	Explosive Bridge Wire	ICD	Interface Control Document
ECO	Engine Cutoff	IECO	Inboard Engine Cutoff
ECS	Environmental Control System	IGM	Iterative Guidance Mode
EDS	Emergency Detection System	IU	Instrument Unit
EDT	Eastern Daylight Time	JSC	Johnson Space Center
EMR	Engine Mixture Ratio	KSC	Kennedy Space Center
EMRC	Engine Mixture Ratio Change	KWJ	Kwajalein
EPO	Earth Parking Orbit	LH <sub>2</sub>	Liquid Hydrogen
		LOS	Loss of Signal

ABBREVIATIONS (CONTINUED)

LOX	Liquid Oxygen	PCM	Pulse Code Modulation
LUT	Launch Umbilical Tower	PEA	Platform Electronics Assembly
LV	Launch Vehicle	PWA	Printed Wiring Assembly
LVDA	Launch Vehicle Data Adapter	PSD	Power Spectral Density
LVDC	Launch Vehicle Digital Computer	PTCS	Propellant Tanking Computer System
MAD	Madrid	PU	Propellant Utilization
MAX Q	Maximum Dynamic Pressure	q	Dynamic Pressure
MCC-H	Mission Control Center - Houston	RDSM	Remote Digital Sub-Multiplexer
MILA	Merritt Island Launch Area	RF	Radio Frequency
ML	Mobile Launcher	RFI	Radio Frequency Interference
MR	Mixture Ratio	RLH	Retrograde Local Horizontal
MSFC	Marshall Space Flight Center	S/A	Service Arm
#, NO.	Number	SACS	Service Arm Control Switches
NASA	National Aeronautics and Space Administration	SC	Spacecraft
NPSP	Net Positive Suction Pressure	SCFM	Standard Cubic Feet per Minute
NPV	Non-Propulsive Vent	SCMS	Standard Cubic Meters per Second
OAT	Overall Test	SL	Skylab
OECO	Outboard Engine Cutoff	SLA	Spacecraft Lunar Module Adapter
OMPT	Observed Mass Point Trajectory	SM	Service Module
OT	Operational Trajectory	STDV	Start Tank Discharge Valve
OWS	Orbital Workshop (Modified S-IVB Stage)	SV	Space Vehicle
PACSS	Project Apollo Coordinate System Standard	SWS	Saturn Workshop

ABBREVIATIONS (CONTINUED)

TAN	Tananarive
TB	Time Base
TCS	Terminal Countdown Sequencer or Thermal Conditioning System
TEX	Corpus Christi, Texas
TVC	Thrust Vector Control
UCR	Unsatisfactory Condition Report
US	United States
UT	Universal Time
VAB	Vertical Assembly Building

## SA-207 MISSION PLAN

The Saturn IB SA-207, designated SL-3, is to boost a manned Command Service Module (CSM) to an 81 x 121 n mi orbit coplanar with the Saturn Work Shop (SWS) orbiting at approximately 234 n mi. The SL-3 space vehicle consists of the Saturn IB-207 launch vehicle and the CSM-117 payload. The launch vehicle is comprised of the S-IB-7 first stage, the S-IVB-207 second stage, and the S-IU-208. SL-3 is the second manned flight in the Skylab Program.

Launch is scheduled to occur on the 28th of July 1973, from Launch Complex 39, Pad B of the Kennedy Space Center (KSC) at 7:10:50 a.m., Eastern Daylight Time. The vehicle is aligned along a 90° azimuth at liftoff. Following liftoff the vehicle rolls to a flight azimuth of approximately 45.0 degrees measured east of north. Vehicle weight at ignition is nominally 1,308,579 lbm.

The S-IB stage powered flight lasts approximately 140 seconds. The S-IVB stage provides powered flight for approximately 453 seconds inserting the CSM into a low earth orbit at the proper altitude and inclination to allow the CSM to enter a phasing orbit for rendezvous.

Following CSM separation the S-IVB/IU/SLA will remain in orbit up to 6 hours, during which time data will be gathered by the Galactic X-Ray Mapping Experiment, S-150. The auxiliary propulsion system will provide attitude control for the experiment to whatever extent that is compatible with deorbit requirements.

During the fourth revolution a controlled deorbit of the spent S-IVB/IU/SLA will be accomplished. The spent vehicle will be oriented to a retrograde attitude and residual propellants in the S-IVB stage tanks will be dumped through the J-2 engine to produce the impulse necessary to deorbit the vehicle. By controlling the vehicle attitude and the time and duration of propellant dump the spent vehicle will be impacted into the uninhabited Pacific Ocean area at a nominal impact point of 23.75 degrees North latitude and 184.50 degrees East longitude.

The CSM Service Propulsion System and Reaction Control System will be used to complete the CSM rendezvous maneuvers and dock axially with the orbiting SWS. The crew will transfer from the CSM and activate the SWS, inhabiting it for a period of up to 59 days. After completion of the scheduled mission activities, the SWS will be prepared for orbital storage, the crew will transfer to the CSM and the SWS will be left in a solar inertial attitude. The CSM will undock from the SWS and deorbit for earth re-entry.

## FLIGHT SUMMARY

The Saturn IB, SA-207 Launch Vehicle was launched at 7:10:50 Eastern Daylight Time on July 28, 1973 from Pad 39B of Kennedy Space Center and placed the Command Service Module containing three crew members into earth orbit for rendezvous with the orbiting Saturn Work Shop. The performance of ground systems supporting the countdown and launch was satisfactory although some concern was expressed during prelaunch countdown about S-IB LOX venting.

The reconstructed flight trajectory (actual) was very close to the Post Launch Operational Trajectory (nominal). The S-IB stage powered the vehicle until Outboard Engine Cutoff (OECO) at 140.73 seconds which was 1.13 seconds later than nominal. The total space-fixed velocity at this time was 0.19 m/s less than nominal. After separation, the S-IB stage continued on a ballistic trajectory until earth impact. The S-IVB burn terminated with guidance cutoff signal and was followed by parking orbit insertion, both 3.14 seconds earlier than nominal. An excess velocity of 0.75 m/s at insertion resulted in an apogee 2.16 km higher than nominal. The parking orbit portion of the trajectory from insertion to CSM/S-IVB separation was close to nominal. The astronaut initiated separation of the CSM from the S-IVB stage occurred at 1080.4 seconds, 124.2 seconds later than nominal.

All aspects of the S-IVB/IU deorbit were accomplished successfully. The propellant dump was modified during real time to establish a reentry trajectory that would enable observation by Kwajalein. This modified plan was accomplished. The velocity change obtained for deorbit was very close to the real-time predicted value. The breakup altitude was 81.7 km, and impact in the primary disposal area.

The S-IB stage propulsion system performed satisfactorily throughout flight. The one propulsion anomaly (possible LOX emanation from the LOX tank vents) occurred during countdown and had no effect on the countdown operations or flight performance. Stage longitudinal site thrust and mixture ratio averaged 0.68 percent and 0.27 percent lower than predicted, respectively. Stage LOX, fuel and total flowrate averaged 0.75 percent, 0.49 percent and 0.68 percent lower than predicted, respectively. Stage specific impulse was within 0.1 percent of predicted. Inboard Engine Cutoff (IECO) occurred at 137.36 seconds (0.76 seconds later than predicted). Outboard Engine Cutoff (OECO) was initiated 3.37 seconds after IECO by thrust OK pressure switch deactuation as planned at 140.73 seconds. At OECO, the LOX residual was 2960 lbm compared to the predicted 3311 lbm and the fuel residual was 6145 lbm compared to the predicted 5988 lbm. The stage hydraulic system performed satisfactorily.

The S-IVB propulsion system performed satisfactorily throughout the operational phase of burn and had normal start and cutoff transients. S-IVB burn time was 448.53 seconds, 4.24 seconds shorter than predicted for the actual flight azimuth of 45.0 degrees. This difference is composed of -0.13 second due to S-IB/S-IVB separation velocity, radius, and weight and -3.90 seconds due to higher than predicted S-IVB performance leaving -0.21 second unexplained. The engine performance during burn, as determined from standard altitude reconstruction analysis, deviated from the predicted Start Tank Discharge Valve (STDV) open +60 second time slice by +0.89 percent for thrust and -0.05 percent for specific impulse. The S-IVB stage engine cutoff (ECO) was initiated by the Launch Vehicle Digital Computer (LVDC) at 592.93 seconds. The S-IVB residuals at engine cutoff were near nominal. The best estimate of the residuals at engine cutoff is 2551 lbm for LOX and 2326 lbm for LH<sub>2</sub> as compared to the predicted values of 2843 lbm for LOX and 1957 lbm for LH<sub>2</sub>. During orbital coast the Auxiliary Propulsion System (APS) demonstrated nominal performance and responded to a disturbing force on the S-IVB/IU stage. LH<sub>2</sub> NPV and Instrument Unit (IU) sublimator operation contributed to the disturbing forces. The level of disturbance attributed to the LH<sub>2</sub> NPV system is within the specified tolerances on nozzle misalignment and area unbalance even if the disturbance were attributed entirely to misalignment or entirely to area unbalance. The disturbance had no effect on mission accomplishment. An engine pitch actuator oscillation of low amplitude and frequency was noted during prelaunch, S-IB boost, and orbital coast thermal cycles while no commands were input to the servovalve. These oscillations were caused by accumulation of micron sized particles in the clearance between the servovalve spool and bushing. Operation was normal during powered flight and deorbit dumps. The impulse derived from the LOX and fuel dumps was sufficient to satisfactorily deorbit the S-IVB/IU. The total impulse provided 104,000 lbf-sec, was in close agreement with the real time nominal predicted value of 103,500 lbf-sec. As expected after the extended LH<sub>2</sub> dump the pneumatic pressure was not sufficient to cause the NPV valves to latch open; however all deorbit safing criteria were met. The APS satisfied control system demands throughout the deorbit sequence.

The structural loads experienced during the flight were well below design values. The maximum bending moment was  $10.6 \times 10^6$  in-lbf (approximately 19 percent of design) at vehicle station 942. The S-IB thrust cutoff transients experienced by SA-207 were smaller than those of SA-206. The S-IVB engine cutoff transient produced oscillations on the gimbal block of 4.25 g peak amplitude with a predominant frequency of 55 Hz. Although this transient exceeded that of SA-206 it was well within the envelope experienced on Saturn V flights. The maximum ground wind experienced by the Saturn IB SA-207 during the prelaunch period was 14 knots (allowable with damper, 55 knots). The ground winds at launch were 13.5 knots from the west (allowable at launch 38 knots).

The stabilized platform and the guidance computer successfully supported the accomplishment of the Launch Vehicle mission objectives. Targeted conditions at orbit insertion were attained with insignificant error. No anomalies nor deviations from nominal performance were noted.

The stabilized platform accelerometers properly reacted to thrust decay vibrations following S-IVB stage guidance cutoff.

The control and separation systems functioned correctly throughout the powered and coast flight. Auxiliary Propulsion System (APS) propellant usage was greater than expected during coast but the quantity available was adequate to fulfill all mission requirements. Engine gimbal deflections were nominal. Bending and slosh dynamics were adequately stabilized. No unusual dynamics accompanied any separation.

The electrical systems and Emergency Detection System (EDS) performed satisfactorily during the flight. Battery performance (including voltages, currents, and temperatures) was satisfactory and remained within acceptable limits. Operation of all power supplies, inverters, Exploding Bridge Wire (EBW) firing units, and switch selectors was nominal.

Environmental pressure data in the S-IB base region compared with pre-flight predictions and/or previous flight data show good agreement.

The thermal environment measured in the SA-207 S-IB base region has been compared with corresponding data from flights SA-203 through SA-206. With the exception of the flame shield radiation heating data (measurement C0603-006), these comparisons show excellent agreement. Two possible causes which would allow more radiation from the engine exhaust plume to reach the flame shield radiometer are, reduction in opacity of the turbine exhaust gas or sustained local burning of the turbine exhaust gases. Neither of these provide a completely satisfactory explanation, but reduced local opacity is the most probable. In all areas the measured thermal environments in the base region of SA-207 were well below the S-IB stage design level.

The S-IB stage engine compartment and instrument compartment require environmental control during prelaunch operations, but are not actively controlled during S-IB boost. The desired temperatures were maintained in both compartments during the prelaunch operation. The Instrument Unit (IU) stage Environmental Control System (ECS) exhibited satisfactory performance for the duration of the IU mission. Coolant temperatures, pressures, and flowrates were continuously maintained within the required ranges and design limits.

The SA-207 vehicle data systems performed satisfactorily except for a failure in the S-IVB telemetry system. This failure resulted in the loss of three S-IVB measurements, but had no impact on vehicle performance or postflight analysis. The overall measurement system reliability was 99.6 percent. The usual telemetry interference due to flame effects and staging were experienced. Usable telemetry data were received until 20,500 seconds (5:41:40). Good tracking data were received from the C-Band radar, with Kwajalein (KWJ) indicating final Loss of Signal (LOS) at 21,175 seconds (5:52:55). The Secure Range Safety Command Systems on the S-IB and S-IVB stages were ready to perform their functions

properly, on command, if flight conditions during launch phase had required destruct. The Digital Command System (DCS) performed satisfactorily from liftoff through deorbit. Instrument Unit (IU) telemetry data needed for real time support of deorbit operations were not available at Mission Control Center-Houston (MCC-H) during the third orbital revolution pass over the Hawaii (HAW) ground station because of improper implementation of ground procedures at HAW and Johnson Space Center (JSC). In general, ground engineering camera coverage was fair being somewhat below the standard set by previous launches. Three S-150 experiment data dumps were satisfactorily accomplished.

Total vehicle mass, determined from postflight analysis, was within 0.21 percent of predicted from ground ignition through S-IVB/spacecraft separation. Hardware weights, propellant loads and propellant utilization were close to predicted values during flight.

Skylab Experiment S-150, Galactic X-Ray Mapping Experiment, was performed during the flight of SA-207. The object of the experiment was to map the X-Ray flux intensity of galactic space. The experiment, which had a planned operating time of 265 minutes, collected X-Ray data for only 110 minutes before the experiment high voltage switched off because of low gas pressure in the X-Ray sensor. Even though the operating time of the X-Ray experiment was less than planned, it was greater than the accumulative time of all preceding similar experiments. The associated spectral data continued to be collected by the experiment star sensors, however, these data are of use principally in determining experiment pointing direction. The lack of one Auxiliary Storage and Playback (ASAP) cycle resulted in loss of this spectral data for the third revolution.

## MISSION OBJECTIVES ACCOMPLISHMENT

Table 1 presents the MSFC Launch Vehicle objective for Skylab-3 as defined in the "Saturn Mission Implementation Plan SL-3/SA-207," MSFC Document PM-SAT-8010.23, Revision A, dated June 8, 1973. An assessment of the degree of accomplishment can be found in other sections of this report as shown in Table 1.

Table 1. Mission Objective Accomplishment

NO.	LAUNCH VEHICLE OBJECTIVE	DEGREE OF ACCOMPLISHMENT	DISCREPANCIES	SECTION IN WHICH DISCUSSED
1	Launch and insert a manned CSM into the earth orbit targeted for during the final launch countdown. [SL-3 was targeted for an 81 x 121 n mi (150 x 224 km) orbit].	Complete	None	4.2

## FAILURES AND ANOMALIES

Evaluation of the launch vehicle and launch vehicle ground support equipment data revealed the following six anomalies and one failure, none of which are considered significant.

Table 2. Summary of Failures and Anomalies

ITEM	VEHICLE SYSTEM	ANOMALY (CAUSE)	SIGNIFICANCE	CORRECTIVE ACTION	SECTION REFERENCE
1	S-1B PRESSURIZATION	POSSIBLE LOX EMANATING OCCASIONALLY FROM THE LOX TANK VENTS FROM APPROXIMATELY T-5.5 HOURS TO VERT CLOSURE AT T-2 MINUTES 43 SECONDS. (UNKNOWN)	NONE TO LAUNCH VEHICLE OR GROUND HARDWARE NONE TO GROUND OPERATIONS EXCEPT POSSIBLY DURING ASTRONAUT BOARDING. (APD 19C ANOMALY)	CLOSED. KSC WILL IMPLEMENT COUNT-DOWN CONTINGENCY PROCEDURES IF THIS PHENOMENON IS OBSERVED PRIOR TO ASTRONAUT BOARDING.	3.4.2.1
2	S-1B FLAME SHIELD	THERMAL RADIATION ENVIRONMENT MORE SEVERE THAN EXPECTED FROM 13 TO 55 SECONDS. (UNKNOWN, POSSIBLY LOCALIZED REDUCED OPACITY OR LOCALIZED AFTERBURNING OF TURBINE EXHAUST GASES.)	NONE. ENVIRONMENT WAS WELL WITHIN DESIGN LIMITS. (APD 19C ANOMALY)	NONE. CLOSED.	13.1
3	S-1VB TELEMETRY	SIX FLIGHT MEASUREMENTS NOT TRANSMITTED ON CP1 LINK AFTER APPROXIMATELY 142 SECONDS. THREE OF THESE WERE CROSS-STRAPPED AND RECOVERED THROUGH IU DP1 LINK. (RANDOM COMPONENT FAILURE IN REMOTE DIGITAL SUB-MULTIPLEXER.)	LOSS OF THREE NON-CRITICAL FLIGHT MEASUREMENTS. (APD 19C FAILURE, APD 44 NON-COMFORMANCE CATEGORY 4.)	NONE. CLOSED.	15.3.1
4	S-1VB HYDRAULIC	PITCH ACTUATOR OSCILLATORY DRIFT AT LOW AMPITUDE AND FREQUENCY DURING PRELAUNCH, S-1B BOOST AND ORBITAL COAST THERMAL CYCLES. (ACTUATOR SERVO VALVE HUNTING DUE TO STICTION CAUSED BY MICRON SIZED CONTAMINANT PARTICLES.)	NONE. (APD 19C ANOMALY.)	NONE. CLOSED.	7.11 10.3.2.1
5	IU/S-1VB ASSEMBLY	UNEXPECTEDLY HIGH S-1VB APS MODULE 2 PROPELLANT CONSUMPTION TO MAINTAIN ATTITUDE CONTROL DURING ORBITAL COAST. (UNPREDICTED ATTITUDE DISTURBANCE FROM WITHIN SPECIFICATION NPV THRUST IMBALANCE AND NOZZLE MISALIGNMENT DURING RELIEF VENTING AND NORMAL IU SUBLIMATOR ACTIVITY.)	NONE. SUFFICIENT PROPELLANTS AVAILABLE FOR ALL MISSION REQUIREMENTS. (APD 19C ANOMALY.)	INCORPORATE TOTAL NPV AND SUBLIMATOR EFFECTS IN FUTURE APS PROPELLANT USAGE PREDICTIONS. CLOSED.	7.8 10.3.2
6	IU TELEMETRY	OPERATIONAL DATA NOT AVAILABLE FOR REAL TIME DISPLAY DURING THIRD ORBITAL REVOLUTION PASS OVER THE HAWAII GROUND STATION. (IMPROPER IMPLEMENTATION OF GROUND PROCEDURES AT HAWAII AND JSC.)	1. DELAYED VERIFICATION OF S-1VB/IU DEORBIT COMMAND. 2. LOSS OF FLIGHT EVALUATION DATA RELATED TO APS ANOMALY. 3. LOSS OF S-150 EXPERIMENT DATA (APD 19C ANOMALY.)	PROBLEM HAS BEEN IDENTIFIED TO JSC FOR APPROPRIATE ACTION. CLOSED.	15.3.2
7	GALACTIC X-RAY (S-150) EXPERIMENT	EXPERIMENT HIGH VOLTAGE SWITCHED OFF PREMATURELY AT 2 HOURS 20 MINUTES DUE TO LOW GAS PRESSURE IN THE X-RAY SENSOR. (GAS LEAKAGE THROUGH THE X-RAY INCIDENT WINDOW)	LOSS OF 2 HOURS AND 35 MINUTES OF EXPERIMENT DATA. (APD 19C ANOMALY.)	IF EXPERIMENT IS FLOWN AGAIN, BROADEN OPERATING BAND OF REGULATOR AND INCREASE KIM-FOL WINDOW THICKNESS TO 0.5 MIL. CLOSED.	18.0

## SECTION 1

### INTRODUCTION

#### 1.1 PURPOSE

This report provides the National Aeronautics and Space Administration (NASA) Headquarters, and other interested agencies, with the results of the SA-207 launch vehicle flight evaluation (Skylab-3 launch). The basic objective of flight evaluation is to acquire, reduce, analyze, evaluate and report on flight data to the extent required to assure future mission success and vehicle reliability. To accomplish this objective, actual flight problems are identified, their causes determined, and recommendations made for appropriate corrective action.

#### 1.2 SCOPE

This report contains the performance evaluation of the launch vehicle systems with special emphasis on problems. Summaries of launch operations and spacecraft performance are included.

The official George C. Marshall Space Flight Center (MSFC) position at this time is represented by this report. It will not be followed by a similar report unless continued analysis or new information should prove the conclusions presented herein to be significantly incorrect.

#### 1.3 PERFORMANCE PREDICTIONS BASELINE

Unless otherwise noted, all performance predictions quoted herein for comparison purposes are those used in or generated by the Skylab-3 (SA-207) Post Launch Predicted Operational Trajectory (OT) S&E-AERO-MFP-114-73, dated July 28, 1973.

## SECTION 2

### EVENT TIMES

#### 2.1 SUMMARY OF EVENTS

Range zero occurred at 07:10:50 Eastern Daylight Time (EDT) (11:10:50 Universal Time [UT]) July 28, 1973. Range time is the elapsed time from range zero, which, by definition, is the nearest whole second prior to liftoff signal, and is the time used throughout this report unless otherwise noted. Time from base time is the elapsed time from the start of the indicated time base. Table 2-1 presents the time bases used in the flight sequence program.

The start of Time Bases T<sub>0</sub> and T<sub>1</sub> were nominal. T<sub>2</sub> and T<sub>3</sub> were initiated approximately 0.8 second and 1.1 seconds late, respectively. These variations are discussed in Section 6 of this document. T<sub>4</sub> was initiated 3.2 seconds early, consistent with the early S-IVB engine cutoff discussed in Section 7. Start of T<sub>5</sub> was initiated by the receipt of a ground command, 0.6 seconds later than scheduled in real time as discussed in Section 5.2.

Figure 2-1 shows the difference between telemetry signal receipt at a ground station and vehicle (Launch Vehicle Digital Computer [LVDC] clock) time. This difference between ground and vehicle time is a function of LVDC clock speed.

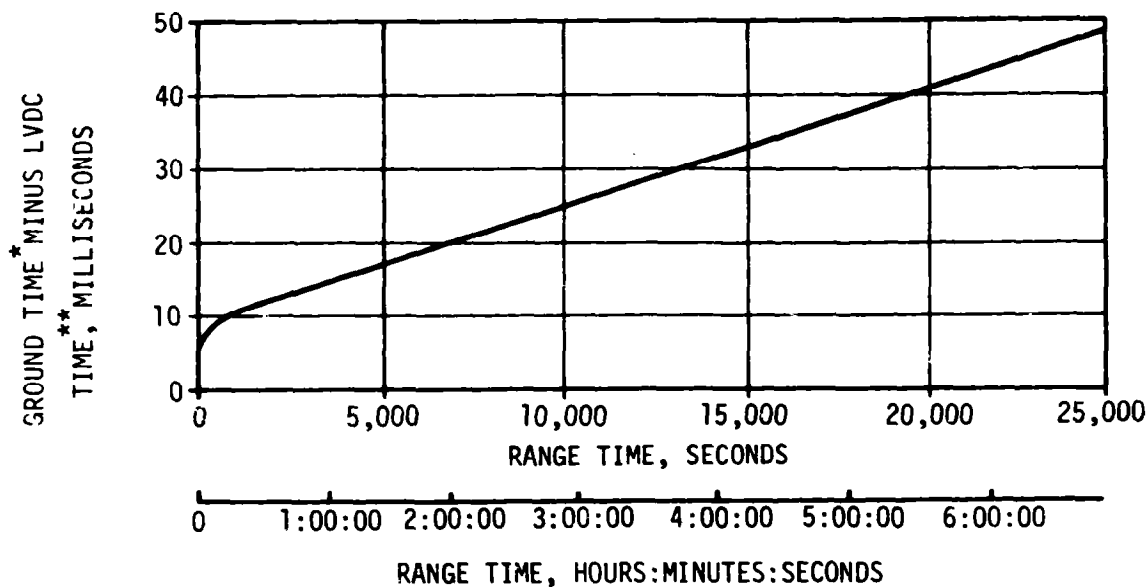
A summary of significant event times for SA-207 is given in Table 2-2. The preflight predicted times were adjusted to match the actual first motion time. The predicted times for establishing actual minus predicted times in Table 2-2 were taken from 68M00001C, "Interface Control Document Definition of Saturn SA-207 and Subs Flight Sequence Program" and from the Skylab-3 (SA-207) Post-Launch Predicted Operational Trajectory (OT) S&E-AERO-MFP-114-73, dated July 28, 1973, unless otherwise noted.

#### 2.2 VARIABLE TIME AND COMMANDED SWITCH SELECTOR EVENTS

Table 2-3 lists the switch selector events which were issued during the flight, but were not programmed for specific times.

Table 2-1. Time Base Summary

TIME BASE	RANGE TIME SECONDS	SIGNAL START
T <sub>0</sub>	-16.95	Guidance Reference Release
T <sub>1</sub>	0.48	IU Umbilical Disconnect Sensed by LVDC
T <sub>2</sub>	134.38	S-IB Low Level Sensors Dry Sensed by LVDC
T <sub>3</sub>	140.72	S-IB DECO Sensed by LVDC
T <sub>4</sub>	593.14	S-IVB ECO (Velocity) Sensed by LVDC
T <sub>5</sub>	19,193.27	Initiated by Receipt of Ground Command



- \* RANGE TIME OF GROUND RECEIPT OF TELEMETERED SIGNAL FROM VEHICLE
- \*\* RANGE TIME OF OCCURENCE AS INDICATED BY UNCORRECTED LVDC CLOCK

Figure 2-1. LVDC Clock/Ground Time Difference

Table 2-2. Significant Event Times Summary

ITEM	EVENT DESCRIPTION	RANGE TIME		TIME FROM BASE	
		ACTUAL SEC	ACT-PRED SEC	ACTUAL SEC	ACT-PRED SEC
1	GUIDANCE REFERENCE RELEASE (GRR)	-17.0	-0.1	-17.4	0.0
2	S-1B ENGINE START COMMAND	-3.1	-0.1	-3.5	0.0
3	S-1B START SIGNAL ENGINE NO. 5	-3.0	-0.1	-3.4	0.0
4	S-1B START SIGNAL ENGINE NO. 7	-3.0	-0.1	-3.4	0.0
5	S-1B START SIGNAL ENGINE NO. 6	-2.9	-0.1	-3.3	0.0
6	S-1B START SIGNAL ENGINE NO. 8	-2.9	-0.1	-3.3	0.0
7	S-1B START SIGNAL ENGINE NO. 2	-2.8	-0.1	-3.2	0.0
8	S-1B START SIGNAL ENGINE NO. 4	-2.8	-0.1	-3.2	0.0
9	S-1B START SIGNAL ENGINE NO. 3	-2.7	-0.1	-3.1	0.0
10	S-1B START SIGNAL ENGINE NO. 1	-2.7	-0.1	-3.1	0.0
11	RANGE ZERO	0.0		-0.5	
12	FIRST MOTION	0.3	0.0	-0.2	0.0
13	TO UMBILICAL DISCONNECT, START OF TIME BASE 1 (T1) LIFTOFF	0.5	0.0	0.0	0.0
14	SINGLE ENGINE CUTOFF ENABLE	3.4	-0.1	3.0	0.0
15	LOX TANK PRESSURIZATION SHUTOFF VALVES CLOSE	6.4	-0.1	6.0	0.0
16	BEGIN PITCH, YAW AND ROLL MANEUVER	10.2	-0.6	9.7	-0.6
17	MULTIPLE ENGINE CUTOFF ENABLE #1	10.4	-0.1	10.0	0.0
18	MULTIPLE ENGINE CUTOFF ENABLE #2	10.6	0.0	10.1	0.0
19	TELEMETER CALIBRATE ON	20.5	0.0	20.0	0.0
20	TELEMETER CALIBRATE OFF	25.4	-0.1	25.0	0.0
21	TELEMETRY CALIBRATOR IN-FLIGHT CALIBRATE ON	27.4	-0.1	27.0	0.0
22	TELEMETRY CALIBRATOR IN-FLIGHT CALIBRATE OFF	32.4	-0.1	32.0	0.0
23	S-150 VENT VALVE OPEN ON	35.4	-0.1	35.0	0.0

Table 2-2. Significant Event Times Summary (Continued)

ITEM	EVENT DESCRIPTION	RANGE TIME		TIME FROM BASE	
		ACTUAL SEC	ACT-PRED SEC	ACTUAL SEC	ACT-PRED SEC
24	S-150 VENT VALVE OPEN OFF	35.6	-0.1	35.2	0.0
25	LAUNCH VEHICLE ENGINES EDS CUTOFF ENABLE	40.4	-0.1	40.0	0.0
26	END ROLL PANEL VER	57.5	1.7	57.0	1.7
27	PACH 1	59.0	1.1	58.5	1.0
28	MAXIMUM DYNAMIC PRESSURE (MAX Q)	75.0	2.0	74.5	2.0
29	TELEMETRY CALIBRATOR IN-FLIGHT CALIBRATE ON	90.6	-0.1	90.2	0.0
30	TELEMETRY CALIBRATOR IN-FLIGHT CALIBRATE OFF	95.6	-0.1	95.2	0.0
31	FLIGHT CONTROL COMPUTER SWITCH POINT NO. 1	100.4	-0.1	100.0	0.0
32	FLIGHT CONTROL COMPUTER SWITCH POINT NO. 2	100.6	-0.1	100.2	0.0
33	TELEMETER CALIBRATION ON	120.2	-0.1	119.8	0.0
34	FLIGHT CONTROL COMPUTER SWITCH POINT NO. 3	120.4	-0.1	120.0	0.0
35	10 CONTROL ACCEL. PWR OFF	120.6	-0.1	120.2	0.0
36	TELEMETER CALIBRATION OFF	125.2	-0.1	124.8	0.0
37	TELEMETER CALIBRATE ON	126.5	-0.1	126.1	0.0
38	TELEMETER CALIBRATE OFF	127.5	-0.1	127.1	0.0
39	EXCESS RATE (P,Y,R) AUTO-ABORT INHIBIT ENABLE	127.7	-0.1	127.3	0.0
40	EXCESS RATE (P,Y,R) AUTO-ABORT INHIBIT AND SWITCH RATE GYRUS SC INDICATION "A"	127.9	-0.1	127.5	0.0
41	S-1B TWO ENGINES CLT AUTO- ABORT INHIBIT ENABLE	128.1	-0.1	127.7	0.0
42	S-1B TWO ENGINES CLT AUTO- ABORT INHIBIT	128.3	-0.1	127.9	0.0
43	PROPELLANT LEVEL SENSORS ENABLE	128.5	-0.1	128.1	0.0
44	TILT ARREST	129.2	-0.8	128.7	-0.8
45	S-1B PROPELLANT LEVEL SENSOR ACTUATION	134.4	0.8	133.9	0.8

Table 2-2. Significant Event Times Summary (Continued)

ITEM	EVENT DESCRIPTION	RANGE TIME		TIME FROM BASE	
		ACTUAL SEC	ACT-PRED SEC	ACTUAL SEC	ACT-PRED SEC
46	START OF TIME BASE 2 (T2)	134.4	0.6	0.0	0.0
47	EXCESS RATE (HULL) AUTO-ABORT INHIBIT ENABLE	134.5	0.7	0.2	0.0
48	EXCESS RATE (HULL) AUTO-ABORT INHIBIT AND SWITCH RATE GYROS SC INDICATION 'B'	134.7	0.7	0.4	0.0
49	INBOARD ENGINES CUTOFF (IECO)	137.36	0.76	2.98	-0.02
50	AUTO-ABORT ENABLE RELAYS RESET	137.7	0.7	3.4	0.0
51	CHARGE CELLAGE IGNITION ERW FIRING UNITS	137.9	0.7	3.6	0.0
52	PREVALVES OPEN	138.0	0.7	4.3	0.0
53	LX DEPLETION CUTOFF ENABLE	138.8	0.7	4.5	0.0
54	FUEL DEPLETION CUTOFF ENABLE	139.4	0.8	5.0	0.0
55	SH-16 OUTBOARD ENGINES CUTOFF (LECO)	140.73	1.13	6.35	0.35
56	START OF TIME BASE 3 (T3)	140.7	1.1	0.0	0.0
57	LX TANK PRESSURIZATION SHUTOFF VALVES OPEN	140.9	1.1	0.2	0.0
58	LX TANK FLIGHT PRESSURE SYSTEM ON	141.0	1.1	0.3	0.0
59	SH-16V ENGINE CUTOFF NO. 1 OFF	141.1	1.1	0.4	0.0
60	SH-16V ENGINE CUTOFF NO. 2 OFF	141.2	1.1	0.5	0.0
61	MIXTURE RATIO CONTROL VALVE OPEN	141.5	1.1	0.8	0.0
62	MIXTURE RATIO CONTROL VALVE BACKUP OPEN	141.6	1.1	0.9	0.0
63	CELLAGE MOTORS IGNITION	141.8	1.1	1.1	0.0
64	SH-16/SH-16V SEPARATION SIGNAL ON	142.0	1.1	1.3	0.0
65	SH-16/SH-16V PHYSICAL SEPARATION	142.1*	1.1	1.4	0.0
66	SH-16V ENGINE IGNITION SEQUENCE START COMMAND	143.4*	1.1	2.7	0.0
67	SH-16V MFCV (FER (4.631 EMF) NO	143.9*	1.1	3.2	0.0

\* CALCULATED - DATA LOST

Table 2-2. Significant Event Times Summary (Continued)

ITEM	EVENT DESCRIPTION	RANGE TIME		TIME FROM BASE	
		ACTUAL SEC	ACT-PRED SEC	ACTUAL SEC	ACT-PRED SEC
68	S-1VB STDV CFEN	144.4 *	1.1	3.7	0.0
69	MAINSTAGE ENABLE ON	144.4 *	1.1	3.7	0.0
70	LP-2 TANK PRESSURIZATION CONTROL SWITCH ENABLE	146.0	1.1	5.3	0.0
71	S-1VB MAINSTAGE CK PRESSURE SWITCH 1	146.2	1.1	5.4	-0.1
72	S-1VB MAINSTAGE	146.8	1.1	6.1	0.1
73	MIXTURE RATIO CONTROL VALVE CLOSE	149.4	1.1	8.7	0.0
74	MIXTURE RATIO CONTROL VALVE CLOSE (9.5:1 EMP)	149.5	1.1	9.2	0.0
75	CHARGE ULLAGE JETTISON ERW FIRING UNITS	150.9	1.1	10.2	0.0
76	ULLAGE MOTORS JETTISON	154.0	1.1	13.3	0.0
77	ENGINE MAINSTAGE ENABLE OFF	154.4	1.1	13.7	0.0
78	ULLAGE ERW FIRING UNITS RESET	160.0	1.1	19.3	0.0
79	ULLAGE MOTORS IGNITION AND JETTISON RELAYS RESET	160.2	1.1	19.5	0.0
80	HEAT-EXCHANGER BYPASS VALVE CONTROL ENABLE	164.7	1.1	24.0	0.0
81	TELEMETRY CALIBRATOR IN-FLIGHT CALIBRATE ON	166.1	1.1	25.4	0.0
82	TELEMETRY CALIBRATOR IN-FLIGHT CALIBRATE OFF	171.1	1.1	30.4	0.0
83	BEGIN IGM PHASE 1	176.6	1.1	35.9	0.0
84	FLIGHT CONTROL COMPUTER SWITCH POINT NO. 4	182.7	1.1	42.0	0.0
85	FLIGHT CONTROL COMPUTER SWITCH POINT NO. 5	344.4	1.1	203.7	0.0
86	TELEMETRY CALIBRATOR IN-FLIGHT CALIBRATE ON	346.1	1.1	205.4	0.0
87	TELEMETRY CALIBRATOR IN-FLIGHT CALIBRATE OFF	351.1	1.1	210.4	0.0
88	LP-2 TANK PRESSURIZATION CONTROL SWITCH DISABLE	443.6	1.1	302.9	0.0

\* CALCULATED - DATA LOST

Table 2-2. Significant Event Times Summary (Continued)

ITEM	EVENT DESCRIPTION	RANGE TIME		TIME FROM BASE	
		ACTUAL SEC	ACT-PREC SEC	ACTUAL SEC	ACT-PREC SEC
89	S-IVB MIXTURE RATIO CONTROL VALVE OPEN	468.8	1.1	328.1	0.0
90	MIXTURE RATIO CONTROL VALVE OPEN (4.831 EMR)	469.0	0.0	328.2	-1.2
91	BEGIN IGM PHASE 2	470.5	0.9	329.8	-0.2
92	TELEMETRY CALIBRATOR INFLIGHT CALIBRATE ON	496.1	1.1	355.4	0.0
93	TELEMETRY CALIBRATOR INFLIGHT CALIBRATE OFF	501.1	1.1	360.4	0.0
94	PROPELLANT DEPLETION CUTOFF ARM	540.7	1.1	400.0	0.0
95	BEGIN TERMINAL GUIDANCE	571.0	2.7	430.2	1.5
96	GUIDANCE CUTOFF SIGNAL (ECO)	592.93	-3.14	452.20	-4.27
97	S-IVB SOLENOID ACTIVATION SIGNAL (K140)	592.9	3.1	452.2	2.0
98	S-IVB MAINSTAGE PRESSURE OK SWITCH 1	593.1	3.0	452.4	1.9
99	S-IVB MAINSTAGE PRESSURE OK SWITCH 2	593.2	3.0	452.5	1.9
100	START OF TIME BASE 4 (T4) INERTIAL ATTITUDE FREEZE	593.1	-3.2	0.0	0.0
101	S-IVB ENGINE CUTOFF NO. 1 ON	593.2	-3.2	0.1	0.0
102	S-IVB ENGINE CUTOFF NO. 2 ON	593.3	-3.2	0.2	0.0
103	PREVALVES CLOSE	593.4	-3.2	0.3	0.0
104	LGX TANK NPV VALVE OPEN ON	593.7	-3.2	0.6	0.0
105	LGX TANK PRESSURIZATION SHUT-OFF VALVES CLOSE ON	593.9	-3.2	0.8	0.0
106	LGX TANK FLIGHT PRESS SYSTEM OFF	594.1	-3.2	1.0	0.0
107	PROPELLANT DEPLETION CUTOFF DISARM	594.9	-3.2	1.8	0.0
108	S-IVB MIXTURE RATIO CONTROL VALVE CLOSE	594.3	-3.2	2.2	0.0
109	S-IVB MIXTURE RATIO CONTROL VALVE BACKUP CLOSE	595.5	-3.2	2.4	0.0

Table 2-2. Significant Event Times Summary (Continued)

ITEM	EVENT DESCRIPTION	RANGE TIME		TIME FROM BASE	
		ACTUAL SEC	ACT-PRED SEC	ACTUAL SEC	ACT-PRED SEC
110	FLIGHT CONTROL COMPUTER S-IVB BURN MODE OFF 'A'	596.6	-3.2	3.5	0.0
111	FLIGHT CONTROL COMPUTER S-IVB BURN MODE OFF 'B'	596.8	-3.2	3.7	0.0
112	AUX HYDRAULIC PUMP FLIGHT MODE OFF	597.0	-3.2	3.9	0.0
113	S/C CONTROL OF SATURN ENABLE	598.1	-3.2	5.0	0.0
114	RATE MEASUREMENTS SWITCH	599.1	-3.2	6.0	0.0
115	ORBIT INSERTION	602.9	-3.1	9.8	0.0
116	S-IVB ENGINE EDS CUTOFF DISABLE	603.1	-3.2	10.0	0.0
117	LH2 TANK LATCHING RELIEF VALVE OPEN ON	603.5	-3.2	10.4	0.0
118	LH2 TANK LATCHING RELIEF VALVE LATCH ON	605.5	-3.2	12.4	0.0
119	LH2 TANK LATCHING RELIEF VALVE OPEN OFF	606.7	-3.2	13.6	0.0
120	LH2 TANK LATCHING RELIEF VALVE LATCH OFF	607.9	-3.2	14.8	0.0
121	CHILDDOWN SHUTOFF VALVES CLOSE	613.1	-3.2	20.0	0.0
122	PITCH MANEUVER TO LOCAL HORIZ	613.5	-2.6	20.4	0.6
123	P.W. INVERTER AND DC POWER OFF	623.1	-3.2	30.0	0.0
124	LX TANK NPV VALVE OPEN OFF	623.7	-3.2	30.6	0.0
125	LX TANK VENT AND NPV VALVES BOOST CLOSE ON	626.7	-3.2	33.6	0.0
126	LX TANK VENT AND NPV VALVES BOOST CLOSE OFF	628.7	-3.2	35.6	0.0
127	CSM SEPARATION ALTERNATE SEQUENCE T4A	1080.4	124.2	487.3	127.3
128	CCS COMMAND S-150 EXPERIMENT	1271.0	0.0	677.9	3.2
129	PREVALVES OPEN	1273.4	-2.9	680.3	0.3
130	CHILDDOWN SHUTOFF VALVES OPEN	1273.6	-2.9	680.5	0.3
131	LH2 TANK LATCHING RELIEF VALVE OPEN ON	1273.8	-2.9	680.7	0.3

Table 2-2. Significant Event Times Summary (Continued)

ITEM	EVENT DESCRIPTION	RANGE TIME		TIME FROM BASE	
		ACTUAL SEC	ACT-PRED SEC	ACTUAL SEC	ACT-PRED SEC
132	LH2 TANK LATCHING RELIEF VALVE OPEN OFF	1274.8	-2.9	681.7	0.3
133	LH2 TANK VENT AND LATCHING RELIEF VALVES BOOST CLOSE ON	1277.8	-2.9	684.7	0.3
134	LH2 TANK VENT AND LATCHING RELIEF VALVES BOOST CLOSE OFF	1279.5	-3.2	686.4	0.0
135	DCS COMMAND EXECUTE +177 DEG. PITCH MANEUVER	1314.0	19.1	720.9	22.2
136	DCS COMMAND EXECUTE -177 DEG. ROLL, 3 DEG. PITCH MANEUVER	2855.0	30.1	2261.9	33.2
137	DCS COMMAND EXECUTE -138 DEG. ROLL MANEUVER	5800.0	45.1	5206.8	48.1
138	DCS COMMAND EXECUTE + 135 DEG. ROLL MANEUVER	6231.0	126.1	5637.8	129.1
139	DCS COMMAND EXECUTE + 45 DEG. ROLL MANEUVER	8930.0	125.1	8336.8	128.1
140	DCS COMMAND EXECUTE - 45 DEG. ROLL MANEUVER	12980.0	125.1	12386.8	128.1
141	DCS COMMAND EXECUTE + 90 DEG. ROLL MANEUVER	14280.0	125.1	13686.8	128.2
142	IU/S-IVB GEORBIT COMMAND	15886.0	-2708.9	15292.8	-2705.8
143	START OF TIME BASE 5 (T5)	19193.3	0.6**	0.0	0.0
144	ENGINE HE CONTROL VALVE OPEN ON (START L2 DUMP)	19227.3	0.6**	34.0	0.0
145	ENGINE MAINSTAGE CONTROL VALVE OPEN OFF (END L2 DUMP)	19672.2	0.5**	478.9	-0.1
146	ENGINE HE CONTROL VALVE OPEN ON (START F2 DUMP)	19702.3	0.5**	509.0	0.0
147	ENGINE IGNITION PHASE CONTROL VALVE CLOSE (STOP H2 DUMP)	20292.3	0.6**	1099.0	0.0
148	S-IVB/IU IMPACT	21692.0	42.7**	21098.8	45.8

\*\* BASED ON REAL-TIME PREDICTIONS, REFERENCE SECTION 5

Table 2-3. Variable Time and Commanded Switch Selector Events

FUNCTION	STAGE	RANGE TIME (SEC)	TIME FROM BASE (SEC)	REMARKS
Water Coolant Valve Closed	IU	480.1	T3 +339.4	LVDC Function
Telemetry Calibrator In-Flight Calibrate ON	IU	676.8	T4 +83.6	Bermuda Revolution 1
TM Calibrate ON	S-IVB	679.8	T4 +86.6	Bermuda Revolution 1
TM Calibrate OFF	S-IVB	680.8	T4 +87.6	Bermuda Revolution 1
Telemetry Calibrator In-Flight Calibrate OFF	IU	681.8	T4 +88.6	Bermuda Revolution 1
S-150 TM Time Correlation ON	IU	3177.8	T4 +2584.6	LVDC Function
S-150 TM Time Correlation OFF	IU	3178.8	T4 +2587.7	LVDC Function
Telemetry Calibrator In-Flight Calibrate ON	IU	6724.8	T4 +6131.7	Madrid Revolution 2
TM Calibrate ON	S-IVB	6727.8	T4 +6134.7	Madrid Revolution 2
TM Calibrate OFF	S-IVB	6728.8	T4 +6135.7	Madrid Revolution 2
Telemetry Calibrator In-Flight Calibrate OFF	IU	6729.8	T4 +6136.7	Madrid Revolution 2
S-150 TM Time Correlation ON	IU	6777.8	T4 +6184.7	LVDC Function
S-150 TM Time Correlation OFF	IU	6778.8	T4 +6185.7	LVDC Function
S-150 Calibrate Command ON	IU	9150.9	T4 +8557.8	LVDC Function
S-150 Calibrate Command OFF	IU	9155.9	T4 +8562.7	LVDC Function
S-150 TM Time Correlation ON	IU	12,177.8	T4 +11,584.7	LVDC Function
S-150 TM Time Correlation OFF	IU	12,178.8	T4 +11,585.6	LVDC Function
Telemetry Calibrator In-Flight Calibrate ON	IU	12,260.8	T4 +11,667.7	Canary Revolution 3
TM Calibrate ON	S-IVB	12,263.8	T4 +11,670.7	Canary Revolution 3

Table 2-3. Variable Time and Commanded Switch Selector Events (Continued)

FUNCTION	STAGE	RANGE TIME (SEC)	TIME FROM BASE (SEC)	REMARKS
TM Calibrate OFF	S-IVB	12,264.8	T4 +11,671.7	Canary Revolution 3
Telemetry Calibrator In-Flight Calibrate OFF	IU	12,265.8	T4 +11,672.7	Canary Revolution 3
S-150 Calibrate Command ON	IU	14,550.9	T4 +13,957.7	LVDC Function
S-150 Calibrate Command OFF	IU	14,555.9	T4 +13,962.7	LVDC Function
Telemetry Calibrator In-Flight Calibrate ON	IU	15,948.9	T4 +15,355.8	Hawaii Revolution 3
TM Calibrate OFF	S-IVB	15,952.9	T4 +15,359.8	Hawaii Revolution 3
Telemetry Calibrator In-Flight Calibrate OFF	IU	15,953.9	T4 +15,360.8	Hawaii Revolution 3
Telemetry Calibrator In-Flight Calibrate ON	IU	17,774.8	T4 +17,181.7	Canary Revolution 4
TM Calibrate ON	S-IVB	17,775.8	T4 +17,182.7	Canary Revolution 4
TM Calibrate OFF	S-IVB	17,776.8	T4 +17,183.7	Canary Revolution 4
Telemetry Calibrator In-Flight Calibrate OFF	IU	17,778.8	T4 +17,185.7	Canary Revolution 4

SECTION 3  
LAUNCH OPERATIONS

3.1 SUMMARY

The performance of ground systems supporting the SA-207/Skylab-3 countdown and launch was satisfactory although some concern was expressed during pre-launch countdown about S-IB LOX venting. This is discussed in paragraph 3.4.2.1.

The space vehicle was launched at 7:10:50 Eastern Daylight Time (EDT) on July 28, 1973, from Pad 39B of the Kennedy Space Center (KSC), Saturn Complex. Damage to the pad, Launch Umbilical Tower (LUT) and support equipment was considered minimal.

3.2 PRELAUNCH MILESTONES

A chronological summary of prelaunch milestones is contained in Table 3-1. All stages, S-IB, S-IVB and Instrument Unit (IU) performed satisfactorily. The S-IB LOX venting anomaly is discussed in paragraph 3.4.2.1.

3.3 TERMINAL COUNTDOWN

The SA-207/Skylab-3 terminal countdown was picked up at T-59 hours (countdown clock time) on July 25, 1973. Scheduled holds were initiated at T-3 hours 30 minutes for a duration of 60 minutes and at T-15 minutes for a duration of 2 minutes. The space vehicle was launched on schedule at 7:10:50 EDT on July 28, 1973.

3.4 PROPELLANT LOADING

3.4.1 RP-1 Loading

The RP-1 system successfully supported countdown and launch. Fuel was placed on board the S-IB stage on July 11, 1973. Tail Service Mast fill and replenish was accomplished at T-8 hours and level adjust/line inert at about T-1 hour. Both operations were completed satisfactorily as planned. Launch countdown support consumed 41,604 gallons of RP-1.

The fuel temperature probe configuration in S-IB Stage Tank F-4 was changed prior to launch due to an intermittent resistance thermometer element. The configuration change electrically removed the intermittent operating element, leaving the two lower probes connected in parallel to provide one temperature output.

Table 3-1. SA-207/Skylab-3 Prelaunch Milestones

DATE	ACTIVITY OR EVENT
August 26, 1971	S-IVB-207 Stage Arrival
Dec. 1, 1972	Command Service Module (CSM) 117 Arrival
March 30, 1973	S-IB-7 Stage Arrival
April 4, 1973	S-IB Erection on Mobile Launcher (ML)-1
May 8, 1973	Instrument Unit (IU) S-IU-208 Arrival
May 28, 1973	S-IVB Erection
May 29, 1973	IU Erection
June 2, 1973	Launch Vehicle (LV) Electrical Systems Test Complete
June 11, 1973	LV Transfer to Pad B
June 12, 1973	Space Vehicle (SV) Electrical Mate
June 19, 1973	LV Propellant Dispersion/Malfunction Overall Test (OAT)
June 20, 1973	SV OAT 1 (Plugs In)
June 29, 1973	SV Flight Readiness Test (FRT) Complete
July 11, 1973	RP-1 Loaded
July 20, 1973	Countdown Demonstration Test (CDDT) Completed (Wet)
July 28, 1973	SL-3 Launch

The fuel temperature was monitored during the launch countdown and at T-1 hour, a final fuel temperature of 66.0°F was projected to ignition. The final fuel density was obtained using the projected temperature.

At approximately 8 1/2 hours prior to launch, the level in the fuel tanks was raised from 600 inches to the level of the overfill sensor (637.2 inches) to ensure that the final fuel level adjust would be a drain. When the overfill sensor indication was received, the Propellant Tanking Computer System (PTCS) mass readout indicated that the level in the fuel tanks was approximately 83 gallons (+1.24 inches) above the overfill

sensor level. This corresponds to an error in the load of approximately 555 pounds. A bias was input to the PTCS, successfully correcting for this error.

### 3.4.2 LOX Loading

The LOX loading system successfully supported countdown and launch. The fill sequence began with S-IB chilldown July 27, 1973, and was completed 1 hour 50 minutes later with all stage replenish. Replenish was automatic through the Terminal Countdown Sequencer (TCS) without incident. LOX consumption during launch countdown was 110,000 gallons.

#### 3.4.2.1 S-IB LOX Venting During Countdown

During the LOX replenishing sequence, LOX was reported emanating randomly and independently from the four outboard tank vent valves from approximately T-5.5 hours to vent closure at T-2 minutes 43 seconds. During video and motion picture coverage of 30 minutes of the countdown beginning at T-1 hour, it appeared that liquid oxygen was erupting from the vent openings of tanks 3 and 4. Alternate camera positions showed what appeared to be LOX emanating from tank 1 and 2 vents, but in that case it could not be determined which specific tank was discharging. Approximately 40 discharges were counted during the period covered by the film, equally distributed between tanks 3 and 4. LOX was not observed venting from the center LOX tank. Figure 3-1 is a series of photographs showing the venting from the outboard tanks.

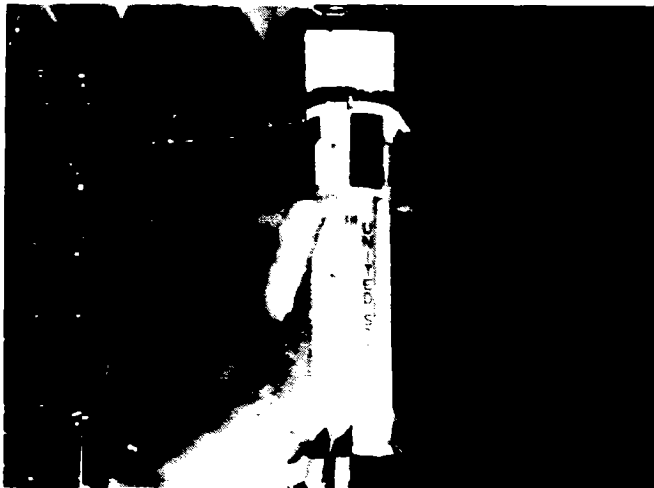
Reconstructed flight performance, as it pertains to the problem, shows nothing unusual. Actual LOX load was within 76 pounds of predicted at ignition command, and LOX pump inlet temperature averaged throughout flight 0.12°F warmer than predicted. Time required to prepressurize the LOX tank was 73 seconds, the same as during the CDDT, which indicated normal ullage volume. The surface wind during the countdown was light. Temperature and relative humidity at the NASA 150 M ground wind tower were 75.0°F and 93 percent, respectively.

Figure 3-2 depicts the relative heights of liquid in the center tank and a windward outer tank. Restricted flow through the 4-in center tank vent valve causes a differential pressure between the tank ullages that is dependent on heat transfer rate and causes an adjustment in liquid levels. Note that with a nominal wind speed of 9.2 knots, the windward outer tank LOX level is approximately 2.7 inches above the center tank LOX level and 23.4 inches below the bottom of the vent duct. A wind increase to 34 knots (maximum expected) would cause the outer tank LOX level to increase approximately 4 inches while the center tank LOX level would be unchanged. Therefore, it is clear that even with such an extreme condition the steady state liquid level is substantially below the vent.

Instrumentation to detect or investigate the phenomenon is inadequate because its intended use was for flight evaluation. However, the eight



EVENT +0 SEC



EVENT +2 SEC



EVENT +5 SEC

Figure 3-1. SA-207 Prelaunch Venting

NOTE: CENTER TANK 4-IN VENT NOT SHOWN.  
TANKS INTERCONNECTED AT BASE.

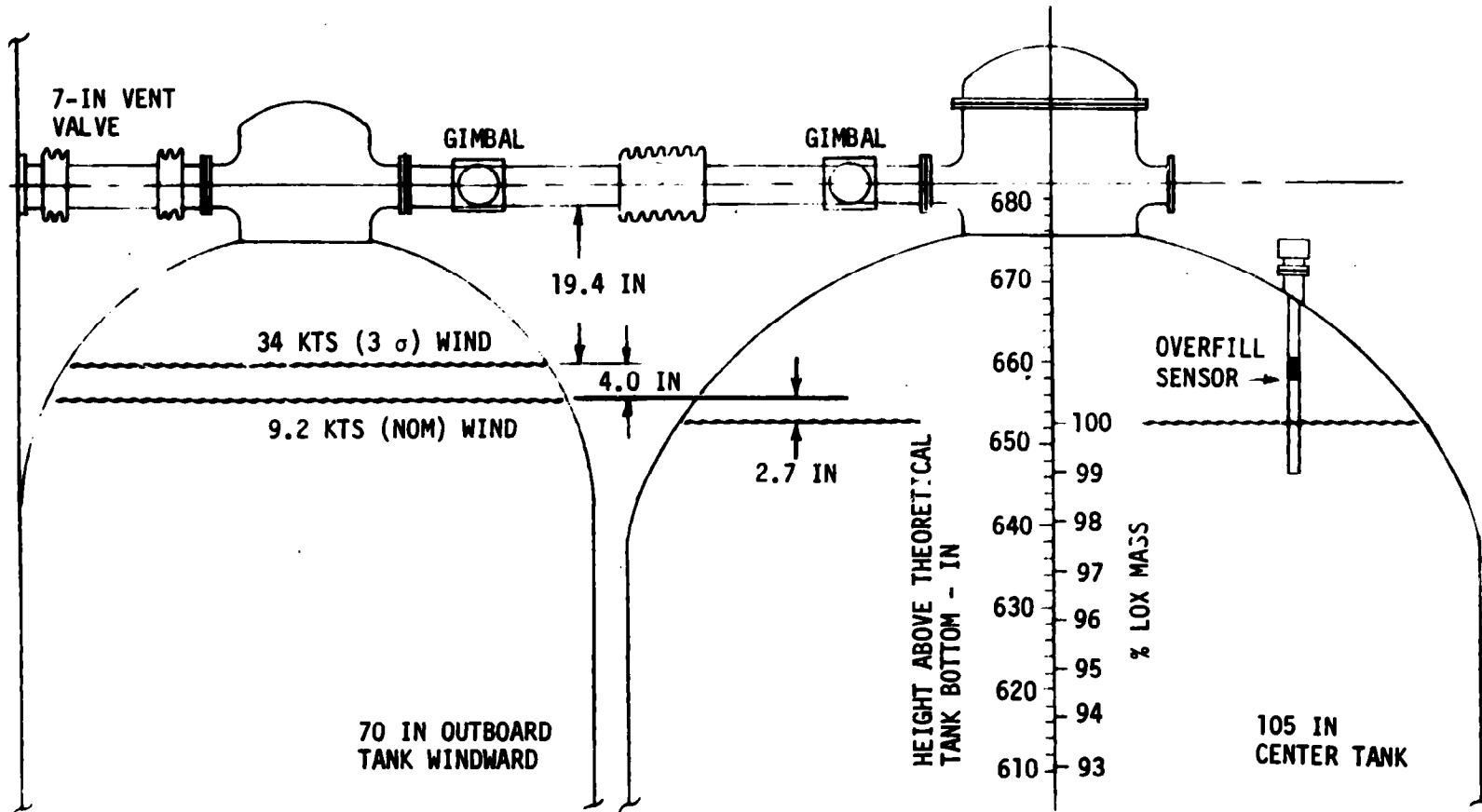


Figure 3-2. Center LOX Tank - Outboard LOX Tank Relationship

LOX pump inlet temperatures (one per engine) were reviewed together with the Engine No. 1 LOX pump inlet pressure for the 8-hour period prior to launch. This period covered start of LOX loading until liftoff. Additionally, center LOX tank ullage pressure was scrutinized for any unusual fluctuations which could be related to the discharges seen on the film. None were noted during the 8-hour period. The overflow sensor, located 21 inches below the vent duct, did not indicate liquid presence during LOX loading. None of these measurements indicated any unusual conditions which would explain the apparent LOX venting.

Review of films taken during SA-206 countdown revealed similar occurrences; however, similar eruptions were not observed during the Countdown Demonstration Test (CDDT) for either SA-206 or SA-207. This indicates the problem is not stage oriented because no stage hardware changes were made between these two events. While the cause is not known, the apparent LOX venting phenomenon had no effect on flight performance or vehicle or ground hardware. All exposed stage and ground hardware involved is capable of satisfactory operation after LOX contact of the type experienced and no corrective action is necessary for stage performance. The only concern is for personnel safety during astronaut boarding.

For the SA-208 countdown, a procedural change will be incorporated in real time if LOX is venting prior to astronaut boarding. The LOX level will be reduced by boiloff and the additional mass required for flight replenished later in the countdown.

### 3.4.3 LH<sub>2</sub> Loading

The LH<sub>2</sub> system successfully supported countdown and launch. The fill sequence began at 00:37:00 EDT, July 28, 1973, and was completed when normal S-IVB replenish was established at 01:26:00 EDT. Replenish was nominal and was terminated at the start of terminal countdown sequence. Launch countdown support consumed about 125,000 gallons of LH<sub>2</sub>.

## 3.5 GROUND SUPPORT EQUIPMENT

### 3.5.1 Ground/Vehicle Interface

In general, performance of the ground service systems supporting all stages of the launch vehicle was satisfactory. Overall damage to the pad, LUT, and support equipment from blast and flame impingement was considered minimal. Detailed discussion of the Ground Support Equipment is contained in KSC Skylab/Saturn IB (SA-207) "Ground Support Evaluation Report."

The Propellant Tanking Computer Systems (PTCS) adequately supported all countdown operations and there was no launch damage.

The Environmental Control Systems (ECS) performed satisfactorily throughout the countdown and launch. Changeover from air to GN<sub>2</sub> occurred at 21:55:00 EDT on July 27, 1973.

The Service Arm Control Switches (SACS) satisfactorily supported SL-3 launch and countdown. The SAC No. 3 primary switch closed at 252 milliseconds and SAC No. 7 primary switch closed at 261 milliseconds after commit. There were no problems and only a minimal amount of heat and blast damage to the SACS.

The Hydraulic Charging Unit and Service Arms (S/A's 1A, 6, 7 and 8) satisfactorily supported the SL-3 countdown and launch. Performance was nominal during terminal count and liftoff.

The damping systems supported the countdown and launch. There were no system failures.

The DEE-3 and DEE-6 systems satisfactorily supported all countdown operation. There was no system damage.

#### 3.5.2 MSFC Furnished Ground Support Equipment

All Ground Power and Battery equipment supported the prelaunch operations satisfactorily. All systems performed within acceptable limits. The Hazardous Gas Detection System successfully supported SL-3 countdown.

## SECTION 4

### TRAJECTORY

#### 4.1 SUMMARY

The Skylab-3 vehicle was launched at 7:10:50 a.m. Eastern Daylight Time, July 28, 1973, from Pad 39B at Kennedy Space Center. The vehicle was launched on an azimuth of 90 degrees east of north. A roll maneuver was initiated at approximately 10 seconds that placed the vehicle on a flight azimuth of 45.003 degrees east of north. The down range pitch program was also initiated at this time.

The reconstructed flight trajectory (actual) was very close to the Post Launch Operational Trajectory (nominal). The S-IB stage powered the vehicle until Outboard Engine Cutoff (OECO) at 140.73 seconds which was 1.13 seconds later than nominal. The total space-fixed velocity at this time was 0.19 m/s less than nominal. After separation, the S-IB stage continued on a ballistic trajectory until earth impact. The S-IVB burn terminated with guidance cutoff signal and was followed by parking orbit insertion, both 3.14 seconds earlier than nominal. An excess velocity of 0.75 m/s at insertion resulted in an apogee 2.16 km higher than nominal.

The parking orbit portion of the trajectory from insertion to CSM/S-IVB separation was close to nominal. The astronaut initiated separation of the CSM from the S-IVB stage occurred at 1080.4 seconds, 124.2 seconds later than nominal.

#### 4.2 TRAJECTORY EVALUATION

##### 4.2.1 Ascent Phase

The ascent phase is defined as the interval from guidance reference release (-16.953 seconds) through parking orbit insertion (602.93 seconds). The ascent trajectory was established by utilizing telemetered guidance velocity data as generating parameters to fit the tracking data from five C-Band stations, listed in Table 4-1. Approximately 3 percent of the C-Band tracking data was rejected due to inconsistencies. The initial launch phase (from first motion to 20 seconds) was established by a least squares curve fit of the initial portion of the ascent trajectory. Comparisons between the resultant best estimate trajectory and the available tracking data show consistency and good agreement.

Telemetered guidance data were used as a model for obtaining proper velocity and acceleration profiles during the transient periods of

Table 4-1. Summary of Available Tracking Data

DATA SOURCE, TYPE	PHASE	RANGE TIME INTERVAL (SEC)
Bermuda, C-Band	Ascent	380 - 610
Bermuda, C-Band	Orbital	250 - 712
Bermuda, S-Band	Orbital	230 - 730
Cape Kennedy, C-Band	Ascent	5 - 424
Hawaii, C-Band	Orbital	15,886 - 16,186
Merritt Island, C-Band	Ascent	5 - 507
Patrick, C-Band	Ascent	25 - 504
Tananarive, C-Band	Orbital	7828 - 8176
Tananarive, C-Band	Orbital	13,390 - 13,660
Wallops Island, C-Band	Ascent/Orbital	255 - 648

Mach 1, maximum dynamic pressure, S-IB thrust cutoff, and S-IVB thrust cutoff.

Actual and nominal altitude, cross range, and surface range for the boost phase are presented in Figure 4-1. Figure 4-2 presents similar comparisons of space fixed velocity and flight path angle. Comparisons of actual and nominal total inertial accelerations are displayed in Figure 4-3. Inspection shows the actual was very close to the nominal values.

Table 4-2 presents the trajectory conditions at engine cutoffs. Trajectory parameters at significant events are presented in Table 4-3. Table 4-4 presents significant parameters at the S-IB/S-IVB and S-IVB/CSM separation events.

The S-IB stage OECO command was issued at 140.73 seconds as a result of LOX depletion. The S-IVB cutoff signal was issued by the Launch Vehicle Digital Computer (LVDC) when end conditions were satisfied at 592.93 seconds.

Mach number and dynamic pressure history comparisons are shown in Figure 4-4. These parameters were calculated using the reconstructed trajectory data and measured meteorological data to an altitude of 62 km. Above

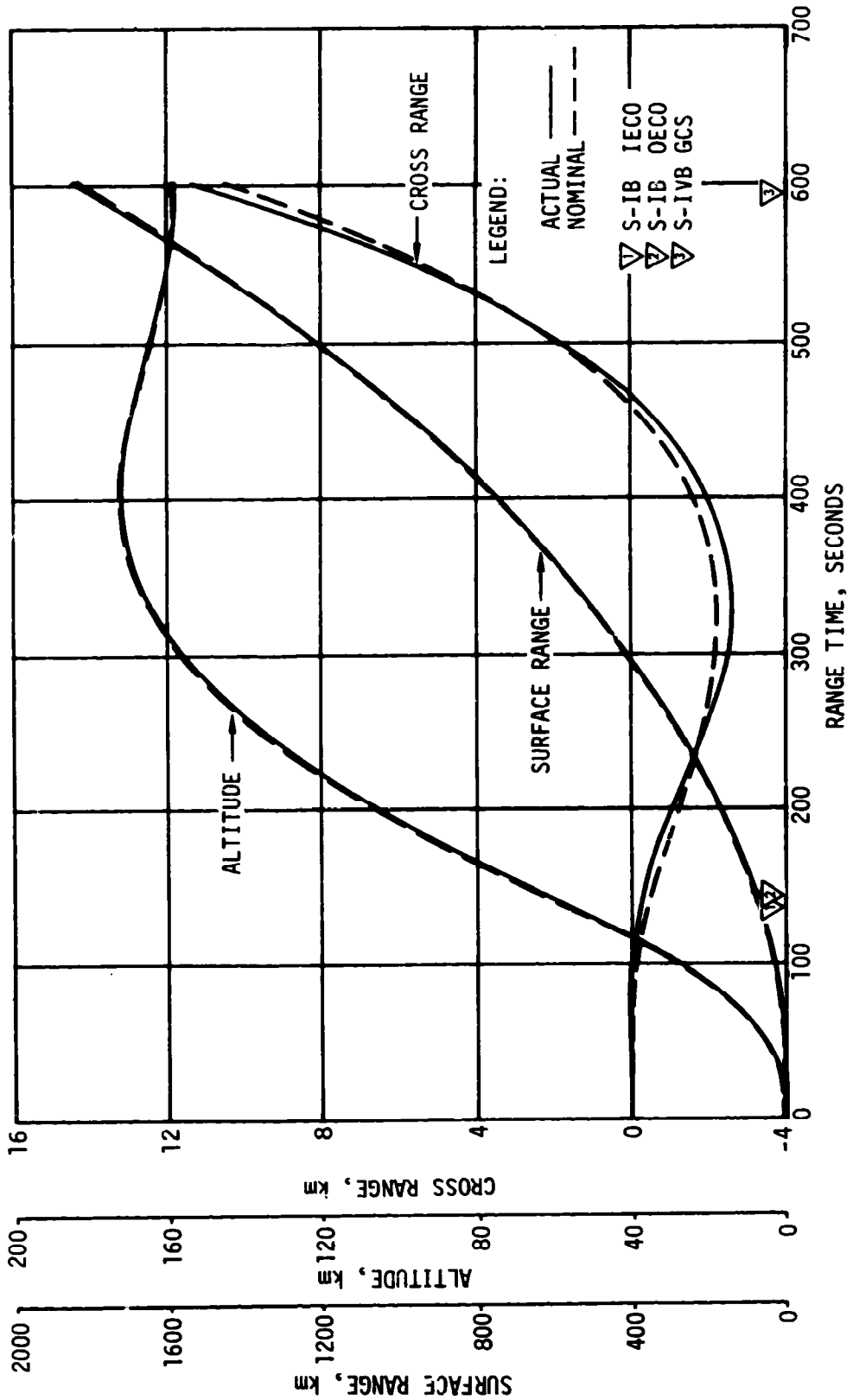


Figure 4-1. Ascent Trajectory Position Comparison

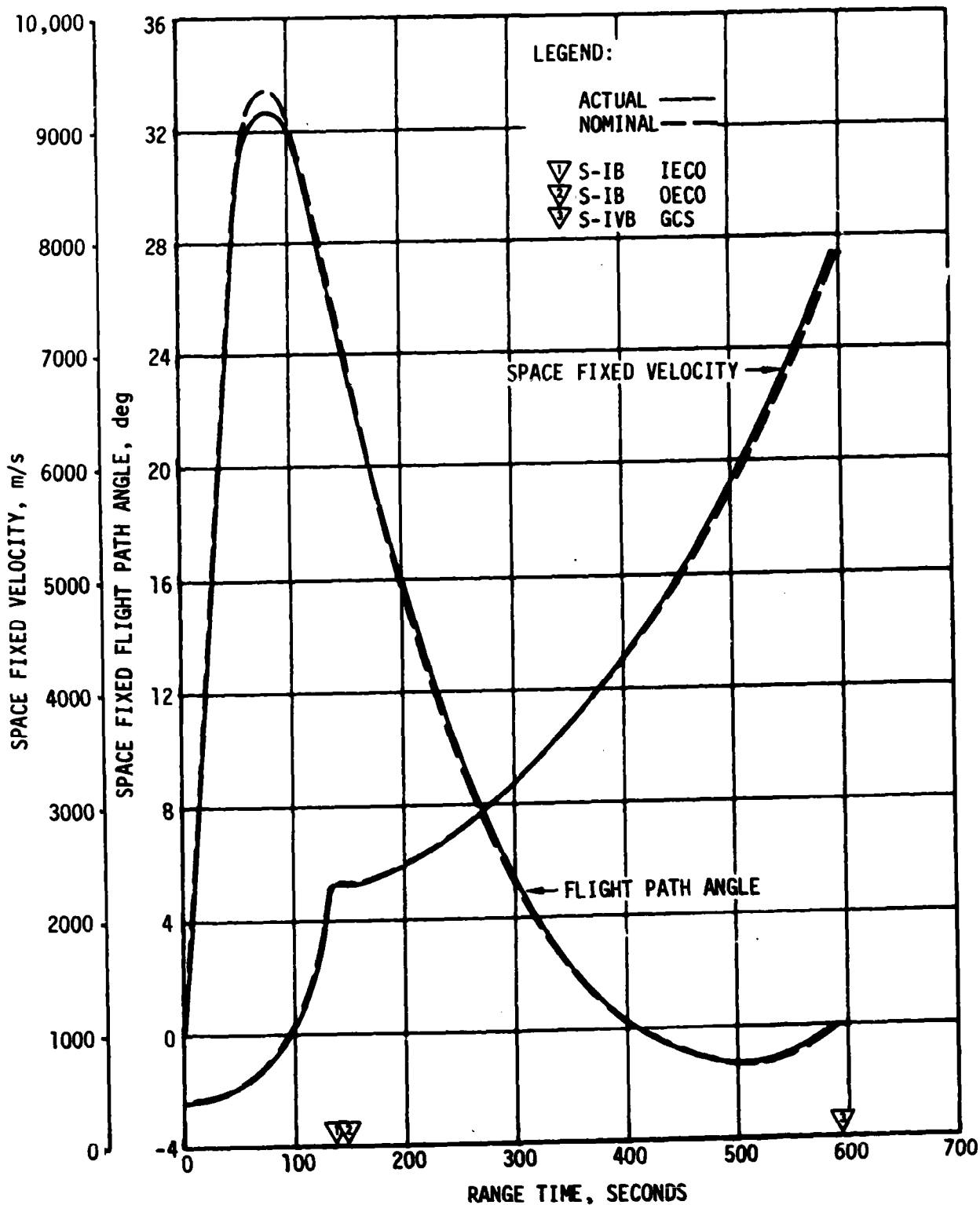


Figure 4-2. Ascent Trajectory Space-Fixed Velocity and Flight Path Angle Comparison

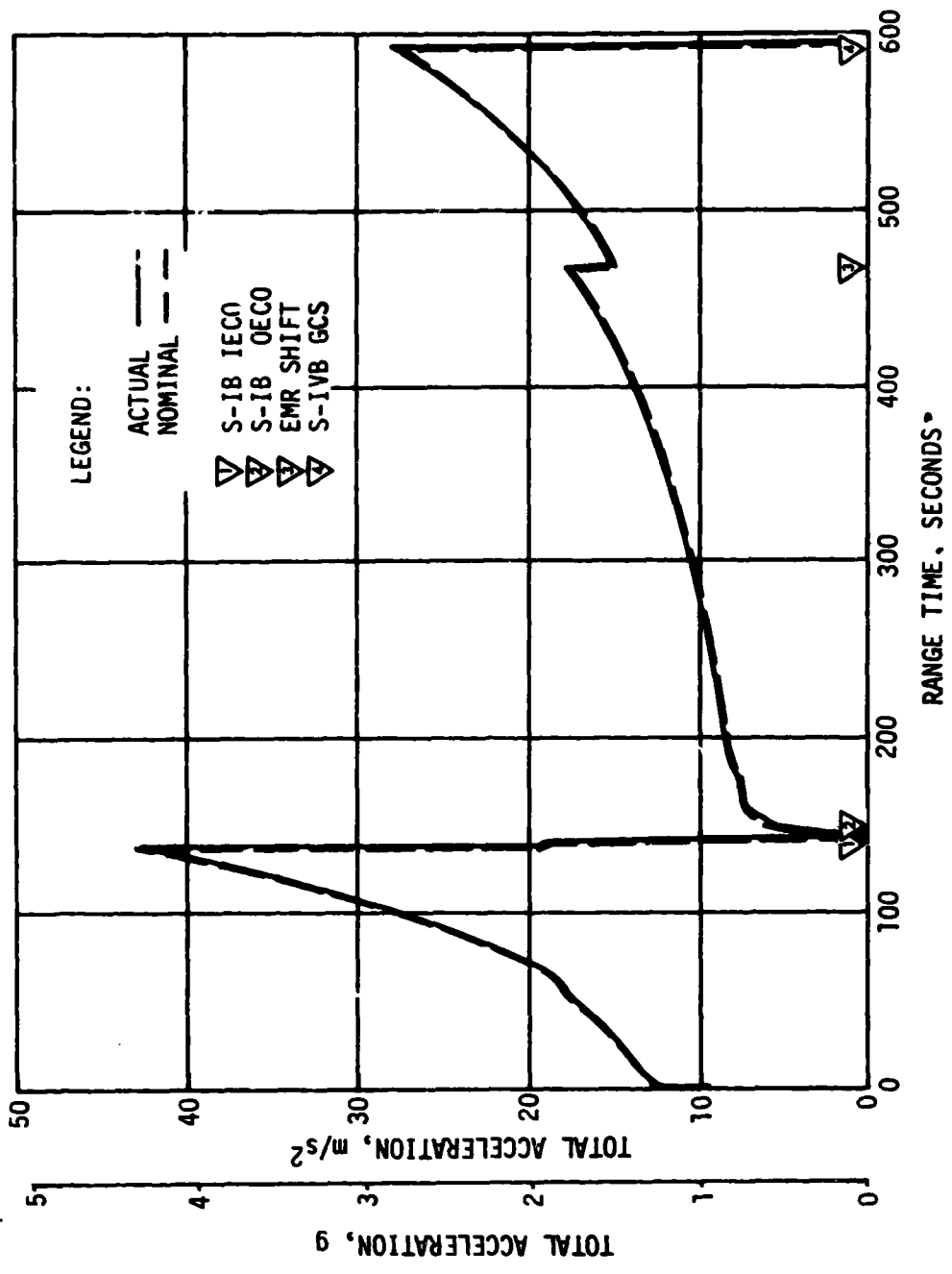


Figure 4-3. Ascent Trajectory Acceleration Comparison

Table 4-2. Comparison of Cutoff Events

PARAMETER	S-IB IECD			S-IB OECD			S-IVB GCS		
	ACTUAL	NOMINAL	ACT-NOM	ACTUAL	NOMINAL	ACT-NOM	ACTUAL	NOMINAL	ACT-NOM
Range Time (sec)	137.36	136.60	0.76	140.73	139.60	1.13	592.93	596.07	-3.14
Altitude (km)	55.41	55.90	-0.49	58.71	58.87	-0.16	158.38	158.52	-0.14
Space-Fixed Velocity (m/s)	2238.27	2244.39	-6.12	2301.84	2302.03	-0.19	7829.73	7829.54	0.19
Flight Path Angle (deg)	25.613	25.927	-0.314	25.053	25.403	-0.350	-0.013	-0.008	-0.005
Heading Angle (deg)	53.150	53.089	0.061	52.911	52.871	0.040	55.803	55.900	-0.097
Surface Range (km)	57.30	57.05	0.25	63.13	62.23	0.90	1797.54	1813.62	-16.08
Cross Range (km)	-0.27	-0.49	0.22	-0.30	-0.52	0.22	10.21	10.11	0.10
Cross Range Velocity (m/s)	-8.42	-10.50	2.08	-8.47	-10.58	2.11	118.18	119.37	-1.19

Table 4-3. Comparison of Significant Trajectory Events

EVENT	PARAMETER	ACTUAL	NOMINAL	ACT-NOM
First Motion	Range Time, sec	0.28	0.28	0.00
	Total Inertial Acceleration, m/s <sup>2</sup>	12.272	12.353	-0.081
Mach 1	Range Time, sec	59.00	57.94	1.06
	Altitude, km	7.54	7.37	0.17
Maximum Dynamic Pressure	Range Time, sec	75.00	73.00	2.00
	Dynamic Pressure, n/cm <sup>2</sup>	3.523	3.454	0.069
	Altitude, km	13.17	12.60	0.57
*Maximum Total Inertial Acceleration:	Range Time, sec	137.346	136.595	0.751
	Acceleration, m/s <sup>2</sup>	42.733	43.147	-0.414
	S-IVB Range Time, sec	592.930	596.070	-3.140
	Acceleration, m/s <sup>2</sup>	27.866	27.543	0.323
Maximum Earth-Fixed Velocity:	Range Time, sec	141.00	140.28	0.72
	Velocity, m/s	2028.24	2027.85	0.39
	S-IVB Range Time, sec	596.00	598.28	-2.28
	Velocity, m/s	7533.97	7533.15	0.82
*Nearest Time Points Available				

Table 4-4. Comparison of Separation Events

PARAMETER	S-IB/S-IVB			S-IVB/CSM		
	ACTUAL	NOMINAL	ACT-NOM	ACTUAL	NOMINAL	ACT-NOM
Range Time (sec)	142.02	140.90	1.12	1080.44	956.27	124.17
Altitude (km)	59.97	60.16	-0.19	169.36	165.80	3.56
Space-Fixed Velocity (m/s)	2302.95	2302.07	0.88	7826.45	7829.74	-3.29
Flight Path Angle (deg)	24.806	25.152	-0.346	0.198	0.146	0.052
Heading Angle (deg)	52.900	52.864	0.036	88.581	78.540	10.041
Geodetic Latitude (deg, North)	29.046	29.042	0.004	50.183	49.224	0.959
Longitude (deg, West)	80.148	80.157	-0.009	22.624	35.266	-12.642
Surface Range (km)	65.42	64.51	0.91	--	--	--
Cross Range (km)	-0.31	-0.53	0.22	--	--	--
Cross Range Velocity (m/s)	-8.44	-10.55	2.11	--	--	--

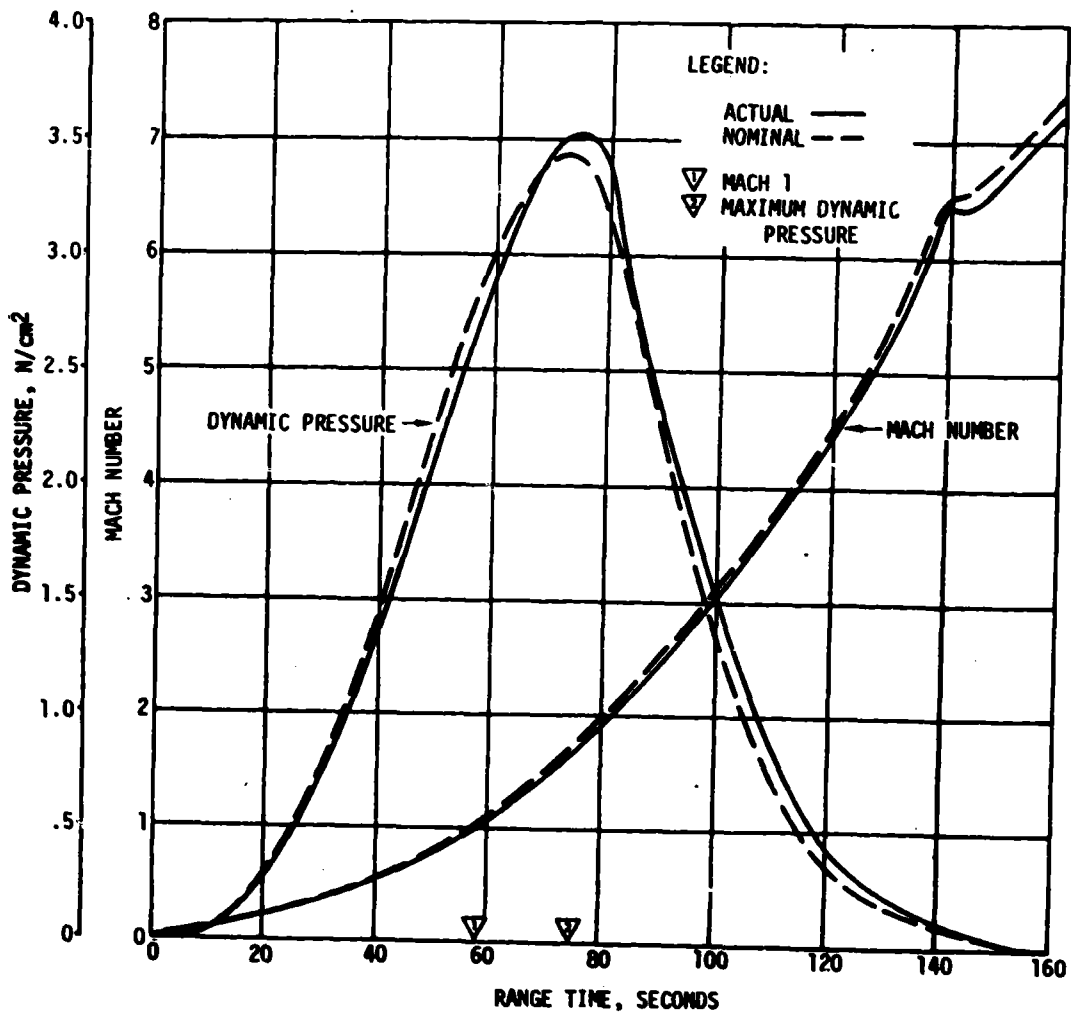


Figure 4-4. Ascent Trajectory Dynamic Pressure and Mach Number Comparison

this altitude the U. S. Standard Reference Atmosphere was used.

A theoretical free flight trajectory was computed for the spent S-IB stage, using initial conditions from the actual trajectory at S-IB/S-IVB separation signal. Three trajectories were integrated from that point to impact using nominal retro-motor performance and outboard engine decay data. The three trajectories incorporate three different drag conditions for 1) stabilized at zero angle of attack (nose forward), 2) tumbling stage, and 3) stabilized at 90 degree angle of attack (broadside). Tables 4-5 and 4-6 summarize the results of these simulations and present the impact envelope. Tracking data were not available, but previous flight data indicate the tumbling drag trajectory to be a close approximation to actual flight. The calculated impact for the tumbling drag trajectory was 31.737 degrees north latitude, 76.907 degrees west longitude, at 539.93 seconds range time.

Table 4-5. Comparison of S-IB Spent Stage Impact Point

PARAMETER	ACTUAL	NOMINAL	ACT-NOM
Range Time (Sec)	539.93	541.11	-1.18
Surface Range (km)	496.67	498.05	-1.38
Cross Range (km)	1.12	-0.10	1.22
Geodetic Latitude (deg, North)	31.737	31.754	-0.017
Longitude (deg, West)	76.907	76.905	0.002
NOTE: Data reflects simulation of tumbling stage.			

Table 4-6. S-IB Spent Stage Impact Envelope

PARAMETER	DRAG SIMULATION		
	NOSE FORWARD	TUMBLING	BROADSIDE
Range Time (sec)	478.08	539.93	581.36
Surface Range (km)	508.69	496.67	488.37
Cross Range (km)	1.28	1.12	1.03
Geodetic Latitude (deg, North)	31.81	31.74	31.69
Longitude (deg, West)	76.81	76.91	76.97

#### 4.2.2 Parking Orbit Phase

The parking orbit originates at orbit insertion and terminates at S-IVB/CSM separation.

Orbital tracking was conducted by the National Aeronautics and Space Administration (NASA) Space Tracking and Data Network. One C-Band (Bermuda) and one S-Band station (Bermuda) were available for tracking coverage during the first revolution. Tananarive provided second and third revolution coverage while Hawaii provided additional third revolution coverage. Some high speed tracking data beyond insertion were available from Wallops Island. These data were edited to provide additional orbital tracking information. The trajectory parameters at orbital insertion were established by adjusting the preliminary estimate to fit the orbital tracking data. A comparison of the actual and nominal parking orbit insertion parameters are delineated in Table 4-7. Figure 4-5 presents the SL-3 ground track from liftoff through CSM separation.

Table 4-7. Comparison of Orbit Insertion Conditions

PARAMETER	ACTUAL	NOMINAL	ACT-NOM
Range Time (sec)	602.93	606.07	-3.14
Altitude (km)	158.52	158.67	-0.15
Space-Fixed Velocity (m/s)	7836.81	7836.06	0.75
Flight Path Angle (deg)	0.001	0.003	-0.002
Heading Angle (deg)	56.268	56.366	-0.098
Cross Range (km)	11.42	11.34	0.08
Cross Range Velocity (m/s)	125.10	126.32	-1.22
Inclination (deg)	50.028	50.031	-0.003
Descending Node (deg)	154.492	154.495	-0.003
Eccentricity	0.0058	0.0056	0.0002
Apogee Altitude (km)	226.29	224.13	2.16
Perigee Altitude (km)	149.87	149.97	-0.10
Period (min)	88.25	88.23	0.02
Geodetic Latitude (deg, North)	39.609	39.698	-0.089
Longitude (deg, West)	65.155	65.601	-0.446

4-11/4-12

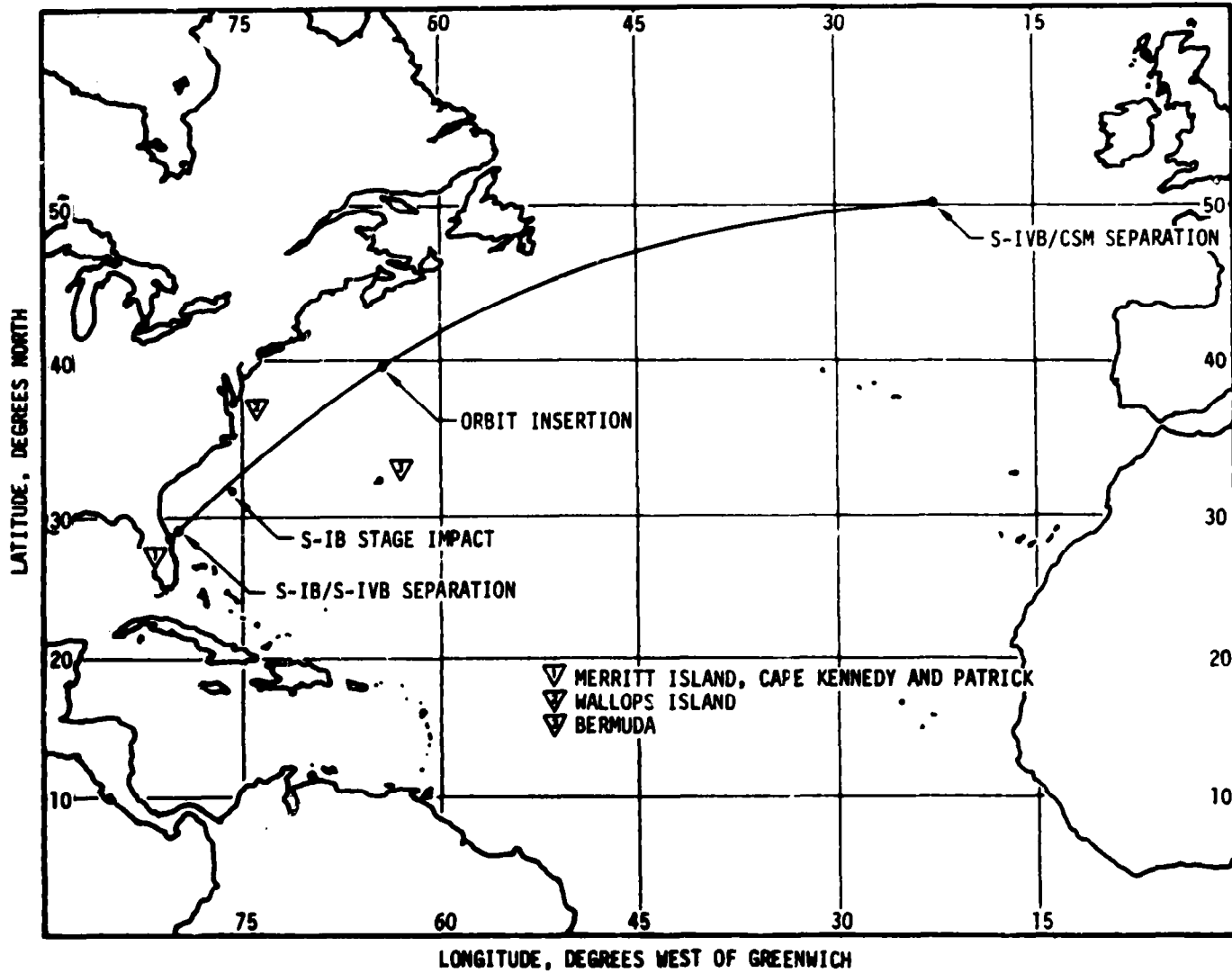


Figure 4-5. Launch Vehicle Ground Track

## SECTION 5

### S-IVB/IU DEORBIT TRAJECTORY

#### 5.1 SUMMARY

All aspects of the S-IVB/IU deorbit were accomplished successfully. The propellant dump was modified during real time to establish a reentry trajectory that would enable observation by Kwajalein. This modified plan was accomplished. The velocity change obtained for deorbit was very close to the real-time predicted value. The breakup altitude was 81.7 km, and impact in the primary disposal area.

#### 5.2 DEORBIT MANEUVERS

Timebase 5 (TB5) was initiated as scheduled by a ground command and started the S-IVB/IU deorbit events at 19,193.3 seconds (310 minutes past Timebase 4). A real-time decision was made to extend the LH<sub>2</sub> tank dump duration in order to improve telemetry coverage of the deorbit, while providing a reentry trajectory allowing Kwajalein to observe breakup. The S-IVB/IU ground track during deorbit with the areas of telemetry coverage are indicated in Figure 5-1.

The velocities achieved from the LOX and LH<sub>2</sub> tank dumps are presented in Figure 5-2 and summarized in Table 5-1. The capabilities predicted in real-time are shown for comparison. As indicated, the actual velocity was only 0.8% greater than predicted. Refer to Section 7.9 for detailed discussion of deorbit propulsion performance.

#### 5.3 DEORBIT TRAJECTORY EVALUATION

The S-IVB/IU orbit trajectory from Command Service Module (CSM) separation to TB5 was reconstructed using the Tananarive and Hawaii C-band radars during revolutions 2 and 3. The available tracking data from these sites are included in the tracking data summary presented in Section 4. A TB5 state vector was obtained from the orbit trajectory reconstruction (actual), and then utilized in simulations of the propellant dump and subsequent reentry trajectory to impact assuming no breakup. Orbit trajectory conditions at TB5 are presented in Table 5-2. A comparison of the actual trajectory and the real-time predicted shows good agreement at this point. This is further illustrated in Figure 5-3 showing the real-time predicted altitude versus range time compared to the postflight reconstructed altitude profile which deviates from the real-time only at the very end.

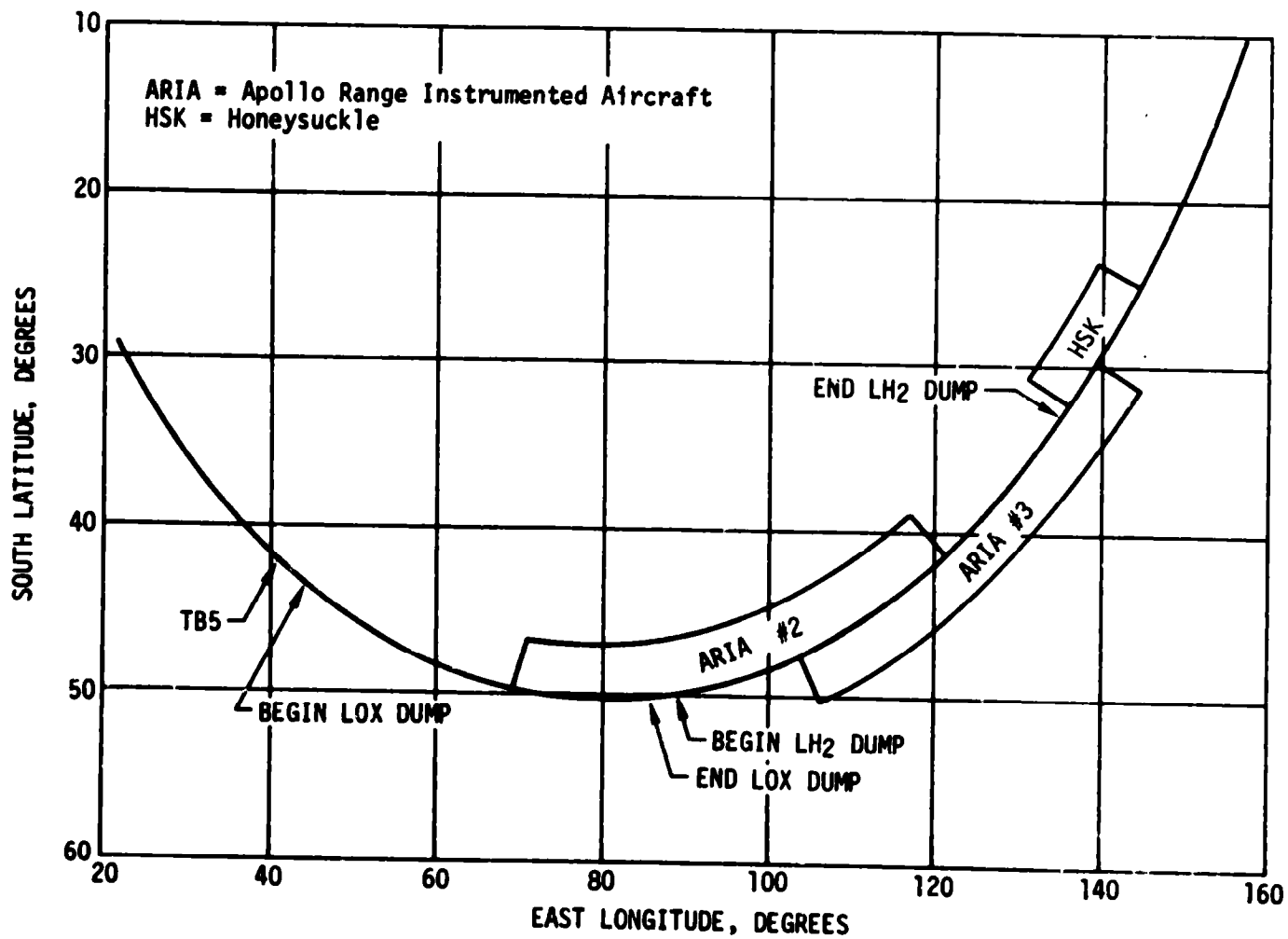


Figure 5-1. S-IVB/IU Ground Track During Propellant Dump

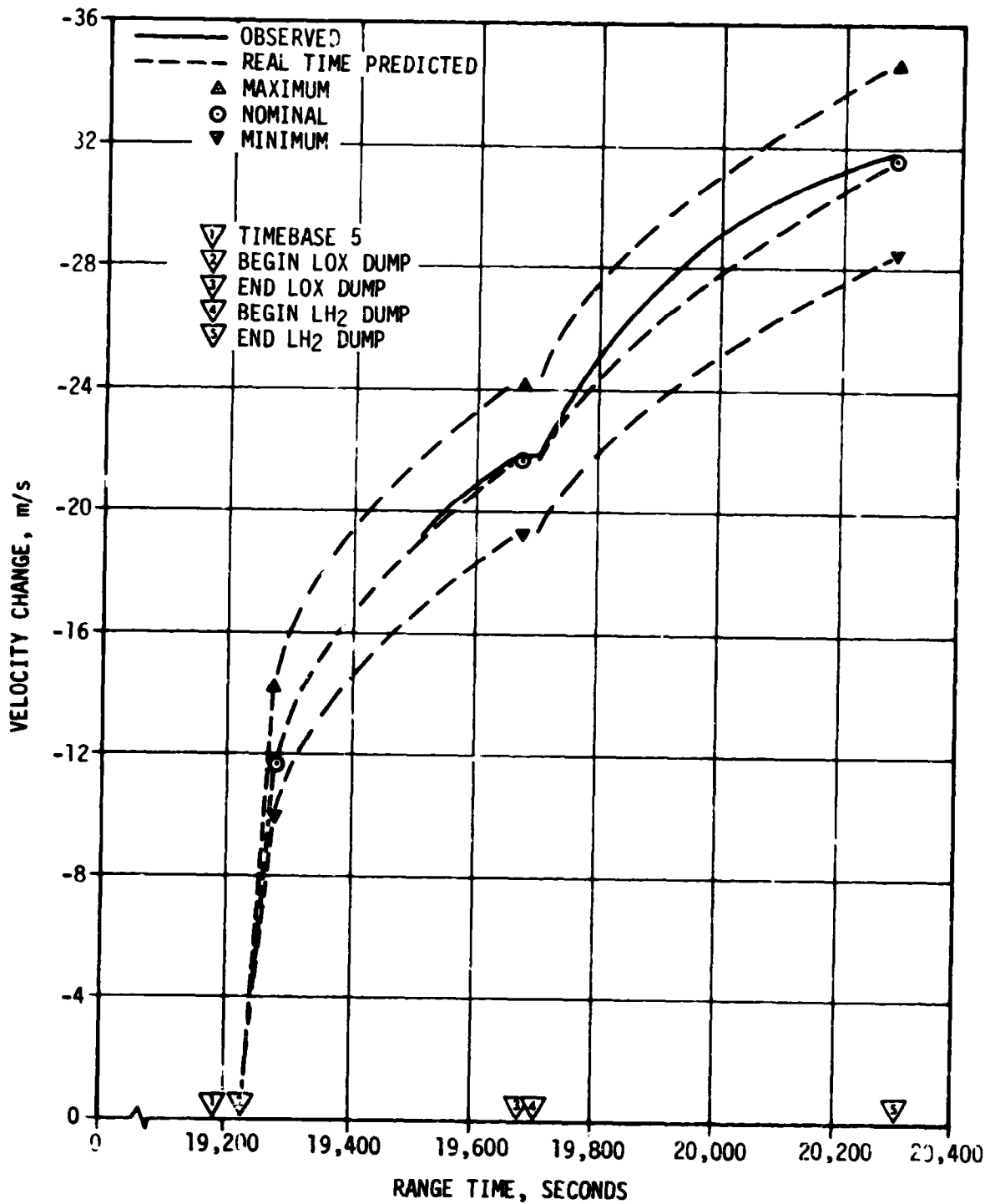


Figure 5-2. S-IVB/IU Deorbit Velocity Change

Table 5-1. S-IVB/IU Propellant Dump Velocity Changes

	ACTUAL	REAL-TIME PREDICTED	ACT-RT
LOX Dump $\Delta V$ (m/s)	21.78	21.63	0.15
LH2 Dump $\Delta V$ (m/s)	9.97	9.86	0.11
Total Dump $\Delta V$ (m/s)	31.75	31.49	0.26

LOX Dump Duration = 445 Seconds

LH2 Dump Duration = 590 Seconds

Table 5-2. S-IVB/IU Orbit Trajectory Components at TB5

	ACTUAL	REAL TIME PREDICTION	ACT - RT
Range Time (sec)	19,193.3 (TB4 +310 min)	19,192.7	0.6
Radius (km)	6599.09	6596.34	2.75
Space-Fixed Velocity (m/s)	7749.42	7751.75	-2.33
Flight Path Angle (deg)	-0.056	-0.059	0.003
Latitude (deg, South)	42.02	42.32	-0.30
Longitude (deg, East)	41.43	41.67	-0.24

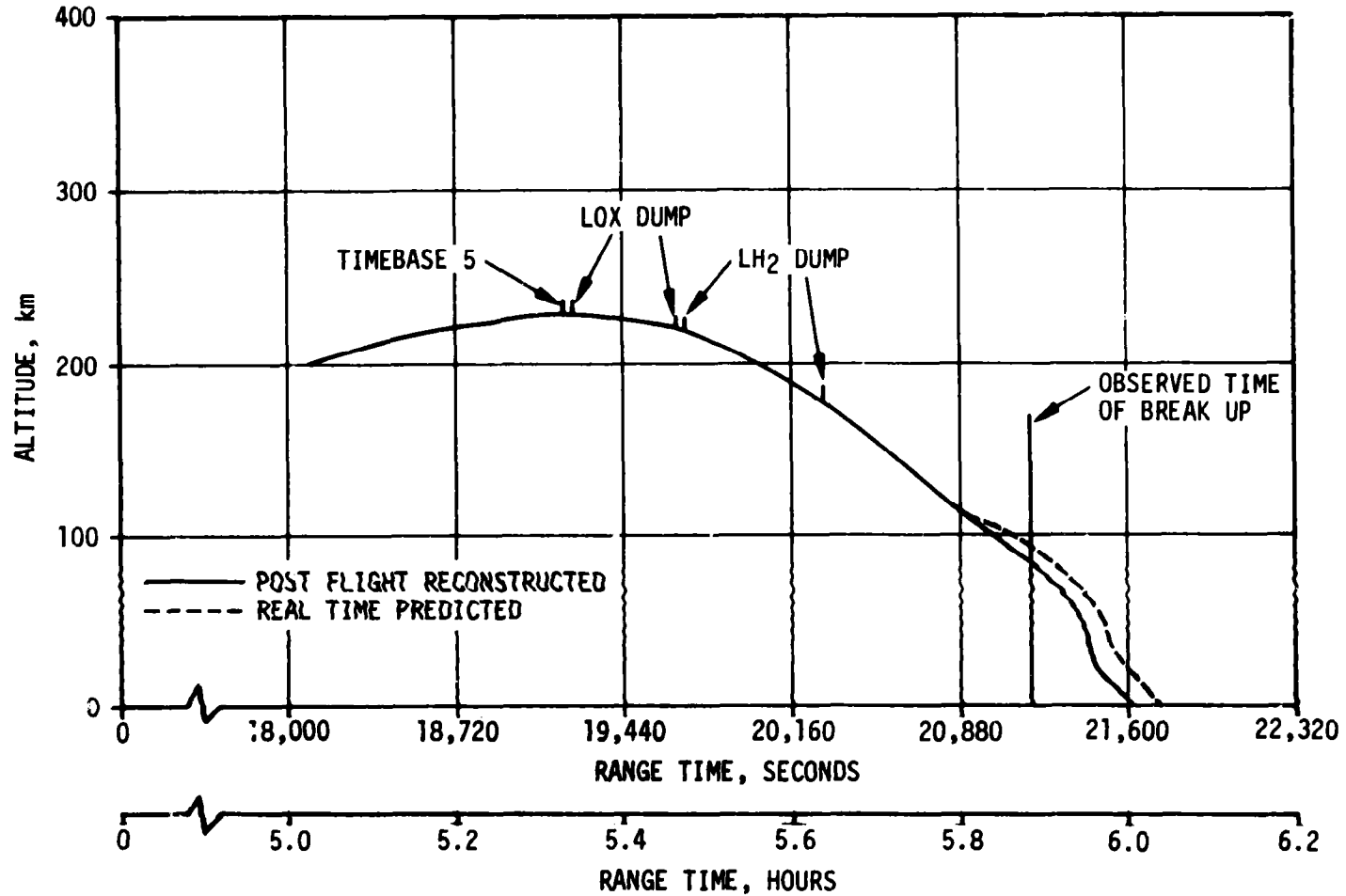


Figure 5-3. S-IVB/IU Deorbit Altitude Profile

Kwajalein radar tracking data established the S-IVB/IU breakup as occurring at 21,175 seconds. The simulated reentry trajectory was compared to the Kwajalein data at this time point. Table 5-3 presents these data, which show reasonable agreement of the breakup location. It should be noted that the Kwajalein site tracked for only a short time and the time of loss of signal has been selected as the most accurate indicator of the breakup time.

#### 5.4 IMPACT

The simulated reentry trajectory discussed above provided the initial conditions for establishing the limits of the impact area. The limits to the impact area were defined by simulation assuming a range of ballistic coefficients ( $W/C_D A$ ) from 47 to 650 kg/m<sup>2</sup>. Table 5-4 presents the short range, nominal, and long range impact point coordinates as they occurred in the plane of the trajectory. These data show that the impact area was approximately 500 n mi in length and well within the planned disposal area.

Table 5-3. S-IVB/IU Deorbit Position at Breakup

	POST FLIGHT RECONSTRUCTED	KWAJALEIN OBSERVED
Altitude (km)	81.7	81.7
Latitude (deg, North)	14.86	15.39
Longitude (deg, East)	176.49	176.96

Table 5-4. SA-207 S-IVB Impact Dispersion Limits

	SHORT RANGE	NOMINAL	LONG RANGE
Range Time (sec)	21,756.	21,650.	21,593.
Latitude (deg, North)	21.73	23.75	27.51
Longitude (deg, West)	177.43	175.50	171.60

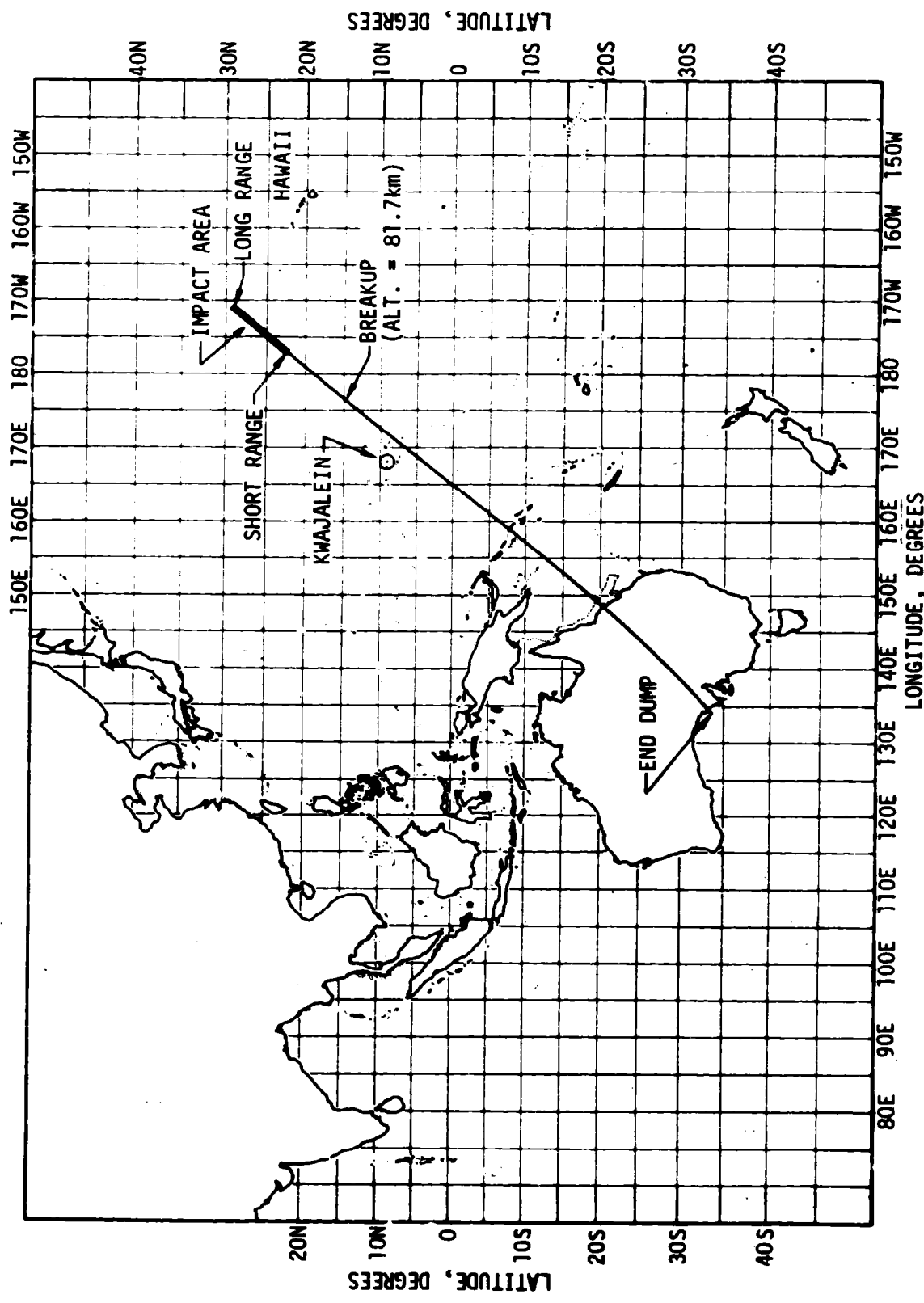


Figure 5-4. S-IVB/IU Ground Track - Dump to Impact

## SECTION 6

### S-IB PROPULSION

#### 6.1 SUMMARY

The S-IB stage propulsion system performed satisfactorily throughout flight. The one propulsion anomaly (possible LOX emanation from the LOX tank vents) occurred during countdown and had no effect on the countdown operations or flight performance. Stage longitudinal site thrust and mixture ratio averaged 0.68 percent and 0.27 percent lower than predicted, respectively. Stage LOX, fuel and total flowrate averaged 0.75 percent, 0.49 percent and 0.68 percent lower than predicted, respectively. Stage specific impulse was within 0.1 percent of predicted. Inboard Engine Cutoff (IECO) occurred at 137.36 seconds (0.76 seconds later than predicted). Outboard Engine Cutoff (OECO) was initiated 3.37 seconds after IECO by thrust OK pressure switch deactuation as planned at 140.73 seconds. At OECO, the LOX residual was 2960 lbm compared to the predicted 3311 lbm and the fuel residual was 6145 lbm compared to the predicted 5988 lbm. The stage hydraulic system performed satisfactorily.

#### 6.2 S-IB IGNITION TRANSIENT PERFORMANCE

All eight engines ignited satisfactorily. The automatic ignition sequence, which schedules the engines to start in pairs with a 100-millisecond delay between each pair, began with time for ignition command at -3.064 seconds range time. The start sequence that occurred was close to optimum. The maximum spread in the start time, defined by the intersection of the maximum chamber pressure or thrust buildup slope with the zero line ( $P_c$  prime times) of engines within a pair was 15 milliseconds and was between engines 5 and 7 (first pair of engines). The smallest interval in the planned 100-millisecond sequence between pairs was 80 milliseconds and was between the third and fourth pair (specifically, between Engines 3 and 4).

Table 6-1 compares predicted and actual start event times. The individual engine thrust buildup curves are shown in Figure 6-1. The thrust values shown are the total engine thrusts and do not account for cant angles.

#### 6.3 S-IB MAINSTAGE PERFORMANCE

S-IB mainstage flight performance was satisfactory although slightly lower than predicted as shown in Figure 6-2. Stage longitudinal site thrust, averaged 12,350 pounds (0.68 percent) lower than predicted. The stage specific impulse during flight was the same as predicted to the nearest 0.1 lbf-s/lbm. Stage mixture ratio averaged 0.0063 (0.27

Table 6-1. S-IB Engine Start Characteristics

ENGINE POSITION AND SERIAL NUMBER	TIME, IGNITION COMMAND TO ENGINE IGNITION SIGNAL (MSEC)		TIME, ENGINE IGNITION SIGNAL TO THRUST CHAMBER IGNITION (MSEC)		TIME, ENGINE IGNITION SIGNAL TO P <sub>c</sub> PRIME (MSEC)	
	ACTUAL (1)	PROGRAMMED	ACTUAL	NOMINAL	ACTUAL	NOMINAL
5 H-4078	105	100	529	584 <sup>(2)</sup>	832	875 <sup>(2)</sup>
7 H-4079	105	100	529	↓	847	↓
6 H-4074	204	200	540	↓	850	↓
8 H-4076	204	200	530	↓	855	↓
2 H-7078	306	300	543	↓	850	↓
4 H-7074	306	300	535	↓	861	↓
1 H-7065	405	400	539	↓	853	↓
3 H-7076	405	400	509	↓	842	↓

(1) Values referenced to event: "Time for Ignition Command".  
 (2) Values presented are mean values S-IB-6 through S-IB-12 static test.

percent) lower than predicted. Total propellant flowrate averaged 43.1 lbfm/sec (0.68 percent) lower than predicted. These averages were taken between range time zero and IECO.

The lower than predicted site thrust and flowrates were primarily the result of the engines performing at lower power levels than expected for rated operating conditions and colder fuel than predicted.

Table 6-2 summarizes the S-IB engines propulsion performance, compared to the predicted performance when reduced to standard sea level conditions.

The average sea level thrust and propellant flowrates were 0.45 percent lower than predicted values which are much closer to the predictions than those of SA-206 where the thrust and propellant flowrates were 0.88 and 0.67 percent lower, respectively.

Postflight evaluation of Saturn IB vehicles SA-201 through SA-205 showed the flight thrust and flowrates to be significantly higher than thrust and flowrates experienced during ground tests, when reduced to standard sea level conditions. Consequently, the flight predictions, based on ground test levels, were biased upwards to compensate for this phenomenon and thus more accurate flight predictions were achieved through vehicle SA-205. SA-206 flight exhibited a contrary trend as the thrust was lower than the levels experienced during ground tests. SA-206 postflight analysis was inconclusive as to the cause of the contrary flight thrust trend which could have been (1) the unique flight performance of the uprated engine (205 klbf) first used on SA-206 or (2) the known inconsistencies in the various SA-206 engine and stage ground tests. Since the thrust levels of SA-207, which also utilize uprated engines, were in agreement with the earlier flights

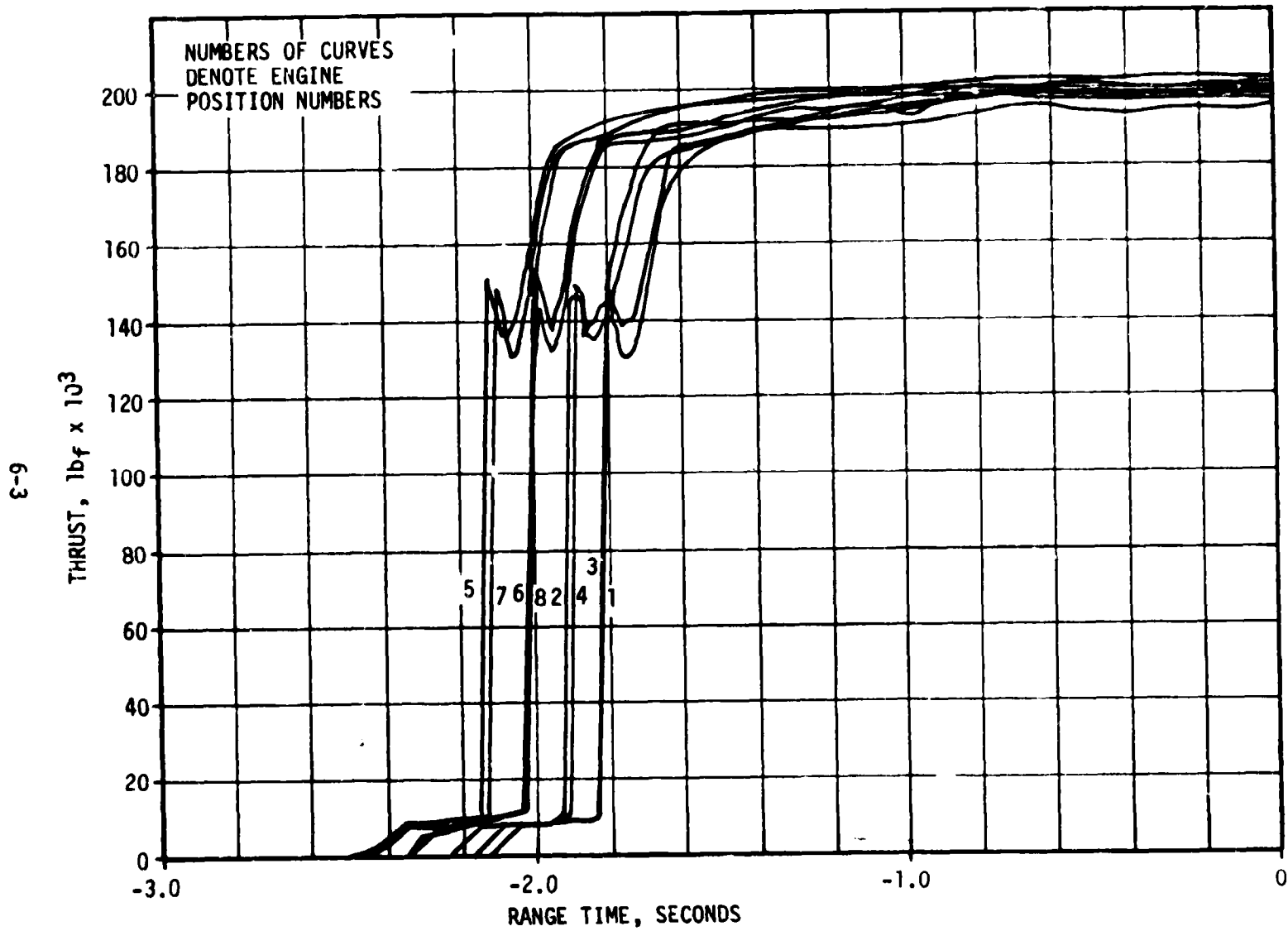
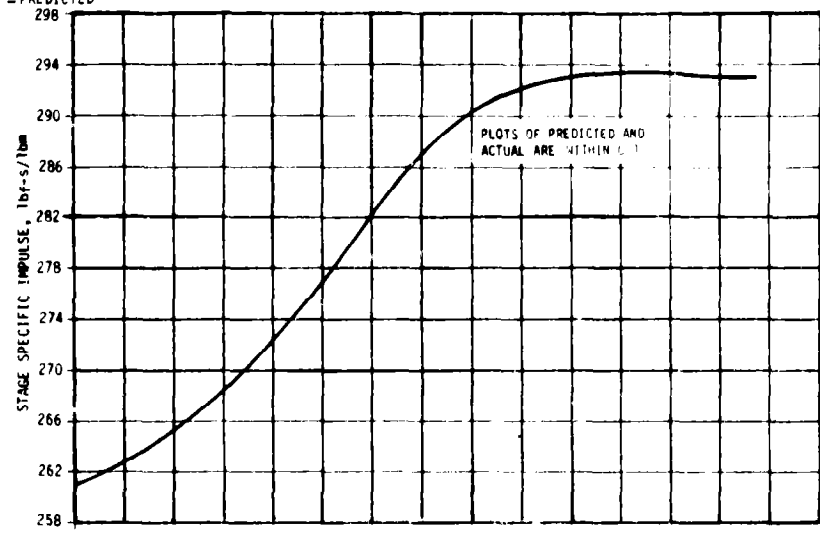
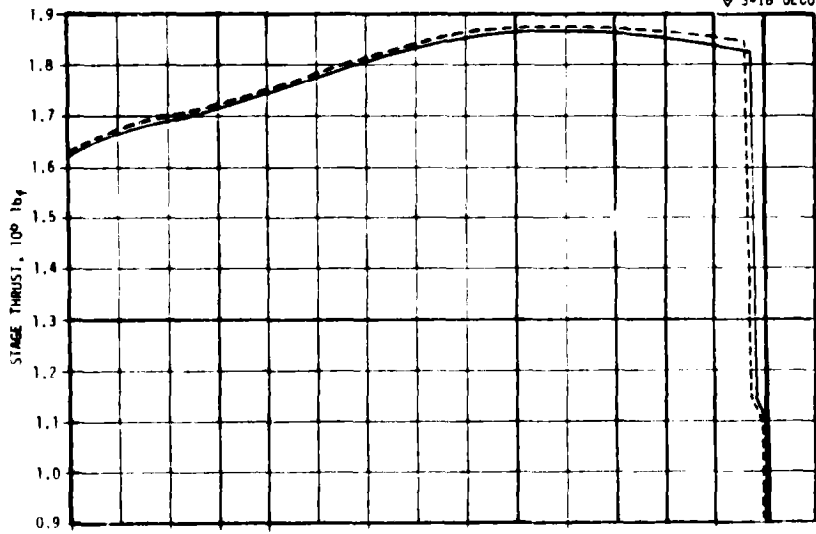


Figure 6-1. S-IB Engines Thrust Buildup

▽ S-1B IEEO — RECONSTRUCTED  
 ▽ S-1B OEEO - - - PREDICTED



6-4-

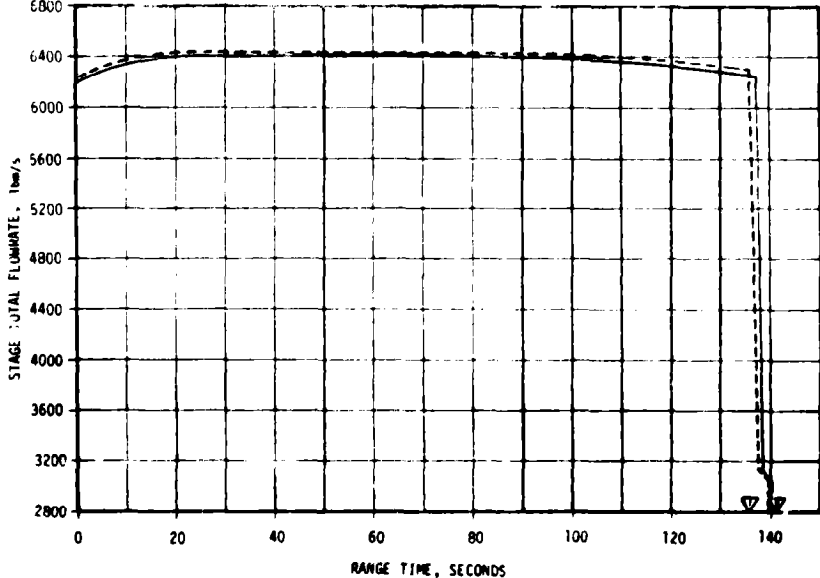
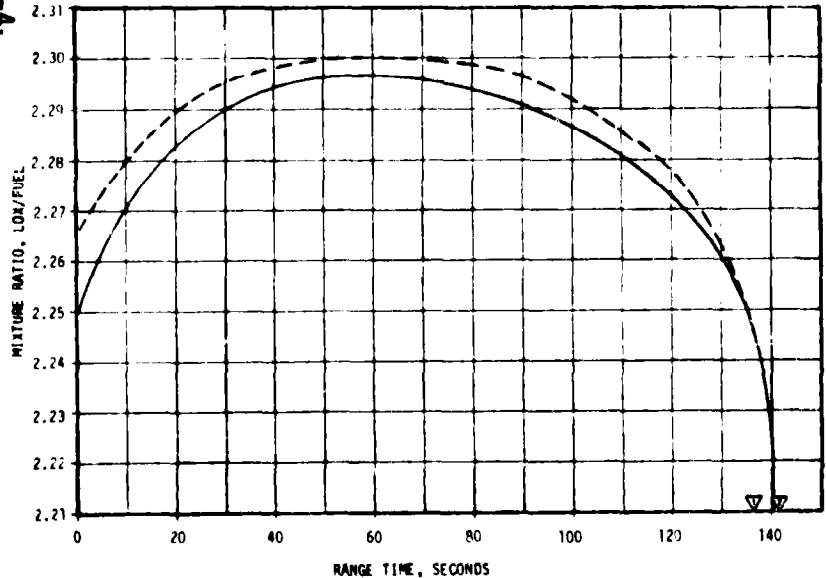


Figure 6-2. S-1B Stage Propulsion Performance

**Table 6-2. S-1B Individual Engine Propulsion Performance\***

ENGINE POSITION	THRUST (LBF)		SPECIFIC IMPULSE (LBF-SEC/LBM)		LOX FLOWRATE (LBM/SEC)		FUEL FLOWRATE (LBM/SEC)		Mixture Ratio					
	PRED	ACTUAL	% DIFF	PRED	ACTUAL	% DIFF	PRED	ACTUAL	PRED	% DIFF				
1	208,753	204,326	-0.89	262.14	262.08	-0.02	541.16	537.91	243.31	241.72	-0.65	2.2260	2.2253	-0.03
2	206,790	205,810	-0.57	262.73	262.71	-0.01	544.53	541.43	242.54	241.21	-0.55	2.2451	2.2446	-0.02
3	206,692	206,777	0.04	263.68	263.86	0.07	542.73	542.61	241.15	241.06	-0.04	2.2506	2.2509	0.01
4	206,046	202,830	-1.56	262.21	261.87	-0.13	544.95	537.03	240.86	237.52	-1.39	2.2625	2.2609	-0.07
5	205,845	206,805	0.47	263.37	263.69	0.12	540.60	542.52	240.98	241.74	0.32	2.2433	2.2422	-0.05
6	205,845	205,464	-0.18	262.65	262.76	0.04	541.58	540.36	242.16	241.60	-0.23	2.2365	2.2365	0.00
7	207,050	206,253	-0.38	263.84	263.85	0.00	542.88	540.76	241.87	240.96	-0.38	2.2445	2.2442	-0.01
8	208,522	207,096	-0.68	263.20	263.14	-0.02	549.08	545.38	243.18	241.62	-0.64	2.2579	2.2571	-0.03
AVG	206,566	205,645	-0.45	262.98	263.00	0.01	543.44	541.00	242.01	240.93	-0.45	2.2458	2.2455	-0.01

\*Performance levels reduced to standard sea level conditions. Data taken at 30 seconds.

LOX density 70.79 lbm/ft<sup>3</sup>  
 Fuel density 50.45 lbm/ft<sup>3</sup>  
 Ambient Pressure 14.67 psia  
 Fuel pump inlet pressure 57 psia  
 LOX pump inlet pressure 65 psia  
 Fuel temperature 60°F

it is now more apparent that the established trend of high flight thrust than ground thrust is valid for the 205 klbf engines and that the SA-206 lower flight thrust was probably due to the inconsistencies in the different ground tests and the subsequent effect of these inconsistencies on the predicted flight levels.

The lower than predicted propellant flowrates caused IECO to be 0.76 second later than predicted. The lower flowrates and a greater than predicted differential between the center and outboard LOX levels at the time of level sensor actuation caused OECO to occur 3.37 seconds after IECO instead of the predicted 3.0 seconds.

Engine No. 7 turbopump gearcase lubricant pressure experienced shifts of +7 and -7 psi at 29 and 44 seconds. These pressure steps are not unusual, the same type having been observed on Engine No. 1 of SA-206, Engine No. 2 of SA-205, and 45 instances during single engine static tests. These shifts are attributed to partial restriction of individual turbopump bearing jets by particles remaining in the lube system cored passages from the casting process, or introduced during turbopump assembly. No evidence of damage due to jet restriction has been experienced or would be expected because redundancy is provided by multiple lubrication jets (three per bearing) in addition to splash lubrication from the gears to the bearings.

#### 6.4 S-IB SHUTDOWN TRANSIENT PERFORMANCE

The cutoff sequence on the S-IB-7 stage began at 134.35 seconds with the actuation of the low-level sensors in LOX tank 02. IECO was initiated 3.01 seconds later by the Launch Vehicle Digital Computer (LVDC) at 137.36 seconds. Thrust decay on each inboard engine was normal. The total IECO impulse was 270,728 lbf-sec. Inboard engine total thrust decay is shown in Figure 6-3. OECO was initiated by thrust OK switch deactuation, as planned, at 140.73 seconds, 1.13 seconds later than predicted. LOX starvation occurred in the four outboard engines. Outboard engine total thrust decay is shown in Figure 6-4. Each engine has three thrust OK pressure switches. As engine thrust level decays during LOX starvation, the first outboard engine to lose thrust OK signal from two-out-of-three switches, will simultaneously cut off all outboard engines. The telemetry system's sampling rate of these signals (12 samples per second) is too low to determine which engine had the earliest two-out-of-three switch drop-out times necessary for OECO.

#### 6.5 S-IB STAGE PROPELLANT MANAGEMENT

Propellant management is the relationship of the propellant consumed to propellant loaded, and is an indication of the propulsion system performance and the capability to load the proper propellant weights. The predicted and actual (reconstructed) percentages of loaded propellants utilized during the flight are shown in Table 6-3.

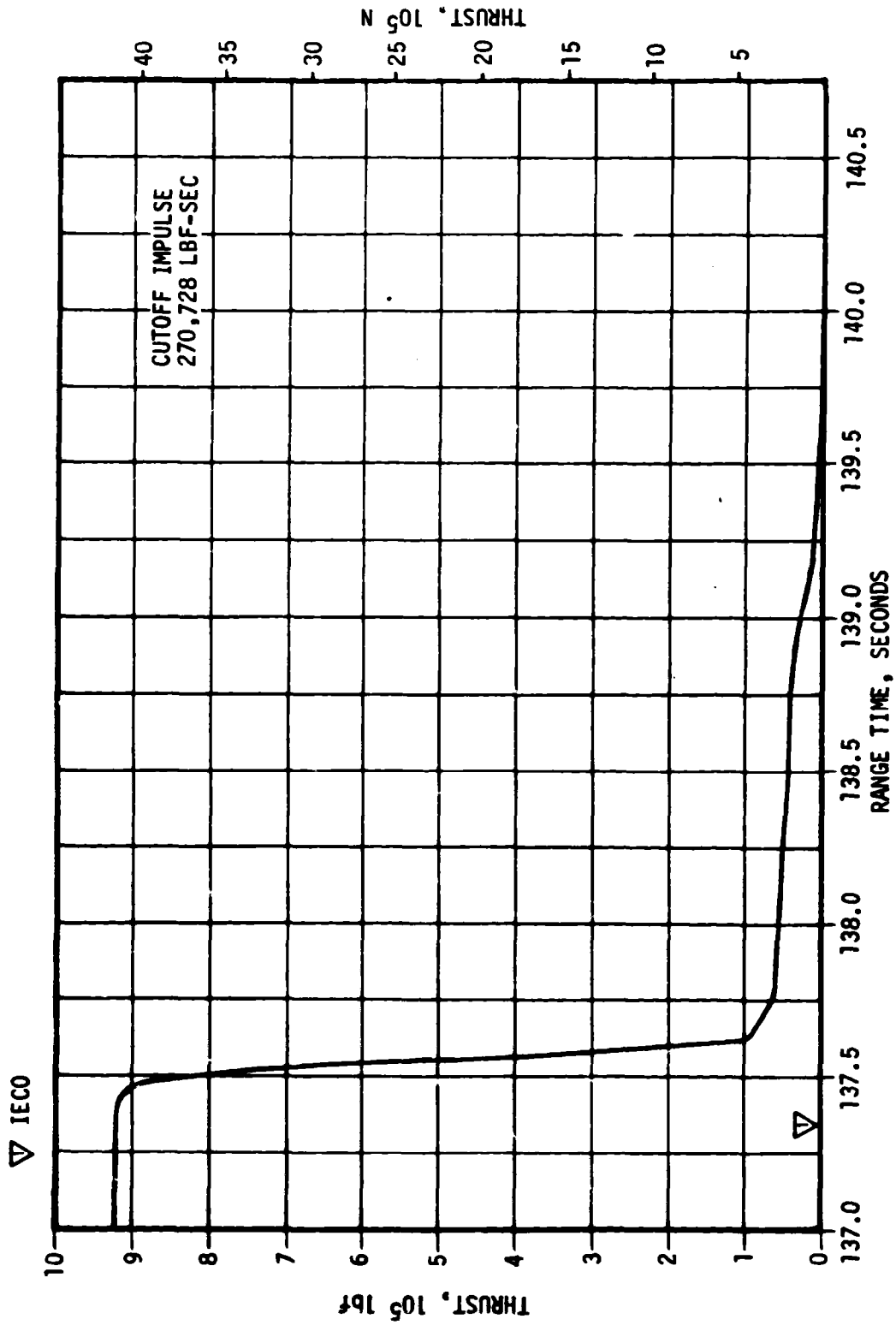


Figure 6-3. S-IB Inboard Engines Total Thrust Decay

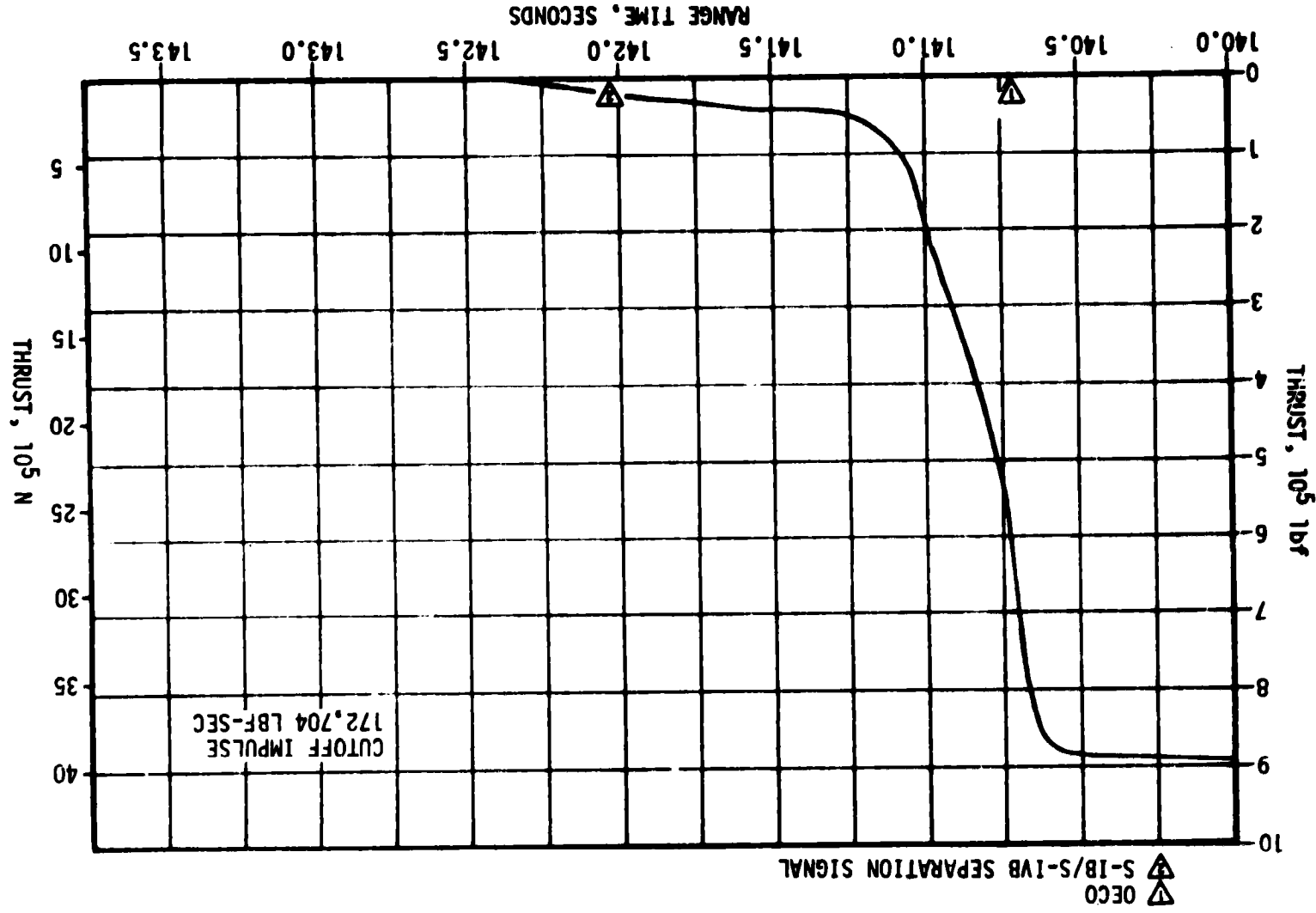


Figure 6-4. S-1B Outboard Engines Total Thrust Decay

8-9

△ OECO  
 △ S-1B/S-1VB SEPARATION SIGNAL

CUTOFF IMPULSE  
 172,704 LBF-SEC

Table 6-3. S-IB Propellant Usage

PROPELLANT	PREDICTED (%)	ACTUAL (%)
Total	99.20	99.20
Fuel	98.34	98.28
LOX	99.58	99.62

The planned mode of OECO was by LOX starvation. The LOX and fuel level cutoff probe heights and flight sequence settings were determined for a 3.00-second time interval between cutoff probe actuation and IECO. The planned time interval between IECO and OECO was 3.00 seconds. OECO was to be initiated by the deactuation of two of the three thrust OK pressure switches on any outboard engine as a result of LOX starvation and the subsequent thrust decay. It was assumed that approximately 271 gallons of LOX in the outboard suction lines were usable. The backup timer (flight sequencer) was set to initiate OECO, 13.00 seconds after level sensor actuation.

To prevent fuel starvation, fuel depletion cutoff probes were located in tanks F2 and F4 container sumps. The fuel bias was 1550 lbm. This fuel mass, included in the predicted residual, was available for consumption to minimize propellant residual due to off-nominal conditions and is not expected to be used during a nominal flight.

The cutoff sequence was initiated by a signal from the cutoff level sensor in tank O2 at 134.35 seconds. The IECO signal was received 3.01 seconds later at 137.36 seconds. OECO was initiated 3.37 seconds after IECO at 140.73 seconds by thrust OK pressure switch deactuation. Fuel depletion probes were not actuated prior to retromotor ignition.

Based on discrete probe data, liquid levels in the fuel tanks were nearly equal and approximately 22.6 inches above theoretical tank bottom at IECO. This level represents a mass of 10,767 lbm of fuel onboard. At that time 10,887 lbm of LOX remained onboard. Corresponding liquid height in the center tank was approximately 14.3 inches and average height in the outboard tanks was approximately 9.7 inches above theoretical tank bottom. Propellants remaining above the main valves after outboard engine decay were 2431 lbm of LOX and 4824 lbm of fuel. Predicted values for these quantities were 2670 lbm of LOX and 4627 lbm of fuel.

Total LOX and fuel masses above the main propellant valves beginning at ignition command are shown in Figures 6-5 and 6-6. A summary of the propellants remaining at major event times is presented in Table 6-4.

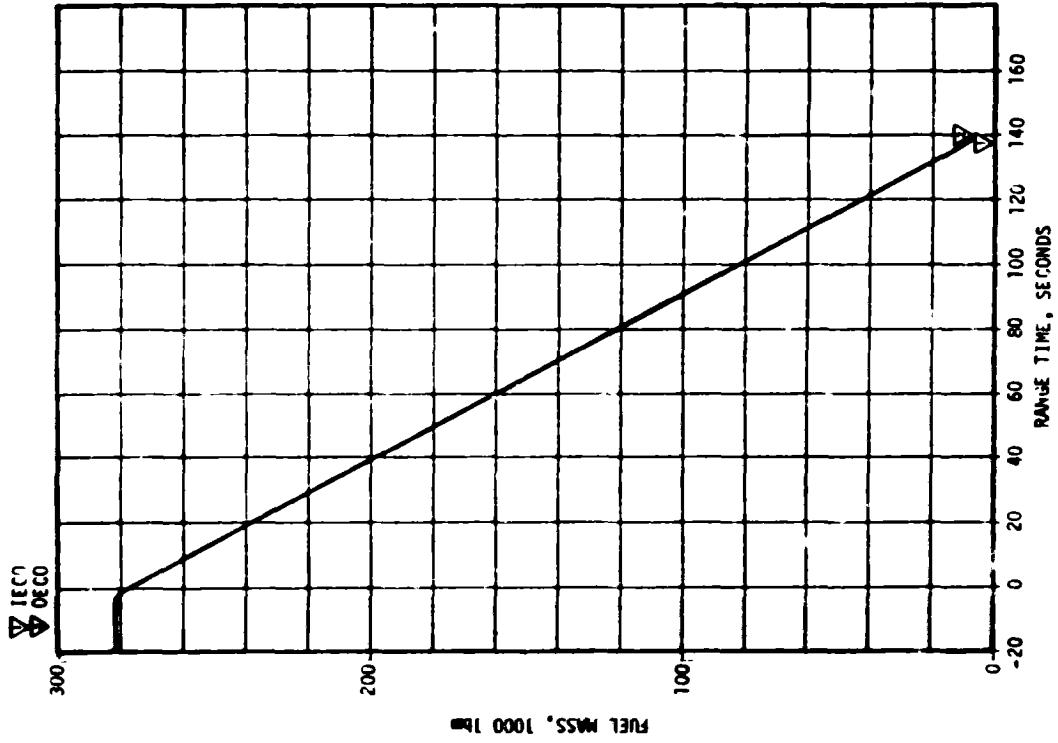


Figure 6-4. S-IB Stage Fuel Mass Above Main Fuel Valve

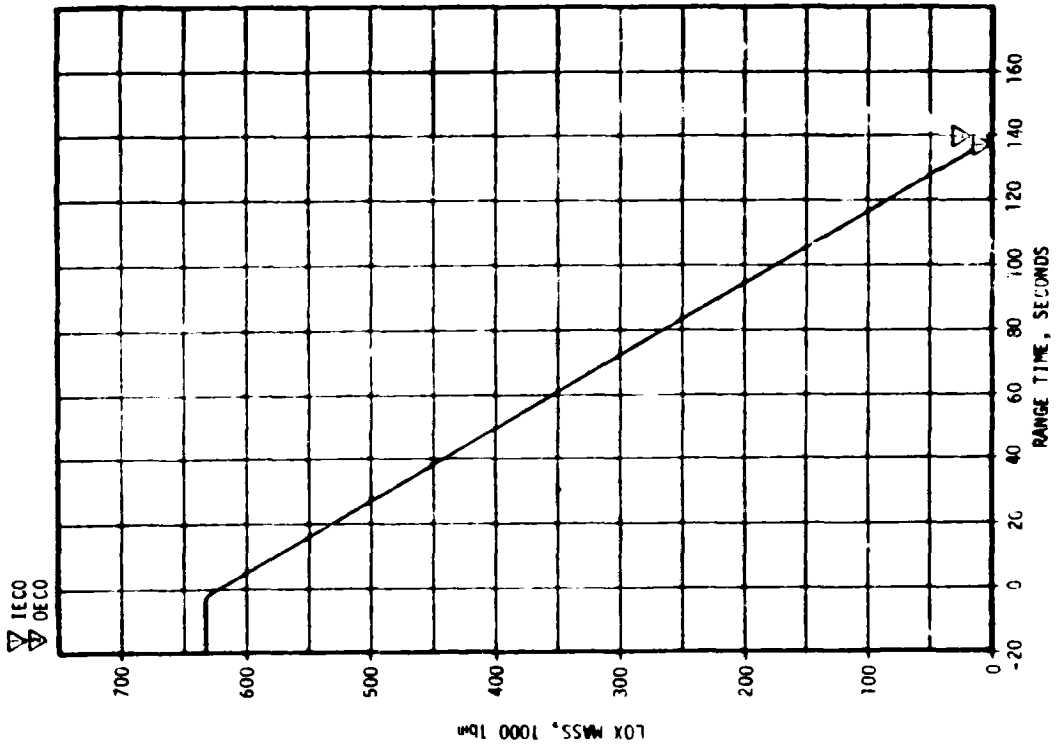


Figure 6-5. S-IB Stage LOX Mass Above Main LOX Valve

Table 6-4. S-IB Propellant Mass History

EVENT	PREDICTED (LBM)			RECONSTRUCTED (LBM)		
	FUEL	LOX	TOTAL	FUEL	LOX	TOTAL
Ignition Command	279,007	632,016	911,023	280,038	631,940	911,978
IU Umbilical Disconnect	275,705	620,864	896,569	276,036	620,788	896,824
IECO	10,265	10,512	20,777	10,767	10,887	21,654
OECO	5,988	3,311	9,299	6,145	2,960	9,105
Separation	4,891	2,753	7,644	5,098	2,514	7,612
Zero Thrust	4,627	2,670	7,297	4,824	2,431	7,255

## 6.6 S-IB PRESSURIZATION SYSTEM

### 6.6.1 Fuel Pressurization System

The fuel tank pressurization system performed satisfactorily during the entire flight. The fuel pump inlet pressure met the minimum Net Positive Suction Pressure (NPSP) requirement throughout flight. A comparison of measured absolute ullage pressure and predicted ullage pressure is presented in Figure 6-7. Measured ullage pressure compared favorably with predicted ullage pressure during the flight and at no time exceeded a difference of 2.0 psi from the predicted value.

Fuel vent valves 1 and 2 closed at the beginning of the pressurization sequence and remained closed. Tank pressurization began at T-160.8 seconds. The 1422-gallon (3.4 percent) ullage volume was pressurized in 2.31 seconds. Due to system cooling, the pressurizing valves opened again at T-119.83 seconds for a period of 0.25 second to repressurize the fuel tank ullage. The pressurizing valves reopened during the engine start sequence at T-1.9 seconds and remained open.

The helium sphere pressure was 2890 psia at ignition, which is lower than it was on S-IB-6, but acceptable. The sphere pressure is shown in Figure 6-8.

Because the fuel temperature and the ullage pressure were different in each of the tanks, liquid levels were also different. Discrete probe data show that the behavior of the fuel tank liquid levels during flight was similar to S-IB-6. The maximum recorded liquid level difference between tanks F1 and F3 was 4.36 inches at 27.0 seconds. The level converged to a difference of 0.6 inch at approximately 137.0 seconds.

### 6.6.2 LOX Pressurization System

The LOX tank pressurization system performed satisfactorily during the

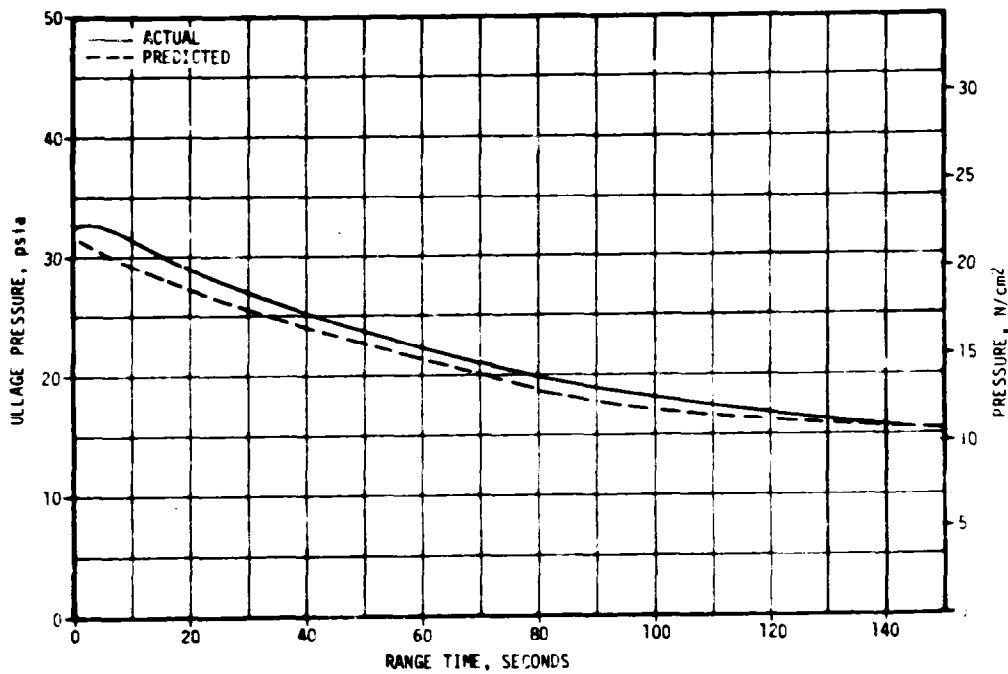


Figure 6-7. S-IB Fuel Tank Ullage Pressure

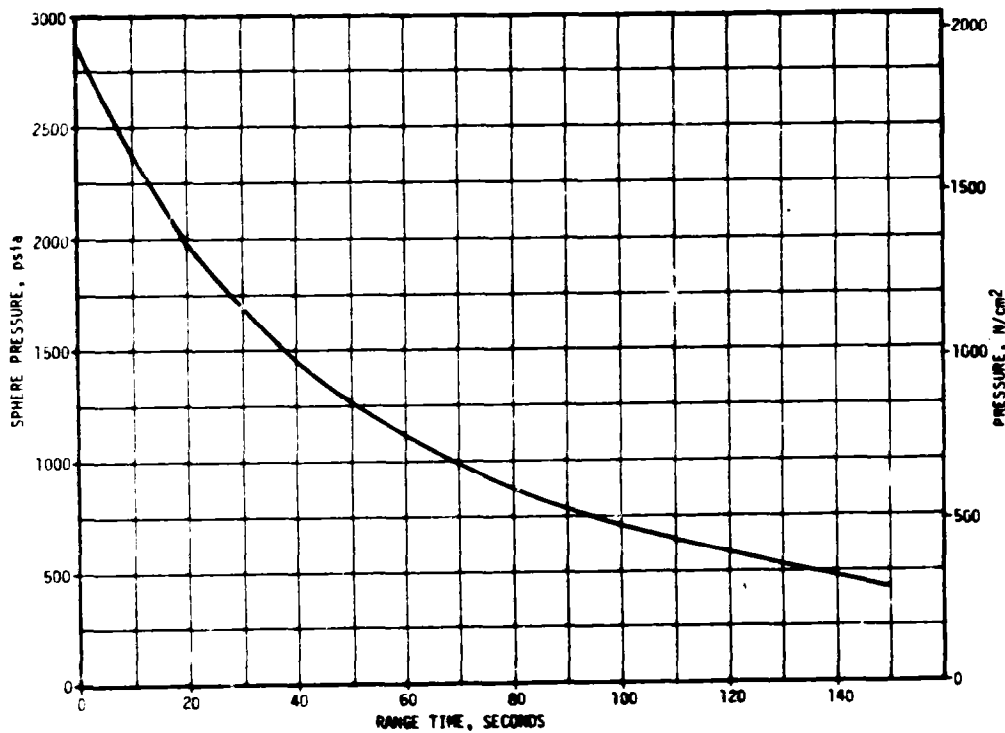


Figure 6-8. S-IB Fuel Tank Helium Pressurization Sphere Pressure

entire flight. The LOX pump inlet pressure met the minimum NPSP requirement throughout flight. On several occasions during the countdown, what appeared to be LOX was seen venting from the outboard tank vents. The apparent LOX venting phenomenon under the LOX loading conditions is not fully understood, and it is unlikely that this phenomenon will be further explained. LOX venting during countdown is not a concern for flight performance. See paragraph 3.1 for more details.

The actual ullage pressure during flight is compared with the predicted pressure and presented in Figure 6-9. The initial pressurization level satisfied the minimum requirement of 80 psia at the LOX pump inlet for engine start. The pressurization system is designed to provide a minimum tank pressure at OECO of 47.5 psia.

The minimum ullage pressure of 48.1 psia occurred during the engine start transient and the maximum pressure of 53.2 psia occurred at 35 seconds. The GOX Flow Control Valve (GFCV) started to close at ignition, and after the normal hesitations during the start transient, reached the fully closed position at 18 seconds and remained closed until 72 seconds as shown in Figure 6-10. The predicted GFCV position is not shown since the valve used for stage test was replaced prior to flight. The GFCV opened 11 seconds earlier than on S-IB-6; which can be attributed to the higher tank pressure at which the GFCV actuated; i.e., 51.6 psia on S-IB-7 versus 50.1 psia on S-IB-6. The GFCV continued to open gradually for the remainder of the flight to 16 percent open at IECO, while the ullage pressure decayed to 49.5 psia.

The pressure upstream of the GFCV was approximately 4.5 percent higher than on S-IB-6 during the period when the valve was closed (18 to 72 seconds), while the temperature was approximately the same as S-IB-6. The higher GOX pressure from 18 to 72 seconds indicates that the GOX flowrate was higher than S-IB-6.

#### 6.7 S-IB PNEUMATIC CONTROL PRESSURE SYSTEM

The S-IB pneumatic control pressure system supplied GN<sub>2</sub> at a regulated pressure of 770 to 781 psia to pressurize the H-1 engine turbopump gearboxes and to purge the LOX and lube seal cavities and the radiation calorimeters. This regulated pressure was also used to close the LOX and fuel prevalues at IECO and OECO.

The 750 psig regulator was replaced during prelaunch checkout and system performance was satisfactory during prelaunch and flight. The actual sphere pressure history remained within the acceptable band as shown in Figure 5-11.

#### 6.8 S-IB HYDRAULIC SYSTEM

The system hydraulic pressures were satisfactory during flight and were similar to those of the SA-206 flight. At zero seconds, the system pressures ranged from 3125 to 3240 psig. The pressure decreased approximately 50 psi on each engine during flight. This normal pressure

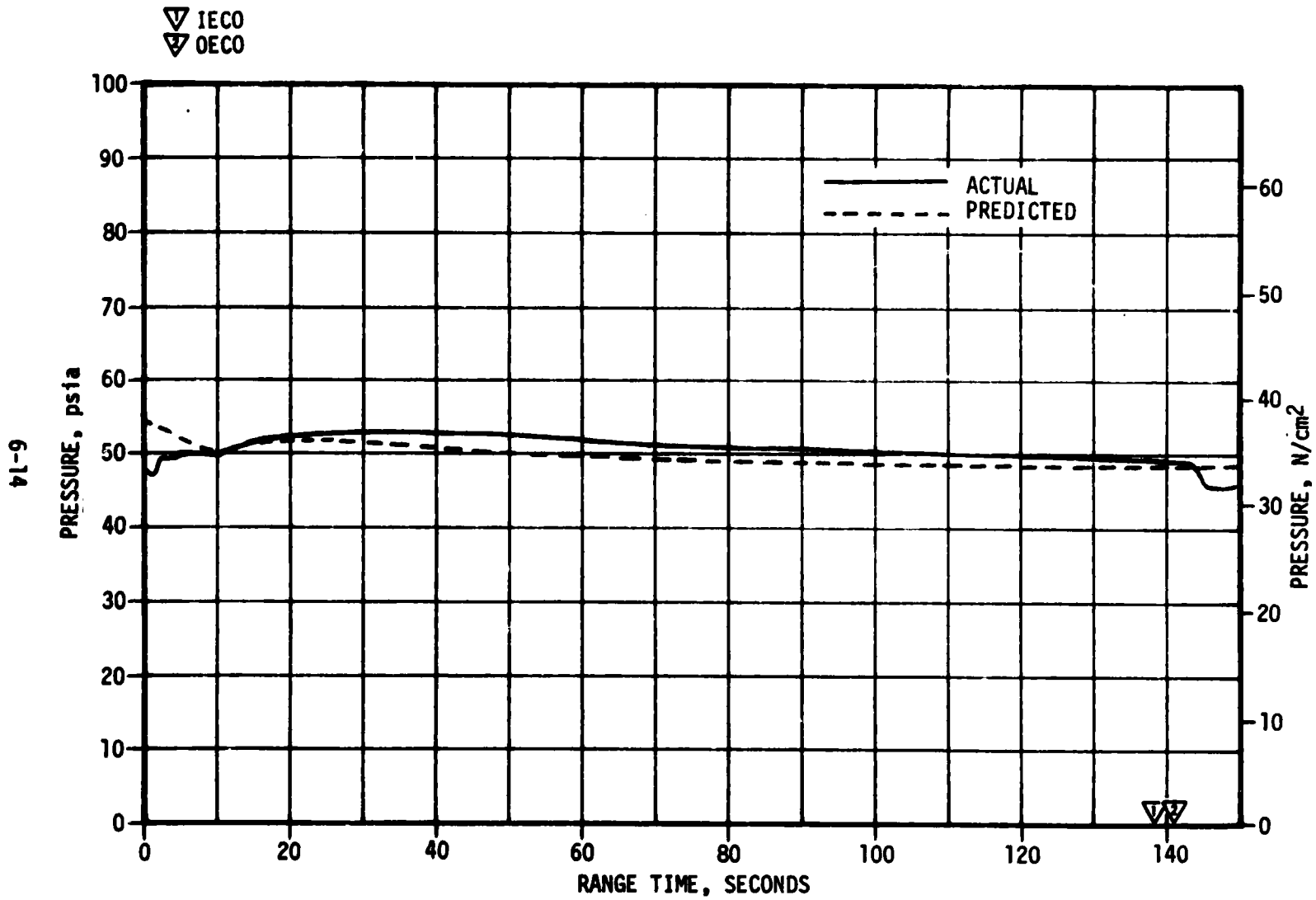


Figure 6-9. S-IB Center LOX Tank Ullage Pressure

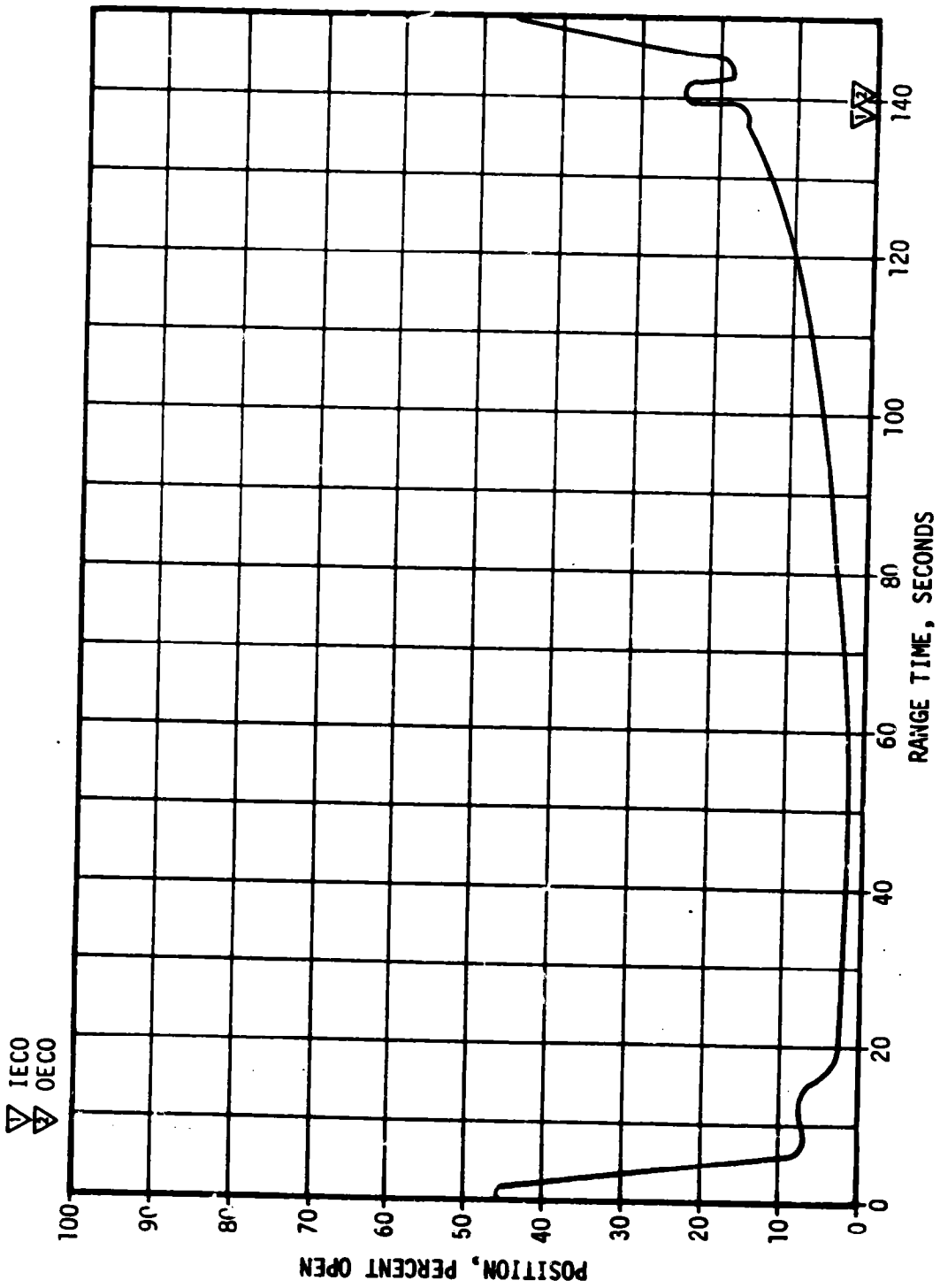


Figure 6-10. S-IB GOX Flow Control Valve Position

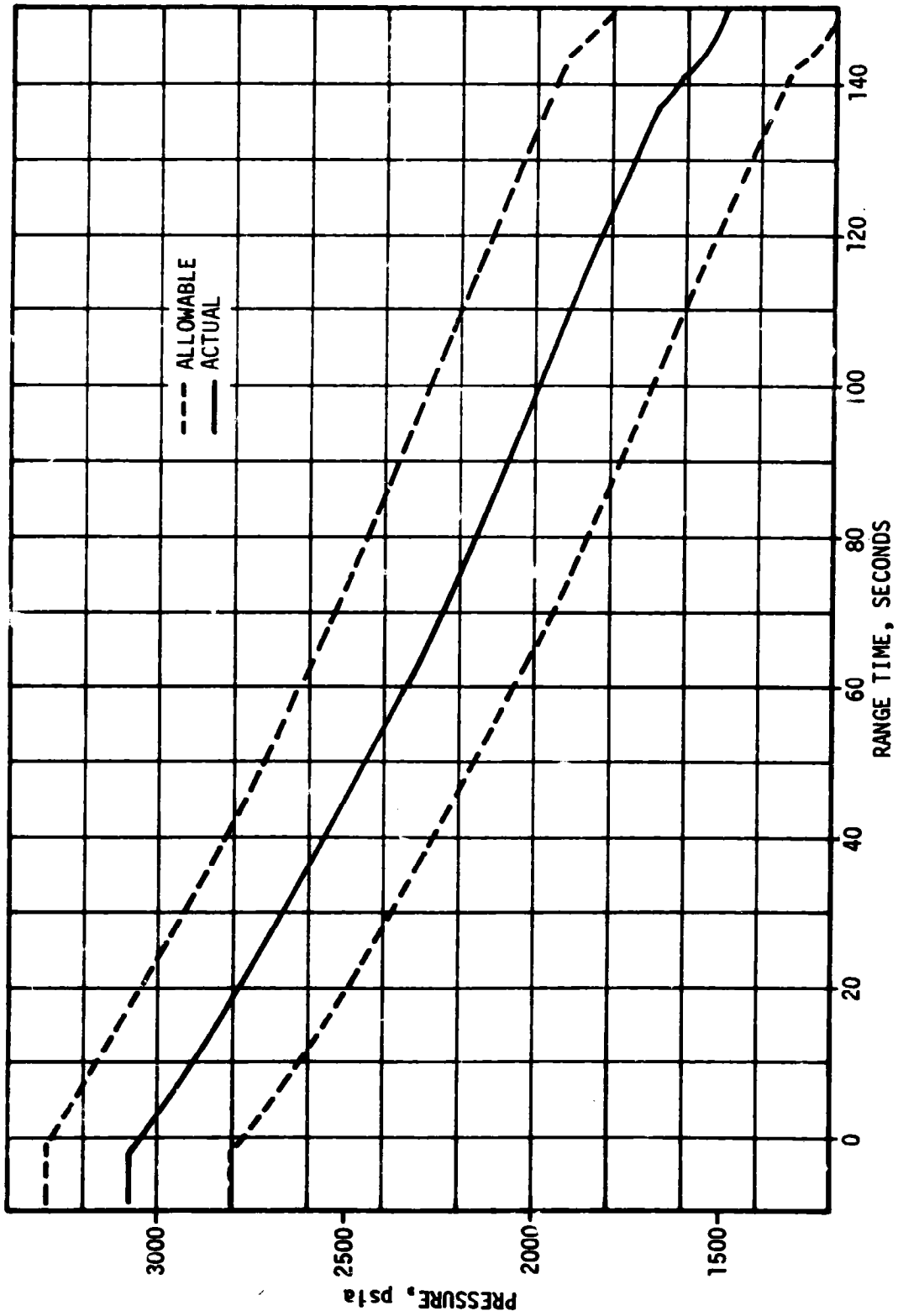


Figure 6-11. S-IB Pneumatic Control Pressure

decrease was due to the main pump temperature increase during the flight.

Reservoir oil levels were also similar to those of the SA-206 flight. There was a rise of approximately 2 percent in each level during flight, indicating about a 7°C rise in each hydraulic system's average oil temperature (not reservoir oil temperature).

The reservoir oil temperatures were satisfactory during flight. Average temperature at liftoff averaged 51°C as compared to an average of 49°C for the four S-IB-6 hydraulic systems. The average temperature decrease during the flight was 9°C for S-IB-7 which was the same for the four S-IB-6 hydraulic systems.

## SECTION 7

### S-IVB PROPULSION

#### 7.1 SUMMARY

The S-IVB propulsion system performed satisfactorily throughout the operational phase of burn and had normal start and cutoff transients. S-IVB burn time was 448.53 seconds, 4.24 seconds shorter than predicted for the actual flight azimuth of 45.0 degrees. This difference is composed of -0.13 second due to S-IB/S-IVB separation velocity, radius, and weight and -3.90 seconds due to higher than predicted S-IVB performance leaving -0.21 second unexplained. The engine performance during burn, as determined from standard altitude reconstruction analysis, deviated from the predicted Start Tank Discharge Valve (STDV) open +60 second time slice by +0.89 percent for thrust and -0.05 percent for specific impulse. The S-IVB stage engine cutoff (ECO) was initiated by the Launch Vehicle Digital Computer (LVDC) at 592.93 seconds. The S-IVB residuals at engine cutoff were near nominal. The best estimate of the residuals at engine cutoff is 2551 lbm for LOX and 2326 lbm for LH<sub>2</sub> as compared to the predicted values of 2843 lbm for LOX and 1957 lbm for LH<sub>2</sub>.

The stage propellant tanks were vented satisfactorily as sequenced following engine cutoff. During orbital coast, the LOX tank pressure increased due to tank heating and liquid boiloff. The pressure stayed within the predicted band. The fuel tank Nonpropulsive Vent (NPV) system satisfactorily controlled fuel ullage pressure during earth orbit.

During orbital coast the Auxiliary Propulsion System (APS) demonstrated nominal performance and responded to a disturbing force on the S-IVB/IU stage. LH<sub>2</sub> NPV and Instrument Unit (IU) sublimator operation contributed to the disturbing forces. The level of disturbance attributed to the LH<sub>2</sub> NPV system is within the specified tolerances on nozzle misalignment and area unbalance even if the disturbance were attributed entirely to misalignment or entirely to area unbalance. The disturbance had no effect on mission accomplishment.

An engine pitch actuator oscillation of low amplitude and frequency was noted during prelaunch, S-IB boost, and orbital coast thermal cycles while no commands were input to the servovalve. These oscillations were caused by accumulation of micron sized particles in the clearance between the servovalve spool and bushing. Operation was normal during powered flight and deorbit dumps.

The impulse derived from the LOX and fuel dumps was sufficient to satisfactorily deorbit the S-IVB/IU. The total impulse provided, 104,000 lbf-sec, was in close agreement with the real time nominal predicted value of 103,500 lbf-sec. A real time decision was made to extend the dump duration in order to improve the Apollo Range Instrumented Aircraft (ARIA) coverage of the deorbit propellant dumps and Kwajalein coverage of stage breakup. As expected after the LH<sub>2</sub> dump the pneumatic pressure was not sufficient to cause the NPV valves to latch open; however all deorbit safing criteria were met. The APS satisfied control system demands throughout the deorbit sequence.

## 7.2 S-IVB CHILLDOWN AND BUILDUP TRANSIENT PERFORMANCE

The thrust chamber temperature at liftoff was -209°F, which was below the maximum allowable redlines limit of -185°F. At S-IVB STDV open signal, the temperature was -182°F, which was within the requirements of -225 +75°F.

The chilldown and loading of the engine GH<sub>2</sub> start tank and pneumatic control bottle prior to liftoff was satisfactory. At liftoff, the engine control sphere pressure and temperature were 2960 psia and -174.7°F and the start tank pressure and temperature were 1315 psia and -189.7°F. At STDV open the engine control sphere pressure and temperature were 2967 psia and -176.3°F. The start tank conditions were 1325 psia and -181.2°F, which was within the start box.

The propellant tank prepressurizations were satisfactory. The propellant recirculation systems operation was satisfactory and operated continuously from before liftoff until just prior to Engine Start Command (ESC). Start and run box requirements for both fuel and LOX were met, as shown in Figure 7-1. At STDV open the LOX pump inlet temperature was -294.7°F and the pump inlet pressure was 40.7 psia. At STDV open the fuel pump inlet temperature was -421.1°F and the pump inlet pressure was 31.4 psia. All conditions were within the start box limits.

Fuel lead followed the expected pattern and resulted in satisfactory conditions as indicated by the fuel injector temperature.

The engine start transient was satisfactory, and the thrust buildup was within the limits set by the engine manufacturer. This buildup was similar to the thrust buildups observed during previous flights. The Mixture Ratio Control Valve (MRCV) was in the closed position, 4.8 Engine Mixture Ratio (EMR), during the buildup. The total impulse from STDV open to STDV open + 2.4 seconds was 172,810 lbf-s.

## 7.3 S-IVB MAINSTAGE PERFORMANCE

The propulsion reconstruction analysis verified that the stage performance during mainstage operation was satisfactory. A comparison of predicted and actual performance of thrust, specific impulse, total flowrate, and EMR versus time is shown in Figure 7-2. Table 7-1 shows the thrust, specific impulse, flowrate, and EMR deviations from predicted at the STDV open +60 second time slice at standard altitude conditions.

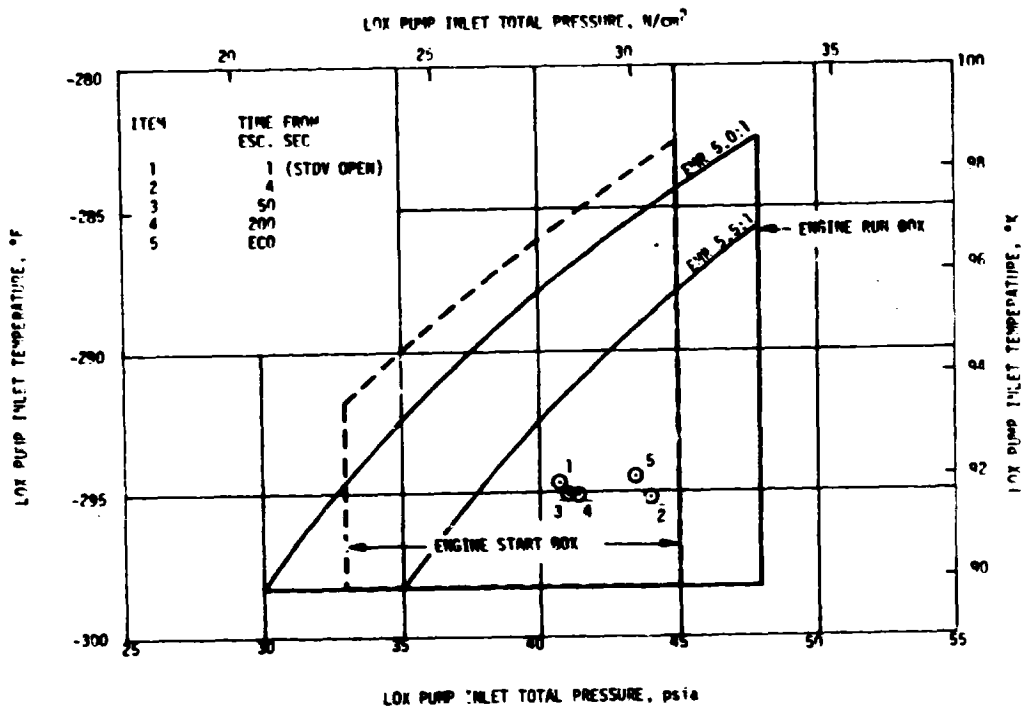
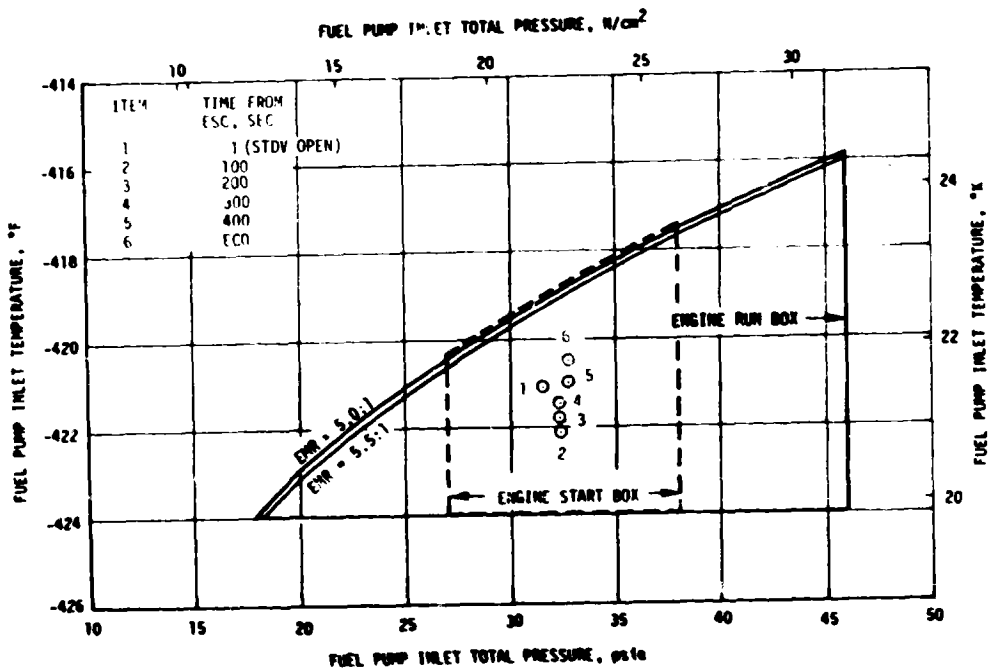


Figure 7-1. S-IVB Start Box and Run Requirements

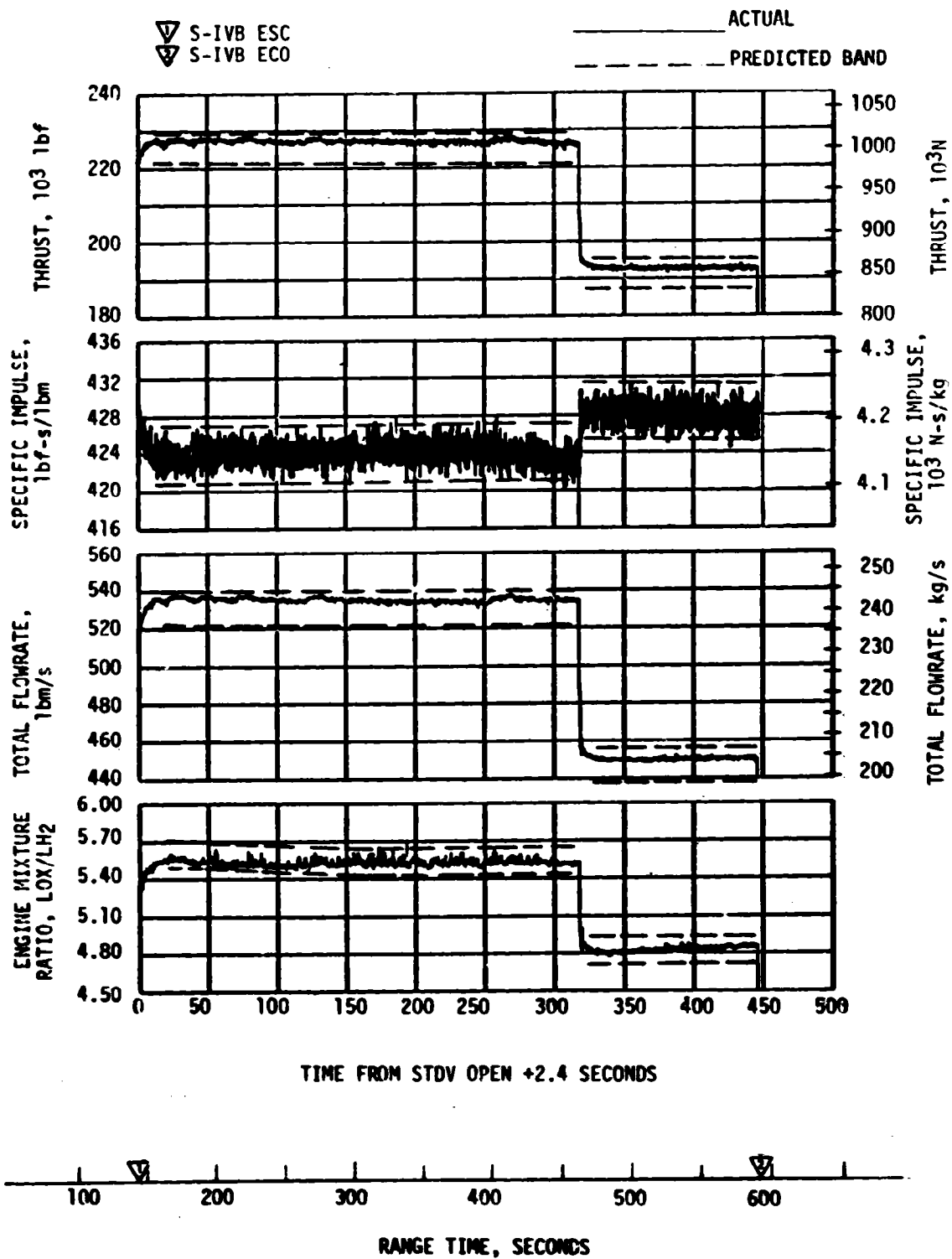


Figure 7-2. S-IVB Steady-State Performance

Table 7-1. S-IVB Steady State Performance (STDV Open +60 Second Time Slice at Standard Altitude Conditions)

	PREDICTED	RECONSTRUCTED	FLIGHT DEVIATION (ACT-PRED)	PERCENT DEVIATION FROM PREDICTED
Thrust, lbf	224,081	226,082	2001	0.89
Specific Impulse, lbf-s/lbm	424.1	423.9	-0.2	-0.05
LOX Flowrate, lbm/s	447.96	452.14	4.18	0.93
Fuel Flowrate, lbm/s	80.47	81.25	0.78	0.97
Engine Mixture Ratio, LOX/Fuel	5.567	5.565	-0.002	-0.04

Specific impulse was slightly less than predicted. Engine burn time was 448.53 seconds which was 4.24 seconds less than predicted for the actual flight azimuth of 45.0 degrees. Of this difference -3.9 seconds was due to higher than predicted S-IVB thrust and flowrate.

The engine helium control system performed satisfactorily during main-stage operation. The engine control bottle was connected to the stage pneumatic supply bottle. An estimated 0.49 lbm of helium was consumed during burn.

#### 7.4 S-IVB SHUTDOWN TRANSIENT PERFORMANCE

S-IVB ECO was initiated at 592.93 seconds by guidance velocity cutoff command. The ECO transient was satisfactory. The total cutoff impulse to zero thrust was 42,484 lbf-s which was 1752 lbf-s lower than the nominal predicted value of 44,236 lbf-s and within the +5320 lbf-s predicted band. Cutoff occurred with the MRCV in the 4.8 EMR position.

IU platform accelerometer oscillations were reported during the cutoff transient about 0.5 second after cutoff command. These IU

oscillations occurred at the same time that oscillations were observed in chamber pressure (D0266-401) and S-IVB gimbal accelerometer data (A0012-401). The peak to peak amplitudes near Engine Cutoff (ECO) +0.5 second were 15 psi and 8.5 g for the chamber pressure and gimbal accelerometer, respectively. The frequency of the oscillations was 55 Hz. Review of previous S-IVB data indicates this condition is within previous flight experience. The oscillation frequency near ECO +0.5 second has varied from 50-75 Hz and the peak to peak amplitudes have varied from 8-45 psi for chamber pressure and 3.0 to 11.0 g for the gimbal accelerometer.

The most probable cause of the IU accelerometer activity is a resonant response to normal thrust chamber pressure oscillations during the cutoff transient which is transmitted through the stage to the IU. Further details are given in Sections 8.2.4 and 9.3.2.

### 7.5 S-IVB STAGE PROPELLANT MANAGEMENT

Comparison of propellant masses at critical flight events, as determined by various analyses, is presented in Table 7-2. The best estimate full load propellant mass for LOX is 195,170 +465 lbm and the best estimate full load propellant mass for LH<sub>2</sub> is 38,367 +186 lbm. The best estimate full load propellant masses were 0.07 percent less for LOX and 0.40 percent greater for LH<sub>2</sub> than predicted. This deviation was well within the required loading accuracy. The best estimate for propellant residuals at end of thrust decay were 2491 lbm for LOX and 2304 lbm for LH<sub>2</sub>. Cutoff transient propellant consumption was 60 lbm for LOX and 22 lbm for LH<sub>2</sub>.

Table 7-2. S-IVB Stage Propellant Mass History

EVENT	UNITS	PREDICTED		PROPELLANT UTILIZATION INDICATED (CORRECTED)		PROPELLANT UTILIZATION VOLUMETRIC		FLOW INTEGRAL		BEST ESTIMATE	
		LOX	LH <sub>2</sub>	LOX	LH <sub>2</sub>	LOX	LH <sub>2</sub>	LOX	LH <sub>2</sub>	LOX	LH <sub>2</sub>
S-IB Liftoff	lbm	195,334	38,216	195,225	38,297	195,053	38,229	195,252	38,495	195,170	38,367
S-IVB ESC	lbm	195,334	38,232	195,225	38,297	195,053	38,229	195,252	38,495	195,170	38,367
S-IVB Cutoff	lbm	3402	2059	2556	2361	2555	2358	2551	2326	2551	2326

The masses shown do not include mass below the main engine valves, as represented in Section 16.

Extrapolation of best estimate residuals data to depletion, using the propellant flow rates, indicated that a LOX depletion (532 lbm) would have occurred approximately 5.4 seconds after the velocity cutoff.

The pneumatically controlled two position MRCV was commanded to the 4.8 EMR engine start position 1.9 seconds prior to ESC. The MRCV does not respond until it receives engine pneumatic power which becomes available at ESC.

The MRCV was commanded to the closed position at ESC +6.0 seconds (approximately 5.5 EMR) and indicated closed at ESC +6.8 seconds. The MRCV was commanded to 4.8 EMR (open) position at ESC +325.4 seconds indicating open at ESC +325.6 seconds where it remained for the duration of powered flight.

The MRCV was commanded to the closed position at ECO +2.4 seconds. The MRCV indicated closed 447 milliseconds after the command was received. No further activities were planned for the MRCV during the rest of the mission.

## 7.6 S-IVB PRESSURIZATION SYSTEM

### 7.6.1 S-IVB Fuel Pressurization System

The LH<sub>2</sub> pressurization system met all of its operational requirements. The LH<sub>2</sub> pressurization system exhibited acceptable performance during prepressurization, boost, burn, earth orbit and deorbit.

The LH<sub>2</sub> tank prepressurization command was received at -119.4 seconds and the tank pressurized signal was received 33.1 seconds later. The ullage pressure reached relief conditions (approximately 31.7 psia) at liftoff, as shown in Figure 7-3.

The LH<sub>2</sub> ullage pressure was 31.4 psia at ESC. The average pressurization flowrate was 0.62 lbm/s until step pressurization, when it increased to 0.88 lbm/s. The total mass used for pressurization during burn was 314 lbm. Throughout the burn, the ullage pressure was at relief (31.6 psia), as predicted. LH<sub>2</sub> tank relief venting was accomplished by an open/close mode, rather than the usual "feathering" mode (see Section 7.10.1), until the venting requirement increased at step pressurization. The open/close venting mode had no effect on tank conditions or pressurization system performance.

The LH<sub>2</sub> pump inlet Net Positive Suction Pressure (NPSP) was calculated from the pump interface temperature and total pressure. These values indicated that the NPSP at STDV open was 13.8 psi. At the minimum point, the NPSP was 4.5 psi above the minimum required value. Throughout the burn, the NPSP had satisfactory agreement with the predicted values. Figure 7-4 summarizes the fuel pump inlet conditions during burn.

### 7.6.2 S-IVB LOX Pressurization System

LOX tank prepressurization was initiated at -167 seconds and increased the LOX tank ullage pressure from ambient to 40.0 psia in 13.2 seconds,

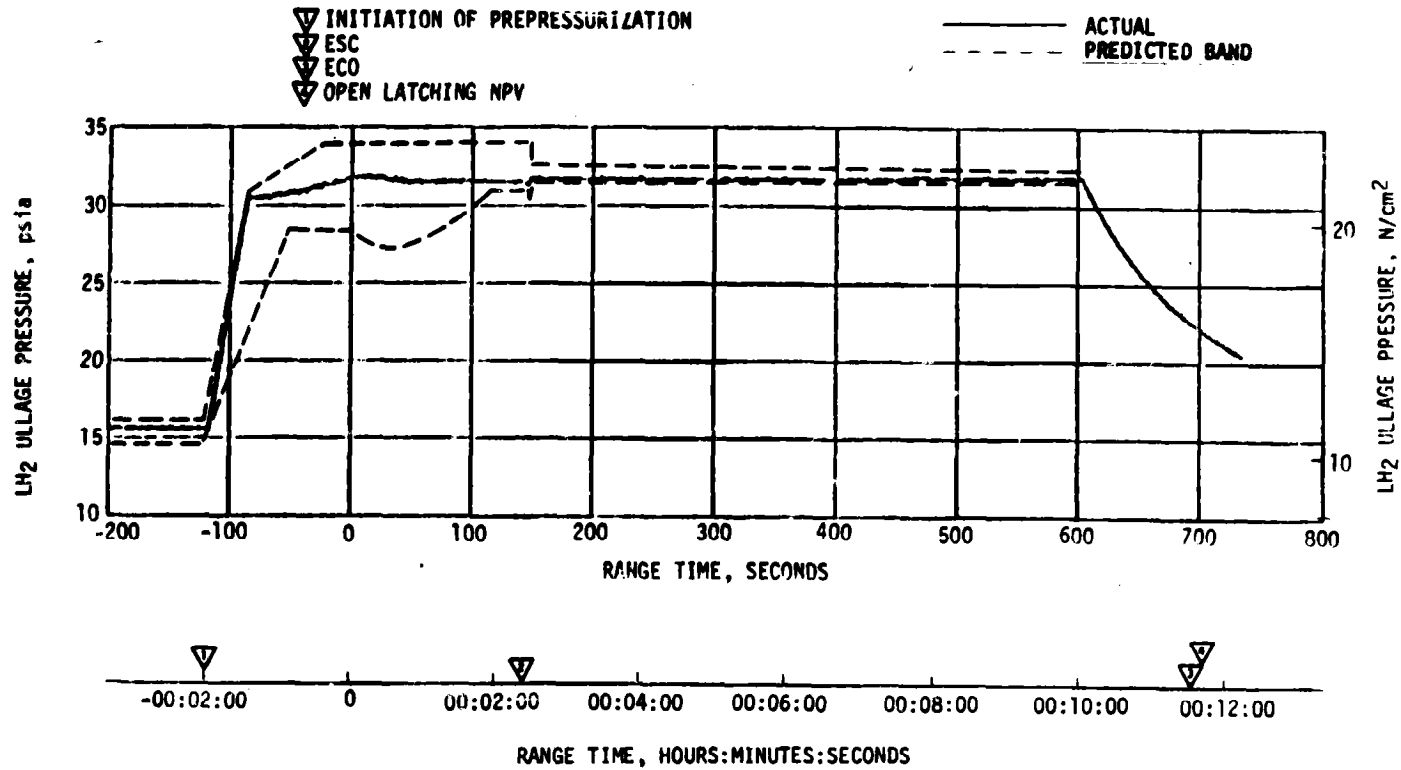


Figure 7-3. S-IVB LH<sub>2</sub> Ullage Pressure - Boost Phase

▽ S-IVB ESC  
 ▽ S-IVB STDV OPEN  
 ▽ S-IVB ECO

— ACTUAL  
 - - - PREDICTED

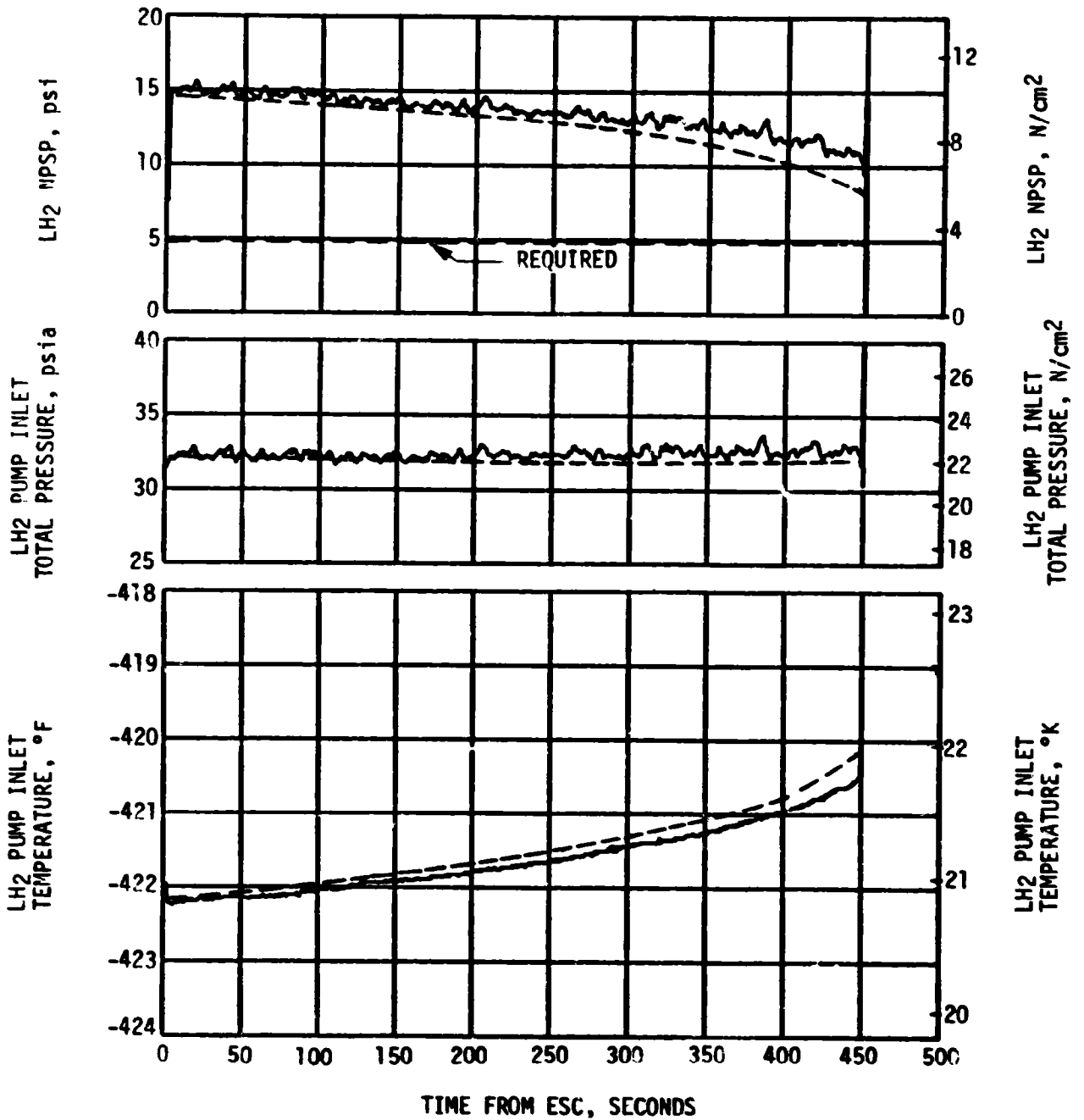


Figure 7-4. S-IVB Fuel Pump Inlet Conditions - Burn

as shown in Figure 7-5. One makeup cycle was required to maintain the LOX tank ullage pressure before the ullage temperature stabilized. A total of 4.61 lbm of helium were required for LOX tank prepressurization. At -119 seconds, fuel tank prepressurization and the vent valve purge caused the LOX tank pressure to increase from 37.8 to 41.0 psia at liftoff.

During boost there was a nominal rate of ullage pressure decay caused by tank volume increase (acceleration effect) and ullage temperature decrease. No makeup cycles could occur because of an inhibit from lift-off +6.0 seconds until ESC -2.5 seconds. LOX tank ullage pressure was 36.4 psia just prior to separation and was increasing at ESC due to a makeup cycle.

During burn, six over-control cycles were initiated, including the programmed over-control cycle initiated prior to ESC. The LOX tank prepressurization flowrate variation was 0.22 to 0.38 lbm/s during under-control and 0.35 to 0.49 lbm/s during over-control system operation. This variation is normal and is caused by temperature effects. Heat exchanger performance during burn was satisfactory.

The LOX NPSP calculated at the interface was 23.8 psi at ESC. This was 11.0 psi above the NPSP minimum requirement for start. The LOX pump static interface pressure during burn follows the cyclic trends of the LOX tank ullage pressure. Figure 7-6 summarizes the LOX pump conditions for burn. The LOX pump run requirements for burn were satisfactorily met.

The cold helium supply was adequate to meet all flight requirements. At ESC, the cold helium spheres contained 255 lbm of helium. At the end of burn, the helium mass had decreased to 96 lbm. Figure 7-7 shows helium supply pressure history.

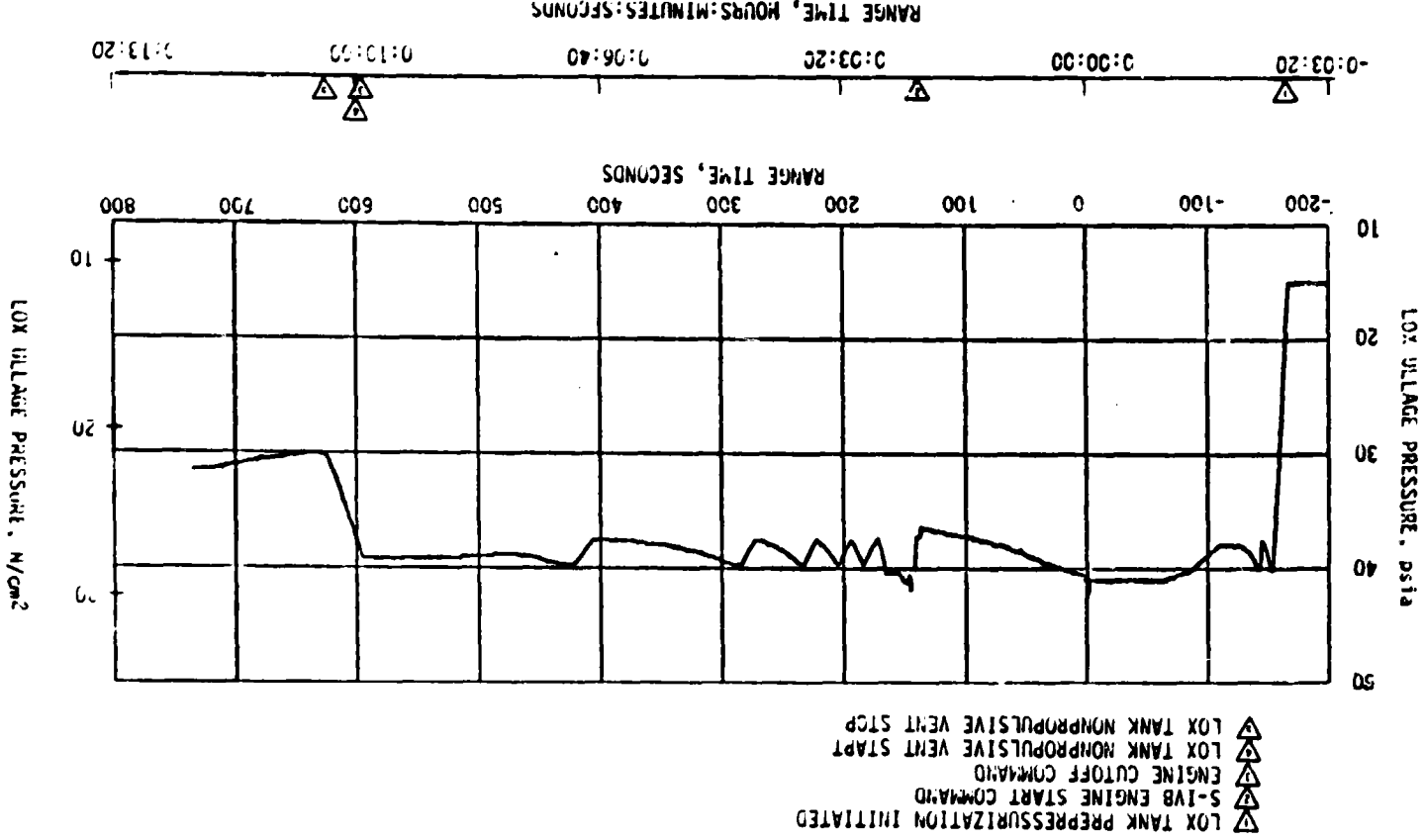
## 7.7 S-IVB PNEUMATIC CONTROL PRESSURE SYSTEM

The stage pneumatic system performed satisfactorily during all phases of the mission. During orbital coast, the pressure decreased from 2835 psia after the prevalues were open to 2430 psia at initiation of propellant dump for deorbit. This decrease was due to the continuous LOX chilldown motor container purge and a temperature decrease in orbit.

The stage pneumatic regulator performance was nominal with a near constant discharge pressure of 467 psia.

This was the second flight with a tie-in of the stage pneumatic sphere and the engine control sphere. The tie-in provides additional helium to hold the engine propellant valves open during dump. System performance was satisfactory with helium being transferred to the engine system during engine burn and propellant dump. The pneumatic sphere pressure at the end of propellant dump was 230 psia.

Figure 7-5. S-1VB LOX Tank Ullage Pressure - Boost Phase



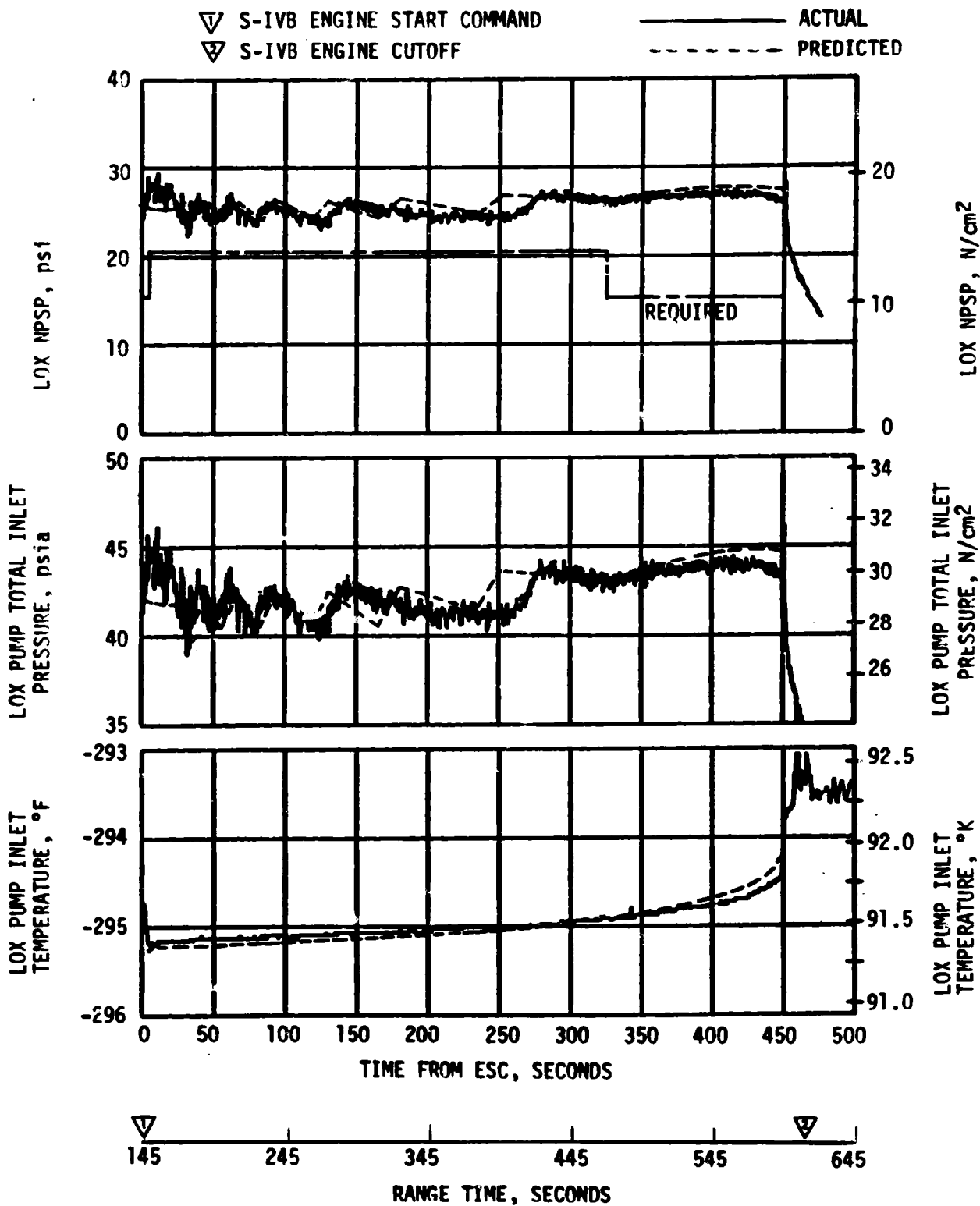


Figure 7-6. S-IVB LOX Pump Inlet Conditions - Burn

- ▽ S-IVB ESC
- ▽ S-IVB ECO
- ▽ START COLD HELIUM DUMP
- ▽ END COLD HELIUM DUMP

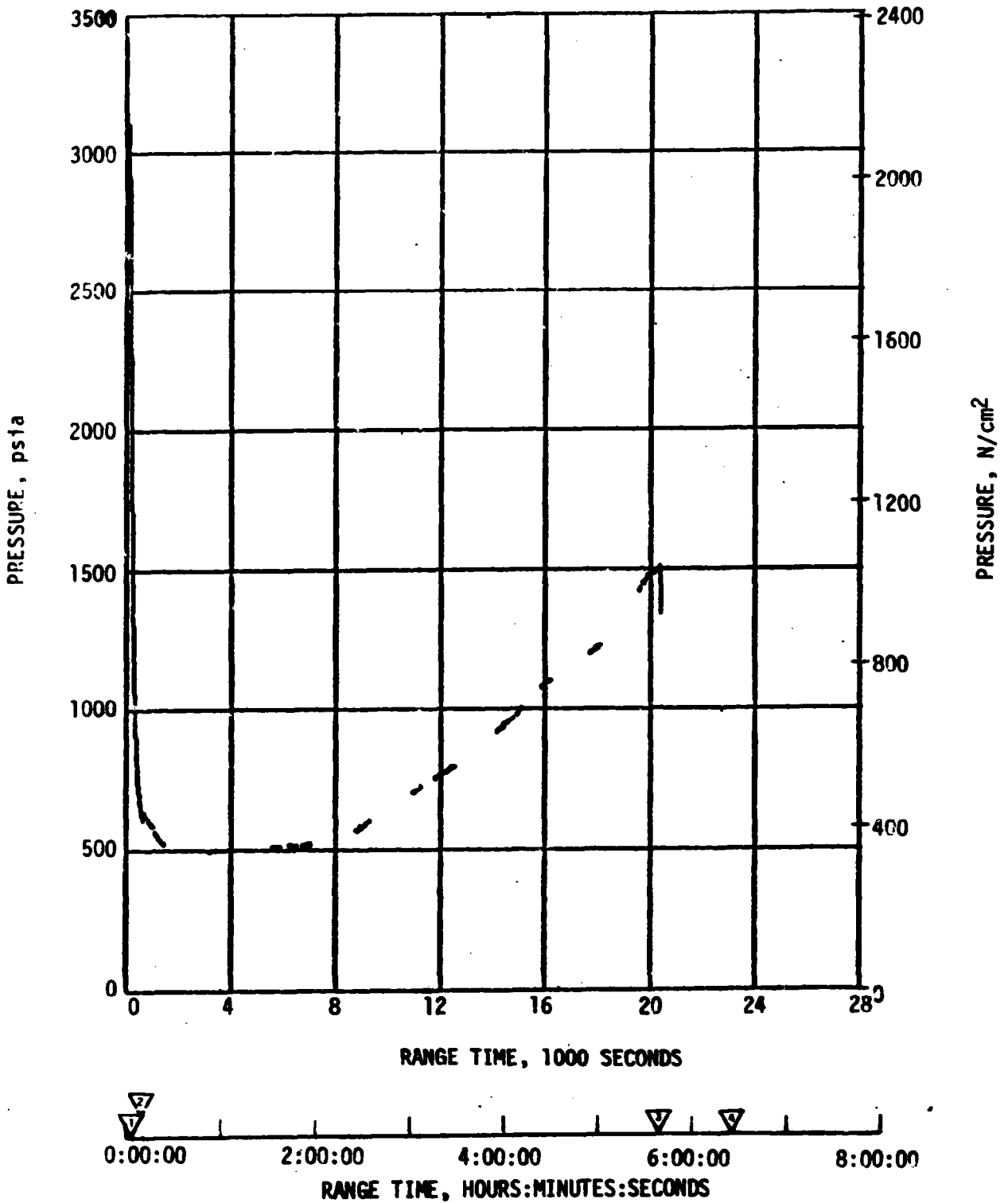


Figure 7-7. S-IVB Cold Helium Supply History

## 7.8 S-IVB AUXILIARY PROPULSION SYSTEM

The APS demonstrated nominal performance throughout the flight and met control system demands, as required through the deorbit sequence.

The Module 2 propellant usage exceeded predicted usage during orbital coast (Figure 7-8). The majority of the extra usage has been attributed to disturbances from the LH<sub>2</sub> NPV and IU sublimator as discussed in paragraph 10.3.2. The disturbances were within allowable tolerances. Neither disturbance was accounted for in the APS propellant usage prediction. The Module 1 propellant usage was nominal. Future flights will incorporate NPV and sublimator thrust perturbations in APS propellant usage predictions. Table 7-3 presents the APS propellant usage during specific portions of the mission. The oxidizer and fuel propellant supply systems performed as expected during the flight. The propellant temperatures ranged from 73°F to 95°F.

The APS pressurant system also functioned nominally. Module No. 1 regulator outlet pressure ranged from 193 to 194 psia. Module No. 2 regulator outlet pressure ranged from 194 to 196 psia.

The performance of the attitude control thrusters was nominal. The thruster chamber pressures ranged from 90 to 100 psia. The average specific impulse for the engines was approximately 200 lbf-sec/lbm.

## 7.9 S-IVB/IU STAGE DEORBIT PROPELLANT DUMP

All aspects of the S-IVB/IU deorbit were accomplished successfully. The impulse derived from the LOX and fuel dumps was sufficient to satisfactorily deorbit the S-IVB/IU. The total impulse provided, 104,000 lbf-sec, was in close agreement with the real time nominal predicted value of 103,500 lbf-sec. The sequence in which the propellant dumps were accomplished is presented in Figure 7-9.

The planned propellant tank safing during the stage passivation sequence following deorbit propellant dump was not accomplished. This was an expected result of the real time decision to extend the LH<sub>2</sub> dump duration to 590 seconds (compared to 125 seconds for SA-206) in order to improve ARIA coverage of deorbit dumps and Kwajalein coverage of stage re-entry. The requirement to hold the main fuel valve open during the extended LH<sub>2</sub> dump bleeds down the stage regulated pneumatic supply to about 230 psia. The propellant tank Non-Propulsive Vent (NPV) valves will actuate open with about 100 psia pneumatic pressure but require 280 psia to latch open. Therefore the NPV valves opened when commanded during the passivation sequence (20,293 seconds predicted time) but closed when the open command was removed a few seconds later. The safing of all stage high pressure storage bottles was accomplished during the passivation sequence according to the planned preflight sequence. Since the propellant tank pressure was reduced to low levels during the deorbit dumps the pressure was acceptably low following the passivation sequence even through normal tank safing was not accomplished.

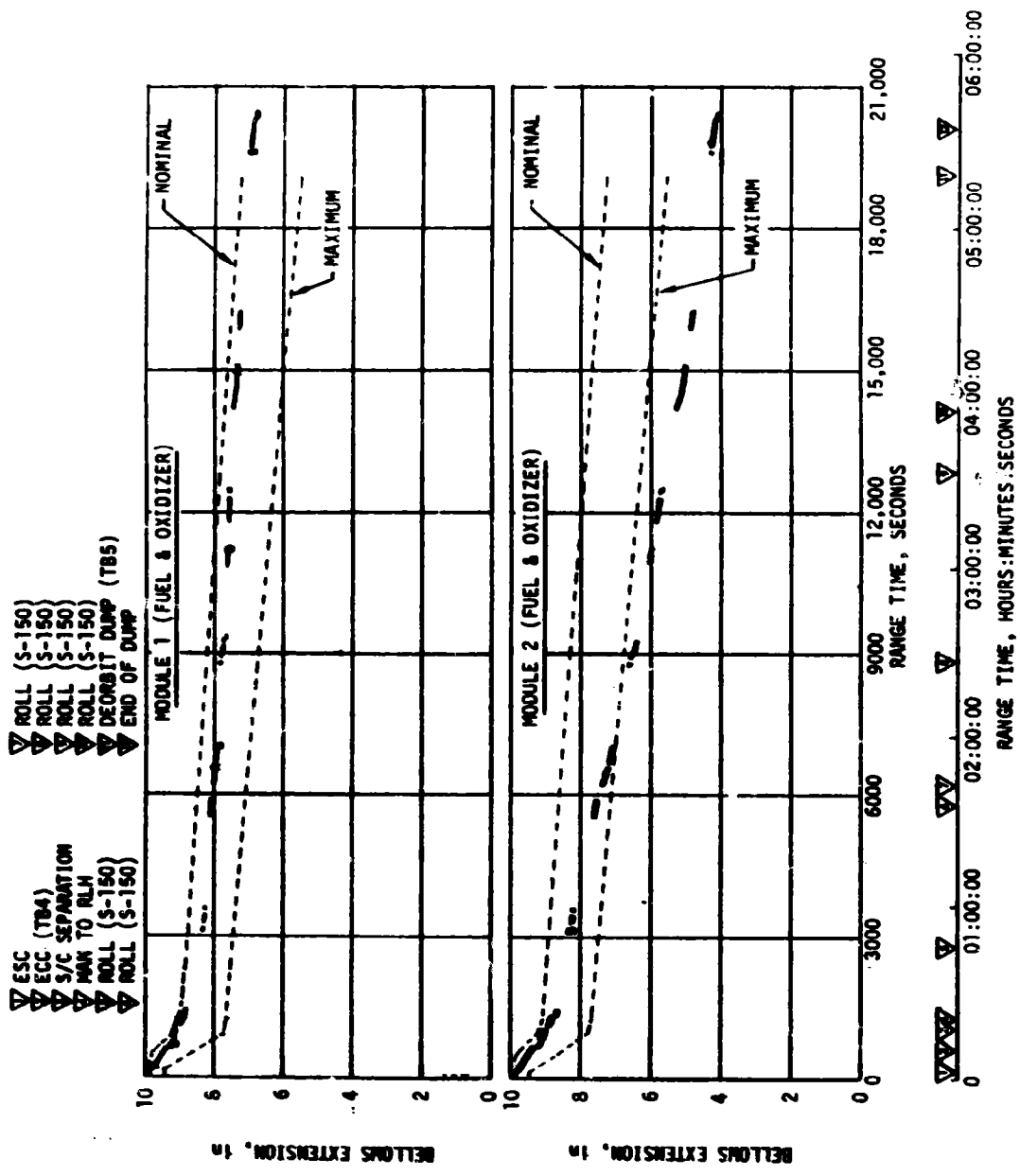


Figure 7-8. S-IVB APS Propellant Usage

Table 7-3. S-IVB APS Propellant Consumption

	MODULE NO. 1				MODULE NO. 2			
	OXIDIZER		FUEL		OXIDIZER		FUEL	
	LBM	PERCENT	LBM	PERCENT	LBM	PERCENT	LBM	PERCENT
Initial Load	39.4	—	23.9	—	39.4	—	23.9	—
Burn (Roll Control)	2.1	5.3	1.2	5.0	1.9	4.8	1.2	5.0
ECO to Spacecraft Separation	1.1	2.8	0.7	2.9	1.6	4.1	1.0	4.2
Spacecraft Separation to Maneuver to Retrograde Local Horizontal	1.2	3.0	0.7	2.9	0.9	2.3	0.5	2.1
Retrograde Local Horizontal (Orbital Coast)	6.7	17.0	4.3	18.0	17.5	44.4	10.8	45.4
Deorbit Dump (Roll Control)	0.8	2.0	0.5	2.1	0.7	1.8	0.4	1.7
End of Dump to 20469 sec.	0.3	0.8	0.2	0.8	0.3	0.8	0.2	0.8
Total Propellant Usage	12.2	30.9	7.6	31.7	22.9	58.2	14.1	59.1

The LOX dump was initiated at approximately 19,227 seconds (05:20:57) and was satisfactorily accomplished. Data were not available until approximately 19,545 seconds which was during the gas portion of the LOX dump. Dump performance was reconstructed for the period when data were not available including the liquid phase. Reconstructed and real-time predicted nominal LOX dump performance (total impulse, mass flow-rate, LOX tank mass and actual and real-time predicted LOX ullage pressure) are shown in Figure 7-10. The reconstruction corresponds to the best fit on available LOX ullage pressure flight data and the calculated velocity change (determined from LVDC accelerometer data) for LOX dump.

The LOX tank ullage pressure decreased from approximately 41.0 to 6.9 psia during the 445 second dump. The maximum negative bulkhead differential pressure following LOX dump was 25.1 psi which was within the allowable 26 psi limit. A reconstructed steady state LOX dump thrust of 809 lbf was attained. Ullage gas ingestion, based on the reconstruction, occurred at 19,275 seconds (05:21:15). LOX dump ended at approximately 19,672 seconds (05:27:52) by closing the Main Oxidizer Valve (MOV).

The reconstructed total impulse before MOV closure was 72,200 lbf-sec, as compared to real time predicted total impulse of 72,000 lbf-sec. The close agreement between the real time predicted and reconstructed total impulse is attributed to the compensating effects of higher than

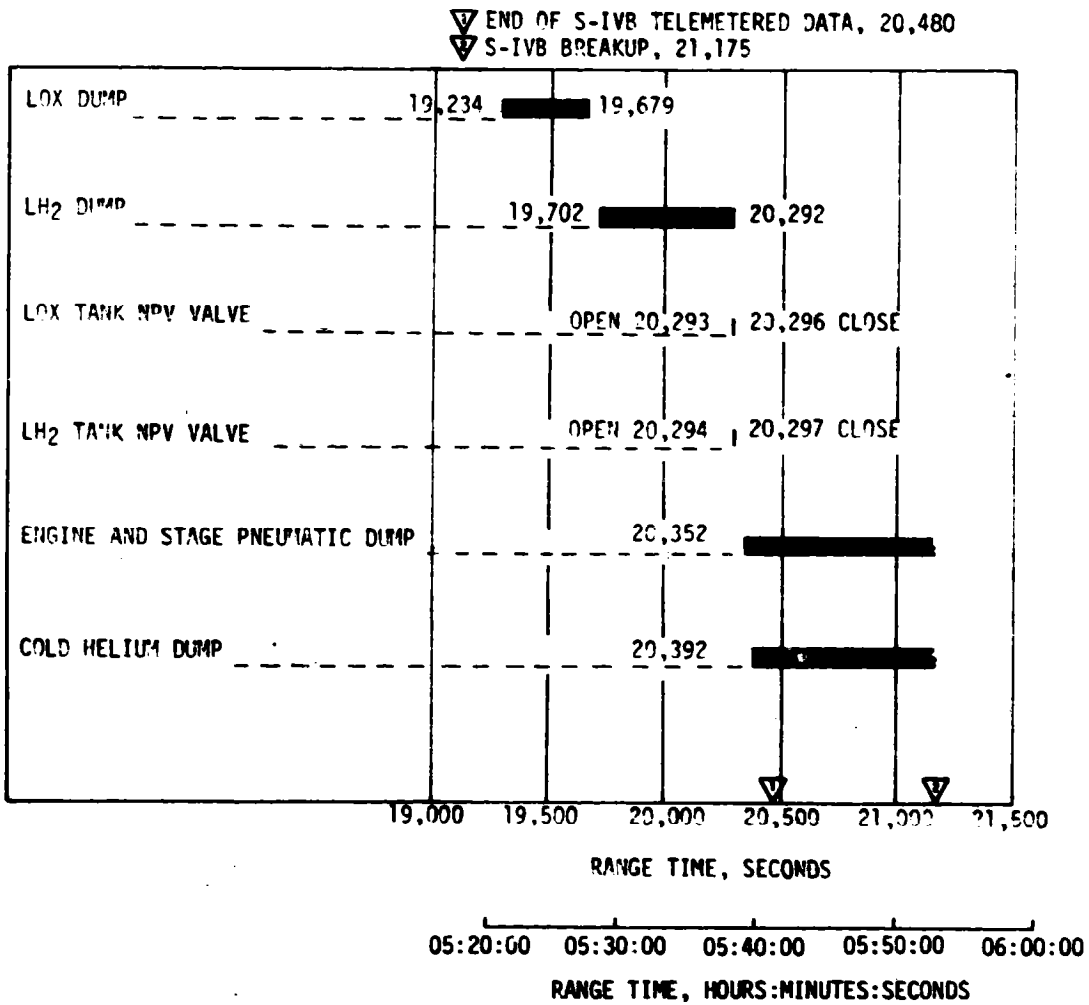


Figure 7-9. S-IVB Deorbit Propellant Dump and Safing Sequence

predicted nominal specific impulse and lower than predicted LOX mass at end of thrust decay. The reconstructed specific impulse during the liquid portion of the dump was 7% higher than predicted, but within the predicted limits. LVDC accelerometer data indicates an S-IVB stage velocity change of 71.46 ft/sec from LOX dump.

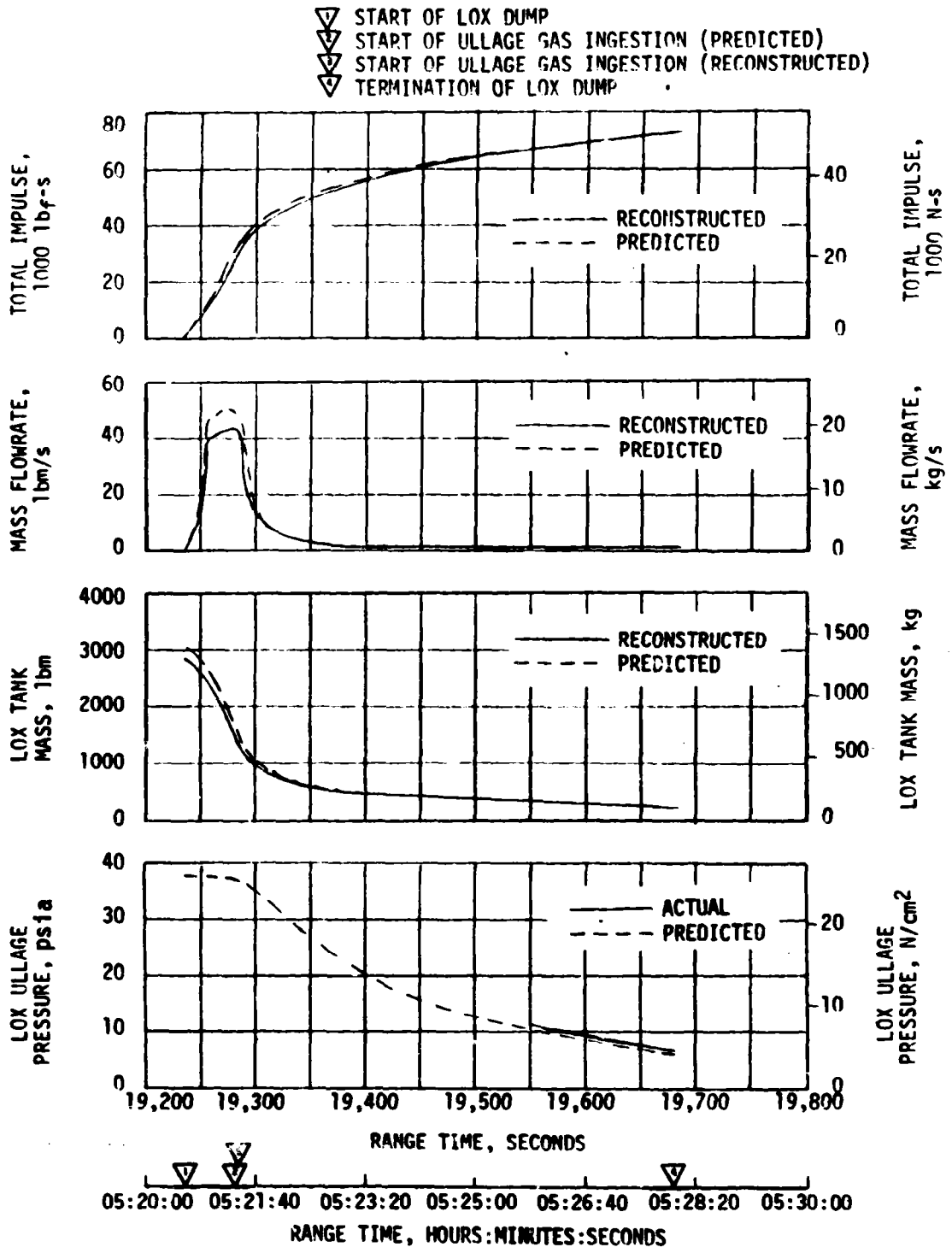


Figure 7-10. S-IVB LOX Dump

Fuel dump was initiated at 19,702 seconds (5:28:22) and was satisfactorily accomplished. Fuel dump impulse, flowrate, mass remaining in fuel tank, and ullage pressure are shown in Figure 7-11. Only GH<sub>2</sub> remained in the tank at dump start. The LH<sub>2</sub> completely boiled off during orbital coast. A reconstruction of dump indicates the dump impulse, 31,800 lbf-sec, was in good agreement with the real time nominal predicted value of 31,500 lbf-sec. The ullage mass at the start of the dump was 343 lbm. Approximately 205 lbm of gaseous hydrogen were dumped through the J-2 engine. The ullage pressure decreased from 32.0 to 7.2 psia during the dump. The dump terminated at 20,292 seconds (5:38:12) when the main fuel valve (MFV) was closed. LVDC accelerometer data indicates the S-IVB stage velocity change due to fuel dump was 32.71 ft/sec.

## 7.10 S-IVB ORBITAL COAST AND SAFING

### 7.10.1 Fuel Tank Orbital Coast and Safing

The fuel tank nonpropulsive vent system satisfactorily controlled the ullage pressure during earth orbit, as shown in Figure 7-12. A 670-second fuel tank vent, initiated at ECO +10.6 seconds, lowered the ullage pressure from 31.8 to 10.9 psia. NPV system data indicate that liquid hydrogen was vented, as expected, during the last 150 seconds of the programmed vent. Liquid venting, which begins about 45 seconds after spacecraft separation, results from the increase in drag experienced after separation. The increased drag forces the LH<sub>2</sub> residual to the top of the tank, near the vent inlet. The liquid venting did not significantly affect fuel dump impulse capability or mission accomplishment.

After the programmed vent the LH<sub>2</sub> tank reached relief at approximately 3250 seconds (0:54:10). Relief venting of the LH<sub>2</sub> tank occurred during most of the mission by an open/close mode as opposed to the usual "feathering" mode of the LH<sub>2</sub> latching valve. This is verified by both the NPV nozzle pressures and the valve closed indication microswitch. A possible explanation of this mode of operation is a more than nominal static friction or "stickiness" of the latching valve pilot poppet. Normally the pilot would open gradually, increasing its stroke with increasing ullage pressure, until enough flow is provided to cause the main poppet to unseat. Increased static friction would delay the pilot opening and cause the ullage pressure to rise slightly in order to overcome this additional force. The pilot, when unseated, would immediately assume a position which would allow sufficient flow to open the main poppet. Reseat of the pilot would occur as the ullage pressure decreased. This establishes an open/close mode of operation. The cycle length was of the order of 10 seconds or more, and is mainly a function of the venting requirements. The venting mode experienced had no effect on tank conditions or mission accomplishment.

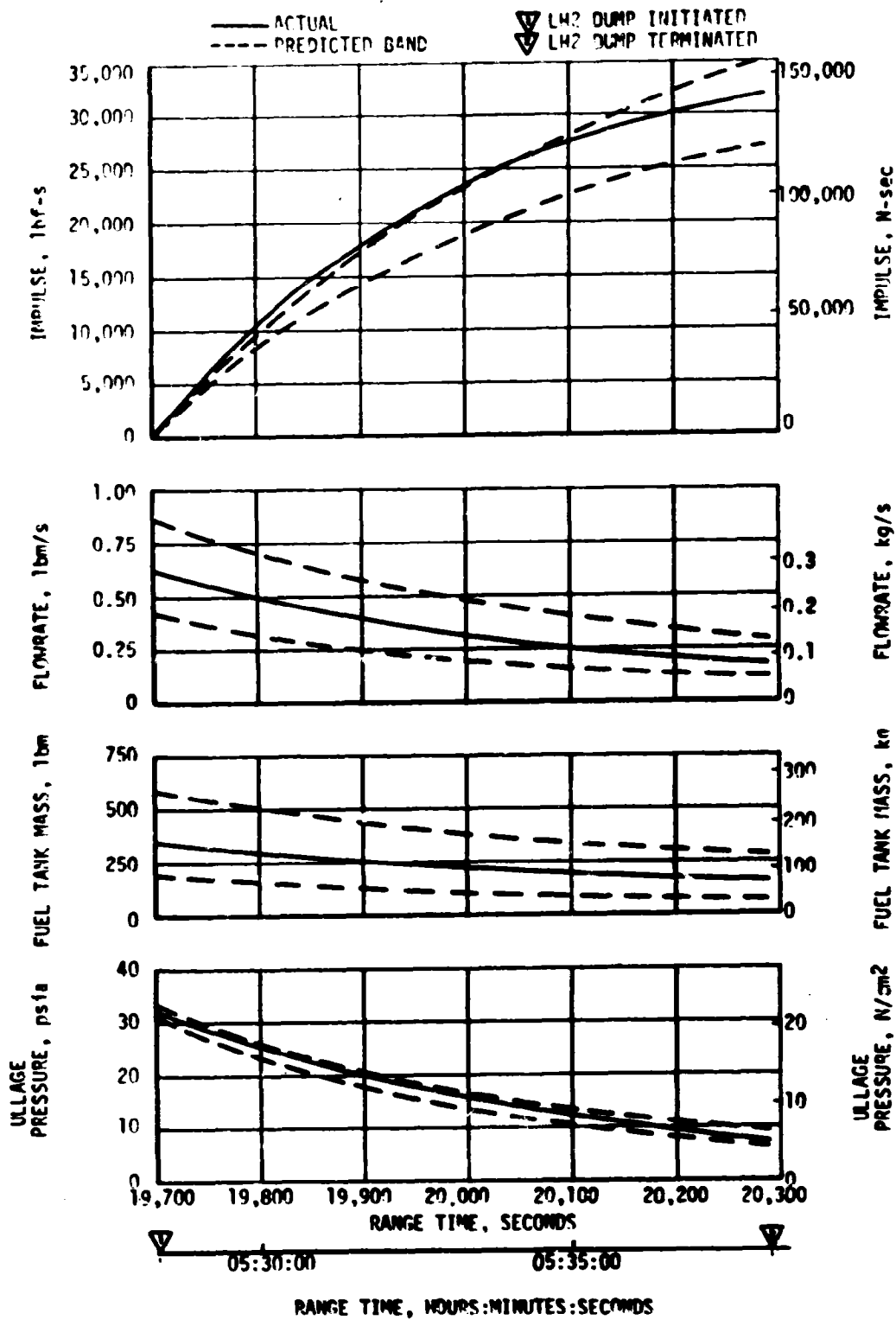


Figure 7-11. S-IVB LH<sub>2</sub> Dump

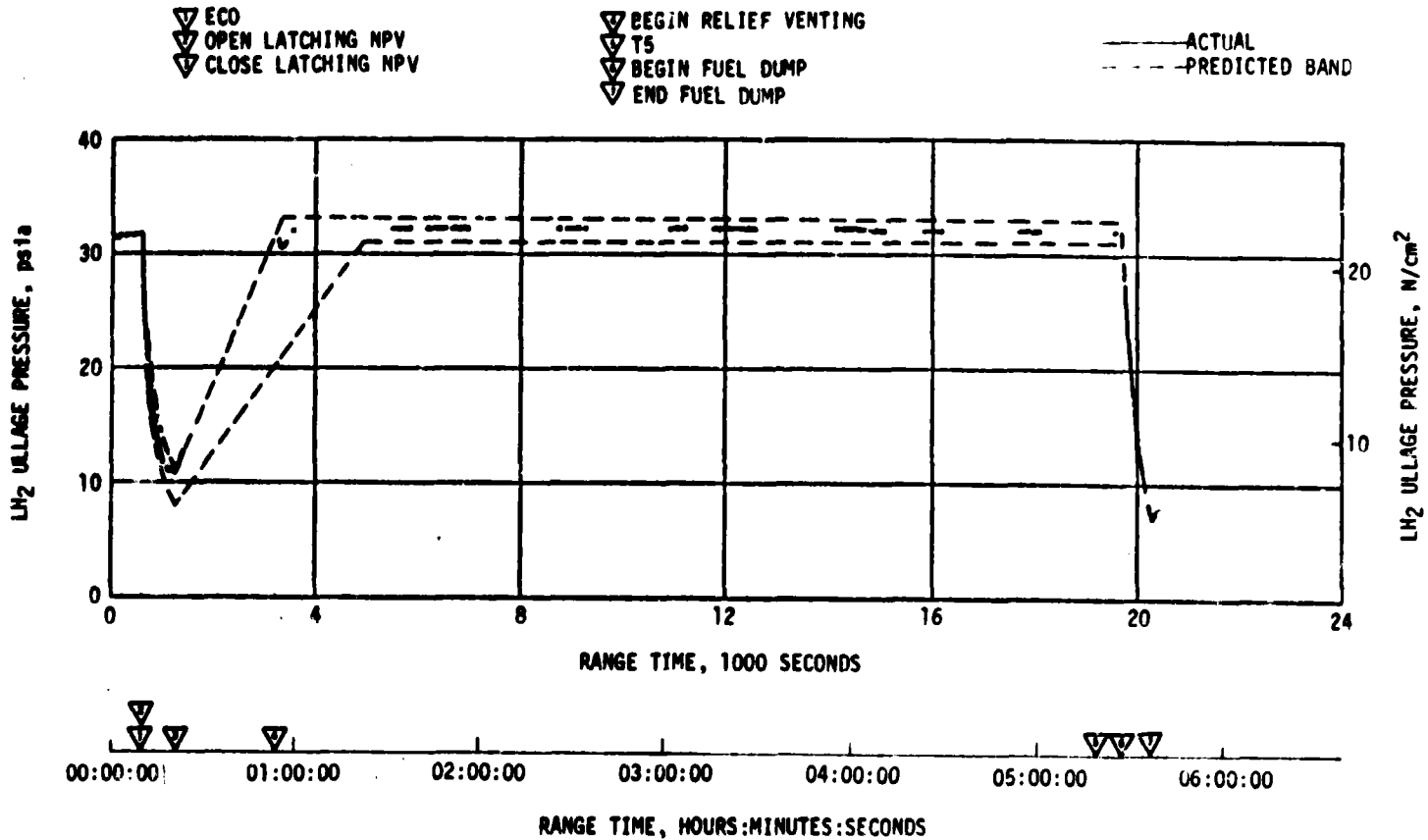


Figure 7-12. S-IVB LH<sub>2</sub> Ullage Pressure - Orbital Coast

A real time decision was made to extend the fuel dump (see Section 7.9) resulting in low stage pneumatic pressure at the end of dump. As expected, the LH<sub>2</sub> latching vent valve did not latch open at 20,293 seconds (5:38:13) and consequently closed when the open command was removed after three seconds. There was no decrease in ullage pressure during the three-second vent interval. The LH<sub>2</sub> ullage pressure increased from 7.2 psia at the end of LH<sub>2</sub> dump (5:38:12) to 8 psia at loss of data (5:41:40). No excessive fuel tank pressures resulted from the failure of the vent valve to latch open.

#### 7.10.2 LOX Tank Orbital Coast and Safing

A programmed 30 second nonpropulsive vent (NPV) starting at 594 seconds (00:09:54) was satisfactorily accomplished. During the vent, LOX tank pressure decreased from 39.0 psia to 29.9 psia (Figure 7-13). Reconstruction of the pressure history during the vent indicates that approximately 30 lbm of gas was vented including 25 lbm of helium and 5 lbm of GOX. At the termination of venting, the ullage consisted of approximately 197 lbm of GOX and 138 lbm of helium.

During orbital coast, the LOX tank pressure increased due to tank heating and liquid boiloff. The pressure stayed within the predicted band (Figure 7-13).

LOX tank safing was not accomplished due to a real time decision to extend the LH<sub>2</sub> dump duration and the subsequent loss of pneumatic pressure as discussed in Section 7.9. As a result of the low pneumatic pressure, the LOX NPV valve did not latch open at 20,293 second (05:38:13) and consequently closed when the open command was removed after three seconds. During these three seconds approximately 1.0 lbm of ullage gas was vented overboard with no detectable change in tank pressure. NPV system nozzle temperature and pressure response was nominal. The tank pressure then increased as a result of cold helium dump from 8.1 psia at 20,392 seconds (05:39:52) to 15.5 psia at data loss 67 seconds later (Figure 7-13). No excessive LOX tank pressure resulted from the failure of the NPV to latch open.

#### 7.10.3 Cold Helium Dump

The cold helium supply was safed by dumping the helium into the LOX tank (see Section 7.10.2). The dump was initiated at 20,392 seconds (5:39:52) and was programmed to continue for 2800 seconds. At loss of data, 67 seconds into dump, the cold helium pressure was approximately 750 psia.

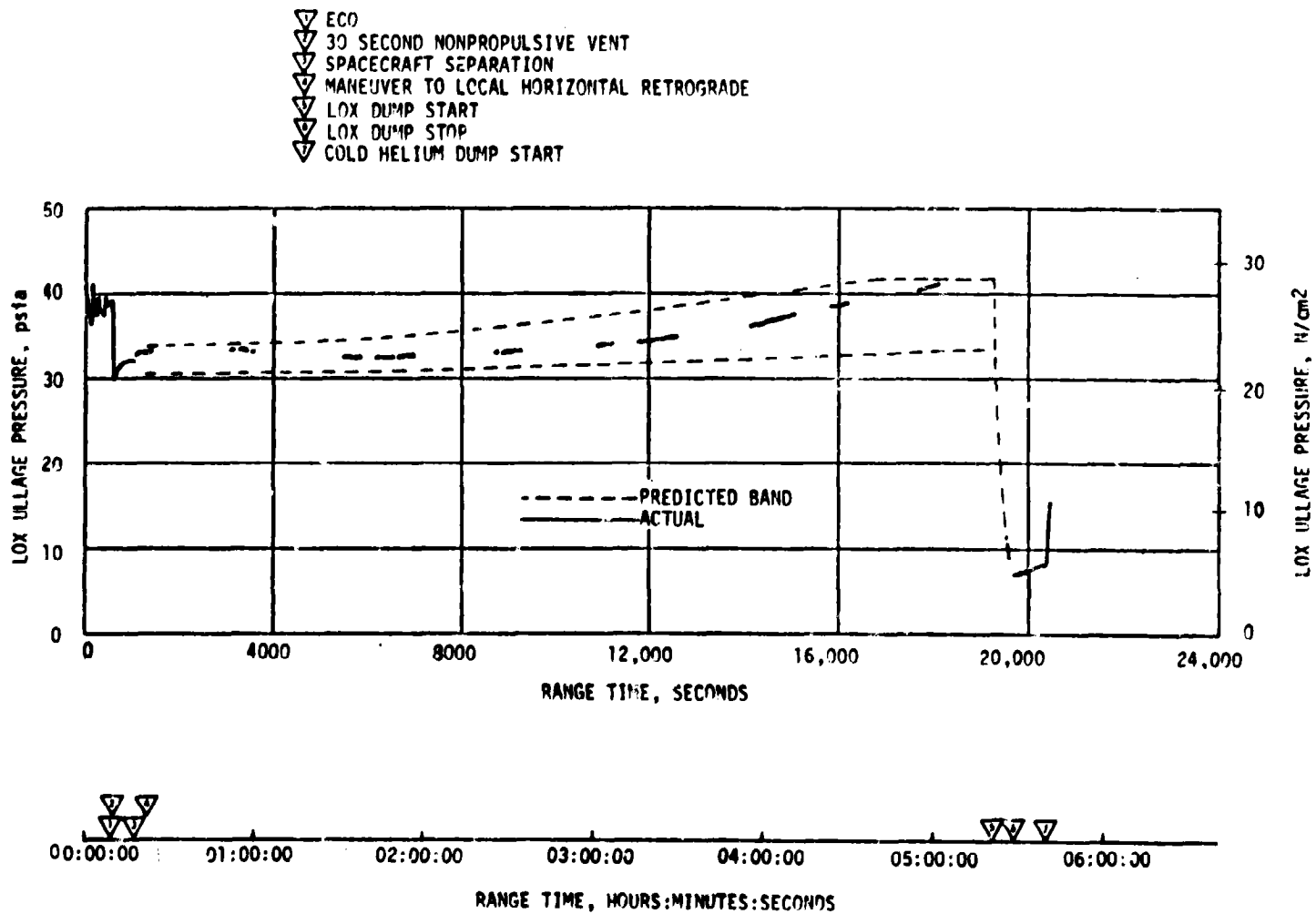


Figure 7-13. S-IVB LOX Tank Ullage Pressure - Orbit, Dump, and Safing

#### 7.10.4 Stage Pneumatic Control and Engine Control Sphere Safing

The interconnection between the stage pneumatic and engine control spheres permitted simultaneous safing of both spheres through the engine purge system. Safing was accomplished by energizing the engine helium control solenoid. Safing was initiated at 20,352 seconds (5:39:12) with a stage sphere pressure of 230 psia. At loss of stage sphere data, 107 seconds into safing, the stage sphere pressure was 175 psia. The engine sphere pressure decreased from approximately 150 psia at initiation of safing to approximately 75 psia at the last available engine sphere data 20,459 seconds; (5:41:39).

#### 7.11 S-IVB HYDRAULIC SYSTEM

The S-IVB hydraulic system performed within the predicted limits after liftoff with no overboard venting of system fluid as a result of hydraulic fluid expansion. Prior to start of propellant loading, the accumulator was precharged to 2450 psia at 85°F. Reservoir oil level (auxiliary pump off) was 90 percent at 84°F.

The auxiliary hydraulic pump was programmed to flight mode "ON" at T-11 minutes. System pressure stabilized at 3650 psia and remained steady. During boost, all system fluid temperatures rose steadily when the auxiliary pump was operating and convection cooling was decreasing. At S-IVB engine start, system pressure increased to 3655 psia and remained steady through the burn period.

System internal leakage rate, 0.50 gal/min (0.4 to 0.8 gpm allowable), was provided for primarily by the auxiliary pump during engine burn as characterized by the auxiliary pump motor current draw. At engine start, and during engine burn system pressure and reservoir pressure histories indicate proper operation of both the auxiliary and engine driven hydraulic pumps.

Prior to engine start, the yaw actuator indicated an offset from zero of +0.24 degree while the pitch actuator indicated -0.10 degrees. While the shift in actuator position is slightly more than noted on previous flights, it is well within an allowable error of 0.40 degrees. The allowable error is based on the null bias and hysteresis effects of the actuator assembly. Actuator positions were offset from null during S-IVB powered flight due to the displacement of the vehicle's center of gravity off the vehicle's vertical axis, the J-2 engine installation tolerances, thrust misalignment, uncompensated gimbal clearances, and thrust structure compression effects.

Following J-2 engine cutoff and prior to the auxiliary hydraulic pump off, the actuators extended beyond the null position indicated prior to J-2 engine start (Figure 7-14). Data review indicated that a valve current bias of .75 to 1.0 milliamps corresponded to the shift in actuator position from the original null positions.

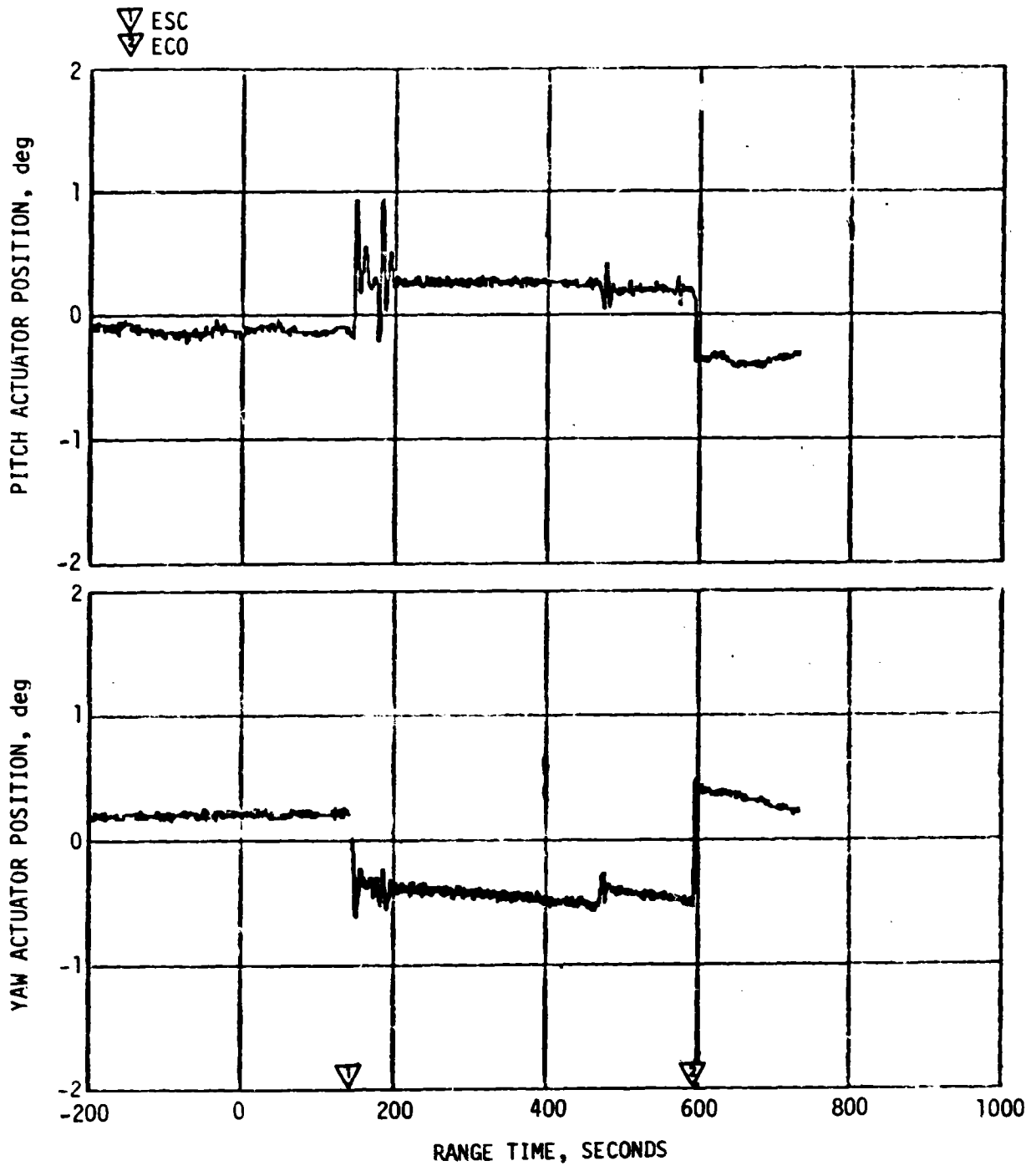


Figure 7-14. S-IVB Hydraulic System - Boost

Pitch actuator oscillations were noted during prelaunch, S-IB boost and orbital coast thermal cycling when the Thrust Vector Control system was inactive. These oscillations were of low amplitude (0.1 to 0.2 degree p-p) and exhibited periods of 100 seconds, 25 seconds and 12 to 20 seconds, respectively. See paragraph 10.3.2.1 for further discussion.

The most probable cause for the actuator motion observed was hunting of the actuator servovalve spool due to increased static friction (stiction) caused by contaminants trapped between the lapped surfaces of the spool and bushing. The servovalve spools are protected by filters which are designed to trap 98 percent of all particles over 5 microns and 100 percent of all particles over 15 microns. However, the flow spool lapped clearance can be less than the filter's absolute rating. Thus, the flow spool is subject to entrapment of microscopic particles between the lapped surfaces which results in spool "stiction." With the spool at its centered position the phenomena of "silting" (buildup of fine particles) at the lapped clearances can be expected to decrease valve leakage. Spool stiction and a decrease in internal leakage were evident from the observed data. The magnitude of erratic actuator motion indicates that less than eight percent of available spool driving force was required to overcome the maximum stiction encountered and therefore this does not represent a control problem. A discussion of the effects of spool stiction on the control system is contained in Section 10.3.2.

Available data during orbital coast indicated all other system measurements indicated nominal system performance. During deorbit, system pressure stabilized at 3650 psia and remained steady. The actuator responded normally to commands during the deorbit phase. The maximum inlet oil temperature noted during this period was 140°F. The actuator oscillation noted during prelaunch, S-IB boost, and orbital coast did not affect hydraulic system performance, and therefore no corrective action is planned.

## SECTION 8

### STRUCTURES

#### 8.1 SUMMARY

The structural loads experienced during the SA-207 flight were well below design values. The maximum bending moment was  $10.6 \times 10^6$  in-lbf (approximately 19 percent of design) at vehicle station 942. The S-IB thrust cutoff transients experienced by SA-207 were smaller than those of SA-206. The S-IVB engine cutoff transient produced oscillations on the gimbal block of 4.25  $\sigma$  peak amplitude with a predominant frequency of 55 Hz. Although this transient exceeded that of SA-206 it was well within the envelope experienced on Saturn V flights.

The maximum ground wind experienced by the Saturn IB SA-207 during the prelaunch period was 14 knots (allowable with damper, 55 knots). The ground winds at launch were 13.5 knots from the west (allowable at launch 38 knots).

#### 8.2 TOTAL VEHICLE STRUCTURES EVALUATION

##### 8.2.1 Longitudinal Loads

The SA-207 vehicle liftoff steady-state acceleration was 1.25 g. Maximum longitudinal dynamic response measured during thrust buildup and release was +0.20 g at the Instrument Unit (IU) and +0.80 g at the Command Module (CM) (Figure 8-1). The SA-206 recorded +0.20 g and +0.60 g, respectively, for the thrust buildup dynamic responses.

The SA-207 Inboard Engine Cutoff (IECO) and Outboard Engine Cutoff (OECO) transient responses were equal to or less than those of previous flights. The maximum longitudinal dynamics resulting from IECO were +0.1 g at the IU and +0.25 g at the CM (Figure 8-2).

The total longitudinal load at station 942, based on strain data, is shown in Figure 8-3 as a function of range time. The envelope of previous flights (S-IB vehicles SA-202 through SA-206) is shown for comparison. The maximum longitudinal load of  $1.37 \times 10^6$  lbf occurred at IECO and was well within design limit capability. The longitudinal load distribution at the time of maximum bending moment (67.2 seconds) and IECO (137.4 seconds) are shown in Figure 8-4. The steady state longitudinal accelerations at these time slices were 1.87 g and 4.35 g, respectively.

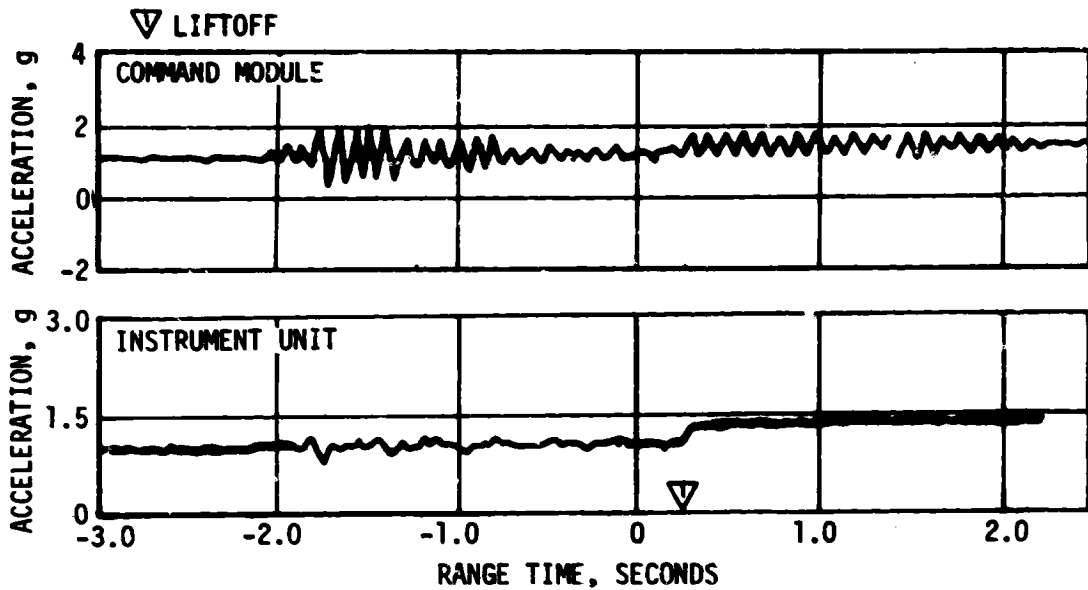


Figure 8-1. SA-207 Longitudinal Accelerations at IU and CM During Thrust Buildup and Launch

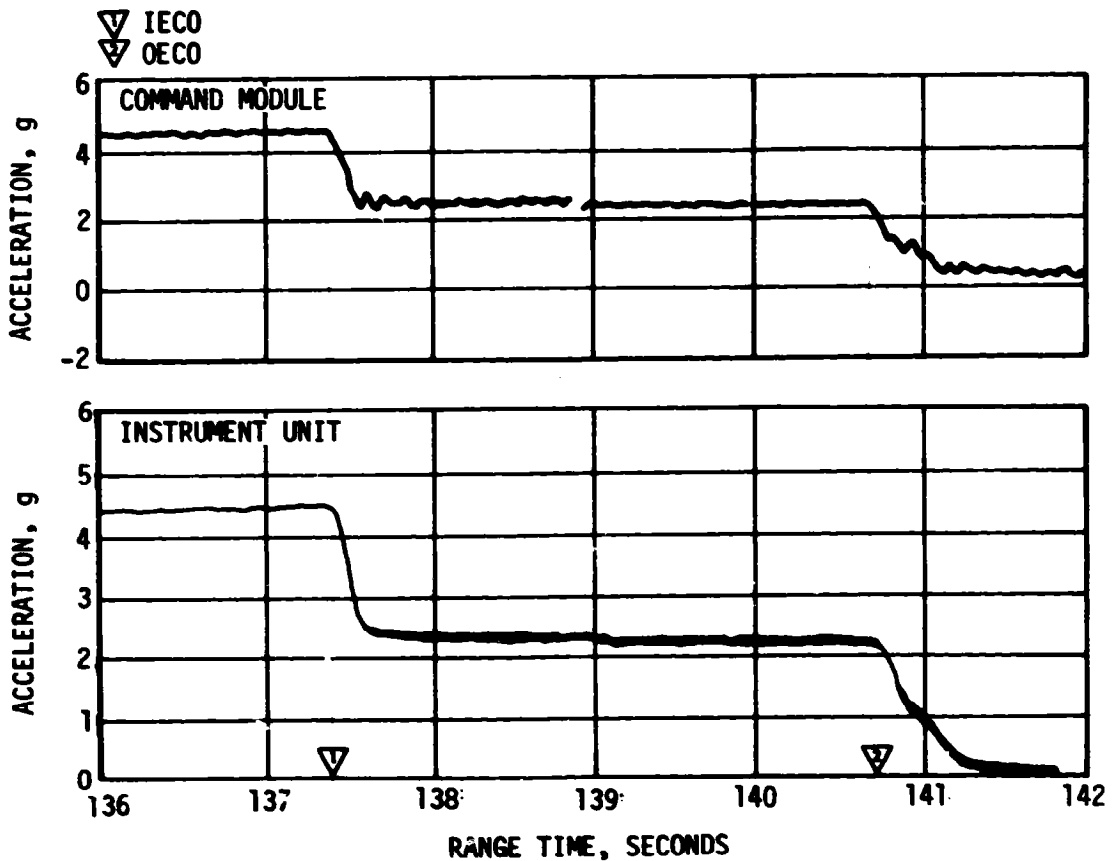


Figure 8-2. SA-207 Longitudinal Acceleration at the IU and CM During S-IB Cutoff

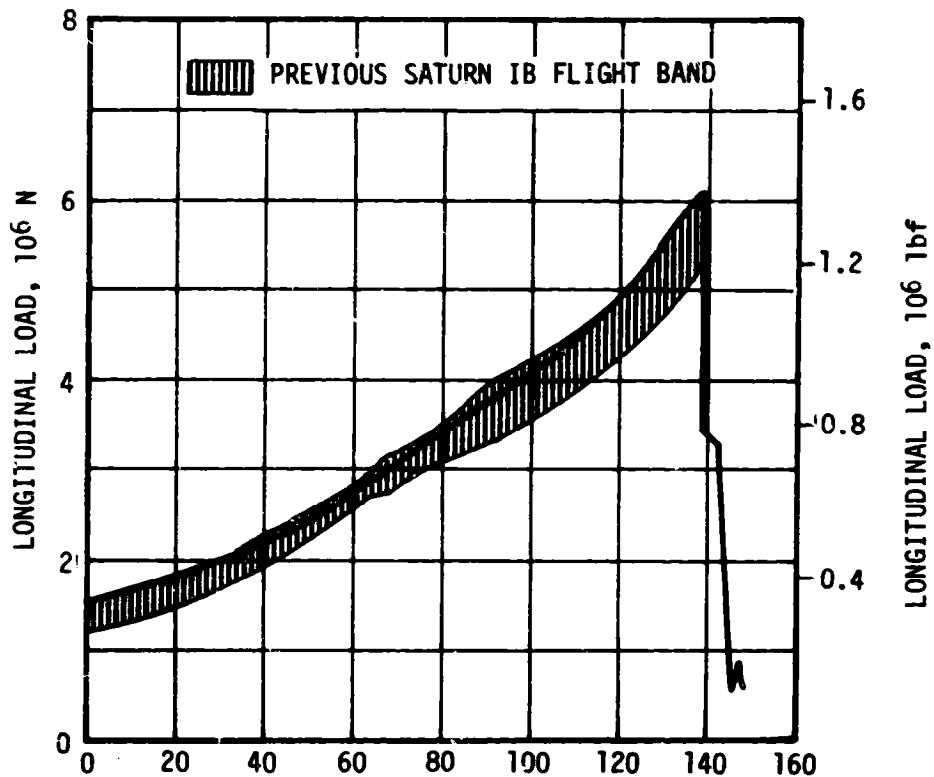


Figure 8-3. S-IB-7 Longitudinal Load from Strain Data at Station 942

### 8.2.2 Bending Moments

The maximum flight bending moment of  $10.7 \times 10^6$  in-lbf occurred at 67.2 seconds. This value was derived from the eight LOX stud strain gage measurements (at station 942) corrected to include the bending moment carried by the center LOX tank which was not instrumented.

The measured flight bending moment, the bending moment distribution (calculated from post flight vehicle mass data and flight trajectory configuration), and the lateral acceleration distribution (normal load factors) are displayed in Figures 8-5 through 8-7. There were no significant lateral modal dynamics contributing to the vehicle bending moment.

### 8.2.3 Combined Loads

Combined compression and tension loads were computed for maximum bending moment (67.2 seconds) and engine cutoff (IECO) conditions using measured S-IVB hydrogen ullage pressure (32.0 psig). An envelope of these results

⊙ STRAIN DATA

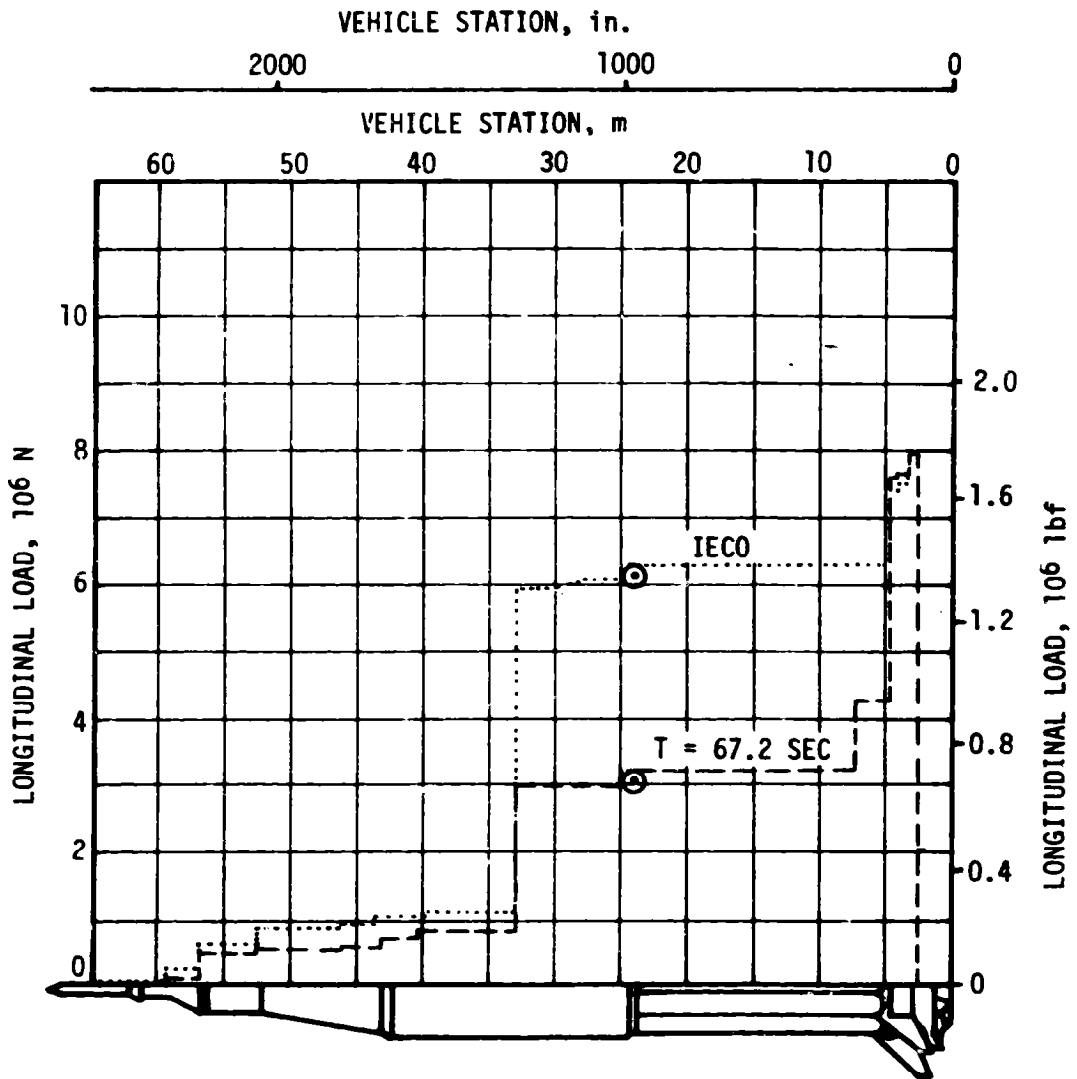


Figure 8-4. SA-207 Longitudinal Load Distribution at Time of Maximum Bending Moment and IECO

**CONDITIONS:**

T = 67.2 SECONDS  
 M = 1.36  
 q = 4.843 PSI  
 α = 0.95 DEGREES  
 β = 0 DEGREES

**LEGEND:**

⊙ BENDING MOMENT  
 DERIVED FROM  
 STRAIN DATA  
 ⬡ DESIGN CRITERION  
 BENDING MOMENT

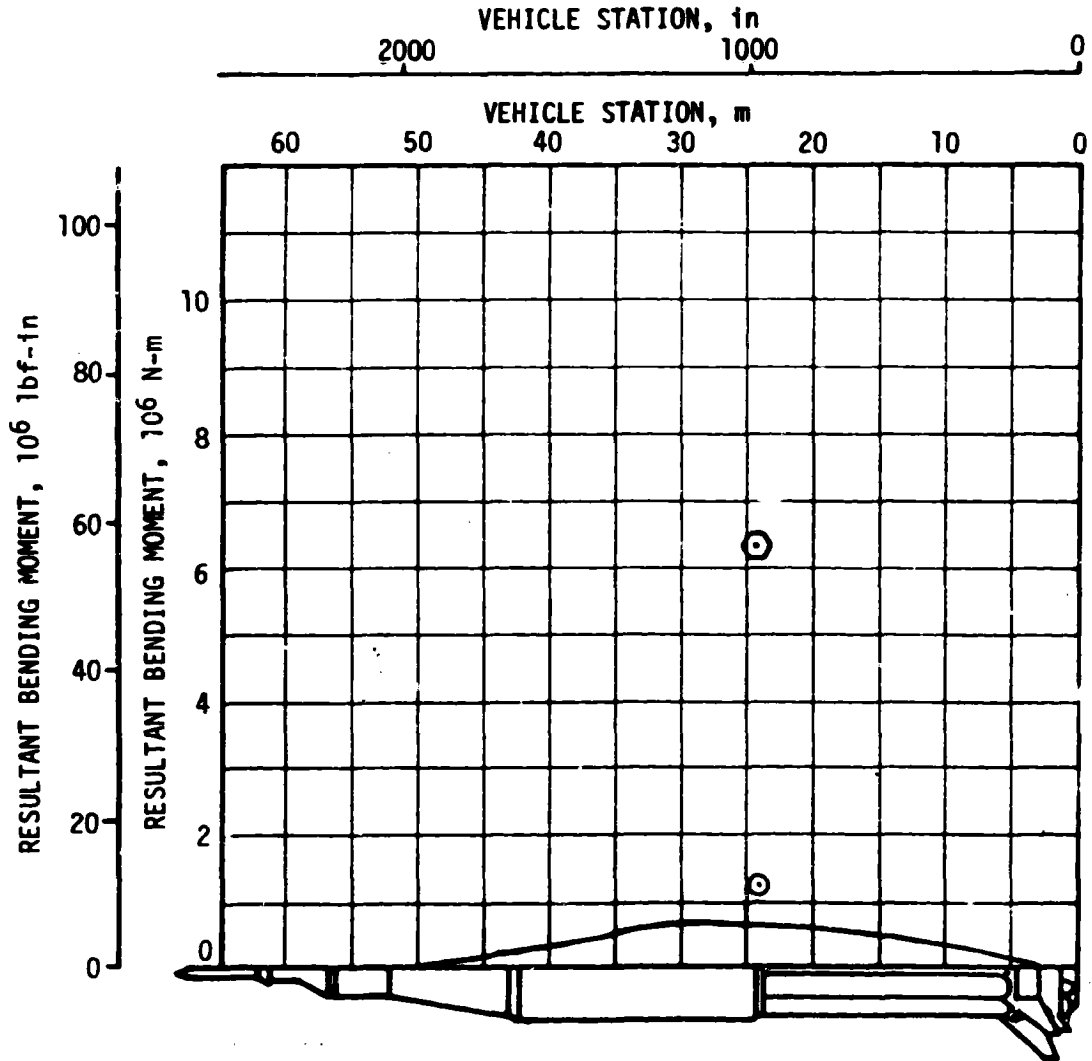


Figure 8-5. SA-207 Resultant Bending Moment Distribution at Time of Maximum Resultant Moment

CONDITIONS:

T = 67.2 SECONDS  
 M = 1.36  
 q = 4.843 PSI  
 $\alpha_p = 0.90$  DEGREES  
 $\beta_p = 0.65$  DEGREES

LEGEND:

- ⊙ BENDING MOMENT DERIVED FROM STRAIN DATA
- ▽ A4-601 ACCELEROMETER DATA
- CENTER OF GRAVITY
- ⊕ DESIGN CRITERION BENDING MOMENT

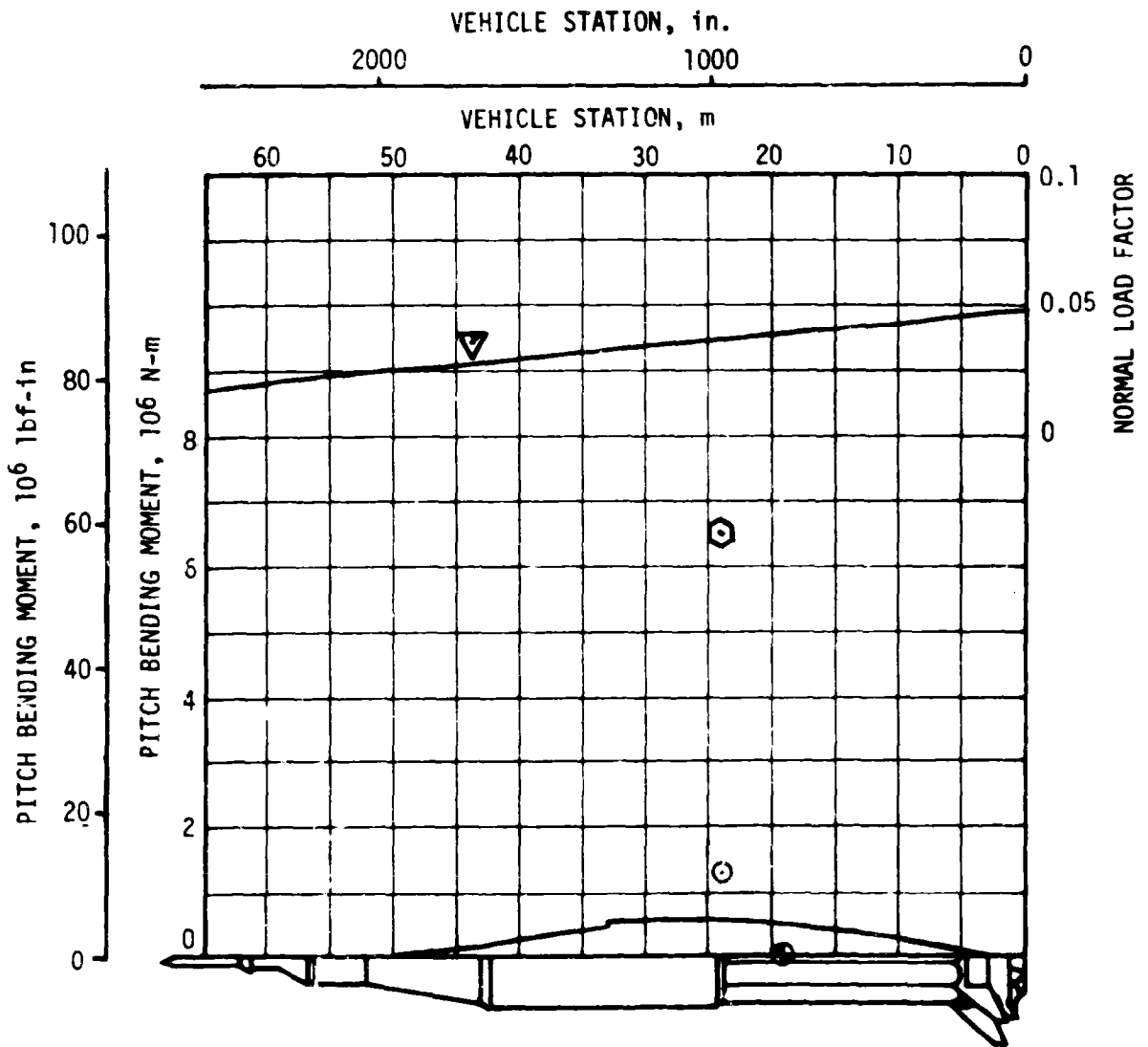


Figure 8-6. SA-207 Pitch Bending Moment and Normal Load Factor Distributions at Time of Maximum Resultant Moment

**CONDITIONS:**

T = 67.2 SECONDS  
 M = 1.36  
 q = 4.843 PSI  
 $\alpha_y = 0.30$  DEGREES  
 $\beta_y = 0.16$  DEGREES

**LEGEND:**

- ⊙ STRAIN DATA
- ▽ A5-603 ACCELEROMETER DATA
- CENTER OF GRAVITY
- ⊙ DESIGN CRITERION BENDING MOMENT

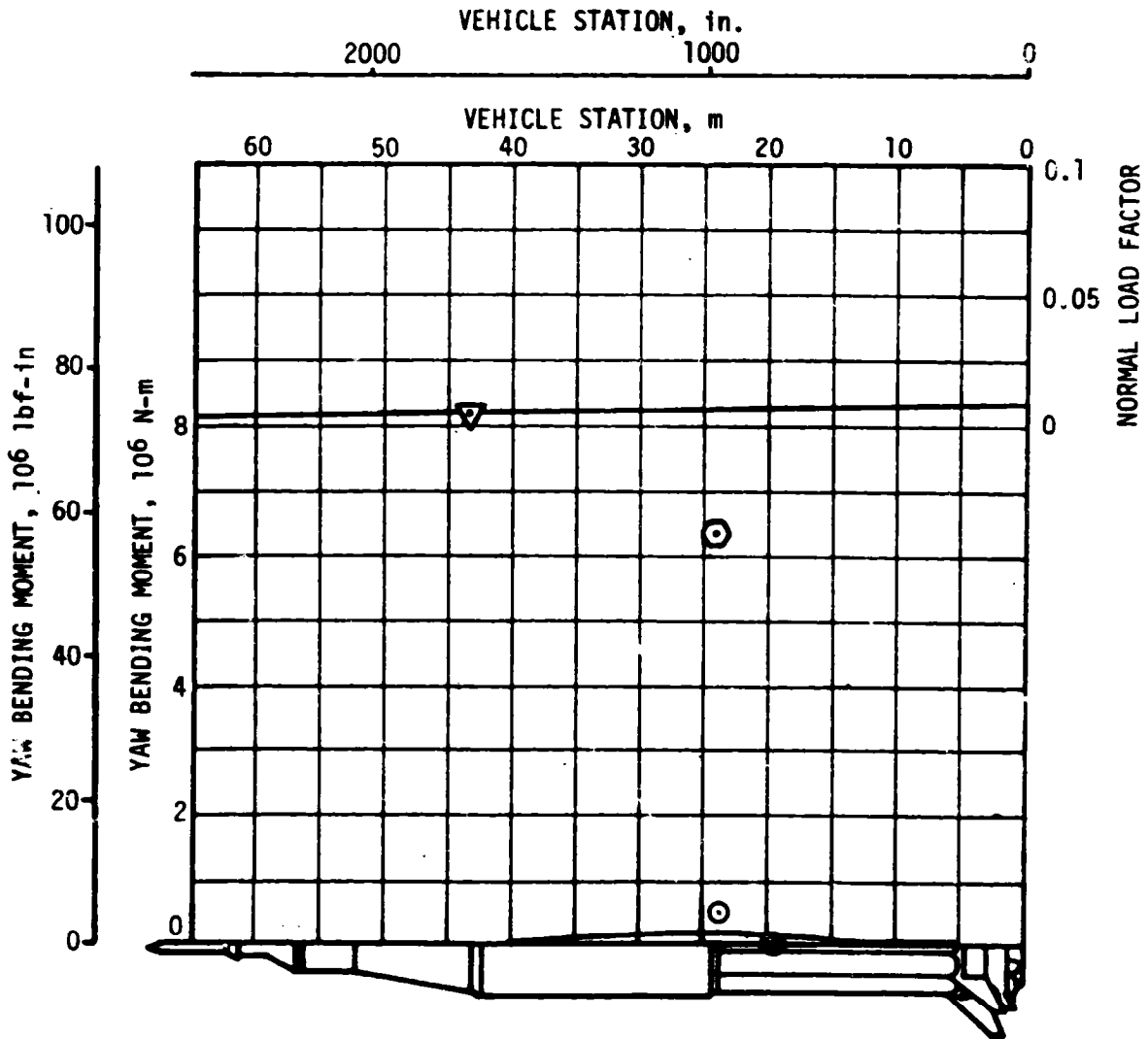


Figure 8-7. Yaw Bending Moment Distributions at Time of Maximum Resultant Moment

plus an envelope of the allowable combined loads are presented in Figure 8-8. The S-IB is not included because the clustered stage does not lend itself to this format.

The minimum safety factors are plotted versus vehicle station in Figure 8-9. The minimum factor of safety of 1.52 at station 1186 was experienced at IECO. The minimum design safety factor is 1.40.

#### 8.2.4 Vehicle Dynamic Characteristics

The longitudinal stability analysis of SA-207 showed all vibration and pressure fluctuations to be smooth and low with no POGO instability.

The first, second and third vehicle bending mode frequencies are compared to the modes predicted by analysis in Figure 8-10. Amplitudes (Figure 8-11) at these frequencies were low and similar to previous Saturn IB flights. In general, the pitch amplitudes were slightly higher than the corresponding yaw amplitudes. The largest recorded amplitude was 0.09 Grms in the pitch direction (station 895) which occurred during the liftoff portion of flight.

The S-IVB stage gimbal block longitudinal low frequency vibration, LOX pump inlet pressure and thrust chamber pressure measurements were similar to the SA-206 flight. Comparison of the overall vibration amplitude during S-IB stage burn for the SA-207 and SA-206 stages is shown in Figure 8-12. With the exception of the initial transient at S-IB engine ignition, the overall amplitudes are lower than the SA-206 flight. The engine ignition transient was  $\pm 0.44$  g with a predominant frequency of 16 Hz.

Low frequency longitudinal vibration and pressure oscillations during S-IVB stage burn are shown in Figure 8-13. The SA-207 vibration and pressure data were generally lower than SA-206, except for the vibration buildup at 45 seconds after engine ignition. The maximum level was  $\pm 0.2$  g with a predominant frequency of 18.6 Hz. This level is within the range ( $\pm 0.04$  to  $\pm 0.25$  g) of levels measured on previous Saturn IB and Saturn V flights.

Spectral density plots at selected time periods are shown in Figure 8-14. These plots show the same characteristics noted on SA-206 and previous Saturn V flights. The 17-19 Hz structural vibration is predominant at 192 seconds and 15-17 Hz near engine cutoff (591 seconds). A mild condition of the 76 Hz "buzz" frequency is again apparent in the oxidizer pump inlet pressure during the period of high Net Positive Suction Pressure (NPSP) [300 seconds].

The S-IVB engine cutoff transient produced 55 Hz oscillations on the gimbal block of  $\pm 4.25$  g. Both the frequency and the amplitudes are within the envelope observed during S-IVB cutoff on previous Saturn flights. This cutoff transient caused unusually large vibrations on the IU ST-124 stabilized platform (Figure 9-5) for this time of flight. Attention was originally focused on this phenomenon because the amplitude of the SA-207 transient measured in the IU was greater than that measured on previous flights.

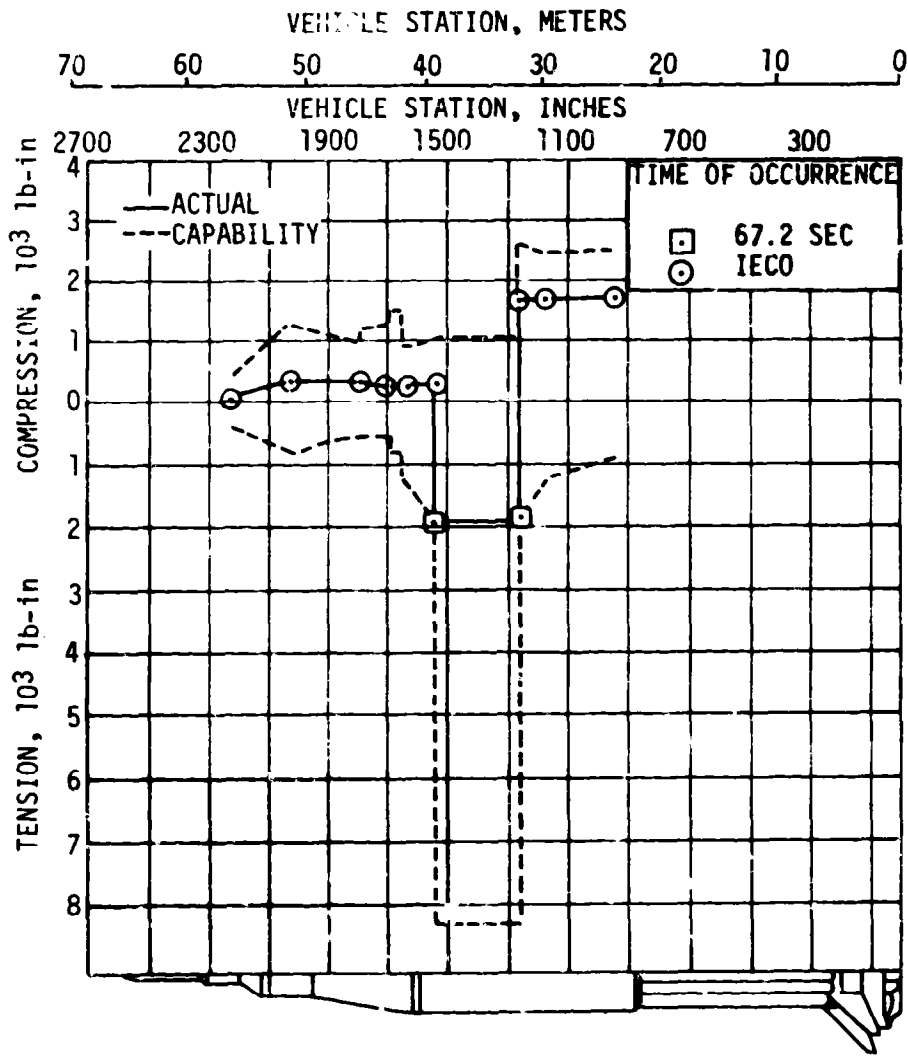


Figure 8-8. Combined Loads Producing Minimum Safety Margins During SA-207 Flight

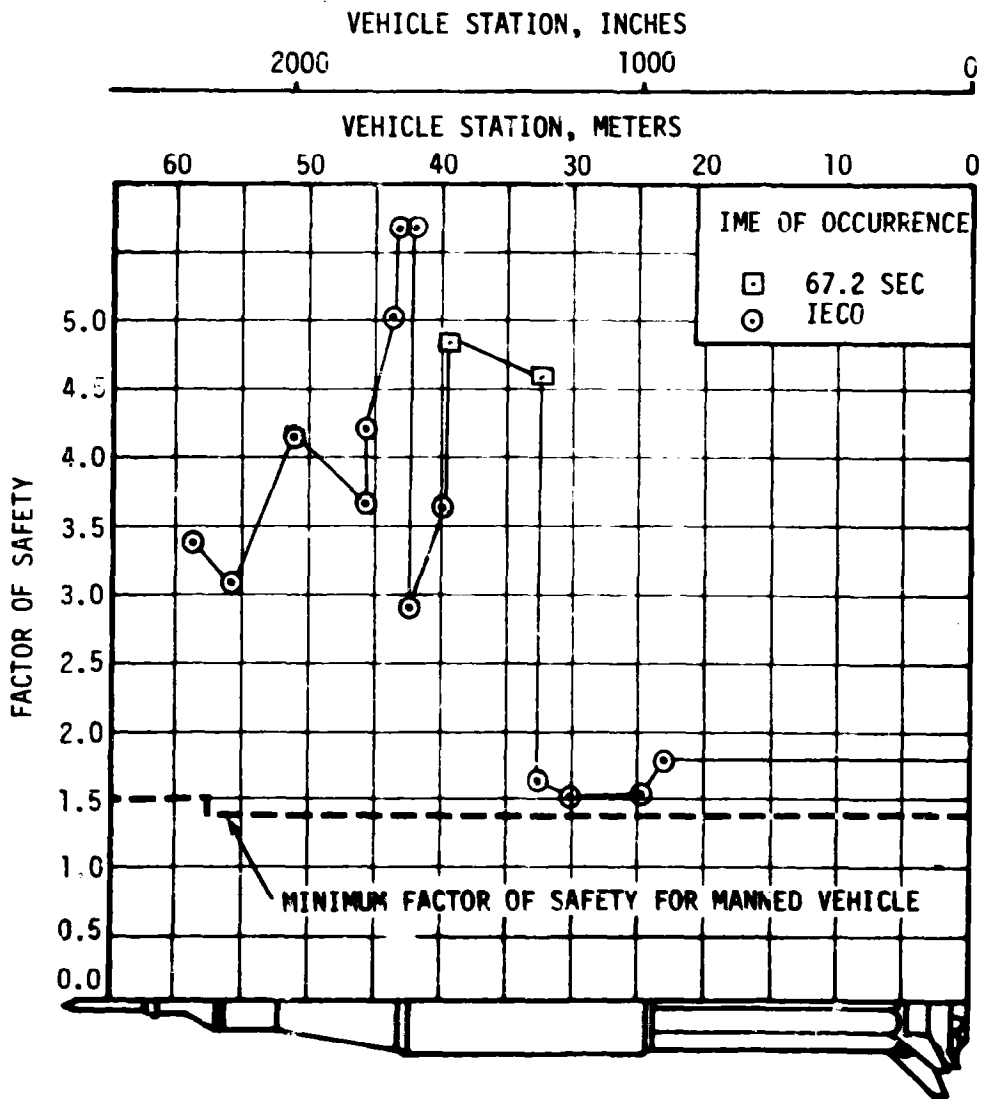


Figure 8-9. Minimum Factor of Safety During SA-207 S-IB Flight

- DYNAMIC ANALYSIS
- 1ST BENDING
- ▲ 2ND BENDING
- ◻ 3RD BENDING

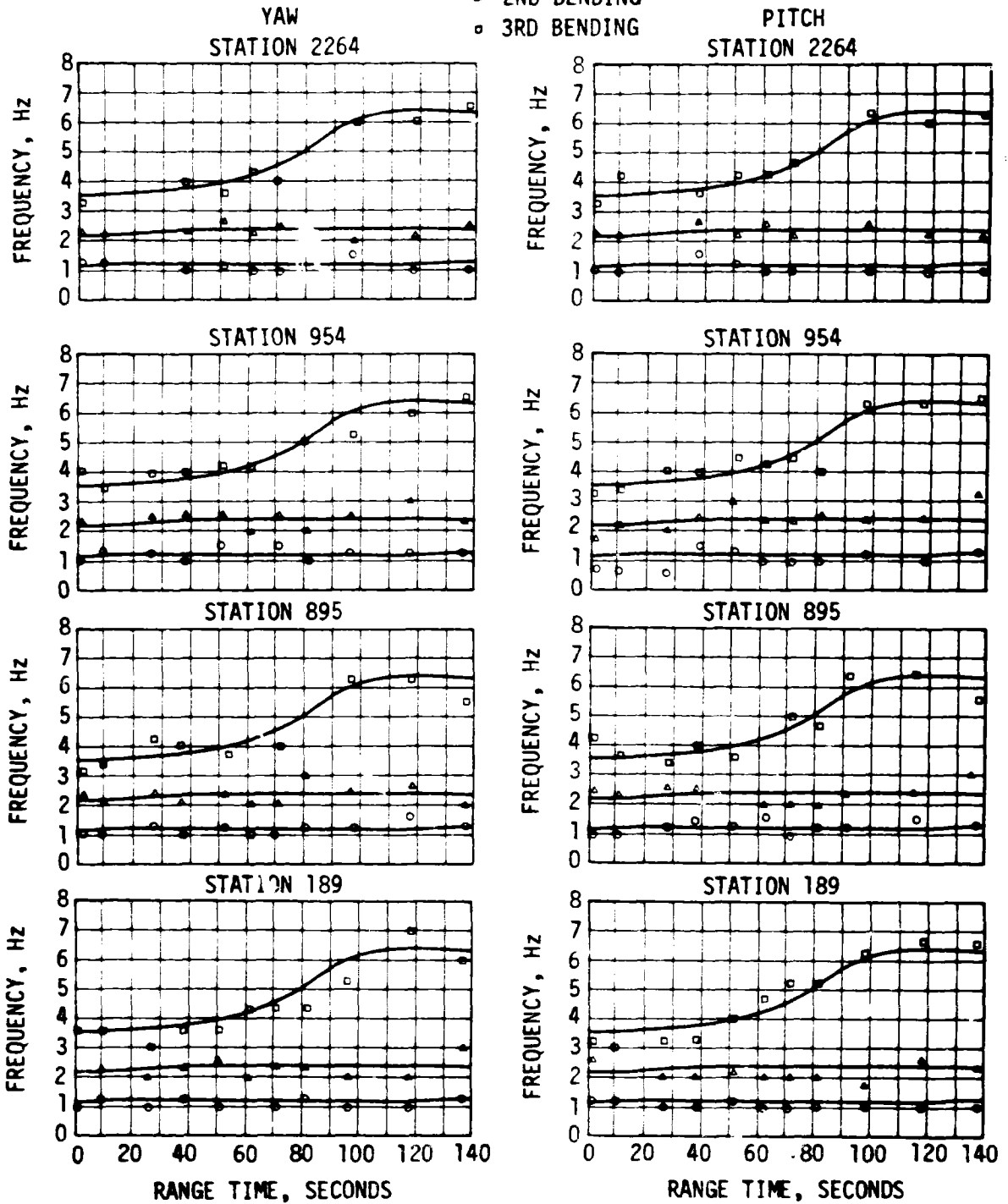


Figure 8-10. Vehicle Bending Frequencies



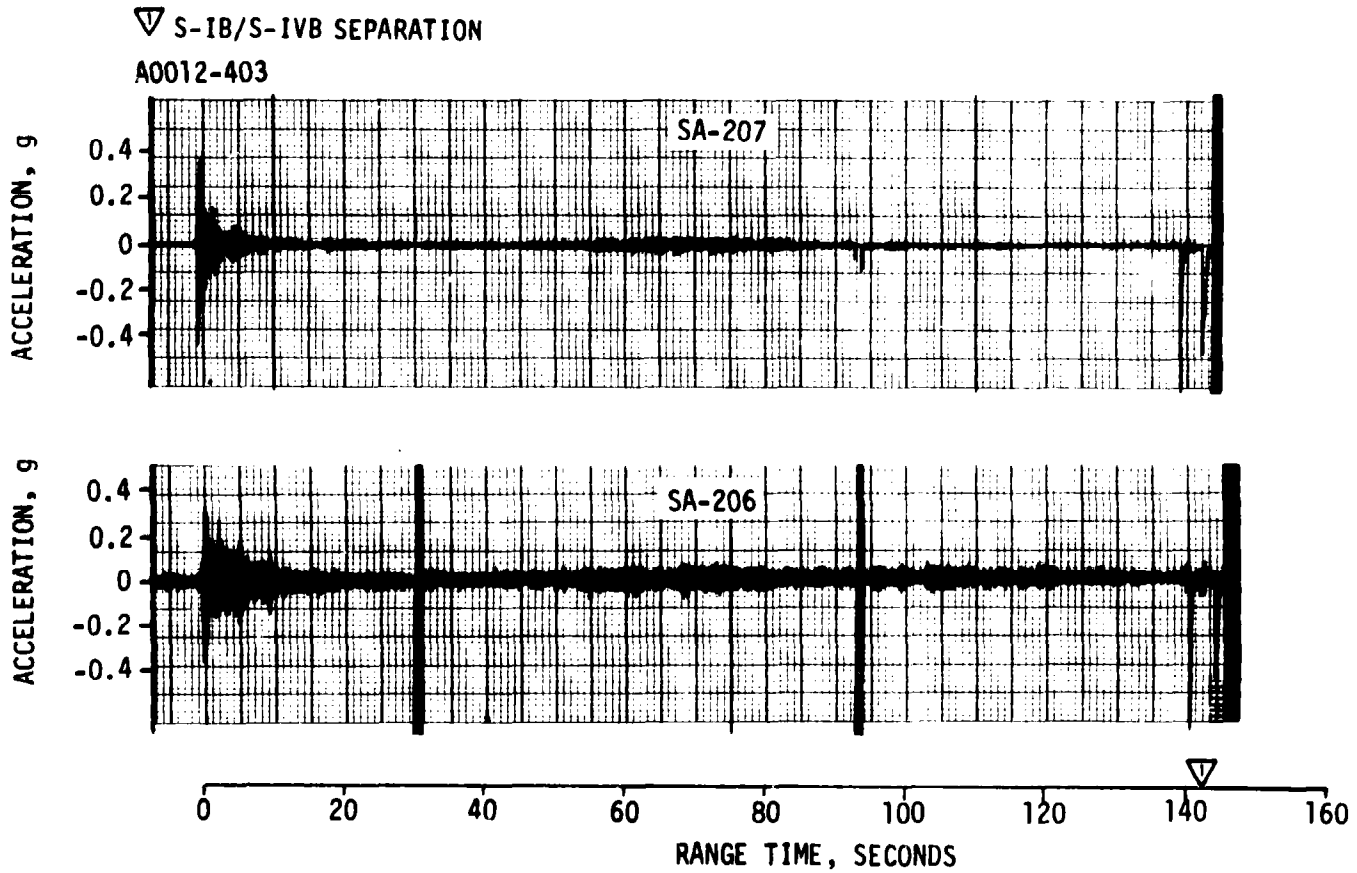


Figure 8-12. Vibration Measured During First Stage Burn



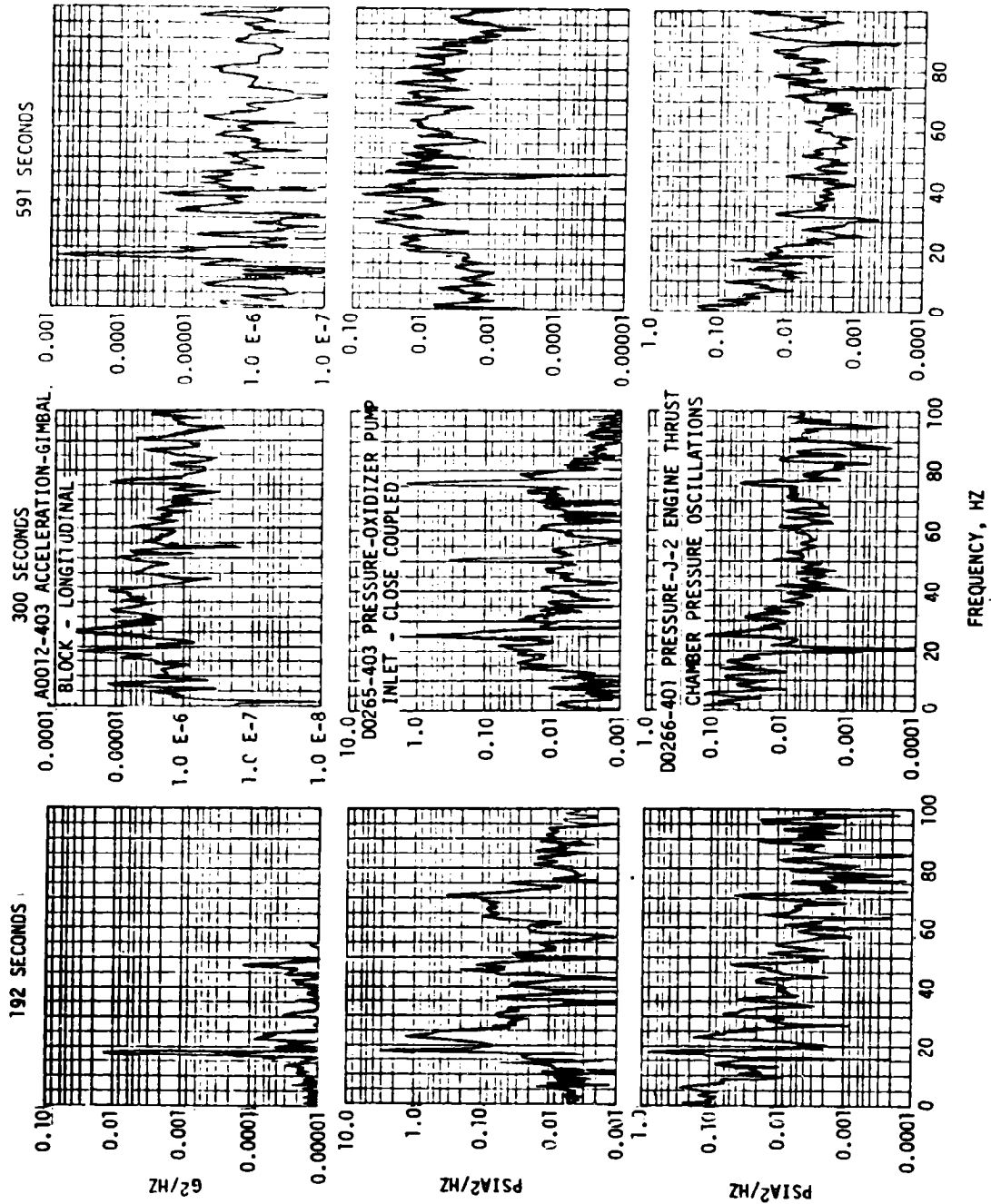


Figure 8-14. Low Frequency Spectral Analysis of Vibration and Engine Pressures

The larger platform response was traced to coupling of the forcing function with a 55 Hz local structural mode. No such coupling occurred on SA-206 since that forcing function was predominately 17 Hz with a 70 Hz component (Figure 8-15). In the event of a forcing function with a strong 55 Hz component on subsequent S-IB vehicles, platform response similar to that seen on SA-207 can be expected again.

The 55 Hz structural resonance did not degrade the platform performance since it coincides with neither the accelerometer servo loop resonance (35 Hz) nor the platform gimbal system resonance (100-150 Hz). Furthermore, more severe vibration environments have been encountered at liftoff, max q and Mach 1 on this and previous flights.

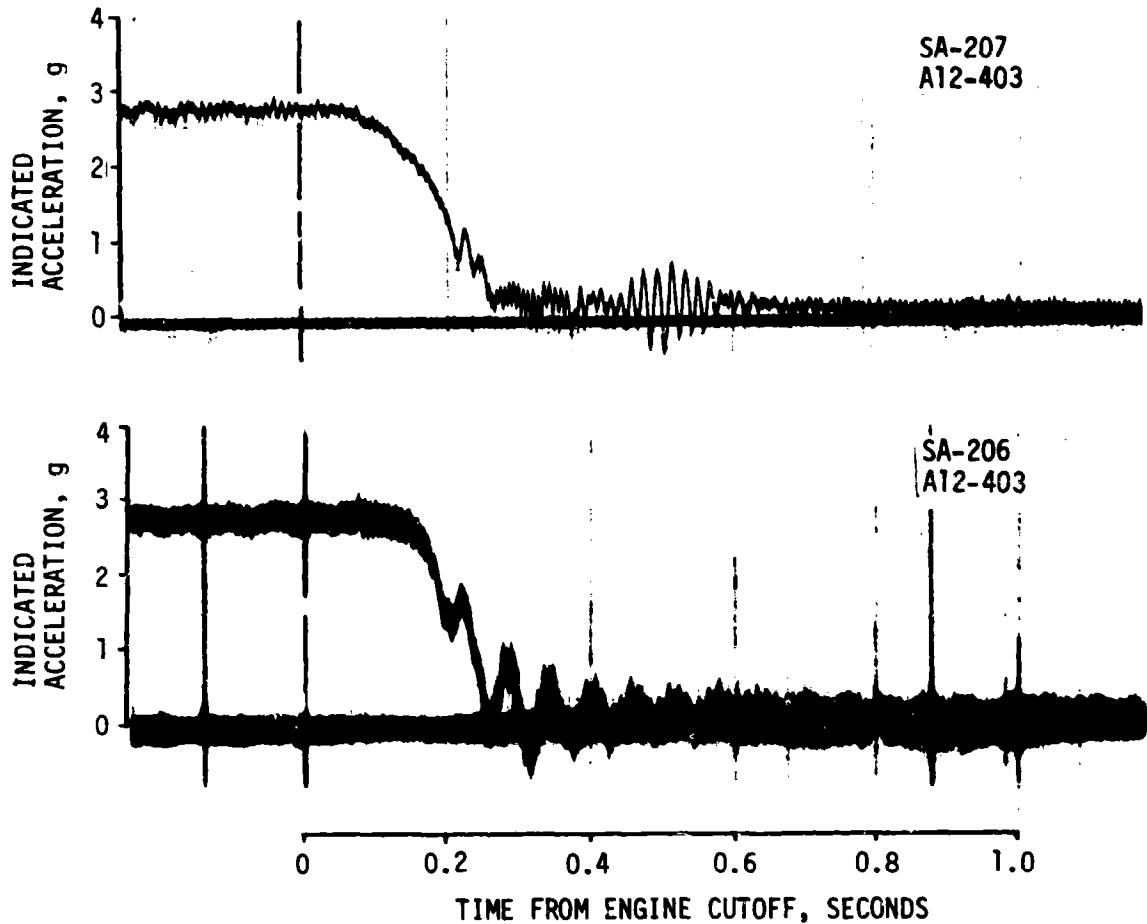


Figure 8-15. S-IVB Cutoff Transients on J-2 Engine Gimbal Block, SA-207 and SA-206

## SECTION 9

### GUIDANCE AND NAVIGATION

#### 9.1 SUMMARY

The stabilized platform and the guidance computer successfully supported the accomplishment of the SA-207 Launch Vehicle mission objectives. Targeted conditions at orbit insertion were attained with insignificant error. No anomalies nor deviations from nominal performance were noted.

The stabilized platform accelerometers properly reacted to thrust decay vibrations following S-IVB stage guidance cutoff.

#### 9.2 GUIDANCE COMPARISONS

The postflight guidance error analysis was based on comparisons of position and velocity data from the onboard guidance computer with corresponding data taken from the final Observed Mass Point Trajectory (OMPT) which was established from external tracking and telemetered velocity data (see Section 4). Comparisons of the inertial platform measured velocities with the OMPT data are shown in Figure 9-1 for boost to orbit insertion. The velocity differences are small and are well within the accuracies of the onboard measuring system and the OMPT. The differences in vertical and downrange velocities indicate offsets of about 0.20 m/s (0.66 ft/s) and 0.05 m/s (0.16 ft/s), respectively. These deviations represent minimum adjustments to telemetered velocities to give the best composite fit of the data from several radars tracking the SA-207 vehicle during boost. The crossrange velocity difference is indicative of misalignment due to some combination of small platform drifts. At orbit insertion, the telemetered crossrange velocity was approximately 0.69 m/s (2.26 ft/s) less than the OMPT value.

The inertial platform velocity measurements at significant event times are shown in Table 9-1. Corresponding data from the OMPT are also shown for comparison. The differences in the velocities at inboard (IECO) and outboard (OECO) engine cutoffs reflect variances in simulating S-IB thrust decay. However, the deviations are small. At S-IVB guidance cutoff signal (GCS) and orbit insertion, the velocity differences are very small.

Velocity gain due to thrust decay after GCS was 7.37 m/s (24.18 ft/s) compared to 6.72 m/s (22.05 ft/s) predicted by the Operational Trajectory (OT). The oscillations in the accelerometer outputs caused by thrust decay vibration (see paragraph 9.3.2) had no accumulative effect.

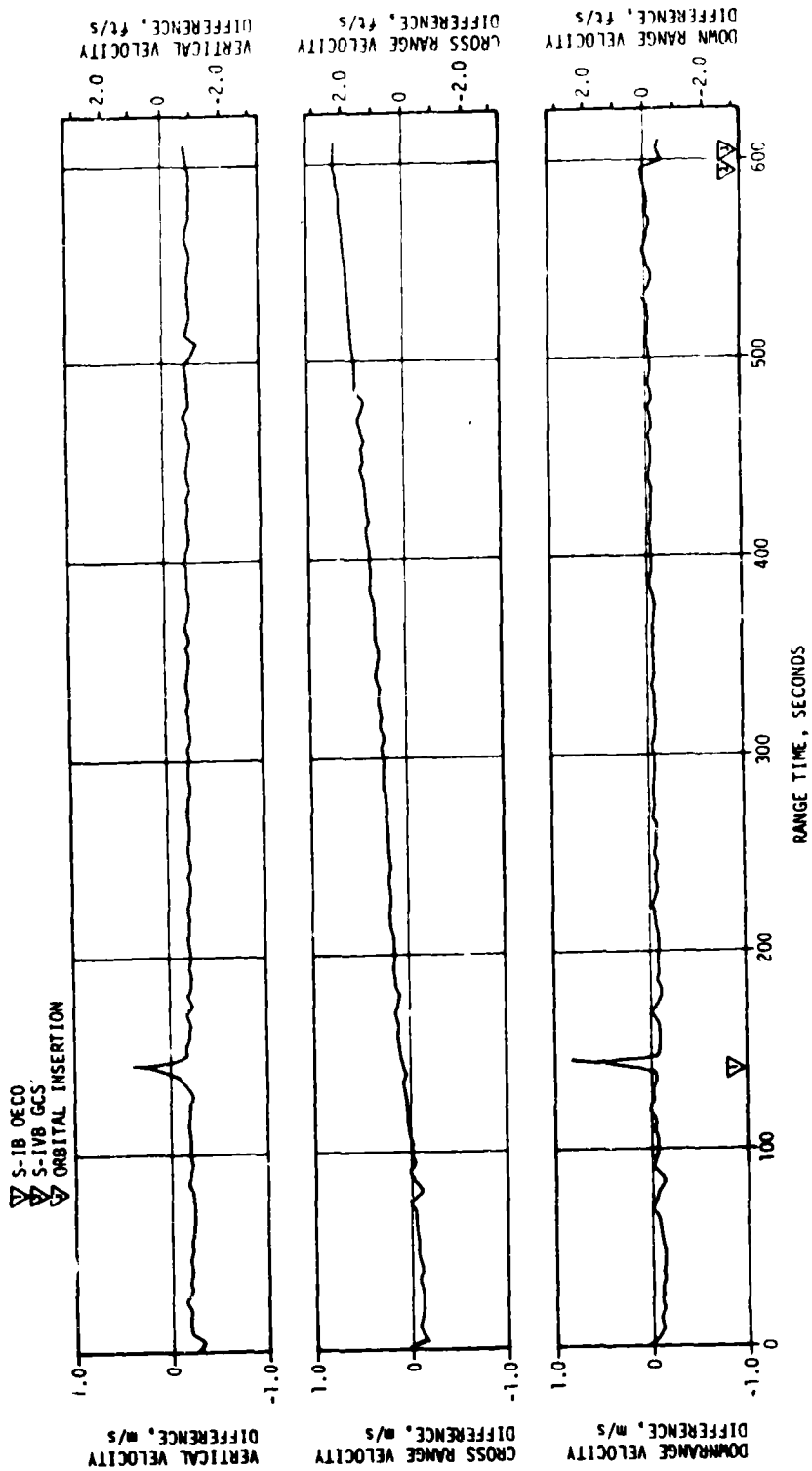


Figure 9-1. SA-207 Trajectory and ST-124M Platform Velocity Comparisons (OMPT Minus LVDC)

Table 9-1. SA-207 Inertial Platform Velocity Comparisons

EVENT	DATA SOURCE	VELOCITY (PACSS-12)*		
		METERS/SECOND (FEET/SECOND)		
		$\dot{X}$	$\dot{Y}$	$\dot{Z}$
S-IB IECO	LVDC	2445.55 (8023.46)	-5.50 (-18.04)	1731.80 (5681.76)
	OMPT	2445.01 (8021.67)	-5.40 (-17.72)	1730.93 (5678.89)
S-IB OECO	LVDC	2482.30 (8144.03)	-5.75 (-18.86)	1801.05 (5908.96)
	OMPT	2481.52 (8141.46)	-5.69 (-18.66)	1800.16 (5906.02)
S-IVB GCS	LVDC	3351.50 (10,995.73)	-97.85 (-321.03)	7724.75 (25,343.67)
	OMPT	3351.16 (10,994.60)	-97.21 (-318.92)	7724.81 (25,343.85)
ORBITAL INSERTION	LVDC	3350.45 (10,992.29)	-98.05 (-321.69)	7732.05 (25,367.62)
	OMPT	3350.17 (10,991.37)	-97.36 (-319.41)	7732.00 (25,367.45)

\*Project Apollo Coordinate System Standard, non-rotating vehicle referenced.

Comparisons of navigation (PACSS-13) positions, velocities, and flight path angle at significant event times are presented in Table 9-2. Differences between the Launch Vehicle Digital Computer (LVDC) and OT data reflect differences in actual and nominal flight environment and vehicle performance. Guidance Cutoff Signal was given with a total velocity 0.03 m/s (0.10 ft/s) and radius vector 27 meters (88 feet) greater than the OT values. At orbit insertion the LVDC total velocity was 0.69 m/s (2.26 ft/s) greater than the OT value.

The LVDC and OMPT data were in very good agreement for the total boost phase. The small transients in velocity comparisons discussed above are reflected in the velocity data shown for S-IB IECO and OECO. At orbit insertion the LVDC total velocity was 0.06 m/s (0.20 ft/s) less than the OMPT value and the radius vector was 138 meters (452 feet) greater. The guidance system was highly successful in guiding the SA-207 launch vehicle to prescribed end conditions as shown in Table 9-3.

Table 9-2. SA-207 Navigation Position and Velocity Comparisons (PACSS-13)

EVENT	DATA SOURCE	POSITIONS METERS (FEET)				VELOCITIES METERS/SECOND (FEET/SECOND)				FLIGHT PATH ANGLE (DEGREES)
		X <sub>s</sub>	Y <sub>s</sub>	Z <sub>s</sub>	R	X <sub>s</sub>	Y <sub>s</sub>	Z <sub>s</sub>	V <sub>s</sub>	
S-1B IECO	LVDC	6,427,727.0 (21,088,343.2)	56,959.7 (186,875.7)	90,180.0 (295,866.1)	6,428,011.9 (21,091,246.4)	937.54 (3075.92)	276.67 (907.71)	2014.67 (6609.81)	2239.29 (7346.75)	25.616
	OMPT	6,427,698.0 (21,088,248.0)	56,956.0 (186,863.4)	90,169.0 (295,830.2)	6,428,582.7 (21,091,150.5)	937.00 (3074.16)	276.70 (907.81)	2013.78 (6606.90)	2238.27 (7343.41)	25.613
	Operational Trajectory	6,428,204. (21,089,909.)	56,524. (185,445.)	89,585. (293,916.)	6,429,077. (21,092,772.)	950.97 (3119.97)	274.76 (901.46)	2014.31 (6608.64)	2244.39 (7363.49)	25.327
S-1B OECO	LVDC	6,430,904.1 (21,098,766.7)	57,893.4 (189,939.0)	97,108.0 (318,595.8)	6,431,897.8 (21,102,026.9)	941.71 (3089.60)	276.10 (905.84)	2083.41 (6835.33)	2302.96 (7555.64)	25.761
	OMPT	6,430,875.4 (21,098,672.5)	57,889.9 (189,927.4)	97,099.1 (318,566.7)	6,431,869.1 (21,101,932.7)	940.94 (3087.08)	276.16 (906.02)	2082.51 (6832.37)	2301.84 (7551.97)	25.753
	Operational Trajectory	6,431,066. (21,099,298.)	57,347. (188,147.)	95,730. (314,074.)	6,432,034. (21,102,474.)	954.31 (3130.95)	274.74 (899.75)	2079.57 (6813.83)	2301.13 (7550.58)	25.403
S-1VB GCS	LVDC	6,218,888.6 (20,403,177.8)	154,861.4 (508,075.5)	1,979,525.2 (6,494,505.2)	6,528,175.6 (21,417,898.9)	-2378.52 (-7803.54)	116.70 (380.97)	7456.64 (24,470.50)	7229.87 (23,687.87)	-0.0107
	OMPT	6,218,751.6 (20,402,728.0)	155,014.1 (508,576.6)	1,979,489.5 (6,494,388.1)	6,528,037.9 (21,417,447.2)	-2378.91 (-7804.83)	116.73 (381.37)	7456.64 (24,470.73)	7229.73 (23,686.10)	-0.1109
	Operational Trajectory	6,213,647. (20,385,982.)	155,117. (508,912.)	1,995,810. (6,547,933.)	6,528,149. (21,417,812.)	-2397.77 (-7966.71)	115.66 (379.45)	7452.45 (24,467.09)	7222.54 (23,687.46)	-0.006
ORBITAL INSERTION	LVDC	6,194,650.2 (20,323,655.5)	156,010.2 (511,844.5)	2,054,030.3 (6,738,944.6)	6,528,175.1 (21,417,397.3)	-2468.45 (-8096.59)	113.81 (373.39)	7436.97 (24,399.51)	7936.75 (25,711.12)	0.0026
	OMPT	6,194,507.7 (20,323,187.7)	156,169.3 (512,366.6)	2,054,004.5 (6,738,859.7)	6,528,037.4 (21,417,439.2)	-2468.73 (-8099.66)	114.17 (375.55)	7436.91 (24,399.30)	7936.81 (25,711.31)	0.0005
	Operational Trajectory	6,189,215. (20,305,824.)	156,261. (512,668.)	2,070,253. (6,792,170.)	6,529,151. (21,417,317.)	-2487.61 (-8161.45)	113.42 (372.11)	7429.86 (24,376.17)	7836.06 (25,708.85)	0.003

NOTE: Project Apollo Coordinate System Standard, non-rotating, earth centered

9-4

REPRODUCIBILITY OF THE ORIGINAL PAGE IS POOR

Table 9-3. SA-207 Boost Terminal Conditions

CONDITION	DESIRED	ACHIEVED	ERROR (ACHIEVED - DESIRED)
Velocity, $V_T$ (m/sec)	7836.04248	7836.06800	0.02552
Radius, $R_T$ (kilometers)	6528.1995	6528.1705	-0.029
Path Angle, $\theta_T$ (deg)	0.0	-.002433	-0.002433
Inclination, $I$ (deg)	50.031132	50.0320279	0.0008959
Descending Node, $\lambda$ (deg)	154.495927	154.496372	0.000445

### 9.3 GUIDANCE AND NAVIGATION SCHEME EVALUATION

The flight program performed all functions properly. Targeted guidance cutoff conditions at orbit insertion were achieved with a high degree of accuracy. All events scheduled at preset times occurred within acceptable tolerances. Times of occurrence of major guidance and navigation events are included in Table 2-2, Section 2.

#### 9.3.1 First Stage Boost

Timebase 1 was initiated at 0.476 seconds, 17.429 seconds after Guidance Reference Release (GRR). The roll and time-tilt maneuver was begun at 10.158 seconds to align the vehicle to a flight azimuth of 45.003 degrees east of north and follow a preset attitude time-history during the atmospheric boost phase, respectively.

The roll maneuver was terminated at 57.471 seconds. Tilt-arrest, signifying completion of the atmospheric boost phase, was commanded at 129.169 seconds with a pitch attitude command of -62.2622 degrees. First stage guidance and navigation was normal.

#### 9.3.2 Second Stage Boost

Second stage guidance was normal with no undue occurrences noted. The desired and achieved guidance terminal conditions for boost are compared in Table 9-3. Observed and predicted vehicle rate-limited commanded attitude angles are shown for comparison in Figures 9-2 through 9-4.

The stabilized platform responded to vibrations during engine thrust decay following guidance-commanded cutoff of the S-IVB stage engine

- ▽ MAX Q
- ▽ S-IB OEEO
- ▽ IGM PHASE 1
- ▽ IGM PHASE 2
- ▽ TERMINAL GUIDANCE
- ▽ S-IVB GCS
- ▽ MANEUVER TO LOCAL HORIZONTAL

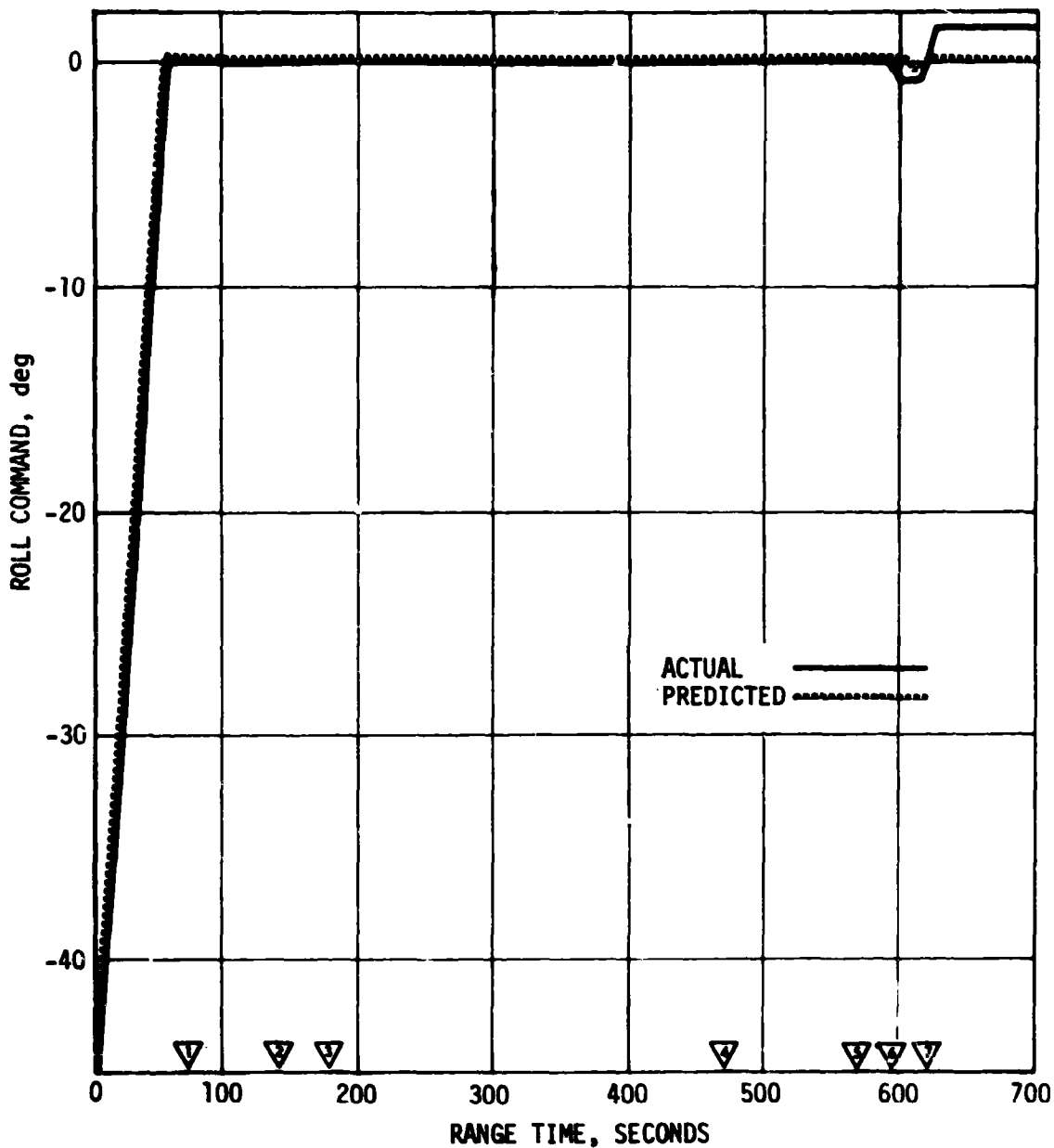


Figure 9-2. Roll Command During Boost

- ▽ MAX Q
- ▽ S-IB OECS
- ▽ IGM PHASE 1
- ▽ IGM PHASE 2
- ▽ TERMINAL GUIDANCE
- ▽ S-IVB GCS
- ▽ MANEUVER TO LOCAL HORIZONTAL

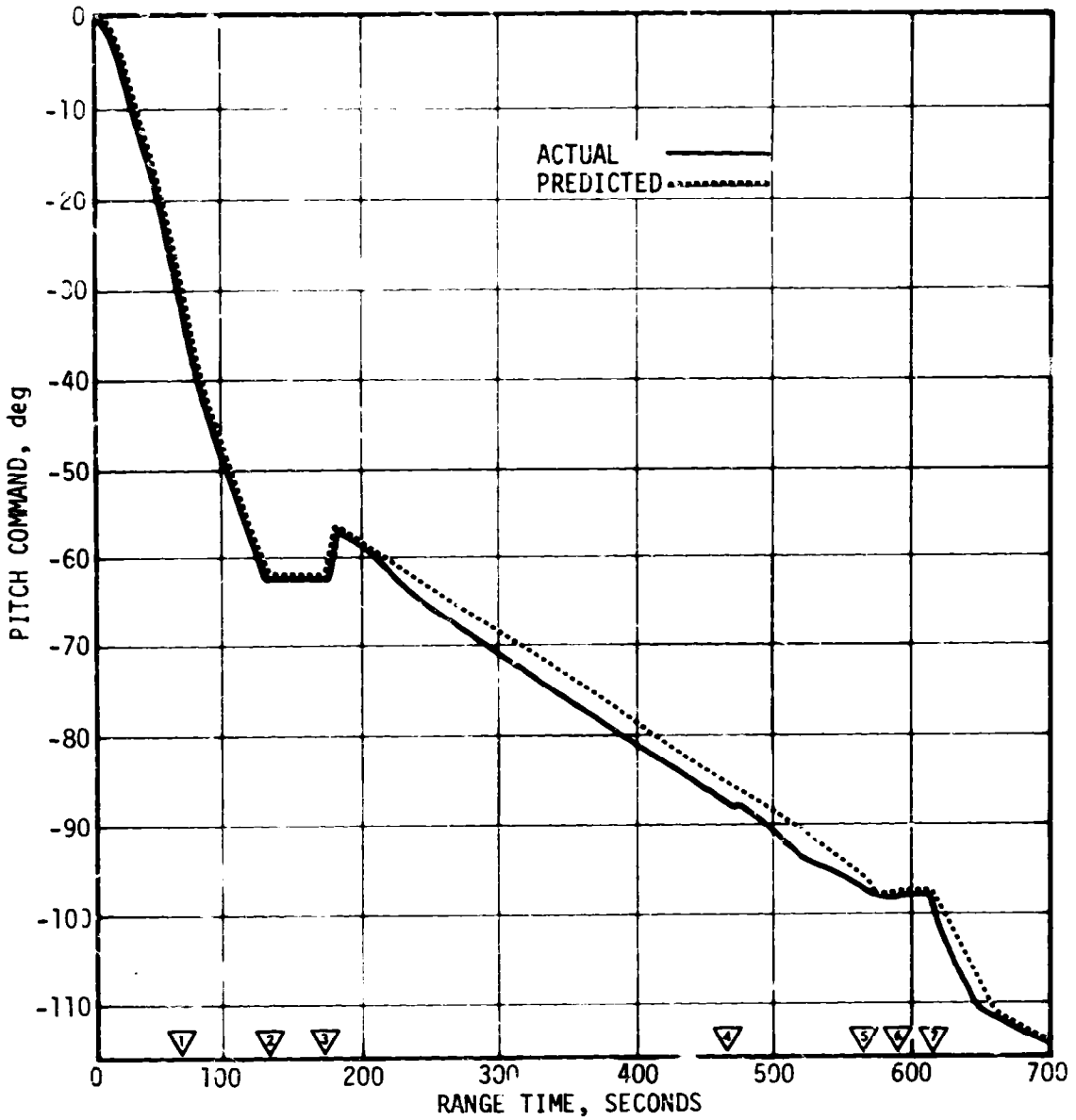


Figure 9-3. Pitch Command During Boost

- ▽ MAX Q
- ▽ S-IB DECO
- ▽ IGM PHASE 1
- ▽ IGM PHASE 2
- ▽ TERMINAL GUIDANCE
- ▽ S-IVB GCS
- ▽ MANEUVER TO LOCAL HORIZONTAL

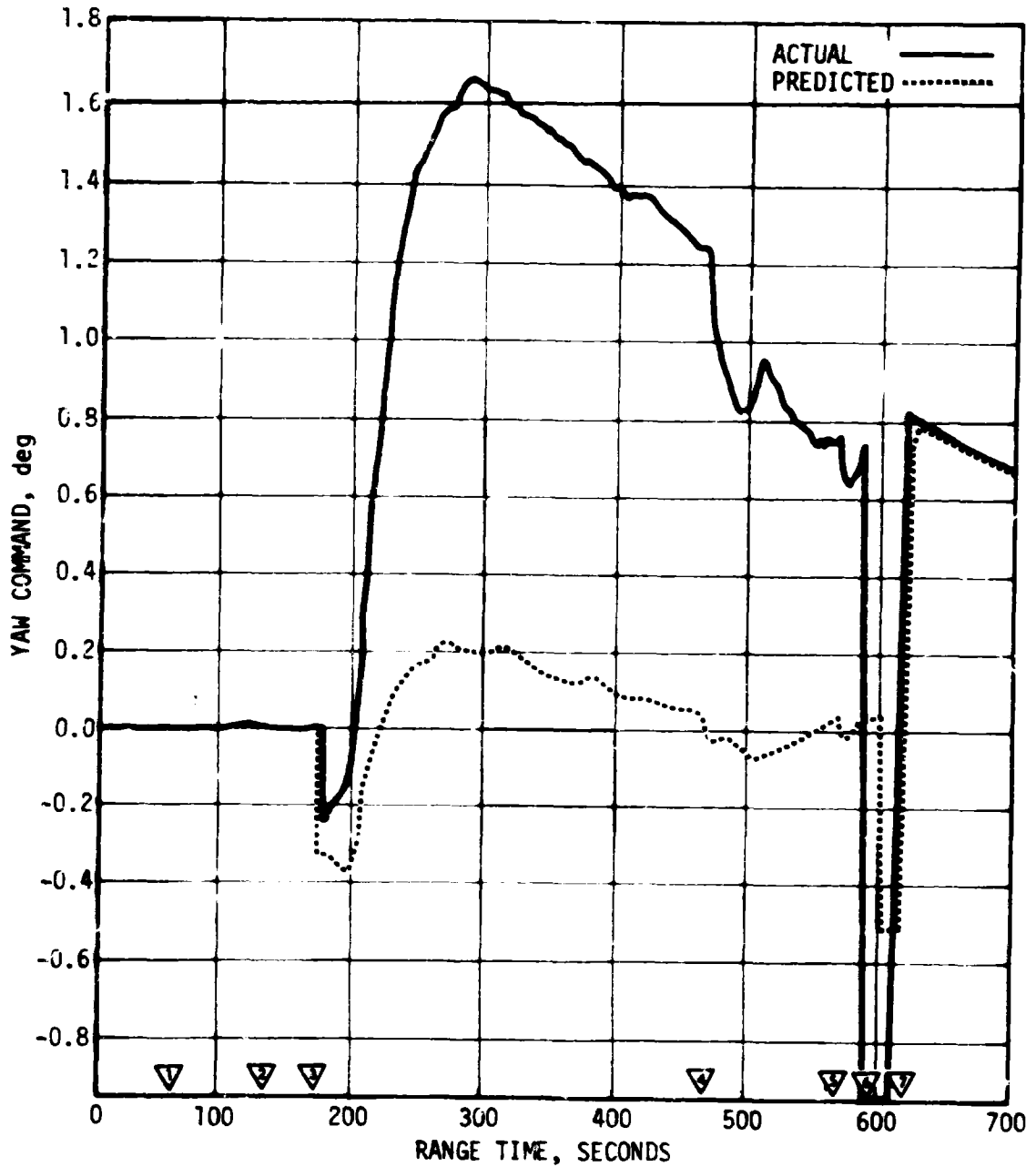


Figure 9-4. Yaw Command During Boost

(see Figure 9-5). The vibration was similar to that noted during the S-IVB thrust decay following the parking orbit cutoff of the last five Apollo/Saturn V vehicles. However, the platform response was much larger for SA-207 than previously noted. The greater response occurred because the vehicle mass for SA-207 was approximately one-half that of the Apollo/Saturn V and the frequency of the burst of vibration from the engine matched the 55 Hz characteristic resonance of the platform structure.

The vibration, discussed additionally in Section 8, was insufficient to cause any degradation in the platform, platform structure or IU structure. The combination of the vibration and its result is interesting because it is a clear presentation of an S-IVB/IU structural characteristic.

### 9.3.3 Orbital Phase

At the start of Timebase 4 an attitude hold (Chi-freeze) was initiated, followed by a local reference maneuver scheduled 20 seconds later. These attitude commands are shown in Table 9-4. Initiation of orbital navigation (implemented at T4 +15.827 seconds) and all orbital events were within the tolerance of one computation cycle. Ground commands for the initial maneuver for the S-150 experiment were issued at approximately T4 +678 seconds. The commanded maneuver start time was T4 +720 seconds. Reference angles for this local reference maneuver were 0, 177 and 0 degrees for X, Y, and Z, respectively.

### 9.3.4 Deorbit Phase

The ground command to initiate the S-IVB/IU deorbit sequence was issued at T4 +15,293 seconds. The deorbit parameters commanded were as follows:

Start Timebase 5 at T4 +18,600 seconds (LOX dump initiated at T5 +34 seconds).

Start sequence for stop LOX dump, start LH<sub>2</sub> dump at T5 +478.9 seconds.

Start sequence for Stop LH<sub>2</sub> dump, safe vehicle at T5 +1098.9 seconds.

These sequences were implemented within the specified tolerances and resulted in deorbit of the S-IVB/IU as planned (see Section 5).

## 9.4 GUIDANCE AND NAVIGATION SYSTEM COMPONENTS

The guidance and navigation hardware satisfactorily supported the accomplishment of mission objectives.

NOTE: Velocity Components per PACSS-12

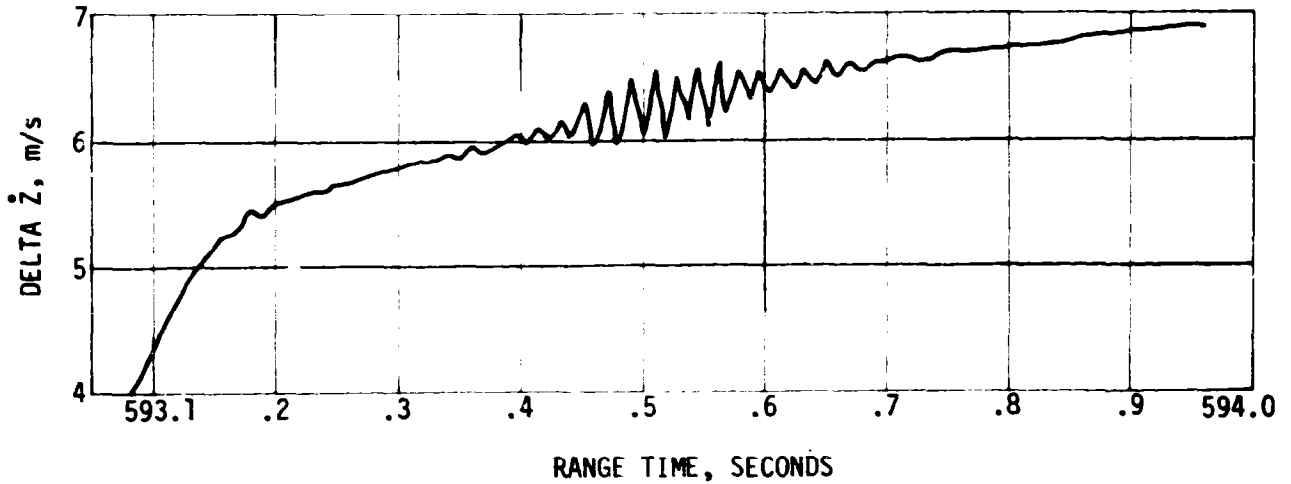
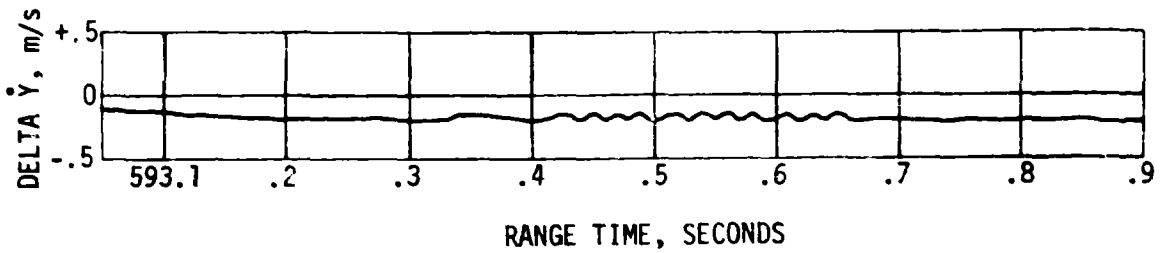
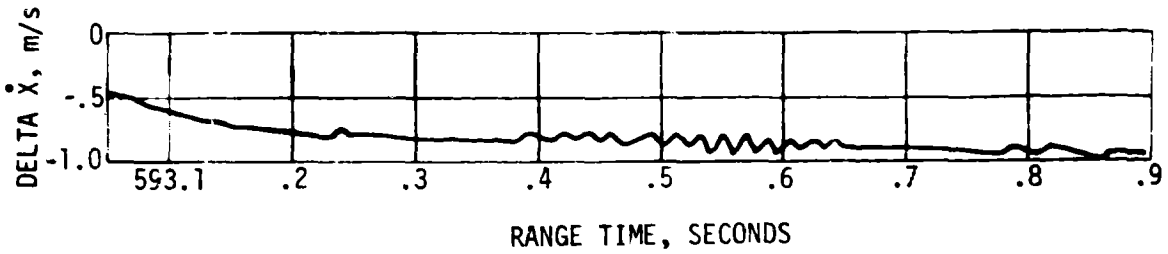


Figure 9-5. Inertial Velocity Component Increments During S-IVB Thrust Decay

Table 9-4. SA-207 Orbital Phase Flight Program Attitude Commands

EVENT	COMMANDED ATTITUDE (DEGREES)		
	ROLL	PITCH	YAW
Time Base 4	-0.7617	-97.9381	-0.9822
Time Base 4 +20 Sec (Local Reference, Implemented at TB4 +20.381 Sec)	0.0000	-109.0778	0.8161

#### 9.4.1 ST-124M Stabilized Platform System

The three gyro servo loops responded properly to all vehicle motions. Maximum gyro pickoff deflection was 0.2 degree during spacecraft separation, as was the case for SA-206. Deflections were below 0.2 degree at all other times.

The three accelerometer servo loops operated within previously experience limits. Maximum pickoff deflections at the significant event times are as follows:

	<u>Z</u>	<u>X</u>	<u>Y</u>
Liftoff	+0.6°	<+0.1°	+0.4°
	-0.3°	<-0.1°	-0.1°
Mach 1/Max Q	+1.7°	+0.6°	+1.6°
	-1.9°	-0.5°	-1.5°
CSM Separation	+0.6°	+2.7°	+2.3°
	-1.6°	-1.8°	-2.4°

There were no gimbal resolver switchovers noted throughout the flight.

Temperature variations noted at the inertial gimbals were less for SA-207 than for SA-206. Comparative values are as follows:

	<u>SA-207</u>	<u>SA-206</u>
Liftoff	40.5°C	41.7°C
End of Mission	37.8°C	35.3°C

This difference is insignificant and may be due to the different sun

angles required by the respective experiments flown on the two vehicles.

The ST-124M stable platform subsystem voltages were nominal during the entire mission.

#### 9.4.2 Guidance Computer

The LVDC and Launch Vehicle Data Adapter (LVDA) performed satisfactorily. No hardware anomalies were observed during any phase of the SA-207 mission.

## SECTION 10

### CONTROL AND SEPARATION

#### 10.1 SUMMARY

The control and separation systems functioned correctly throughout the powered and coast flight of SA-207. Auxiliary Propulsion System (APS) propellant usage was greater than expected during coast but the quantity available was adequate to fulfill all mission requirements. Engine gimbals deflections were nominal. Bending and slosh dynamics were adequately stabilized. No unusual dynamics accompanied any separation.

#### 10.2 S-IB CONTROL SYSTEM EVALUATION

No abnormal dynamics developed as a result of launch from the pedestal. Tower clearance was adequate. Table 10-1 summarizes liftoff misalignments. Effective roll misalignment of the inboard engines was greater than the predicted value, but resulted in a roll error of less than 0.5 degree.

Table 10-1. Misalignment Summary

	PREDICTED 3 $\sigma$ RANGE			LAUNCH		
	PITCH	YAW	ROLL	PITCH	YAW	ROLL
Thrust Misalignment, deg	+0.46	+0.46	+0.19	0.0	0.0	-0.05
Inboard Engine Misalignment, deg	+0.25	+0.25	+0.25	0.0	0.0	0.30
Vehicle Stacking and Pad Misalignment, deg	+0.39	+0.39	0.0	0.0	0.0	0.0

The SA-207 control system performed as expected during S-IB boost. Jim-sphere measurements indicate wind velocities below the 84th percentile levels for July. The wind peak was 13.2 meters per second at 13.8 kilometers altitude from an azimuth of 14 degrees. In the high dynamic pressure region, the maximum total angle of attack of 1.31 degrees occurred predominantly in the yaw plane in response to a wind peak. The control system adequately stabilized the vehicle response to all winds.

Maximums of about 21 percent of the available yaw gimbal angle and 12 percent of the available pitch gimbal angle were used. Both peak deflections were due to wind speed peaks and associated shears. Bending and sloshing dynamics were properly stabilized with neither response exhibiting any divergent trend.

Time histories of pitch, yaw and roll dynamics and control deflections are shown in Figures 10-1 through 10-4. The maximums are summarized in Table 10-2. Vehicle dynamics in the region between liftoff and 50 seconds resulted primarily from steering commands. Between 50 and 100 seconds, the vehicle responded normally to the roll and pitch steering programs and the wind. Dynamics from 100 seconds to S-IB outboard engine cutoff were caused by Inboard Engine Cutoff (IECO), tilt arrest, separated air-flow aerodynamics, and high altitude winds. Pitch and yaw plane control accelerometers were deactivated at 120 seconds.

The effects of thrust unbalance, offset center of gravity (cg), thrust vector misalignment and control system misalignments resulted in attitude errors which were within predicted envelopes. The effective thrust vector misalignments were negligible in both pitch and yaw. Only roll plane thrust misalignments could be detected in this flight, and they averaged  $-0.05$  degrees for all eight engines,  $0.30$  degrees for the four inboard engines and  $-0.17$  degrees for the four outboard engines, see Table 10-1.

The peak angles of attack in the high dynamic pressure region were small,  $-1.31$  degrees in yaw and  $1.13$  degrees in pitch, and did not occur simultaneously. Time histories of the free stream angles of attack are presented in Figure 10-4. The peak average engine deflections required to trim out the aerodynamic moments in this region were  $0.91$  degrees in pitch and  $-1.66$  degrees in yaw. The peak engine deflection for roll control occurred just prior to this region and was  $0.24$  degrees.

### 10.3 S-IVB CONTROL SYSTEM EVALUATION

The S-IVB thrust vector control system provided satisfactory pitch and yaw control during boost and during the deorbit propellant dumps. The APS provided satisfactory roll control while the vehicle was under thrust vector control. The APS also provided satisfactory, pitch, yaw, and roll control during orbital coast. APS Module 2 propellant usage was larger than predicted, due principally to LH<sub>2</sub> Non-Propulsive Vent (NPV) imbalance and IU sublimator operation. Servo valve spool stiction caused a low amplitude oscillation in the J-2 engine pitch actuator when the thrust vector control system was inactive.

#### 10.3.1 S-IVB Control System Evaluation During Burn

During S-IVB burn, control system transients were experienced at S-IB/S-IVB separation, guidance initiation, Engine Mixture Ratio (MR) shift and terminal guidance mode ( $\chi$  tilde) and S-IVB Engine Cutoff (ECO).

- ▽ BEGIN PITCH/ROLL MANEUVER
  - ▽ BEGIN ACCELEROMETER CONTROL
  - ▽ END ROLL MANEUVER
  - ▽ MACH 1
  - ▽ MAX q
  - ▽ 1ST GAIN SWITCH
  - ▽ END ACCELEROMETER CONTROL
  - ▽ 2ND GAIN SWITCH
  - ▽ TILT ARREST
  - ▽ INBOARD ENGINE CUTOFF
  - ▽ OUTBOARD ENGINE CUTOFF
  - ▽ STAGING
- MEASURED ——— SIMULATED - - -

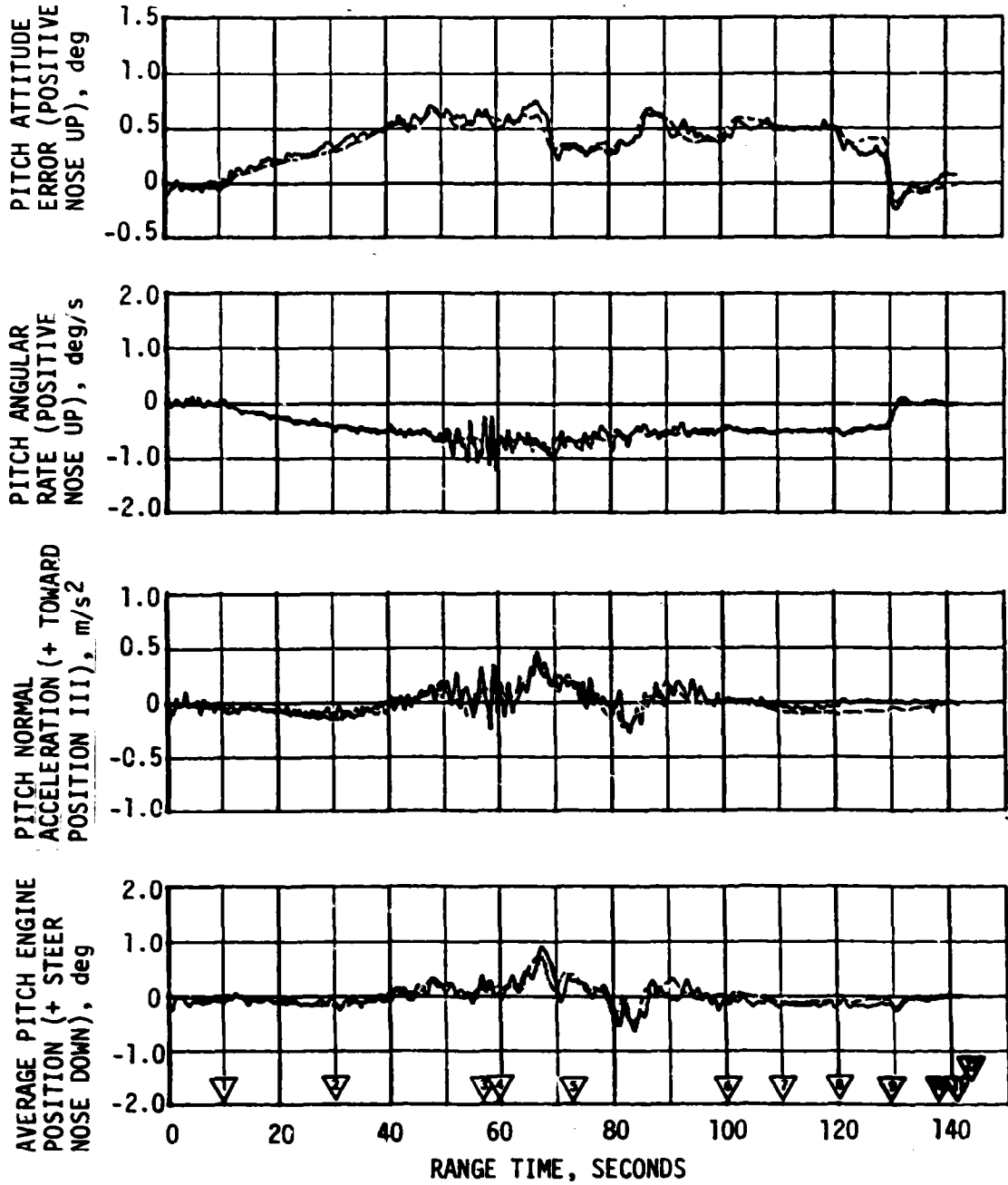


Figure 10-1. Pitch Plane Dynamics During S-IB Burn

- ▽ BEGIN PITCH/ROLL MANEUVER
- ▽ BEGIN ACCELEROMETER CONTROL
- ▽ END ROLL MANEUVER
- ▽ MACH 1
- ▽ MAX q
- ▽ 1ST GAIN SWITCH
- ▽ END ACCELEROMETER CONTROL
- ▽ 2ND GAIN SWITCH
- ▽ TILT ARREST
- ▽ INBOARD ENGINE CUTOFF
- ▽ OUTBOARD ENGINE CUTOFF
- ▽ STAGING

— MEASURED    - - - SIMULATED

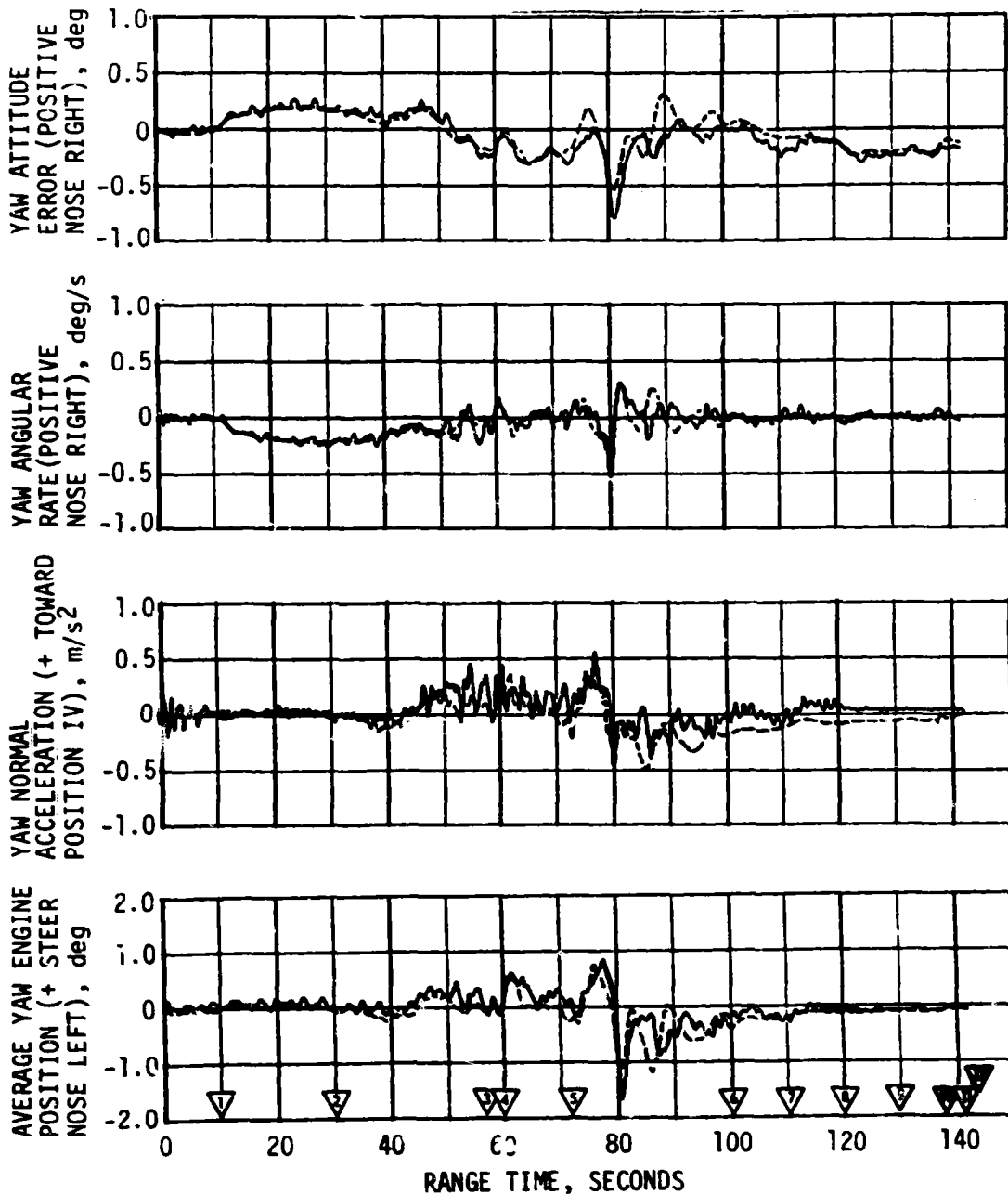


Figure 10-2. Yaw Plane Dynamics During S-IB Burn

- ▽ BEGIN PITCH/ROLL MANEUVER
  - ▽ BEGIN ACCELEROMETER CONTROL
  - ▽ END ROLL MANEUVER
  - ▽ MACH 1
  - ▽ MAX q
  - ▽ 1ST GAIN SWITCH
  - ▽ END ACCELEROMETER CONTROL
  - ▽ 2ND GAIN SWITCH
  - ▽ TILT ARREST
  - ▽ INBOARD ENGINE CUTOFF
  - ▽ OUTBOARD ENGINE CUTOFF
  - ▽ STAGING
- MEASURED    - - - SIMULATED

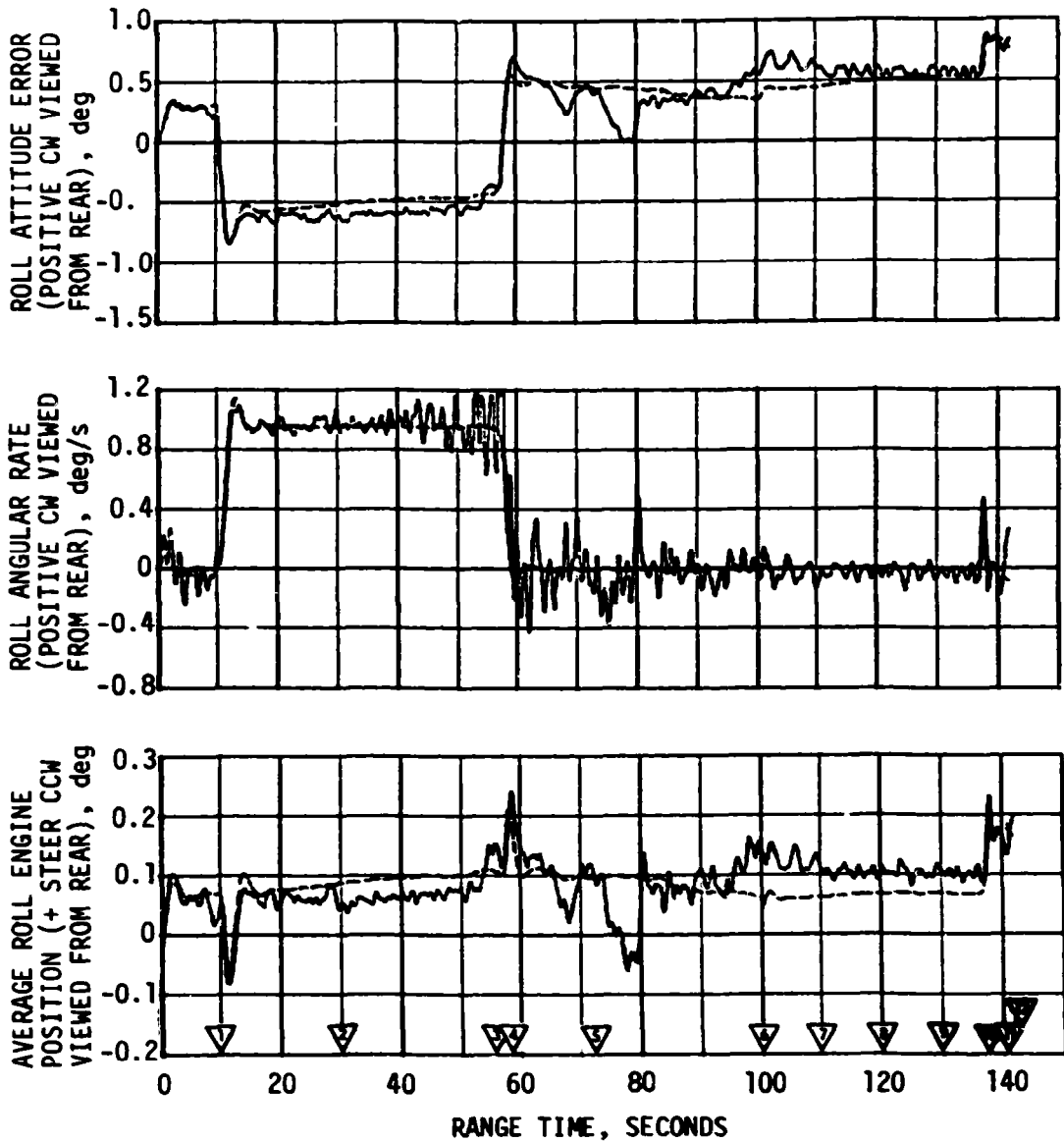


Figure 10-3. Roll Plane Dynamics During S-IB Burn

- ▽ BEGIN PITCH/ROLL MANEUVER
- ▽ BEGIN ACCELEROMETER CONTROL
- ▽ END ROLL MANEUVER
- ▽ MACH 1
- ▽ MAX q
- ▽ 1ST GAIN SWITCH
- ▽ END ACCELEROMETER CONTROL
- ▽ 2ND GAIN SWITCH
- ▽ TILT ARREST
- ▽ INBOARD ENGINE CUTOFF
- ▽ OUTBOARD ENGINE CUTOFF
- ▽ STAGING

— SIMULATED

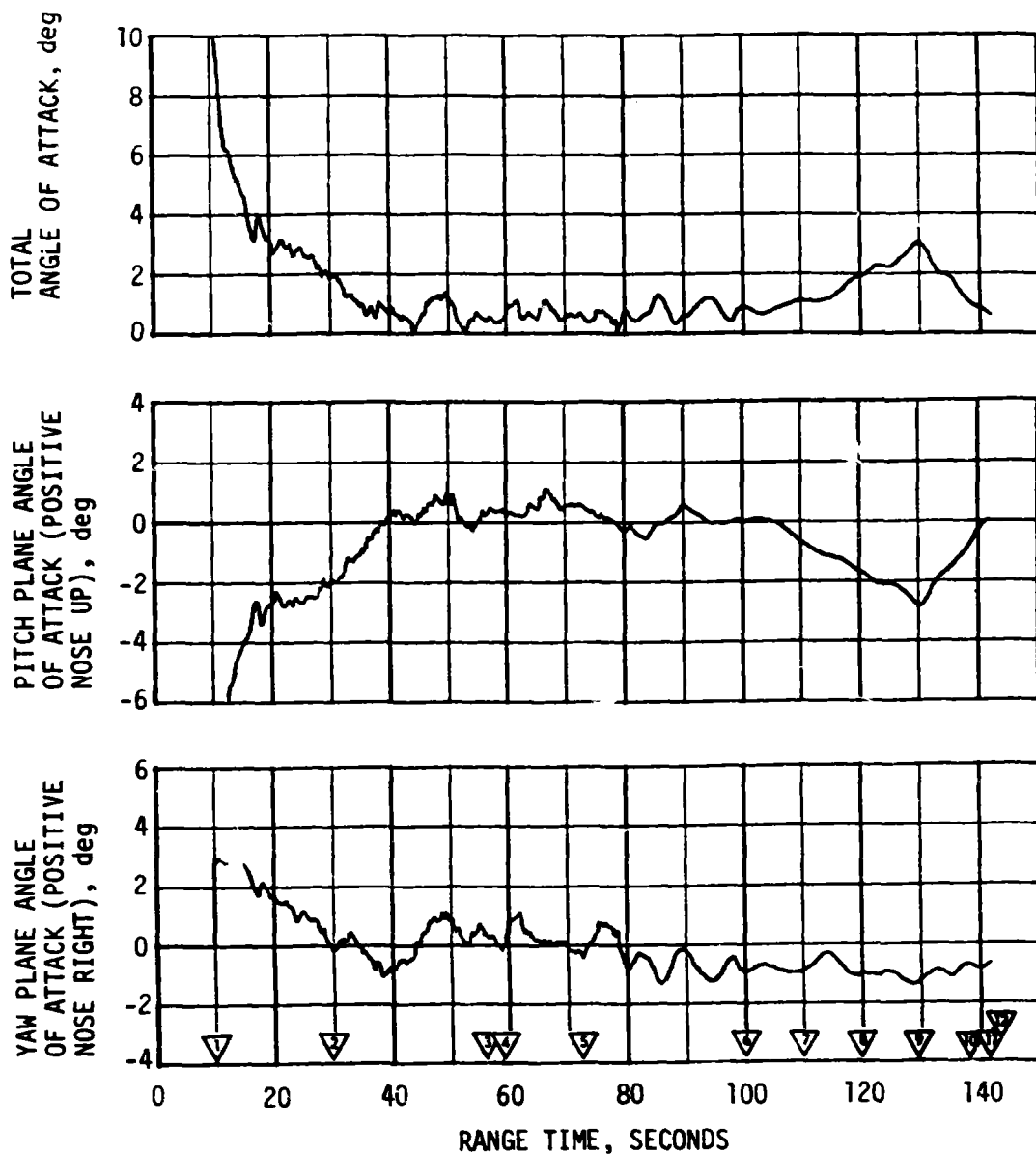


Figure 10-4. Pitch and Yaw Plane Free Stream Angle of Attack During S-IB Burn

Table 10-2. Maximum Control Parameters During S-IB Burn

PARAMETER	PITCH PLANE		YAW PLANE		ROLL PLANE	
	AMPLITUDE	RANGE TIME (SEC)	AMPLITUDE	RANGE TIME (SEC)	AMPLITUDE	RANGE TIME (SEC)
Attitude Error, deg	0.75	67.1	-0.83	81.0	0.89	136.3
Angular Rate*, deg/s	-1.02	69.7	-0.52	80.2	1.12	13.7
Average Gimbal Angle, deg	0.91	67.4	-1.66	80.7	0.24	58.6
Angle of Attack, deg	1.13	67.2	-1.31	86.0	--	--
Angle of Attack Dynamic Pressure Product, deg-N/cm <sup>2</sup> (deg-lbf/ft <sup>2</sup> )	3.84 (802)	67.2	-3.52 (-735)	86.0	--	--
Normal Acceleration, m/s <sup>2</sup> (ft/s <sup>2</sup> )	0.47 (1.54)	66.9	0.56 (1.84)	76.9	--	--

\*Angular rates are not considered valid due to the low sample rate and high noise content of the data from 50 to 60 seconds.

The transients were expected and were well within the capabilities of the control system. A discussion of the structural response resulting from the S-IVB cutoff transient is contained in Section 8.2.4.

The S-IVB burn pitch attitude error, angular rate, and actuator position are presented in Figure 10-5. The yaw plane burn dynamics are presented in Figure 10-6. The maximum attitude error and rate occurs for the pitch axis at IGM initiation. A summary of the maximum values of critical flight control parameters is presented in Table 10-3.

The pitch and yaw effective thrust vector misalignments during the first part of burn (prior to MR shift) were +0.43 and +0.36 degrees, respectively. Following the MR shift, the misalignments were +0.24 and -0.20 degrees for pitch and yaw, respectively. A steady state roll torque prior to MR shift of 39.3 N-m (29.0 lbf-ft) counterclockwise looking forward required roll APS firings. The steady state roll torque following MR shift was 37.7 N-m (27.8 lbf-ft) counterclockwise looking forward and required roll APS firings. The steady state roll torque experienced on previous flights has ranged between 51.4 N-m (45.3 lbf-ft) counterclockwise and 54.2 N-m (40.0 lbf-ft) clockwise.

- ▽ S-IVB BURN MODE ON "B"
- ▽ GUIDANCE INITIATION
- ▽ MIXTURE RATIO SHIFT
- ▽ CHI TILDE
- ▽ CHI FREEZE
- ▽ S-IVB ENGINE CUTOFF

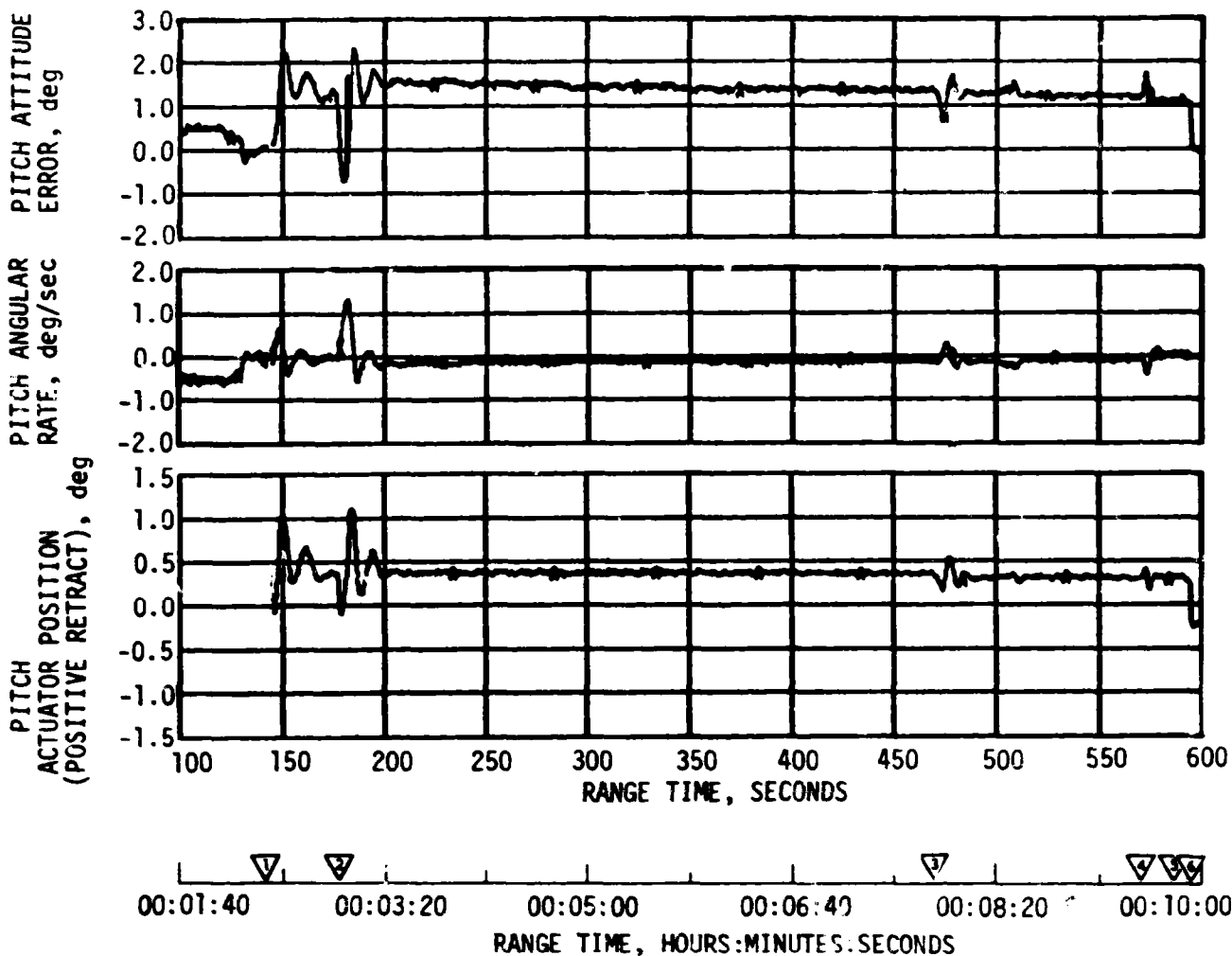


Figure 10-5. Pitch Plane Dynamics - S-IVB Burn

- ▽ S-IVB BURN MODE ON "B"
- ▽ GUIDANCE INITIATION
- ▽ MIXTURE RATIO SHIFT
- ▽ CHI TILDE
- ▽ CHI FREEZE
- ▽ S-IVB ENGINE CUTOFF

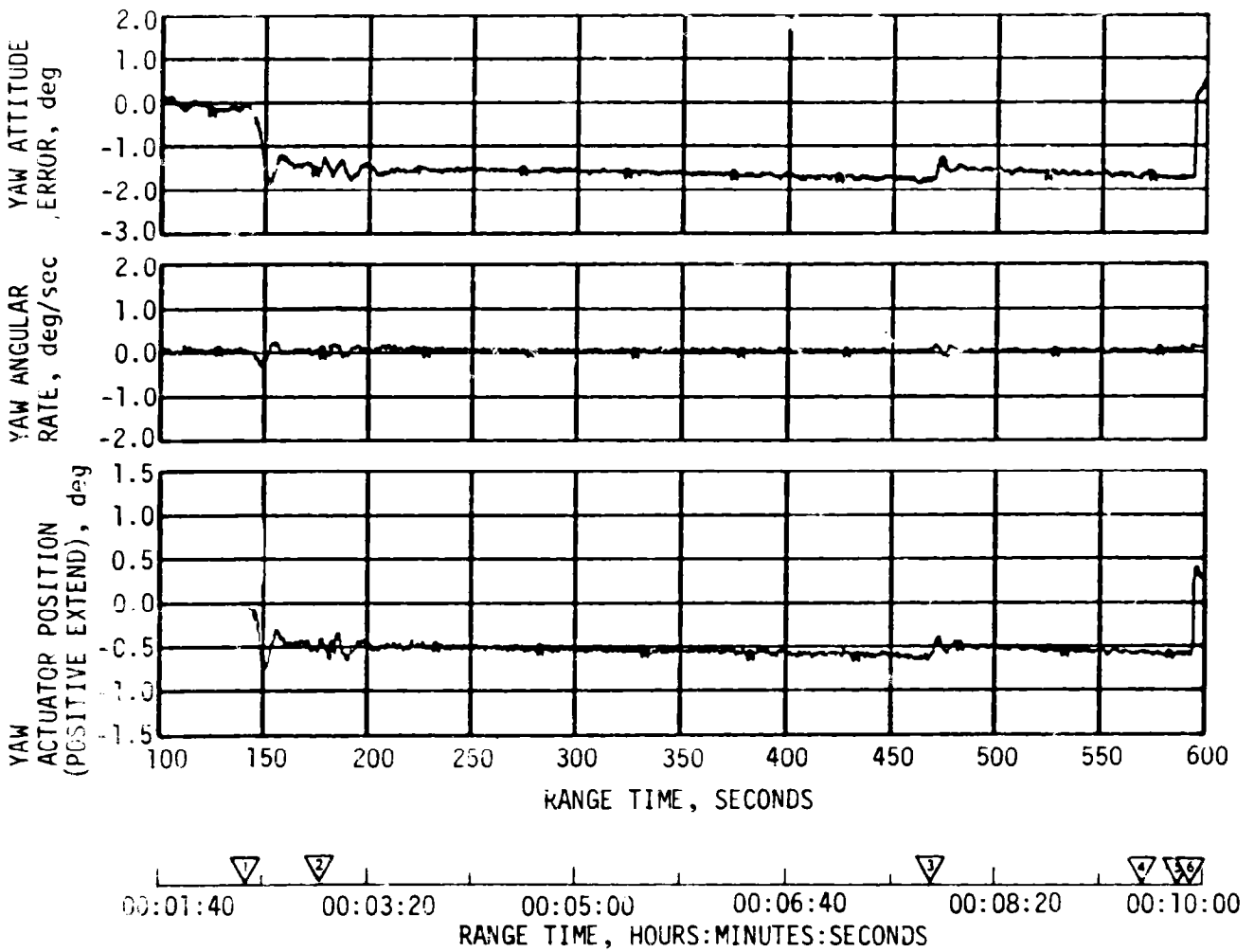


Figure 10-6. Yaw Plane Dynamics - S-IVB Burn

Table 10-3. Maximum Control Parameters During S-IVB Burn

PARAMETER	ROLL		PITCH		YAW	
	AMPLITUDE	RAISE TIME SEC	AMPLITUDE	RAISE TIME SEC	AMPLITUDE	RAISE TIME SEC
Attitude error, deg	±0.5	1.5	±0.5	1.5	±0.5	1.5
Angular Rate, deg/s	±0.5	1.5	±0.5	1.5	±0.5	1.5
Maximum in-plane angle, deg	±0.5	1.5	±0.5	1.5	±0.5	1.5
* Data involved						

Propellant sloshing during burn was observed on data obtained from the Propellant Utilization (PU) mass sensors and on the pitch and yaw actuator position and actuator valve current data. The propellant slosh had a negligible effect on the operation of the attitude control system.

### 10.3.2 S-IVB Control System Evaluation During Orbit

The APS provided satisfactory orientation and stabilization during orbit. Telemetry data following the deorbit propellant dumps and prior to reentry indicated that the vehicle was stabilized. Higher than predicted APS Module 2 propellant usage was observed.

Significant events related to orbital coast attitude control were the maneuver to the in-plane local horizontal following S-IVB cutoff, spacecraft separation, and seven maneuvers for the S-150 experiment. Table 10-4 describes the maneuvers during orbit. The pitch attitude error and angular rate for events during which telemetry data were available are shown in Figure 10-7.

Following S-IVB cutoff and switching to the orbital coast control mode, the vehicle was maneuvered to the in-plane posigrade local horizontal (position I down), and the orbital pitch rate was established. This maneuver began at 613 seconds (00:10:13) and consisted of approximately -15 degrees in pitch, +1.8 degrees in yaw, and +0.7 degrees in roll.

Spacecraft separation, which occurred at approximately 1080 seconds (00:18:00), produced vehicle disturbances similar to SA-206. See Section 10.5.2 for a discussion of vehicle motion during CSM separation.

At 1314 seconds (00:21:54) the first of a series of seven S-150 experiment maneuvers was begun. Table 10-4 describes the type of maneuver, time of maneuver, and the change in vehicle attitude. The first maneuver placed the vehicle 3 degrees from a retrograde local horizontal attitude. The second maneuver placed the vehicle in the retrograde local horizontal

Table 10-4. Attitude Maneuvers During Orbit

MANEUVER	TIME OF MANEUVER (SEC)	PITCH ATTITUDE (DEG)	YAW ATTITUDE (DEG)	ROLL ATTITUDE (DEG)
Maneuver to Local Horizontal (Position I Down)	613 to 670	262.3 to 247	-1.0 to 0.8	-0.7 to 0.0
Pitch Maneuver to +177° from Local Horizontal	1314 to 1800	203 to 350	-0.5 to 0.6 (Note 2)	0.0
Maneuver to Retrograde Local Horizontal and Roll -177 Degrees	2855 to 3155	274 to 277	1.0 (Note 2)	0.0 to -177.0
-138 Degree Roll Maneuver	5800 to 6500	(Note 1)	(Note 2)	-177.0 to 45.0
+135 Degree Roll Maneuver (Position III Down)	6231 to 6500	(Note 1)	(Note 2)	45.0 to 180.0
+45 Degree Roll Maneuver	8930 to 9030	(Note 1)	(Note 2)	180.0 to 225.0
-45 Degree Roll Maneuver (Position III Down)	12,980 to 13,070	(Note 1)	(Note 2)	225.0 to 180.0
+90 Degree Roll Maneuver (Position IV Down)	14,280 to 14,460	(Note 1)	(Note 2)	180.0 to 270.0
<p>Note 1 Orbital Pitch Rate of Approximately -0.068 deg/sec</p> <p>Note 2 Yaw Attitude Maintained in Orbit Plane</p>				

10-11

▽ INITIATE MANEUVER TO LOCAL HORIZONTAL  
 ▽ SPACECRAFT SEPARATION

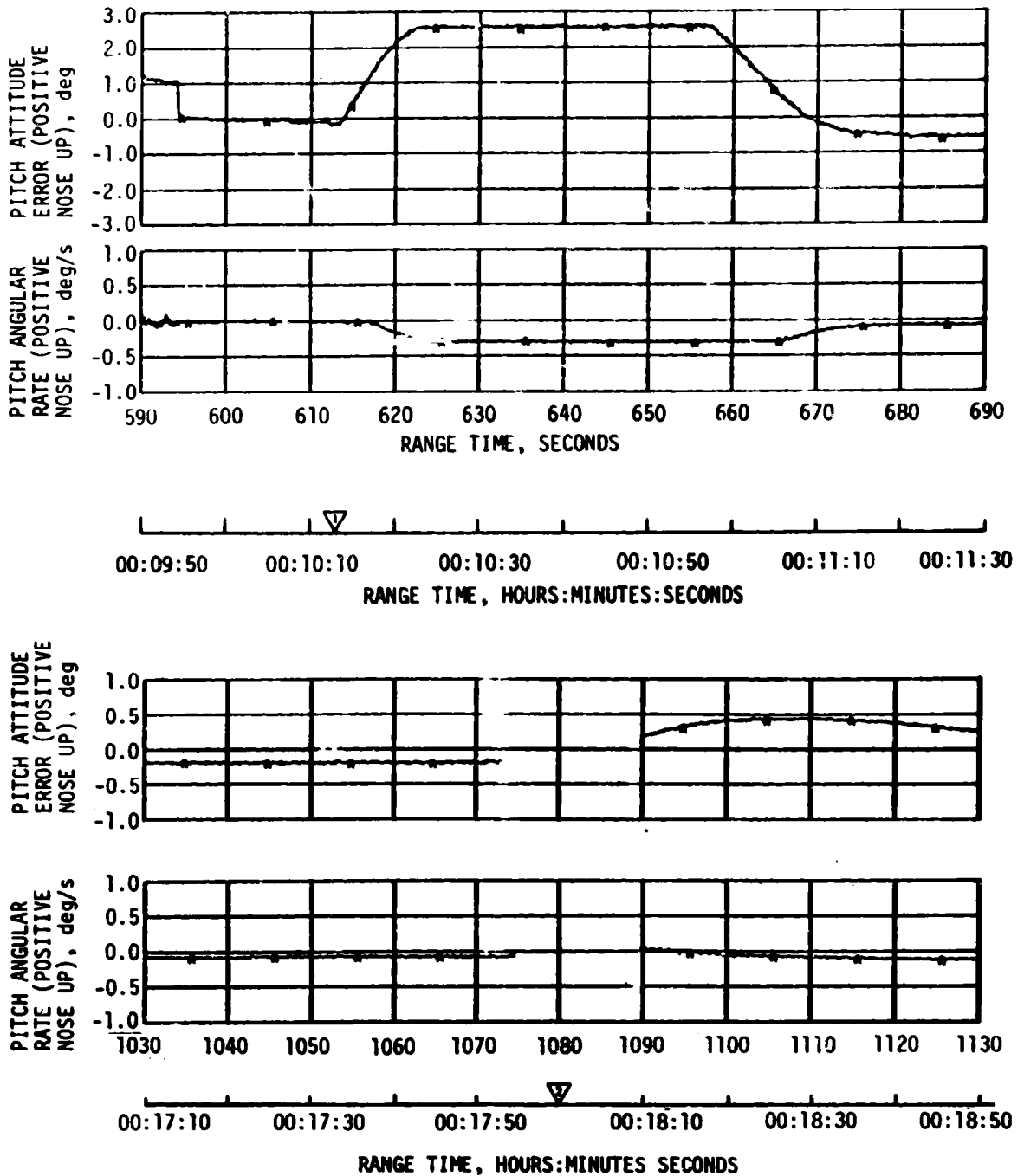


Figure 10-7. Pitch Plane Dynamics During Orbit (Sheet 1 of 4)

▽ INITIATE +177 DEGREE PITCH MANEUVER  
 (TERMINATE +177 DEGREE PITCH MANEUVER =1800 SECONDS)

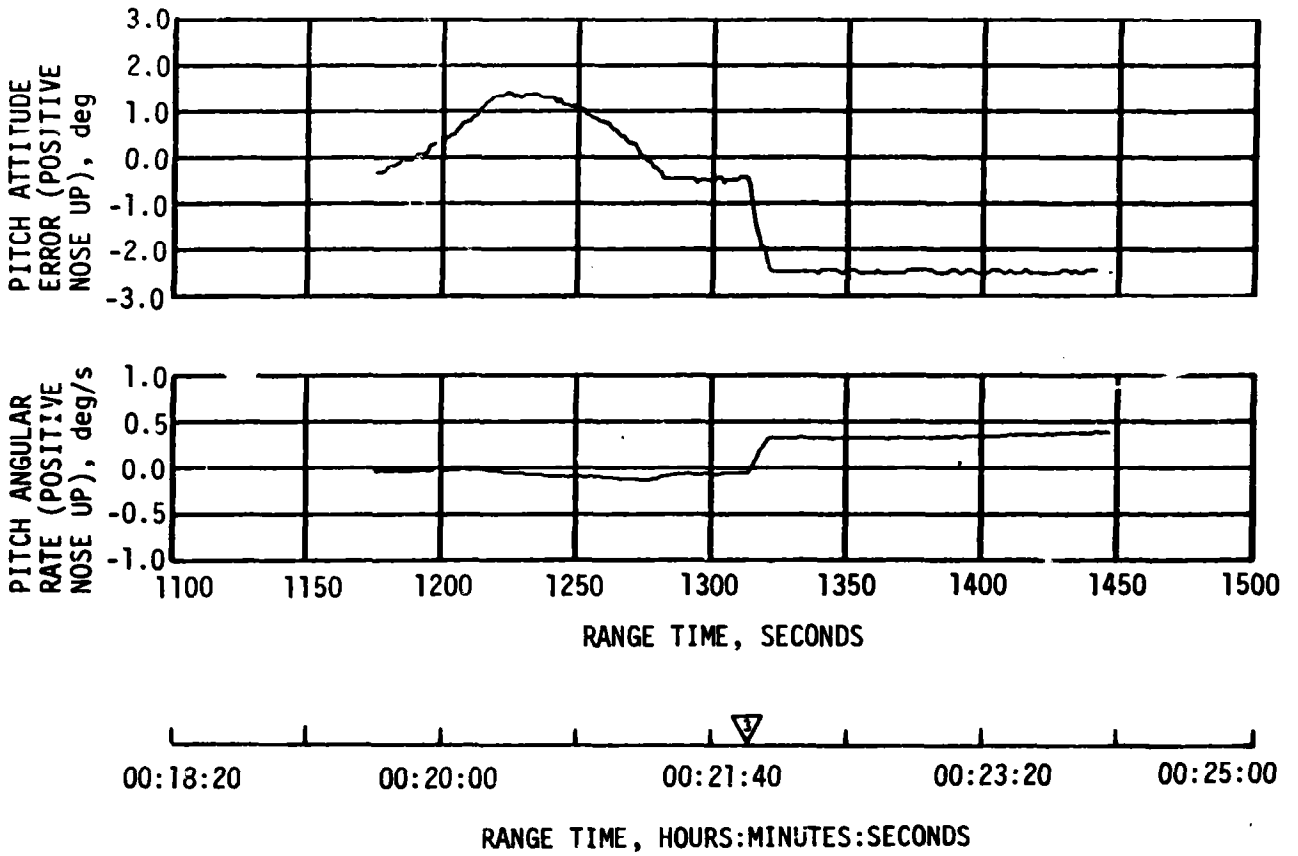


Figure 10-7. Pitch Plane Dynamics During Orbit (Sheet 2 of 4)

- ▽ TERMINATE - 177 DEGREE ROLL MANEUVER  
(INITIATE -177 DEGREE ROLL MANEUVER =2855 SEC)
- ▽ INITIATE +135 DEGREE ROLL MANEUVER
- ▽ TERMINATE +135 DEGREE ROLL MANEUVER

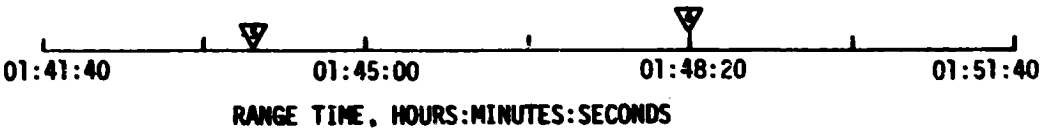
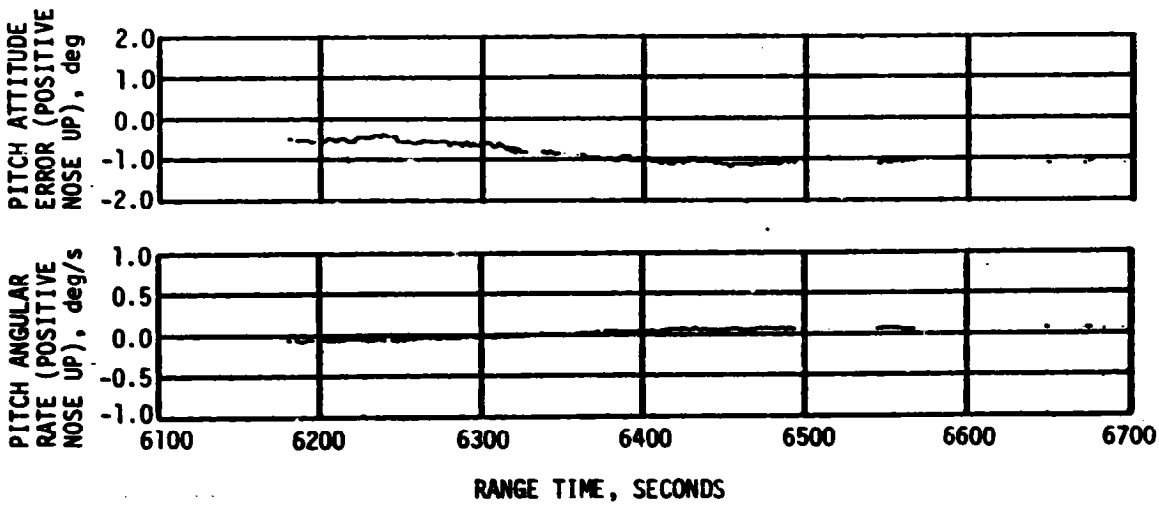
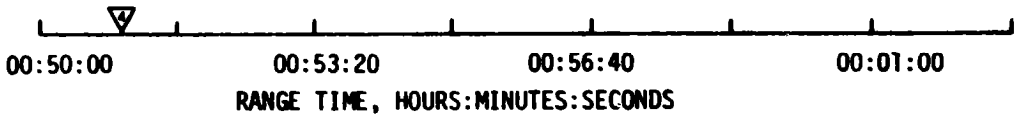
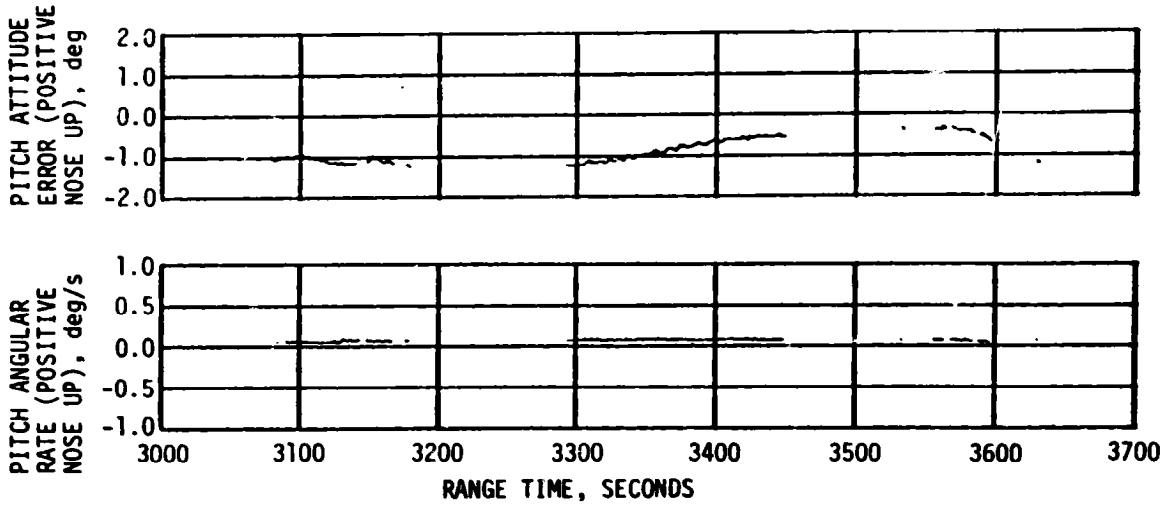


Figure 10-7. Pitch Plane Dynamics During Orbit (Sheet 3 of 4)

- ▽ INITIATE +45 DEGREE ROLL MANEUVER
- ▽ TERMINATE +45 DEGREE ROLL MANEUVER
- ▽ INITIATE +90 DEGREE ROLL MANEUVER
- ▽ TERMINATE +90 DEGREE ROLL MANEUVER

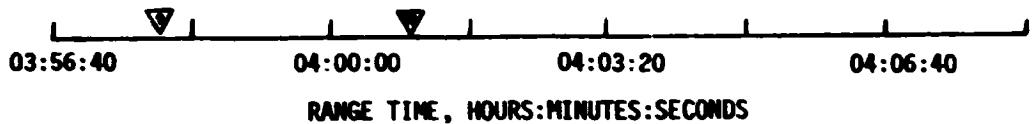
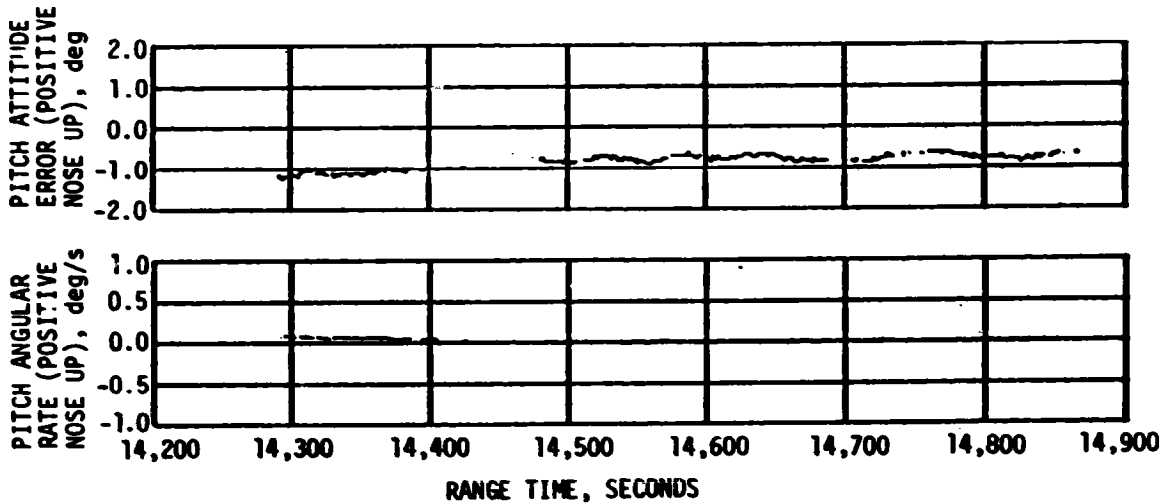
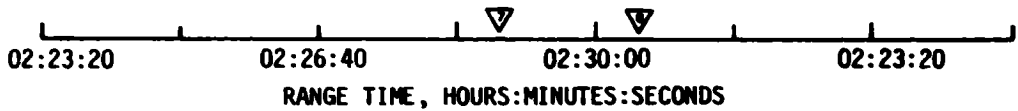
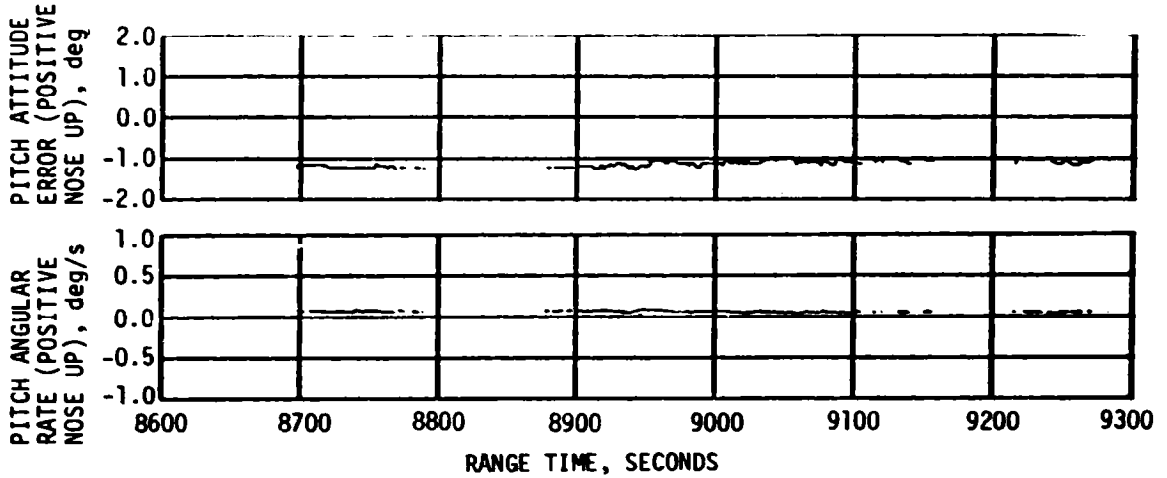


Figure 10-7. Pitch Plane Dynamics During Orbit (Sheet 1 of 4)

attitude, where the vehicle remained for the duration of the mission. The remaining maneuvers were all about the roll axis.

Propellant usage rate from APS Module 2 was higher than predicted throughout most of time base 4 (refer to Section 7.8 for APS consumption data). Prior to the flight, both modules were predicted to use approximately the same amount of propellant. A postflight reconstruction of disturbances using APS thruster firing histories indicated that the S-IVB LH<sub>2</sub> Non-Propulsive Vent (NPV) and the IU Environmental Control System (ECS) sublimator were the major contributors to the higher than predicted propellant usage.

The effect of the LH<sub>2</sub> NPV is shown in Figure 10-8. The pitch and roll attitude errors reflect a disturbing moment concurrent with the onset of LH<sub>2</sub> relief venting at 3560 seconds (00:59:20). It is estimated that the average NPV pitch disturbing moment was between two and three ft-lb and that the NPV accounted for 50 to 70 percent of the increased APS propellant usage. Reconstruction of the total pitch disturbing moment (Figure 10-9) shows a correlation with sublimator water valve cycles. The yaw disturbing moment was also observed to change direction in a cyclic manner which correlated with sublimator operation. Net yaw moment was slightly more than 1.0 ft-lb prior to a water valve cycle and approximately -1.0 ft-lb immediately following.

The NPV effect was less than that which can be produced by allowable tolerances of NPV thrust imbalance and vent misalignment. Demands originating from the IU sublimator were minor and resulted from normal operation.

#### 10.3.2.1 Pitch Actuator Disturbance

The pitch actuator exhibited a low frequency small amplitude oscillation during several periods when the thrust vector control system was inactive and the auxiliary hydraulic pump was on for thermal conditioning. Available data shows that actuator motion occurred during the following periods:

1. For approximately 300 seconds prior to start of S-IVB burn.
2. Following S-IVB cutoff until normal hydraulic pressure decay (approximately 90 seconds after burn mode off signal).
3. For approximately the first ten seconds of auxiliary pump cycle #2 (5656 seconds to 5704 seconds).
4. During auxiliary pump cycle #4 (11,056 seconds to 11,104 seconds).
5. During auxiliary pump cycle #6 (15,646 seconds to 16,126 seconds).

Prior to S-IVB burn and during auxiliary pump cycles number 4 and number 6, the pitch actuator motion was periodic with periods of 100 seconds, 25 seconds and between 12 and 20 seconds, respectively. The peak-to-peak

▽ END -177 DEGREE ROLL MANEUVER  
 ▽ LH<sub>2</sub> NPV RELIEF CYCLE

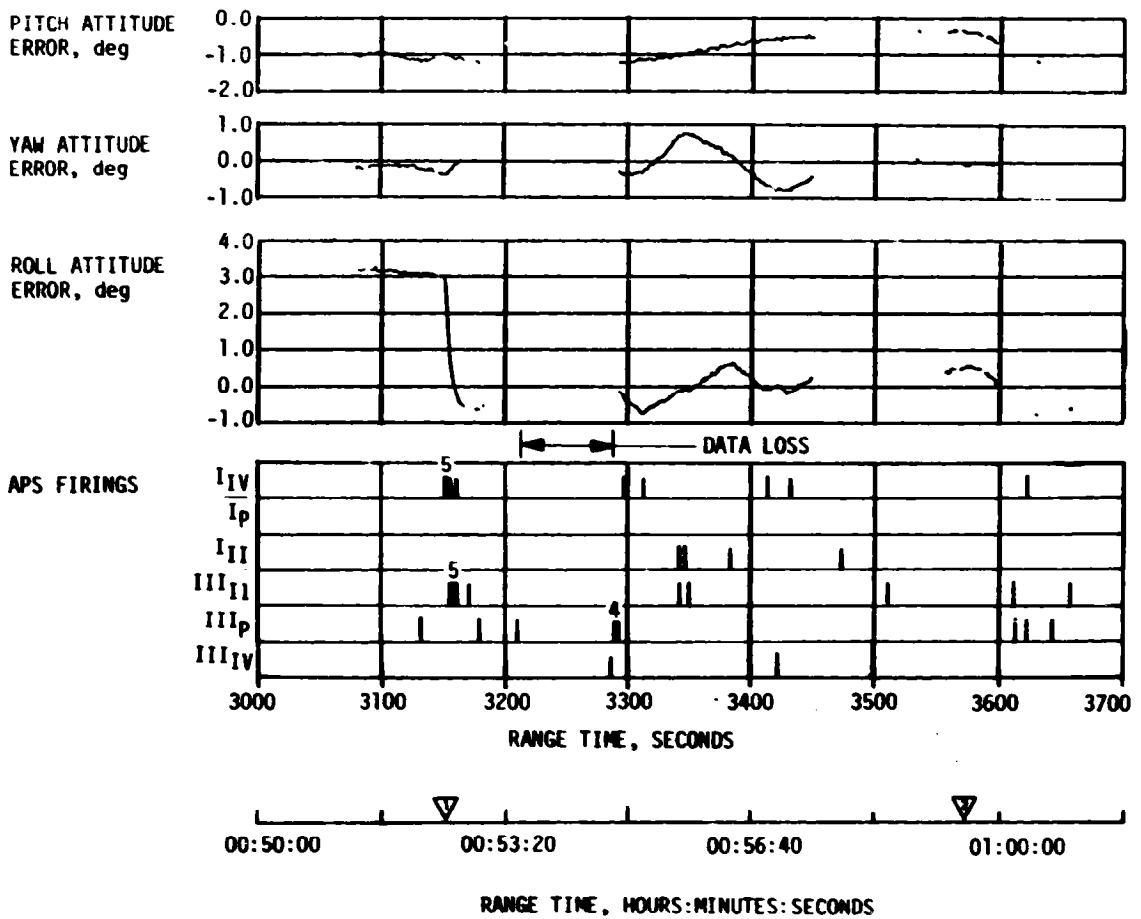


Figure 10-8. APS Activity During LH<sub>2</sub> NPV Relief Venting (Sheet 1 of 2)

▽ END -177 DEGREE ROLL MANEUVER  
 ▽ LH<sub>2</sub> NPV RELIEF CYCLE

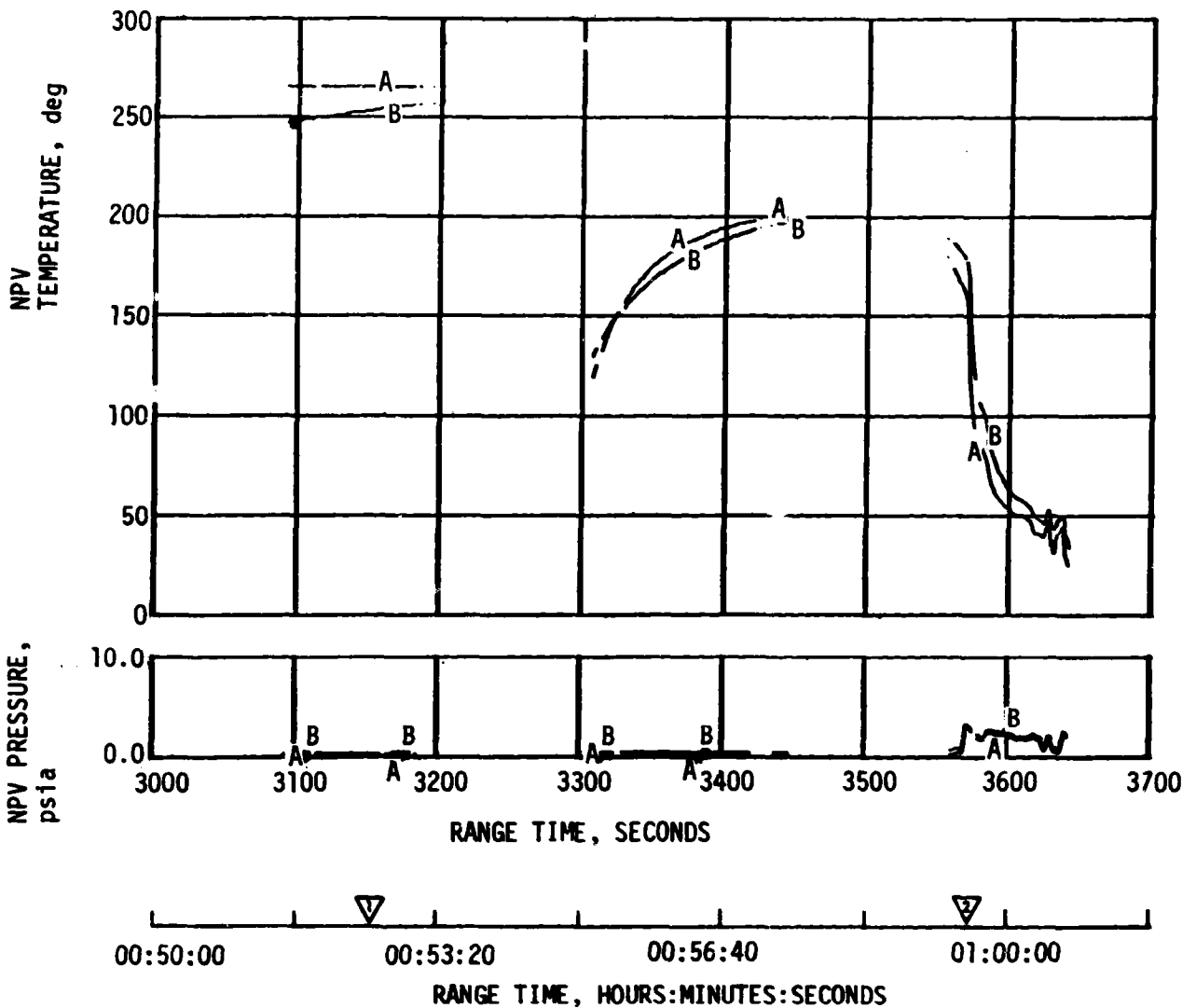


Figure 10-8. APS Activity During LH<sub>2</sub> NPV Relief Venting (Sheet 2 of 2)

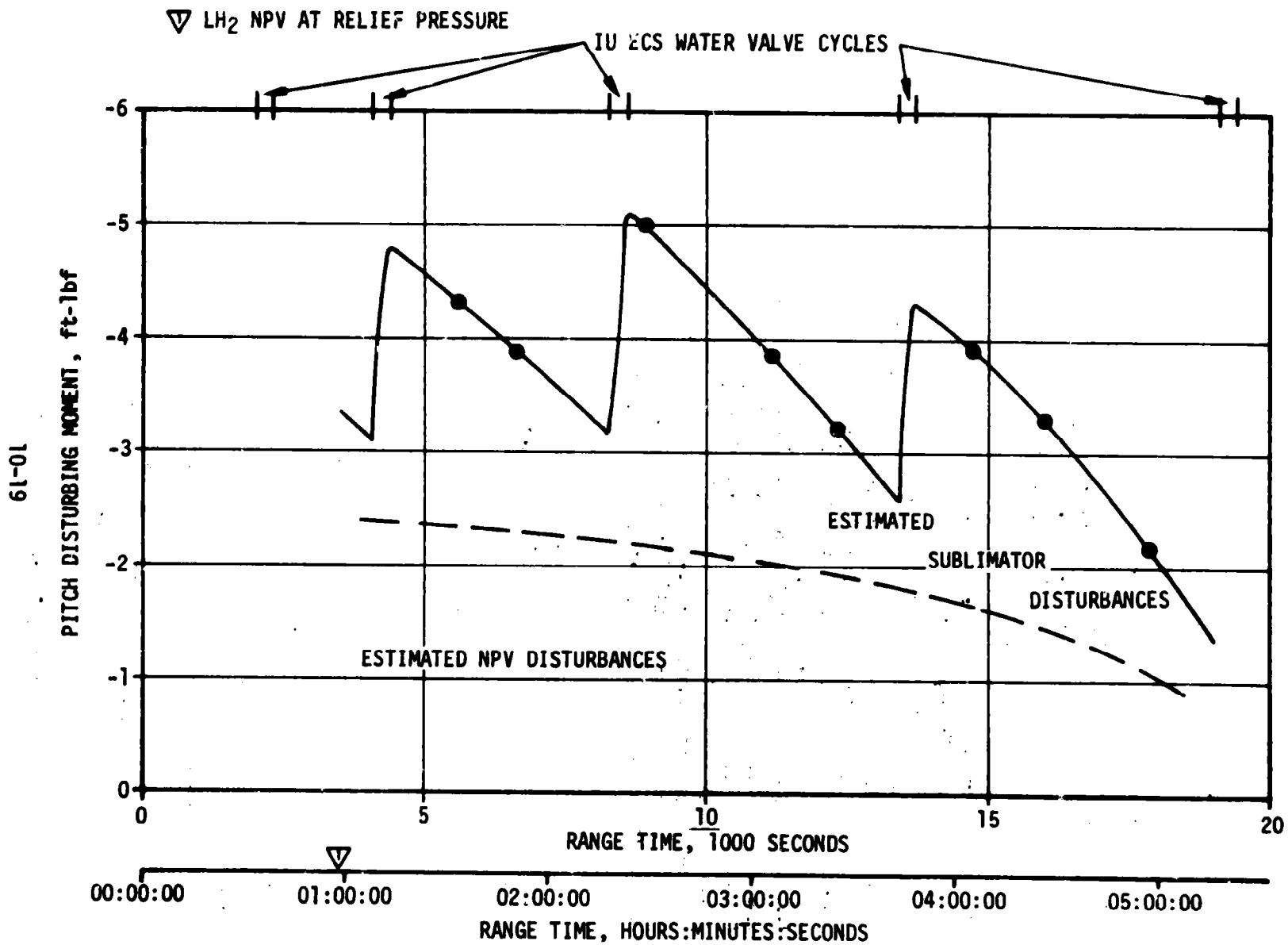


Figure 10-9. S-IVB Pitch Disturbance During Coast

amplitude of the motion ranged between 0.1 and 0.2 degrees of engine deflection. In addition to the motion observed on the pitch actuator, the engine position null offset observed during auxiliary pump on cycles was larger than noted on previous flights. SA-206, for example, showed a maximum pitch and yaw null offset for these periods of approximately 0.1 degree, while on SA-207 null offsets were observed to be approximately -0.30 degree in pitch and 0.4 degree in yaw. While larger than observed on previous flights, these null offset values are within the specification range for the servo valve.

An analog computer simulation of the valve actuator dynamics was implemented to investigate the low amplitude oscillation characteristics of the system with non-linear characteristics in the valve. Stiction (static friction) in the valve spool (due to minute contaminants in the valve), suspected to be the cause of low amplitude oscillations, was included in the simulation. Figure 10-10 presents a comparison of a simulation generated engine position and the actual engine position during auxiliary pump cycle number 6. A small amount of spool stiction (equivalent to 0.01 inch-pounds of torque-motor torque) is all that was required to produce the oscillations. A slight asymmetry in the stiction characteristic was included to achieve the asymmetric engine position trace. These simulation results substantiate the conclusion that spool stiction caused the low amplitude oscillations observed and that the level of this stiction was quite low, having a negligible effect on system performance at higher amplitudes such as during powered flight or during deorbit dump.

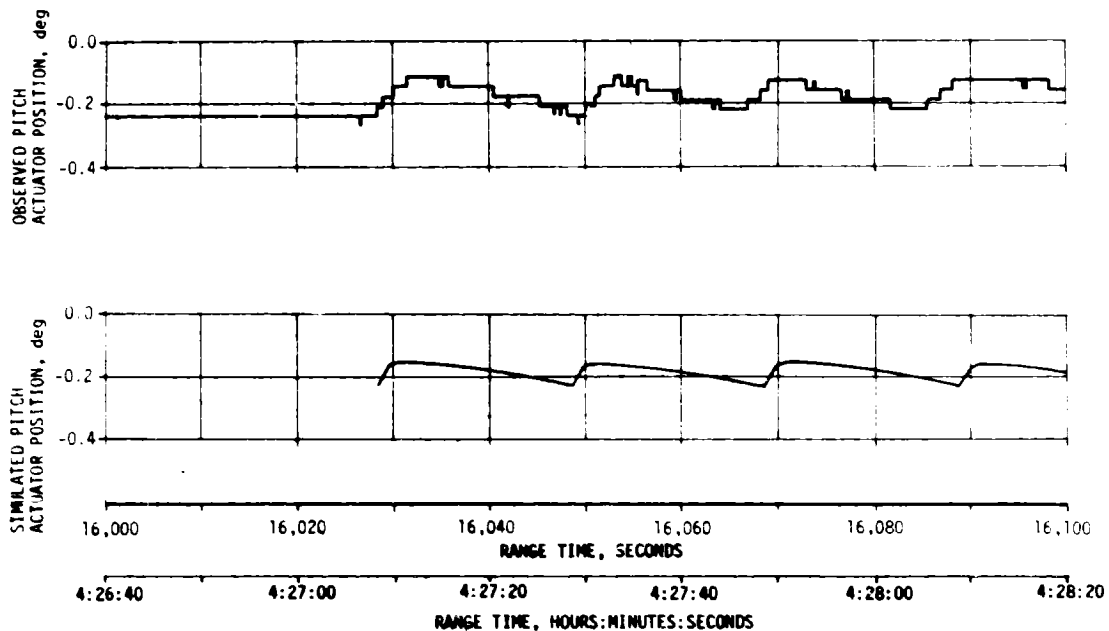


Figure 10-10. Comparison of Measured S-IVB Pitch Actuator Motion with Simulation Incorporating Effects of Stiction

### 10.3.3 S-IVB Control System Evaluation During Deorbit

Satisfactory vehicle stability and control characteristics were observed during the deorbit propellant dump. Thrust Vector Control (TVC) was used for pitch and yaw, while the APS was used for roll control. Attitude error and attitude rate data for the pitch, yaw and roll axes along with APS firing data are presented in Figure 10-11 (Sheet 1 of 2) for the last 132 seconds of the 445 second LOX dump and the 590 second LH<sub>2</sub> dump. The figure also shows the 30 second period between LOX and LH<sub>2</sub> dump, during which time there is no thrust to provide pitch and yaw control moment.

Although telemetry data could not be obtained for the first 313 seconds of the LOX dump, a comparison of the steady-state value of the attitude error data in the figure with predicted maximum values shows that, in general, performance was better than predicted. For example, the steady-state pitch attitude error was predicted to be approximately -3.12 degrees, while the actual is observed to be approximately -0.15 degree. The predicted maximum value is based on the known attitude error contribution due to center of gravity (cg) offset, which is approximately -1.12 degrees and a worst case thrust vector misalignment (in magnitude and direction) which adds an additional -2.00 degrees. A comparison of the average yaw attitude error shows a similar improvement over the predicted values. The predicted maximum steady-state yaw attitude error is approximately -3.7 degrees, while the actual is only -2.1 degrees. The predicted yaw attitude error is also based on contribution due to cg offset, which is known to be -1.7 degrees, and the worst case thrust vector misalignment contribution of -2.00 degrees of attitude error.

Analysis of the observed data shows that, in addition to attitude errors due to cg offset and thrust vector misalignment, actuator null bias provided a significant contribution to the total attitude error. (Actuator null bias is obtained as the difference between the observed actuator position and the commanded actuator position.) Actuator null bias on previous flights has been near zero. For example, SA-206 actuator null bias during deorbit was not measurable and during powered flight amounted to approximately -0.06 degree and 0.07 degree in pitch and yaw actuator position, respectively. On the other hand, the SA-207 average null bias amounted to -0.1 and 0.27 degrees in pitch and yaw, respectively, during powered flight and -0.26 and 0.40 degrees during deorbit. Including the actuator null bias in the analysis of the SA-207, the average pitch attitude error during deorbit shows that the observed value of -0.15 degrees is composed of (a) -1.12 degrees of attitude error due to the known cg offset, (b) 0.52 degrees of attitude error due to null bias and (c) 0.45 degrees of attitude error due to the effective thrust vector misalignment. A similar breakdown for the average yaw attitude error shows that the observed value of -2.1 degrees is composed of (a) -1.70 degrees of attitude error due to the known cg offset (b) -0.80 degrees of attitude error due to null bias and (c) 0.40 degrees of attitude error due to thrust vector misalignment.

During the 30 second period between LOX and LH<sub>2</sub> dump (19,672 seconds [05:27:52] to 19,702 seconds [05:28:22]), in which there is no thrust

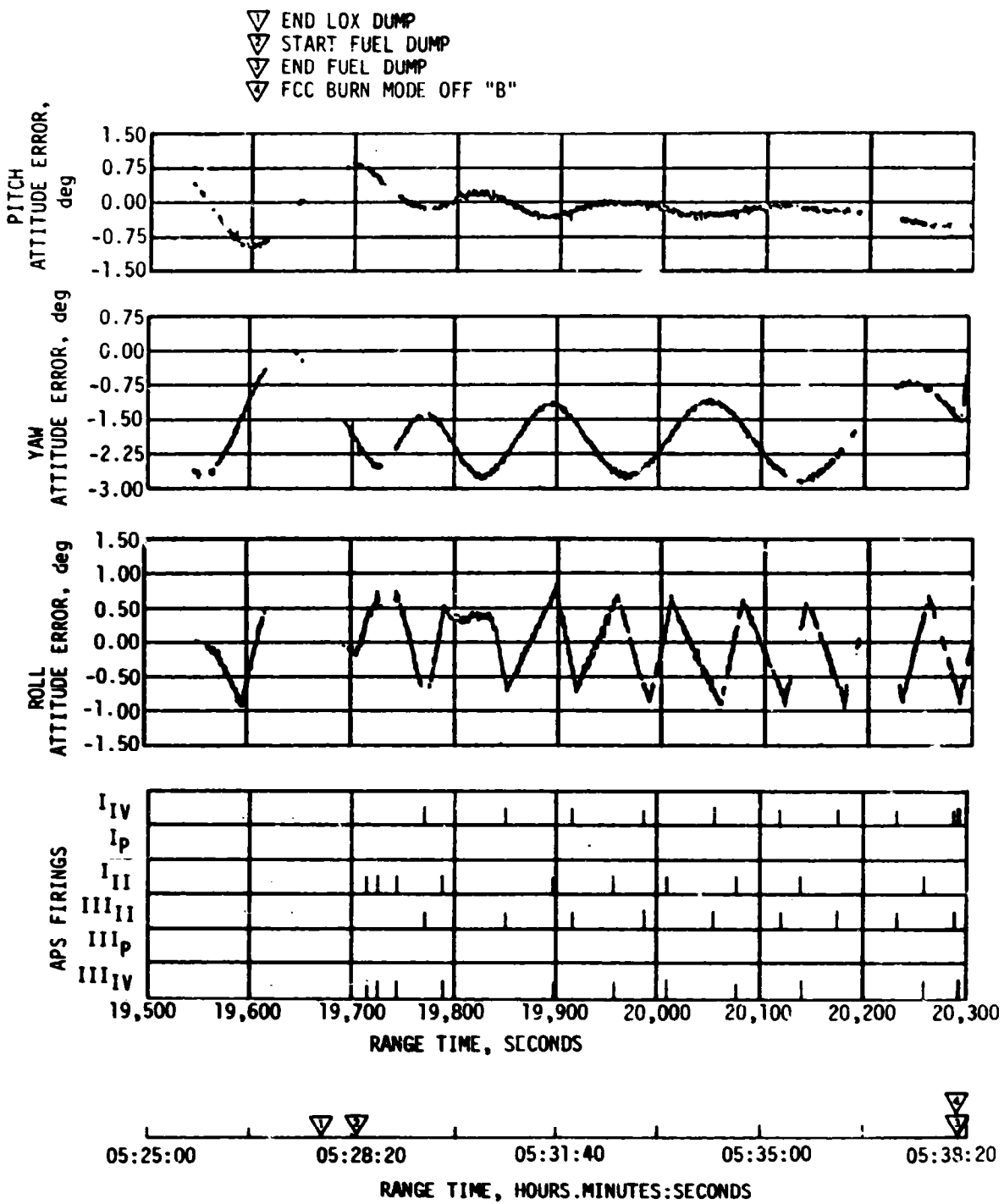


Figure 10-11. Vehicle Dynamics During Deorbit (Sheet 1 of 2)

▽ FCC BURN MODE OFF "B"

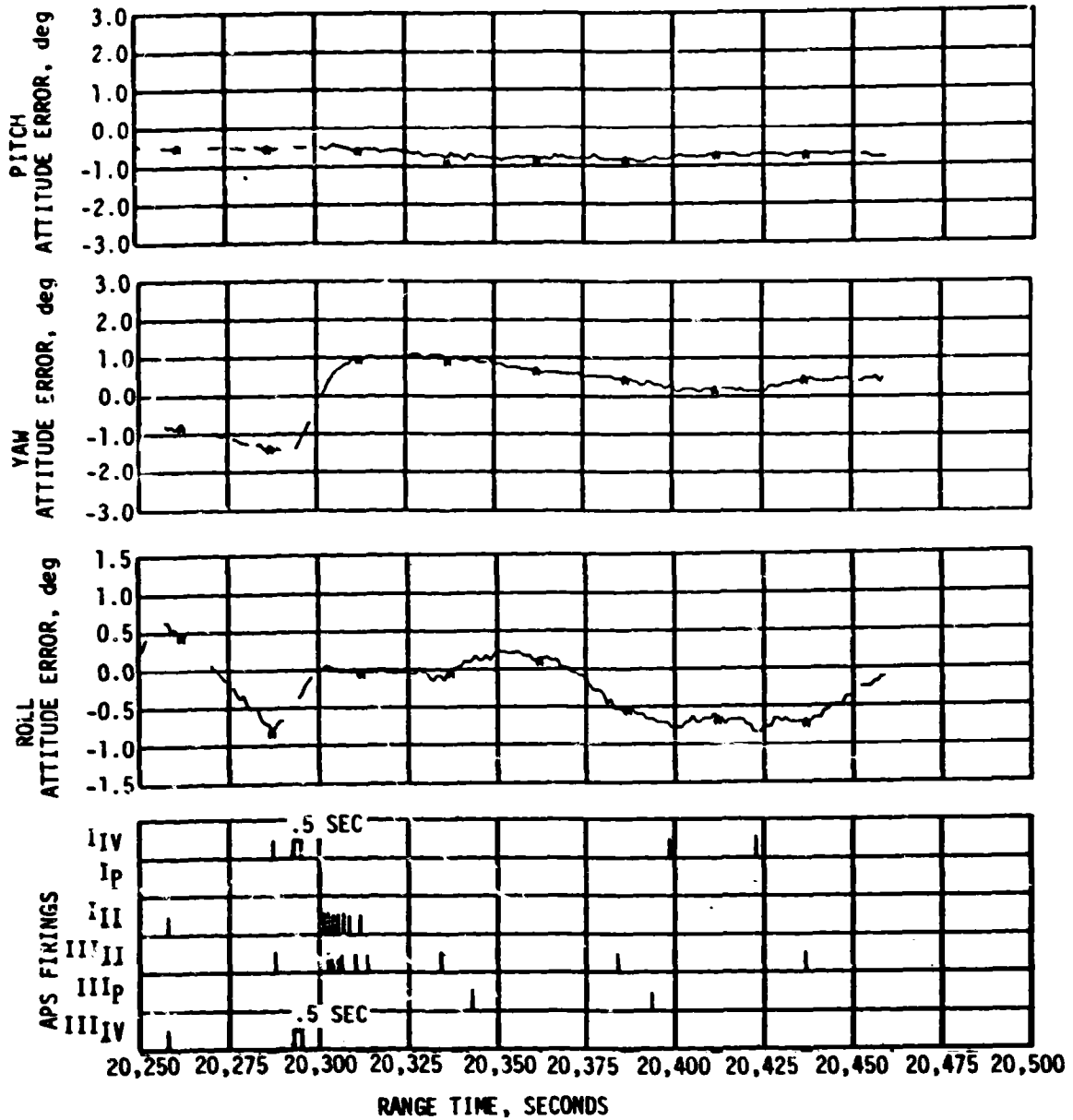


Figure 10-11. Vehicle Dynamics During Deorbit (Sheet 2 of 2)

for control, it is noted from the figure that the delta increase in attitude error is much larger in yaw than in pitch. The reason for this is that the residual yaw rate at LOX dump termination is much larger than the residual pitch rate (-0.2 degrees/second versus approximately 0.03 degrees/second). In both axes, the sense of the rate tends to increase the attitude errors during the uncontrolled period.

A comparison of the maximum peak to peak amplitudes for SA-206 and SA-207 attitude error data shows the SA-207 data to be well within that reported previously for SA-206. For example, the maximum peak to peak amplitude occurred in yaw for SA-206 and was approximately 4.6 degrees. The SA-207 maximum peak to peak attitude error also occurred about the yaw axis but was only 2.7 degrees.

The vehicle was observed to be limit cycling in the roll axis during LOX and LH<sub>2</sub> propellant dumps, thus indicating a very low or no roll torque on the vehicle during the propellant dumps. There was a slight roll disturbance at approximately 19,800 seconds (05:30:00) which required one pair of roll APS firings to control.

The programmed command for S-IVB burn mode off "B" was commanded at 20,292.9 seconds (05:38:12.9), completing the requirements for transferring pitch and yaw attitude control from the thrust vector control system to coast attitude control system.

Initial conditions for coast attitude control were as follows:

Pitch Attitude Error	-0.4 deg	Pitch Angular Rate	0.1 deg/sec
Yaw Attitude Error	-1.2 deg	Yaw Angular Rate	-0.1 deg/sec
Roll Attitude Error	-0.4 deg	Roll Angular Rate	0.1 deg/sec

These attitude errors and angular rates were nulled out by the coast attitude control system. As can be seen from Figure 10-11, disturbances on the vehicle following the propellant dumps were small.

#### 10.4 INSTRUMENT UNIT CONTROL COMPONENTS EVALUATION

The control subsystem functioned properly throughout the SA-207 mission. All planned maneuvers occurred at or near the anticipated times of flight. Gain switching and the limited use of control accelerometers during S-IB boost were accomplished properly.

#### 10.5 SEPARATION

##### 10.5.1 S-IB/S-IVB Separation

A detailed reconstruction of the separation dynamics was not possible, since S-IVB data dropped out for approximately 2.3 seconds following

separation. The separation analysis was done by comparing SA-205 data with the available SA-207 data. Comparison of S-IB and S-IVB longitudinal acceleration and body rates with SA-205 data showed essentially nominal separation.

Figure 10-12 shows the S-IB/S-IVB longitudinal acceleration, and Figure 10-13 shows pitch, yaw, and roll angular rates during S-IB/S-IVB separation. Vehicle dynamics were nominal and well within staging limits.

#### 10.5.2 S-IVB/CSM Separation

S-IVB/CSM separation was accomplished on SA-207 with the vehicle in the in-plane local horizontal attitude with an orbital pitch rate of approximately  $-0.068$  degrees/second. S-IVB disturbances due to spacecraft separation were first observed at 1080.6 seconds (00:18:00.6) on APS engine firing data. However, disturbances may have occurred earlier, but were not evidenced due to data dropout during separation. The S-150 experiment deployment sequence which is referenced to S-IVB/CSM separation indicates that S-IVB/CSM separation occurred at approximately 1080.4 seconds (00:18:00.4). Maximum vehicle rates following separation were 0.09 degrees/second pitch,  $-0.09$  degrees/second yaw, and 0.0 degrees/second roll. APS firings occurred for approximately 30 seconds following separation in response to separation-induced disturbances.

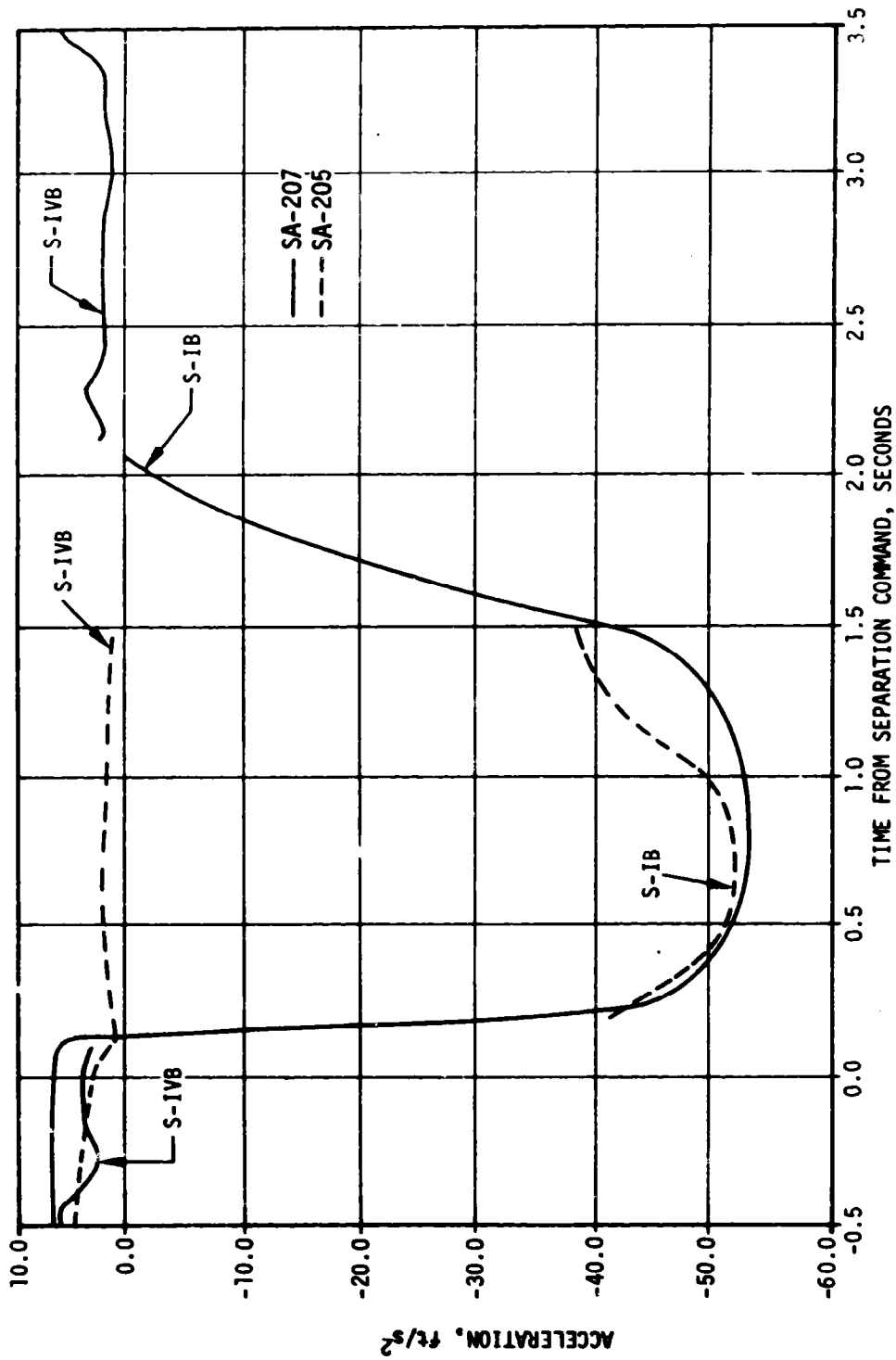


Figure 10-12. S-IB/S-IVB Longitudinal Acceleration During Separation

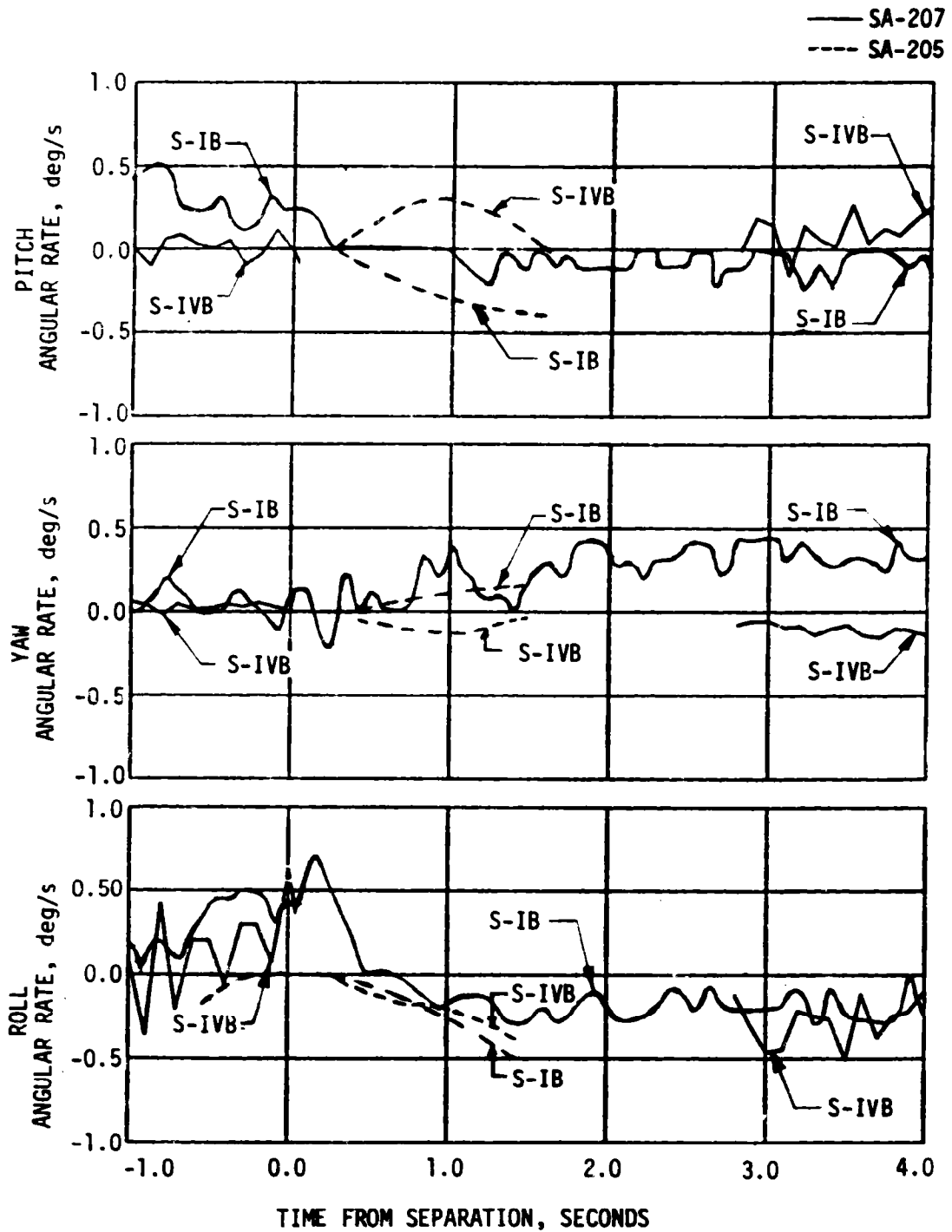


Figure 10-13. Angular Velocities During S-IB/S-IVB Separation

## SECTION 11

### ELECTRICAL NETWORKS AND EMERGENCY DETECTION SYSTEM

#### 11.1 SUMMARY

The electrical systems and Emergency Detection System (EDS) of the SA-207 launch vehicle performed satisfactorily during the flight. Battery performance (including voltages, currents, and temperatures) was satisfactory and remained within acceptable limits. Operation of all power supplies, inverters, Exploding Bridge Wire (EBW) firing units, and switch selectors was nominal.

#### 11.2 S-IB STAGE ELECTRICAL SYSTEM

The S-IB-7 stage electrical system was modified to eliminate a single-point failure mode in the premature ignition detection circuit and to add shielding to the Remote Digital Sub-Multiplexer signal input and signal return wires. There were no malfunctions associated with the changes.

The S-IB stage electrical system operated satisfactorily. Battery voltage and current excursions during flight coincided with significant vehicle events as predicted. Voltages of the 1D10 and 1D20 batteries averaged 29.0 and 28.3 V, respectively, from power transfer to S-IB/S-IVB separation and remained within the allowable range of 27 to 30 V. The current from batteries 1D10 and 1D20 averaged 10.2 and 19.2 amperes, respectively, throughout the boost phase. The most pronounced power drains were caused by the H-1 engines conax valve firings and pre-vent operations during S-IB stage engine cutoff. Battery power consumption was within the rated capacity of each battery as shown in Table 11-1.

The three measuring voltage supplies performed satisfactorily and remained within the allowable range of  $5.000 \pm .0125$  V.

All switch selector channels functioned as commanded by the Instrument Unit (IU) and were within the required time limits.

The separation and retro motor EBW firing units were armed and triggered as programmed. Charging time and voltage characteristics were within performance limits.

The range safety command system EBW firing units were in a state-of-readiness for vehicle destruct had it been necessary.

Table 11-1. S-IB Stage Battery Power Consumption

BATTERY	RATED CAPACITY (AMP-HR)	POWER CONSUMPTION*	
		AMP-HR	PERCENT OF CAPACITY
1D10	33.3	4.7	14.0
1D20	33.3	5.3	15.8
*From activation until end of telemetry (at 386 seconds).			

### 11.3 S-IVB STAGE ELECTRICAL SYSTEM

The S-IVB stage electrical system performed satisfactorily. The battery voltages and currents remained within the normal range.

Battery temperatures remained within specified limits indicating that all battery heater controllers operated properly.

Battery voltage, current and temperature plots are shown in Figures 11-1 through 11-4.

Battery power consumption was within the rated capacity of each battery as shown in Table 11-2. The three 5 V and five 20 V excitation modules all performed within acceptable limits. The LOX and LH<sub>2</sub> chilldown inverters performed satisfactorily and fulfilled load requirements.

All switch selector channels functioned properly, and all sequencer outputs were issued within required time limits.

Performance of the EBW circuitry for the separation system was satisfactory. Firing unit charge and discharge responses were within predicted time and voltage limits. The command destruct firing units were in the required state-of-readiness had vehicle destruct been necessary.

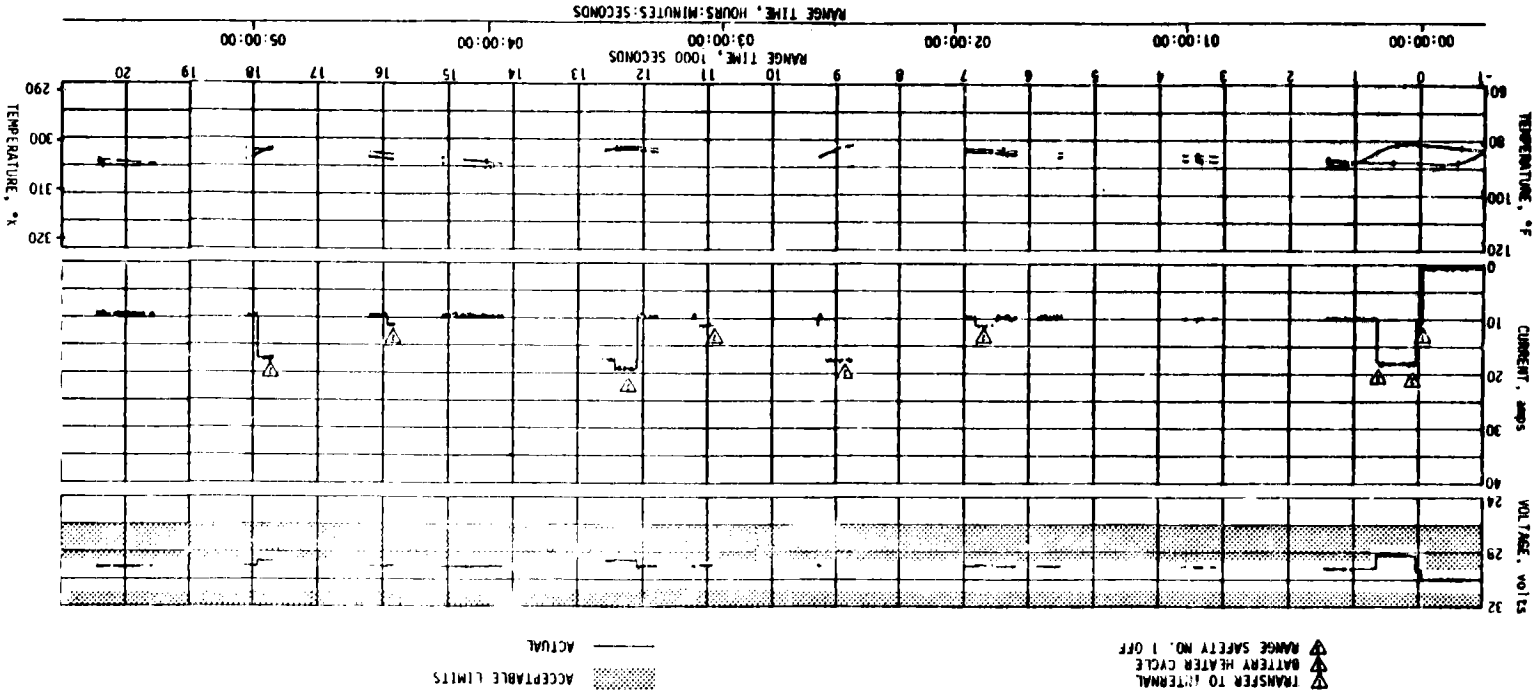


Figure 11-1. S-IVB Stage Forward No. 1 Battery Voltage, Current, and Temperature

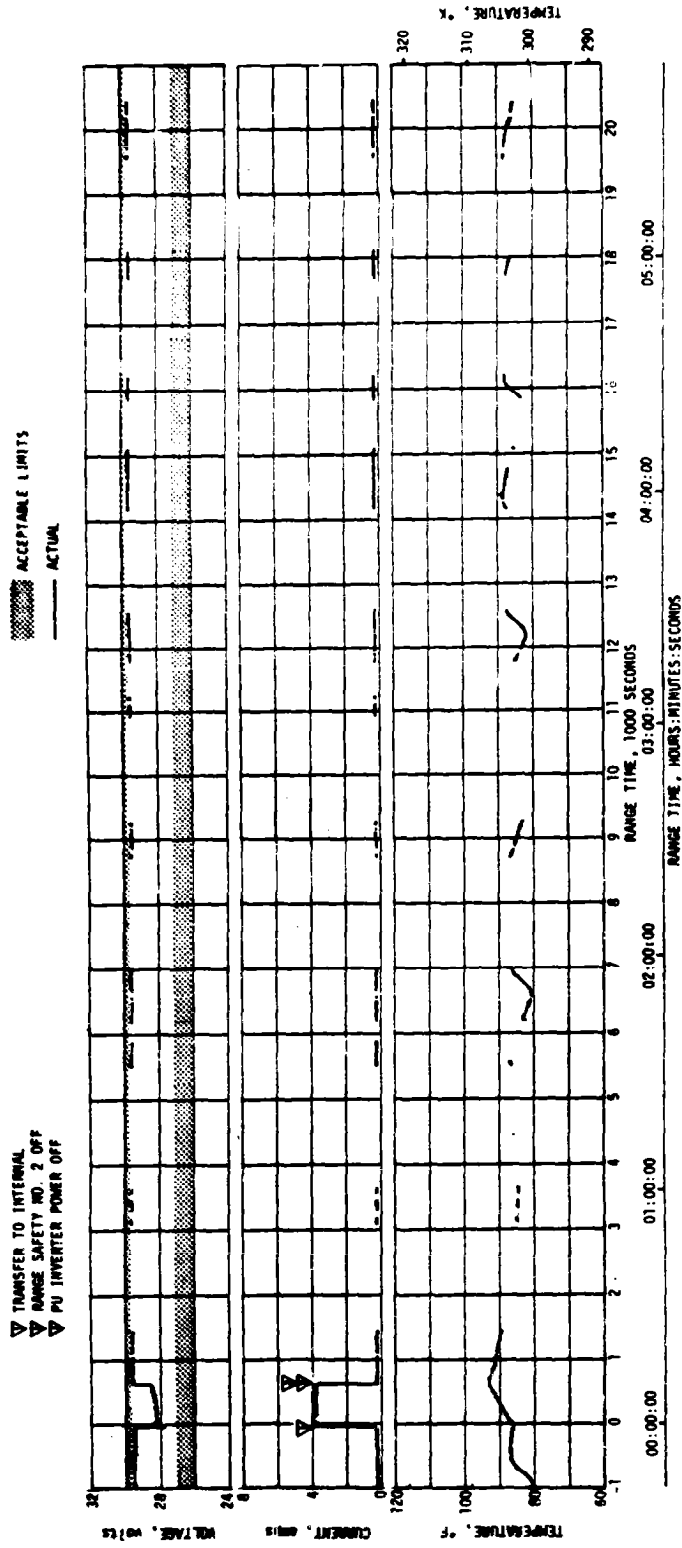


Figure 11-2. S-IVB Stage Forward No. 2 Battery Voltage, Current, and Temperature

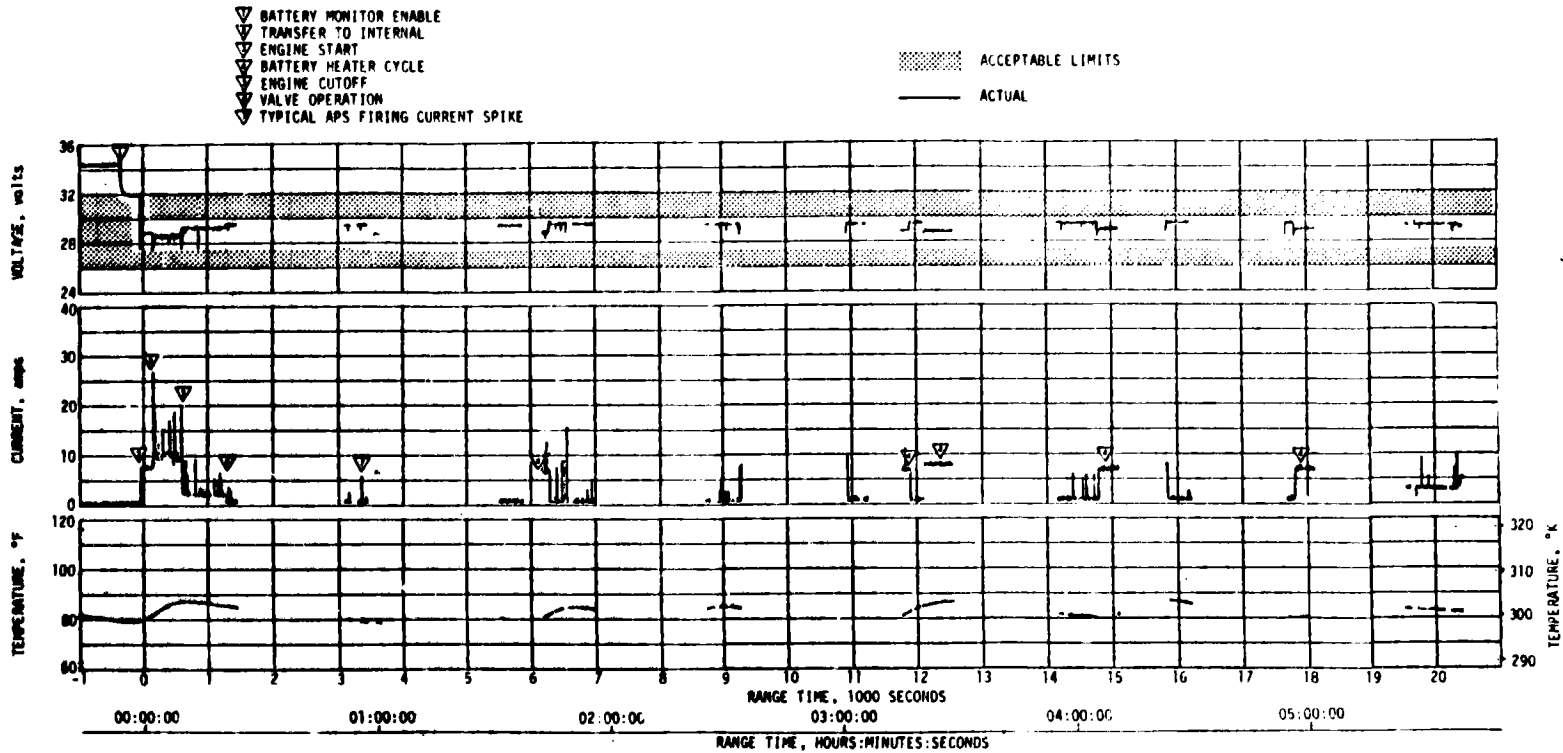


Figure 11-3. S-IVB Stage Aft No. 1 Battery Voltage, Current, and Temperature

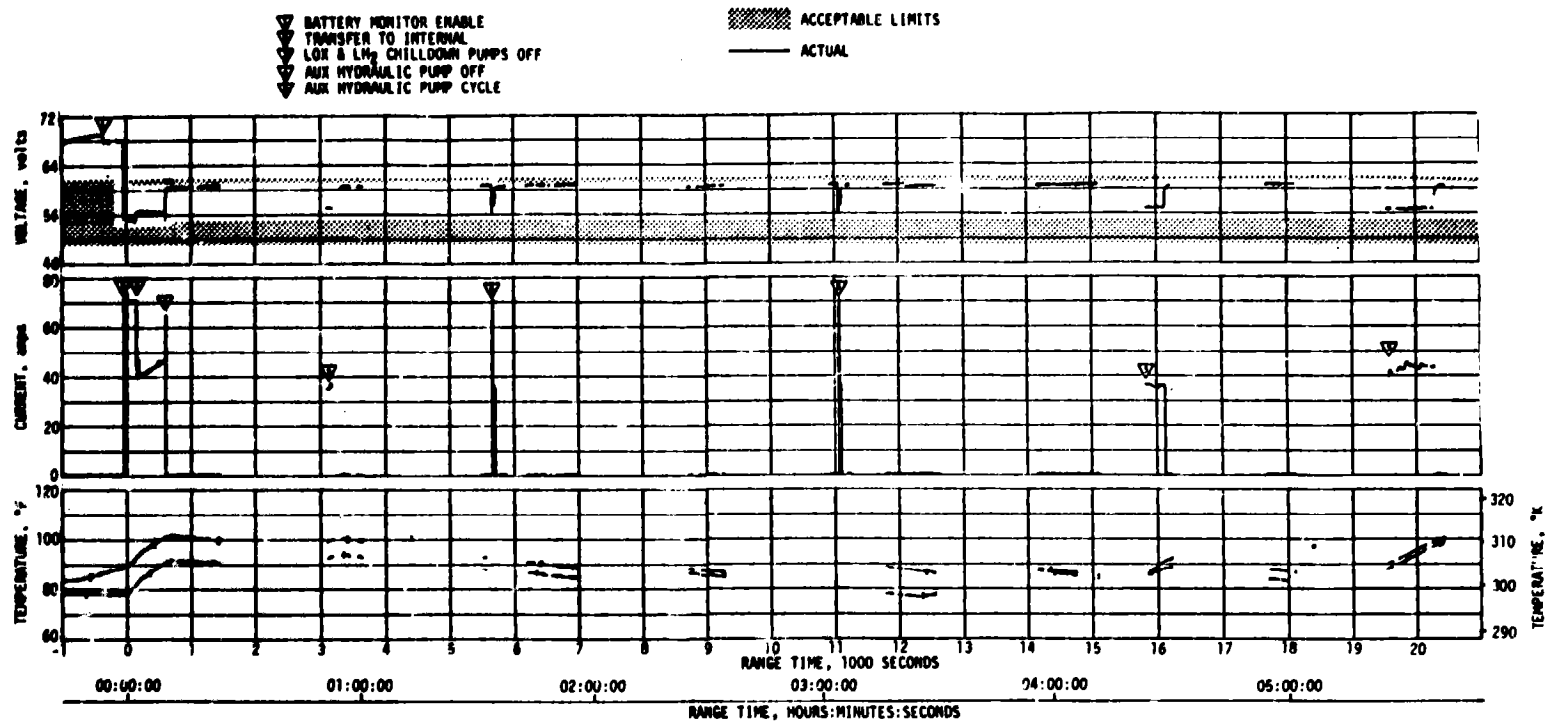


Figure 11-4. S-1VB Stage Aft No. 2 Battery Voltage, Current, and Temperature

Table 11-2. S-IVB Stage Battery Power Consumption

BATTERY	RATED CAPACITY (AMP-HR)	POWER CONSUMPTION*	
		AMP-HR	PERCENT OF CAPACITY
Forward No. 1 (4D30)	227.5	89.5	39.3
Forward No. 2 (4D20)	3.5	3.4	97.1
Aft No. 1 (4D10)	59.8	15.7	26.3
Aft No. 2 (4D40)	66.5	55.1	82.9

\*From battery activation until end of telemetry (at 20,459 seconds)

#### 11.4 INSTRUMENT UNIT ELECTRICAL SYSTEM

The IU electrical system was modified to incorporate the Galactic X-Ray (S-150) experiment. Experiment power was provided from the 6D30 battery through the 6D31 bus by the addition of an experiment distributor and associated cabling.

The IU electrical system functioned satisfactorily. All battery voltages remained within performance limits of 26 to 30 V. The battery temperature and current were nominal. Battery voltages, currents and temperatures are shown in Figures 11-5 through 11-7.

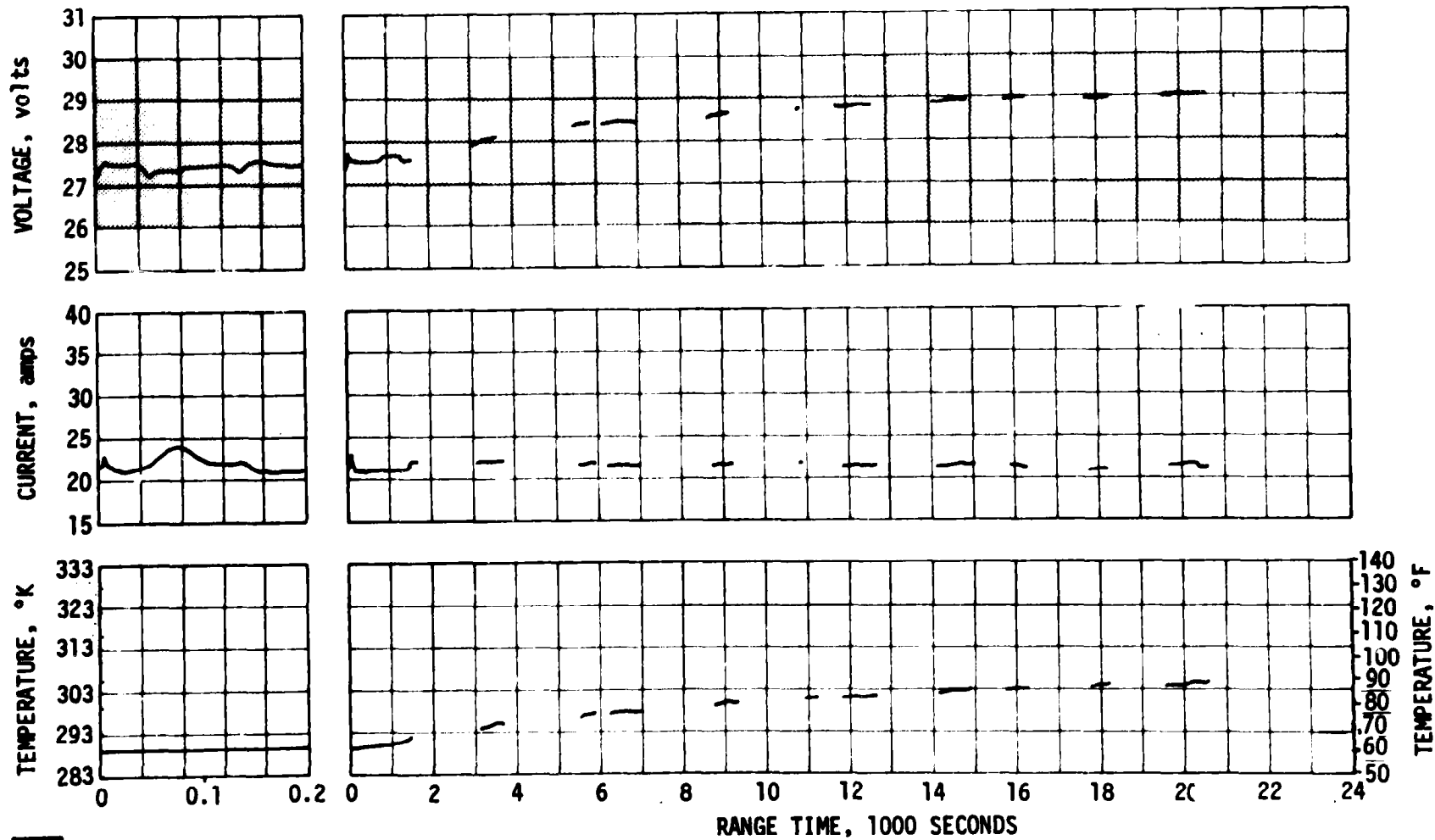
Battery power consumption and capacity for each battery are shown in Table 11-3. As expected, addition of the S-150 experiment equipment increased battery power consumption.

The current sharing of the 6D10 and 6D30 batteries, to provide redundant power to the ST-124M platform was satisfactory throughout the flight. During the S-IB burn, current sharing reached a maximum of 24 and 25.5 amperes from the 6D10 and 6D30 battery, respectively.

The 56 volt power supply maintained an output voltage of 55.5 to 56.5 V which is well within the required range of 56  $\pm$ 2.5 V.

The 5 volt measuring power supply performed nominally, maintaining a constant voltage within specified tolerances.

8-11

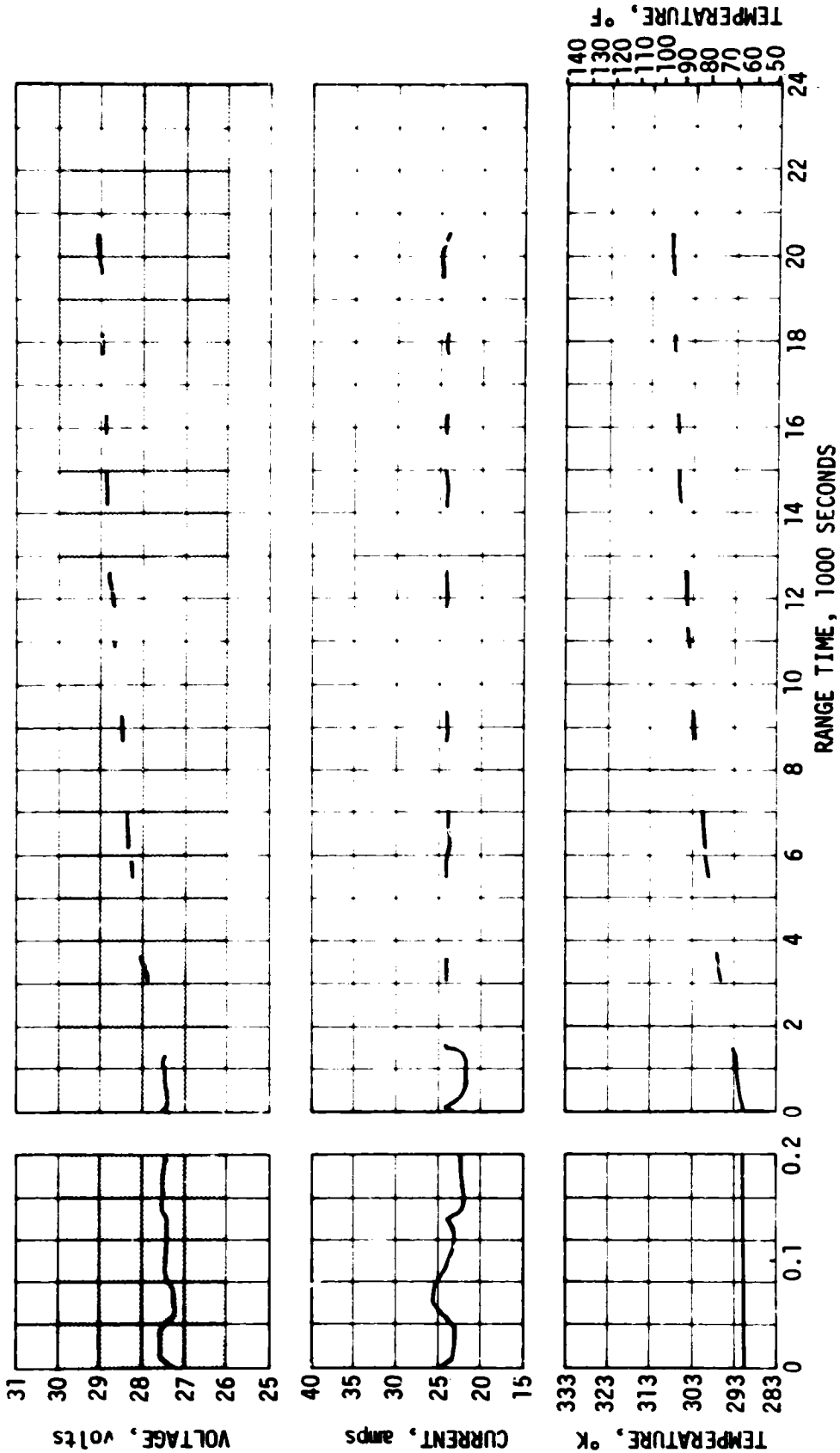


ACCEPTABLE VOLTAGE  
ACTUAL

00:00:00 03:20:00 06:40:00

RANGE TIME, HOURS:MINUTES:SECONDS

Figure 11-5. IU 6D10 Battery Parameters



ACCEPTABLE VOLTAGE 00:00:00 03:20:00 06:40:00  
ACTUAL  
RANGE TIME, HOURS:MINUTES:SECONDS

Figure 11-6. IU 6D30 Battery Parameters

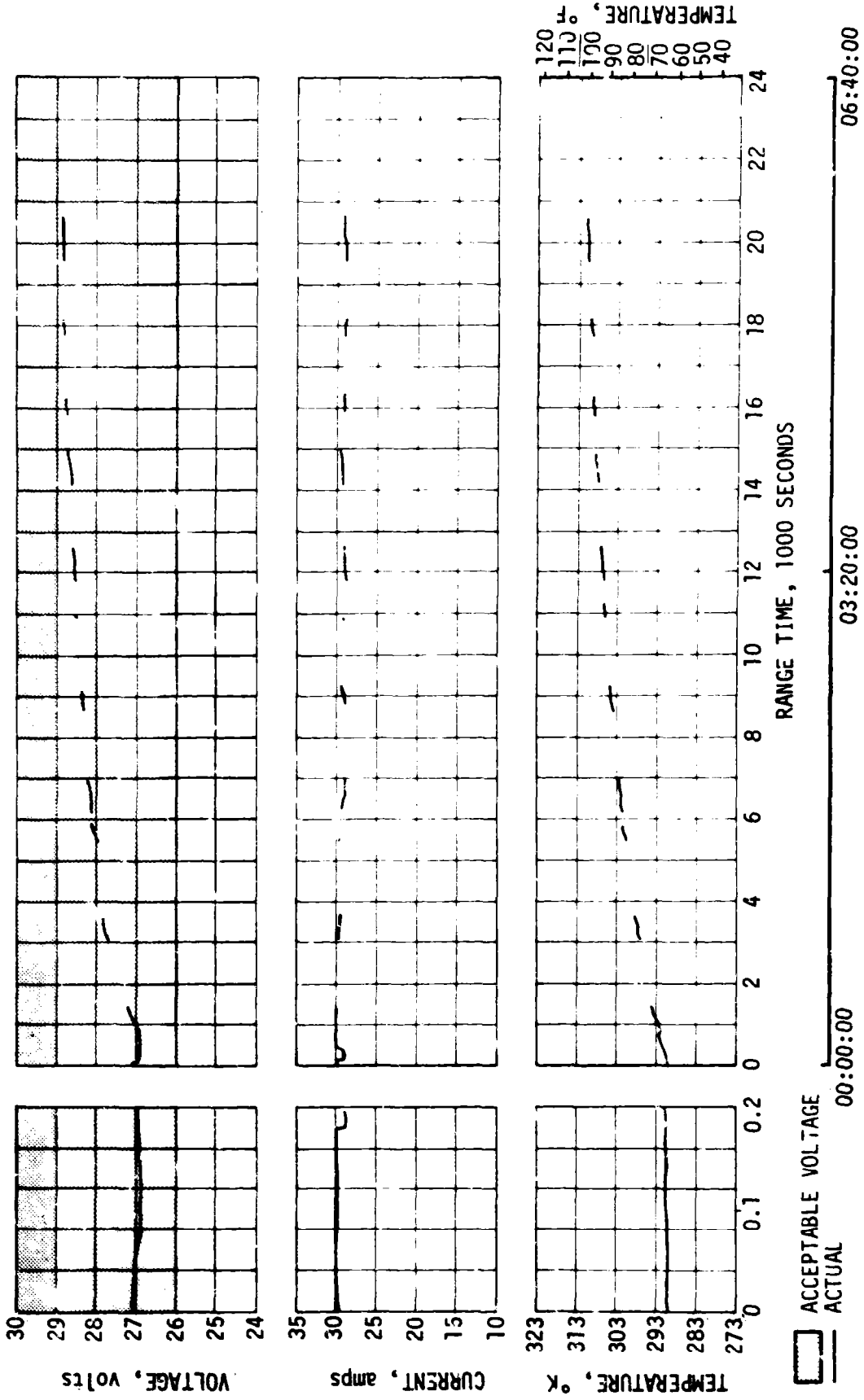


Figure 11-7. IU 6DA0 Battery Parameters

The switch selector, electrical distributors and network cabling performed nominally.

Table 11-3. IU Battery Power Consumption

BATTERY	RATED CAPACITY (AMP-HR)	POWER CONSUMPTION*	
		AMP-HR	PERCENT OF CAPACITY
6D10	350	132.6	37.9
6D30	350	150.1	42.9
6D40	350	183.2	52.3

\*From battery activation until end of telemetry (at 20,500 seconds).

#### 11.5 EMERGENCY DETECTION SYSTEM

The performance of the SA-207 EDS was normal and no abort limits were exceeded. All switch selector events associated with EDS for which data are available, were issued at the scheduled times. The discrete indications for EDS events also functioned normally. The performance of all thrust OK pressure switches and associated voting logic, which monitors engine status, was nominal insofar as EDS operation was concerned. S-IVB tank ullage pressures remained below the abort limits. EDS displays to the crew were normal.

As shown in Section 10, none of the rate gyros gave an indication of angular overrate about the pitch, yaw, or roll axis. The maximum angular rates were well below the abort limits.

The operation of the EDS Cutoff Inhibit Timer was nominal. The timer ran for 41.58 seconds which is within the specified limits of 40 to 42 seconds.

## SECTION 12

### VEHICLE PRESSURE ENVIRONMENT

#### 12.1 S-IB BASE PRESSURE

Environmental pressure data in the S-IB base region of SA-207 have been compared with preflight predictions and/or previous flight data and show good agreement. Base drag coefficients were also calculated using the measured pressures and actual flight trajectory parameters. There were three base pressure measurements in the S-IB base region; two on the heat shield and one on the flame shield. One measurement on the heat shield was a differential pressure across the shield, whereas the other two measurements were of absolute pressures.

Results of the heat shield and flame shield absolute pressure measurements are shown in Figures 12-1 and 12-2, respectively. These data are presented as the difference between measured base pressures and ambient pressure and in coefficient form ( $[\text{measured-ambient}]/\text{dynamic pressure}$ ). Values are compared with the band of data obtained from previous S-IB flights of similar vehicle base configuration and show good agreement. Both the heat shield and flame shield pressure measurements were almost identical to the data from SA-206 flight. The data indicate that during the first 70 seconds of flight (up to 6 n mi) the H-1 engine exhausts and base flow were aspirating the heat shield region, resulting in base pressures below ambient pressures. In the flame shield area, the aspirating effect was terminated at an altitude of 4 n mi. Above these altitudes the reversal of engine exhaust products, due to plume expansion, resulted in base pressures above ambient as was expected.

Pressure loading, measured near the outer perimeter of the SA-207 heat shield, is compared with data from previous flights in Figure 12-3. The SA-207 data remained on the lower side of the data band during flight at altitudes below 5 n mi. This also occurred on the SA-206 flight and the two sets of flight data agree very well.

Also shown in the figure is the predicted differential pressure band for the heat shield. The flight values were well within these limits during the entire flight. Above 15 n mi altitude, the SA-207 flight data returned to near zero indicating the engine compartment had vented to near base pressure. This is normal and occurred on all previous flights except SA-205.

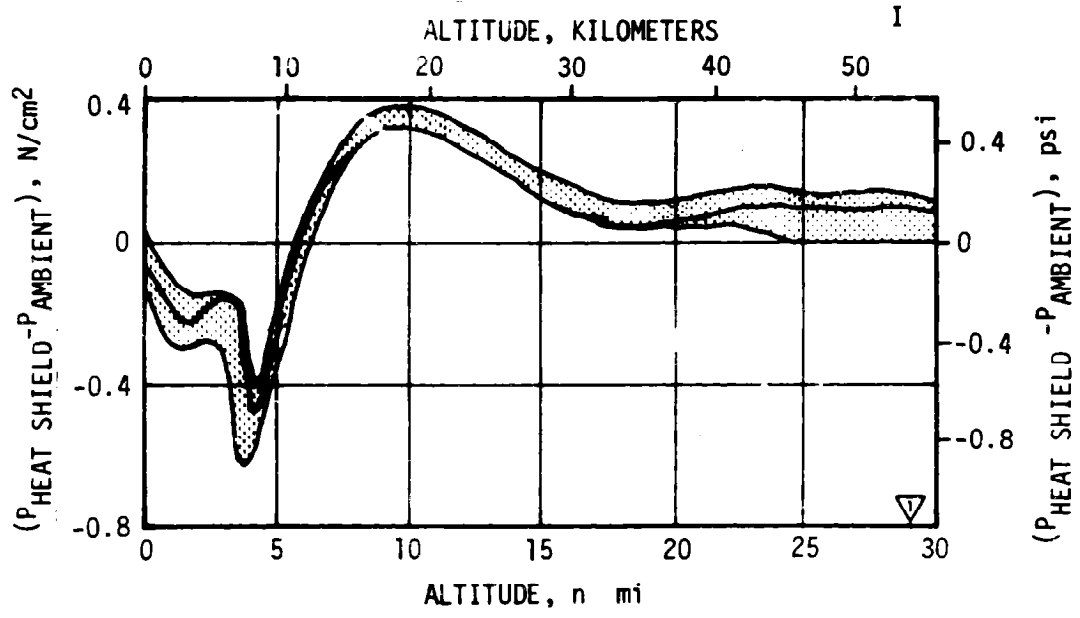
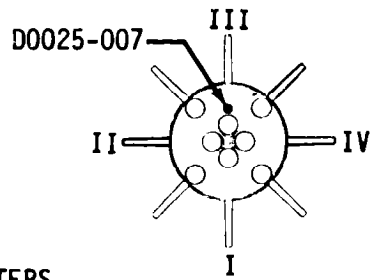
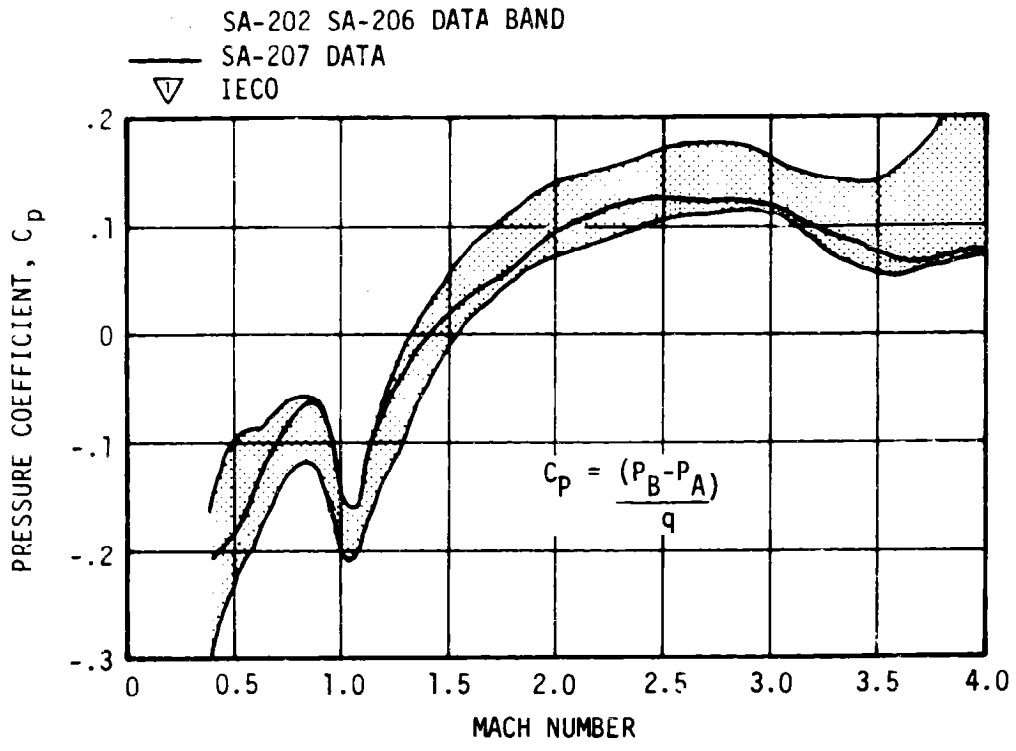


Figure 12-1. S-1B Stage Heat Shield Pressure  
 12-2

SA-203 THRU SA-206 DATA BAND  
 SA-207 DATA  
 IECO

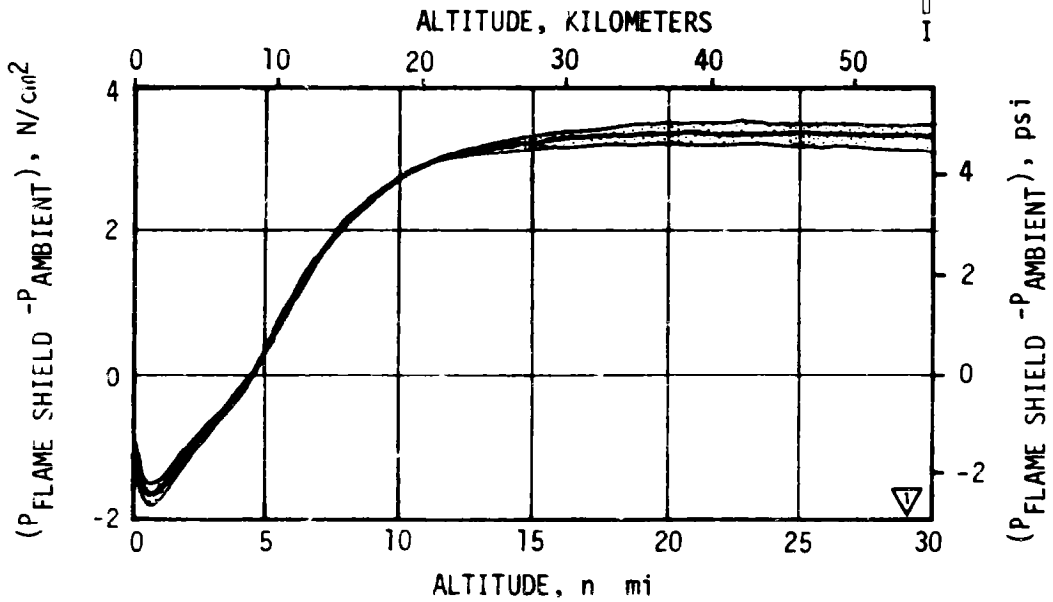
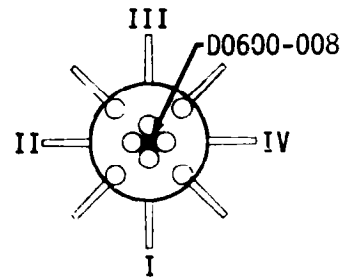
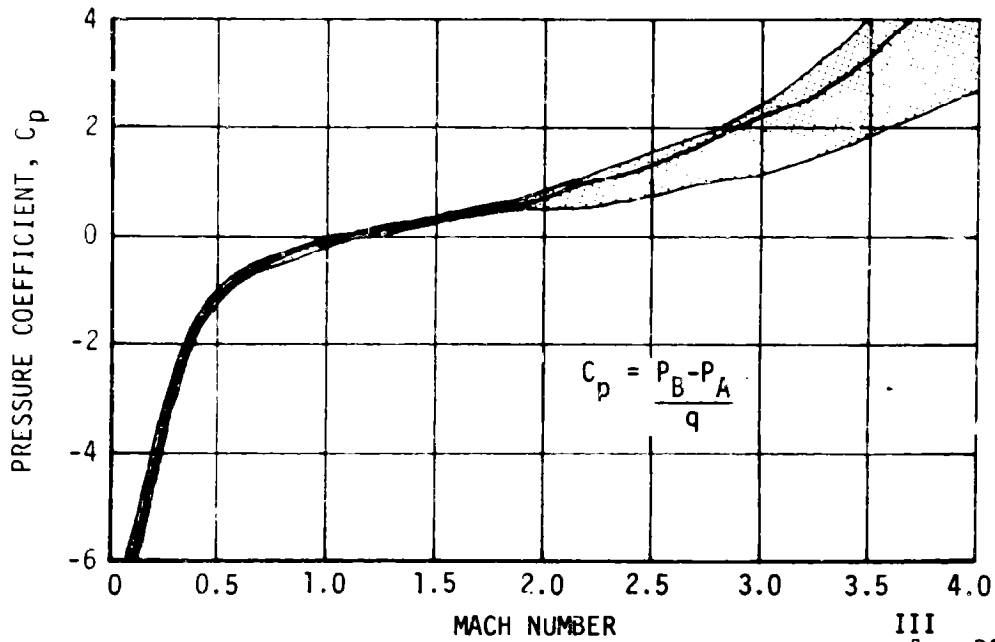


Figure 12-2. S-IB Stage Flame Shield Pressure

- - - SA-207 PREDICTED BAND  
 [Stippled Area] SA-201 THRU SA-206 DATA BAND  
 [Solid Line] SA-207 DATA  
 ▽ IECO

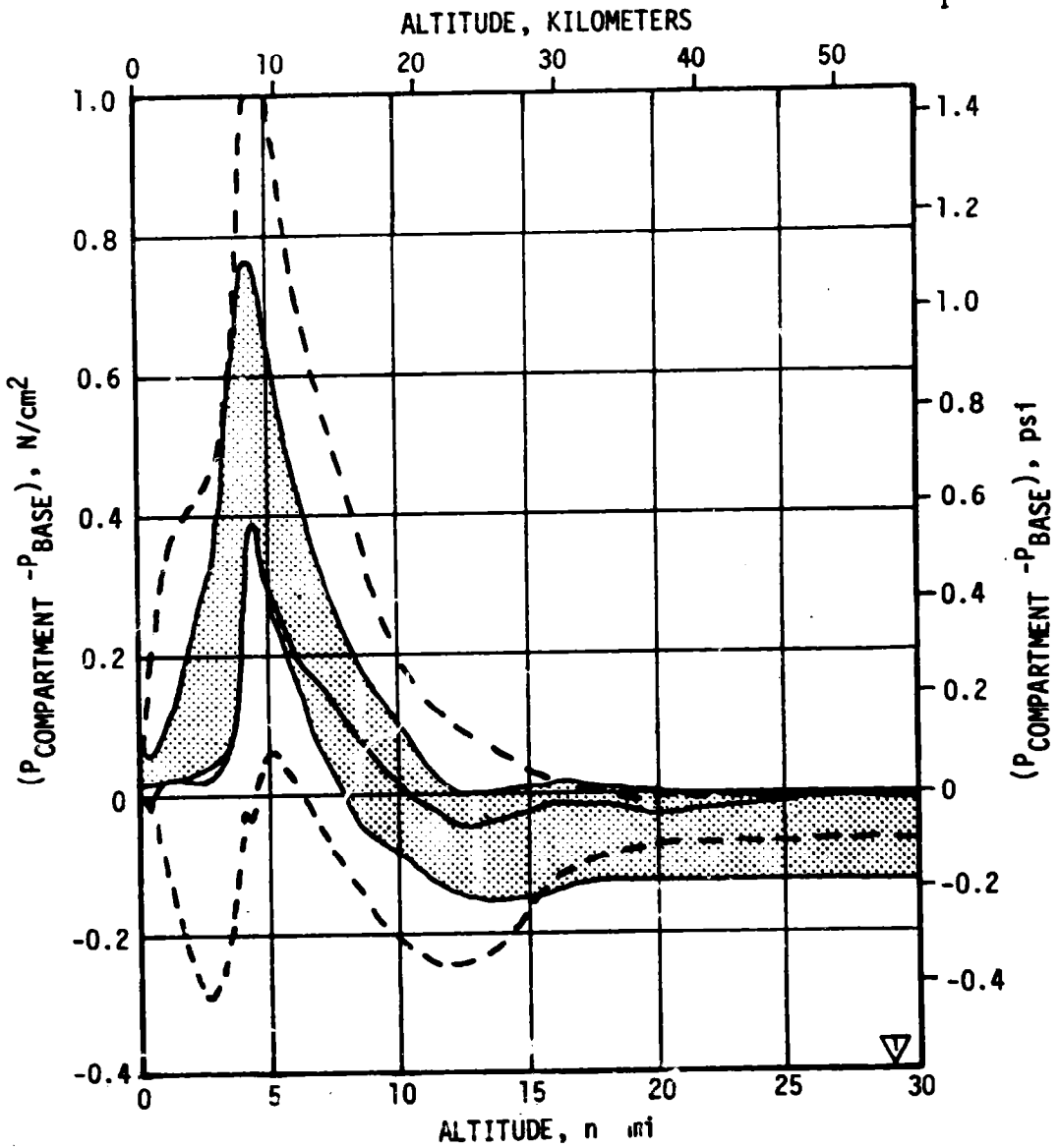
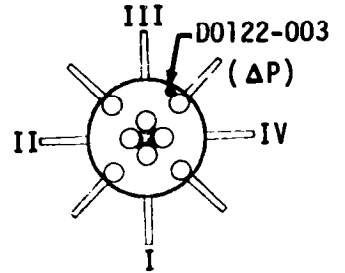


Figure 12-3. S-IB Stage Heat Shield Loading

Base drag coefficients calculated from the SA-207 data are compared to the data band from previous flights in Figure 12-4. The comparison is very good considering that the drag coefficients were determined from measurements taken at only two locations on the base. However, these measurements are representative of average base pressures.

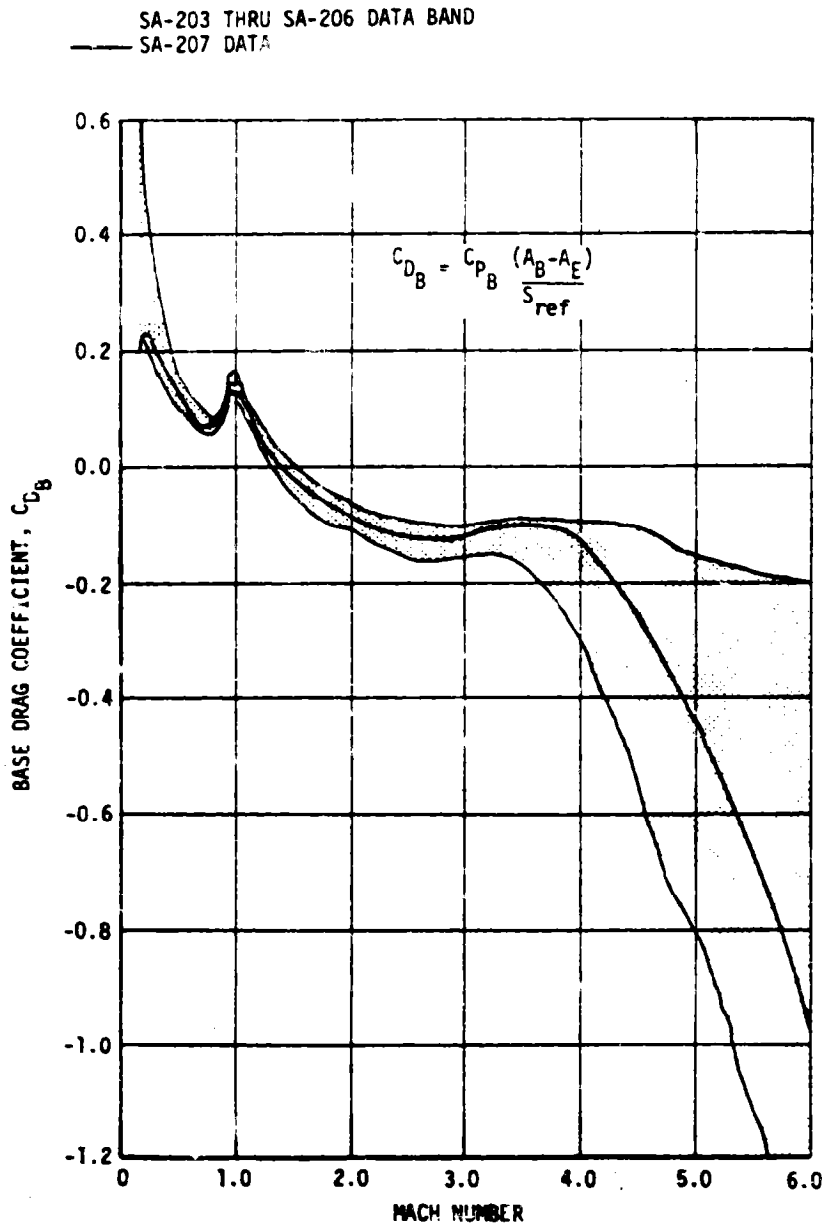


Figure 12-4. S-IB Stage Base Drag Coefficient

12-5/12-6

SECTION 13  
VEHICLE THERMAL ENVIRONMENT

13.1 S-IB BASE HEATING

The thermal environment measured in the SA-207 S-IB base region has been compared with corresponding data from flights SA-203 through SA-206. With the exception of the flame shield radiation heating data (measurement C0603-006), these comparisons show excellent agreement. In all areas the measured thermal environments in the base region of SA-207 were well below the S-IB stage design level. There were seven base region thermal environment measurements flown on SA-207.

Heat shield thermal environment data are presented as a function of vehicle altitude in Figures 13-1 through 13-4. The trend and magnitude of the SA-207 data traces are consistent with the bands formed by data from SA-203 through SA-206. These data are also consistent with the base pressure data presented in Figure 12-2, showing the effect of exhaust gas reversal into the heat shield region beginning at an altitude of approximately 5 n mi. Additionally, these data show that there is a sustained reversal of exhaust gases into the region at altitudes above 15.5 n mi.

Data from the three flame shield thermal measurements are presented in Figures 13-5, 13-6, and 13-7. The bands formed by the data recorded on previous flights are also shown for comparison.

Measured flame shield total heating rates from SA-207 (Figure 13-5) were about as expected, being in the upper portion of the band of previous data between the altitudes of 0.4 and 2.5 n mi. The slight drop below this band at 4 to 5 n mi altitude is minor and of little significance.

Gas temperatures, presented in Figure 13-6, also show generally good agreement with a slight deviation from the previous data band between the altitudes of 0.25 and 1.25 n mi. These temperature data then tended to remain near or just above the previous data band up to an altitude of 2.7 n mi. Beyond this point, the SA-207 data followed the normal drop in gas temperature to a value that is comparable to the turbine exhaust gas exit temperature. This drop in flame shield gas temperature is brought about by the reversal of engine exhaust gases that trap the cooler (approximately 800°K) turbine exhaust gases below the flame shield.

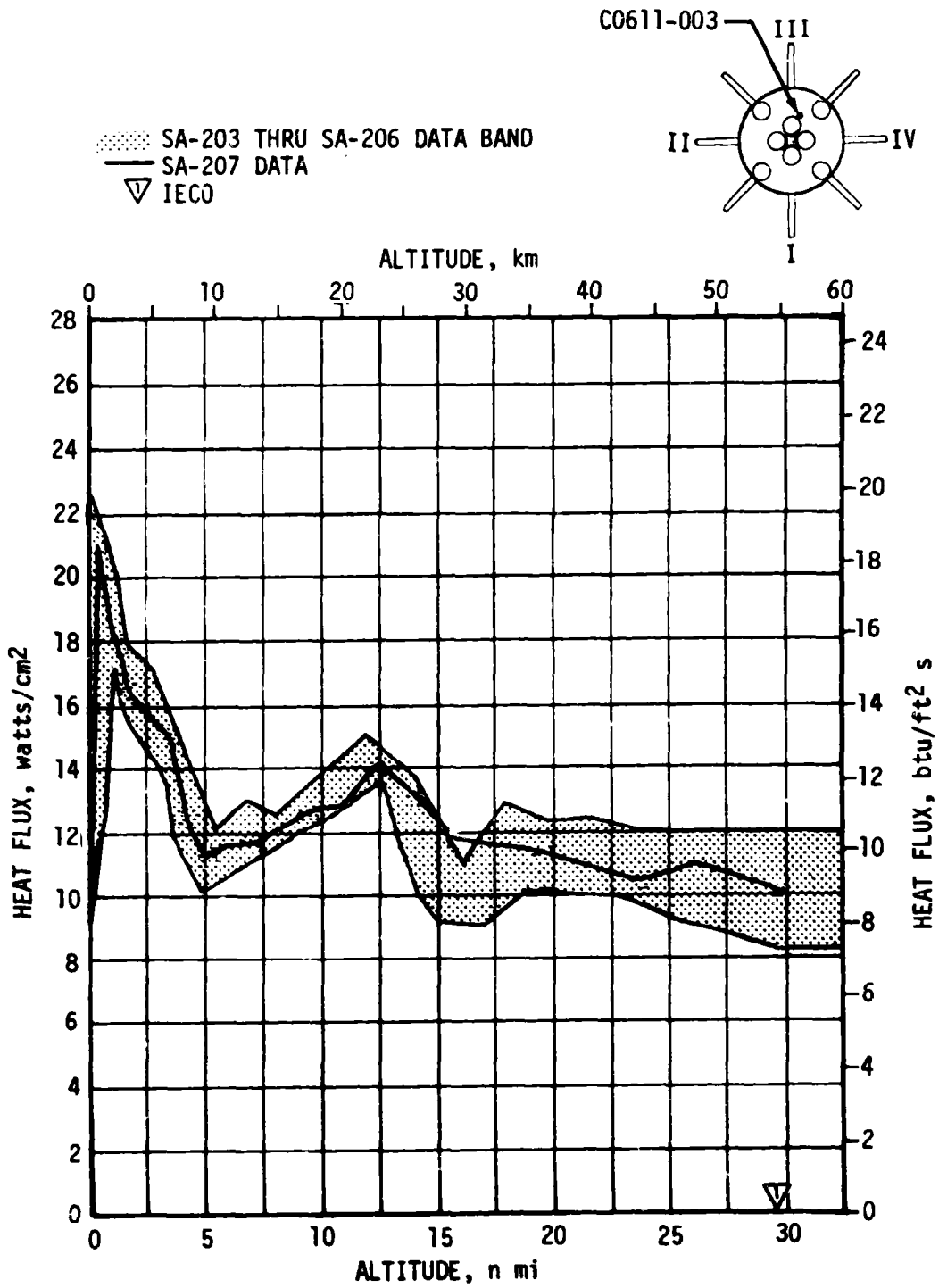


Figure 13-1. S-IB Stage Heat Shield Inner Region Total Heating Rate

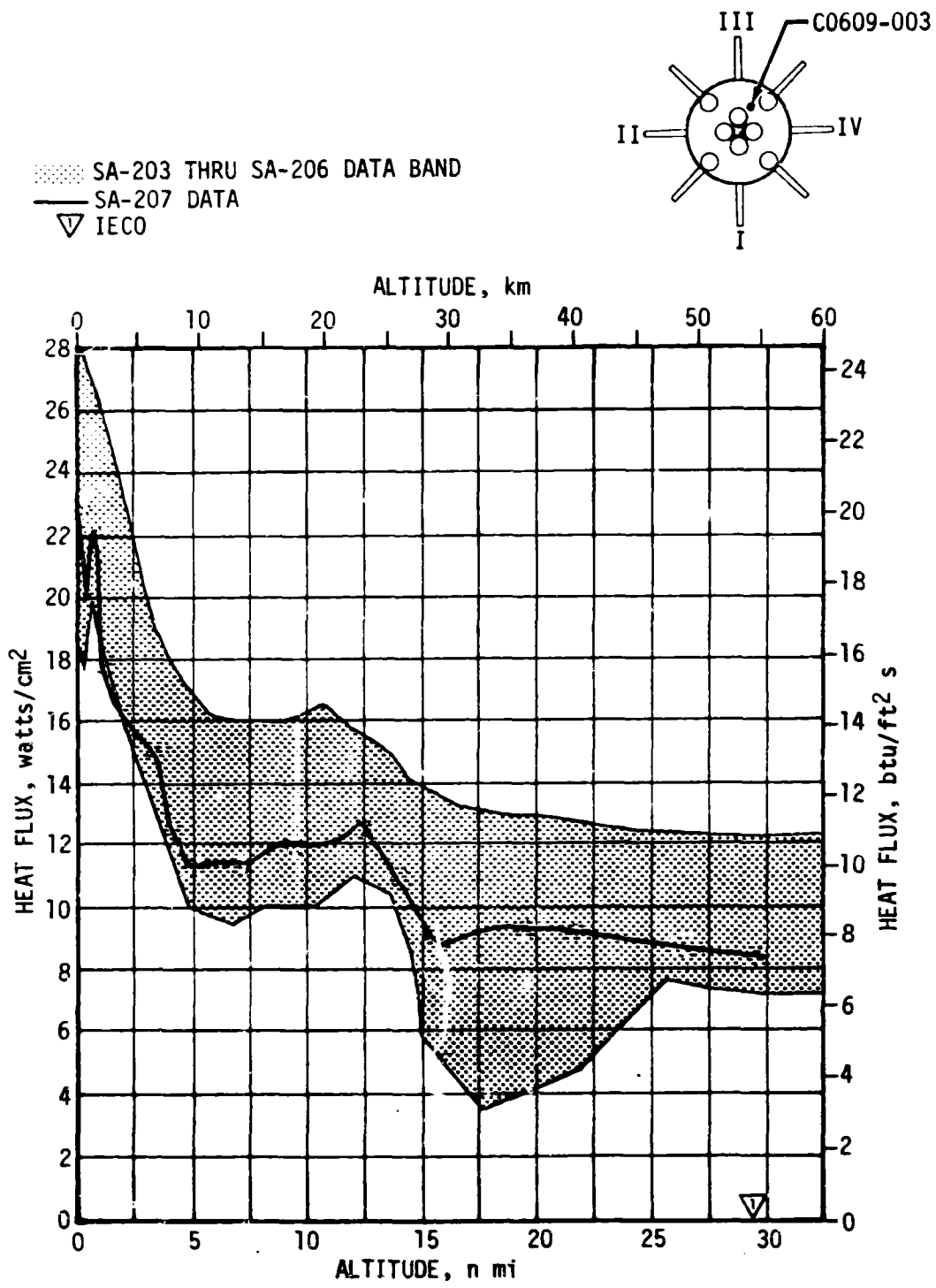


Figure 13-2. S-IB Stage Heat Shield Inner Region Radiation Heating Rate

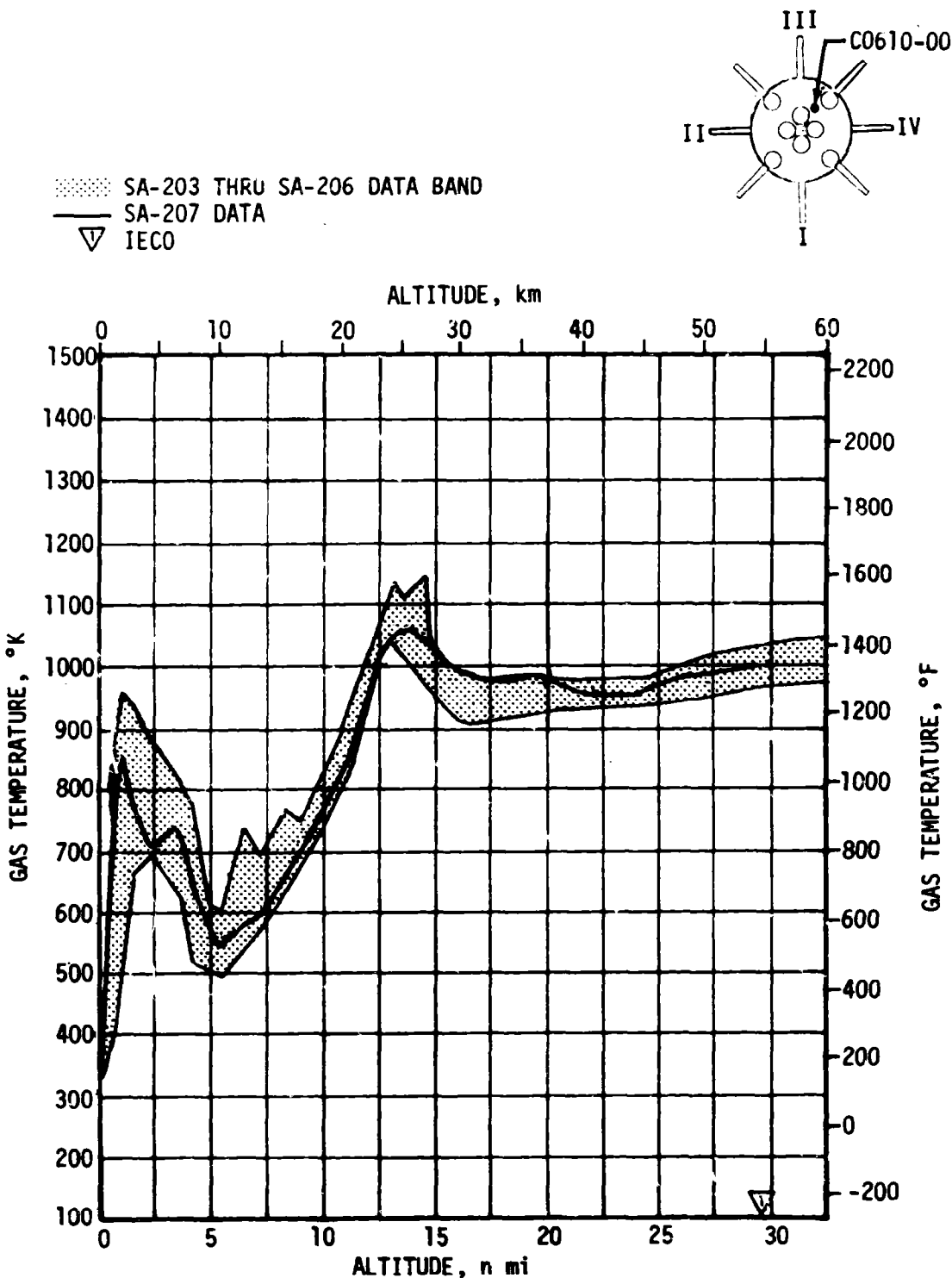


Figure 13-3. S-IB Stage Heat Shield Inner Region Gas Temperature

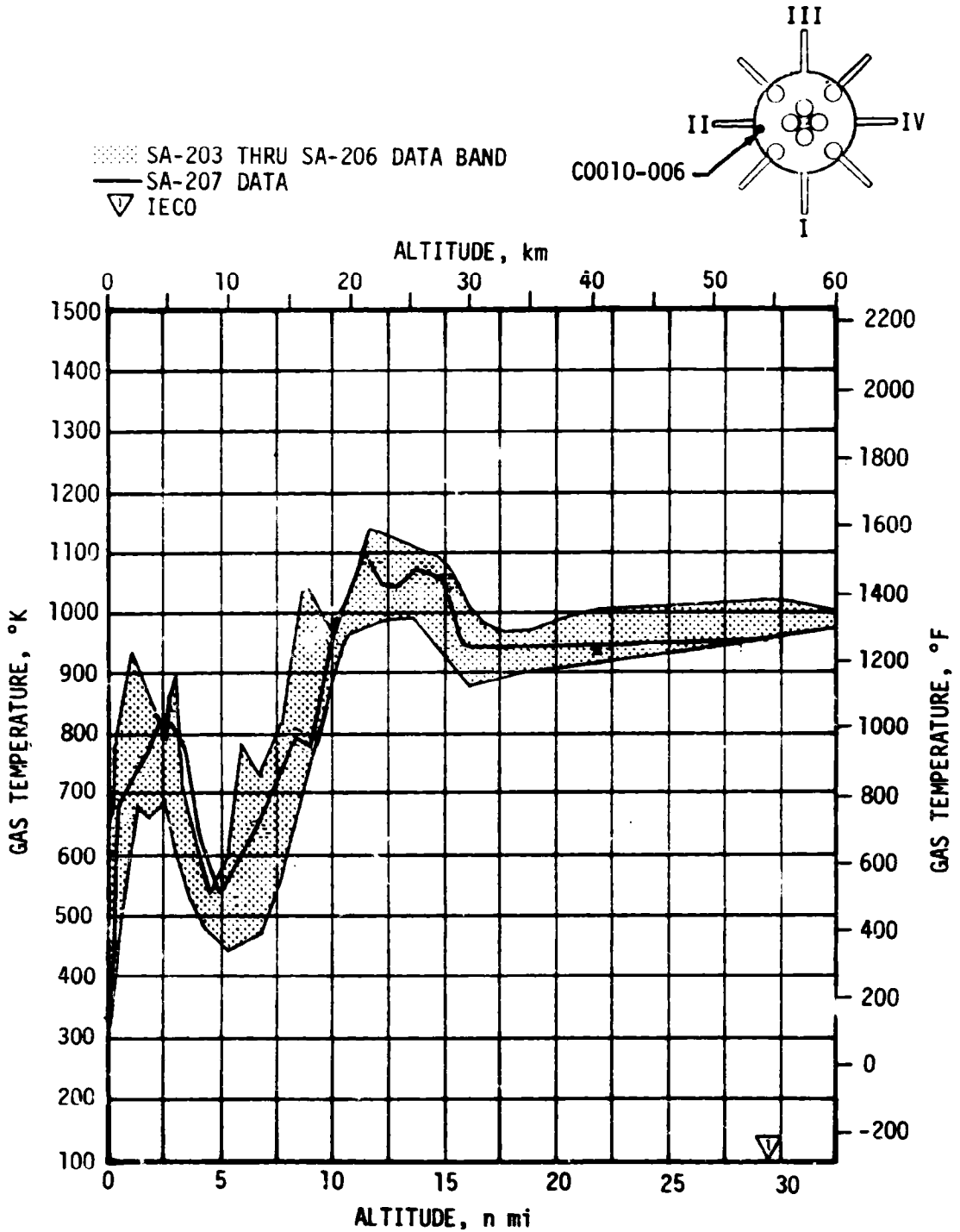


Figure 13-4. S-IB Stage Heat Shield Outer Region Gas Temperature

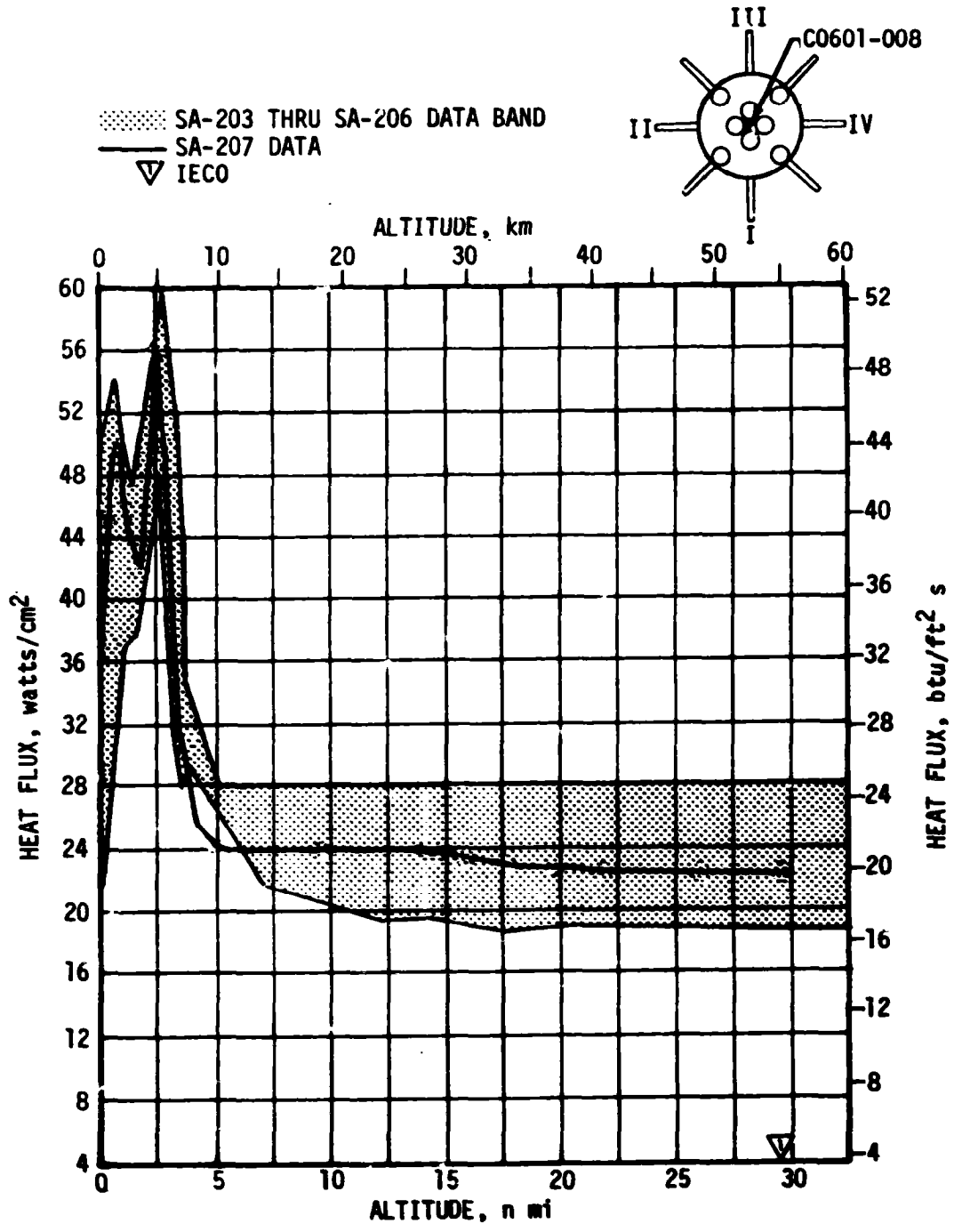


Figure 13-5. S-IB Stage Flame Shield Total Heating Rate

SA-203 THRU SA-205 DATA BAND  
 SA-207 DATA  
 IECO

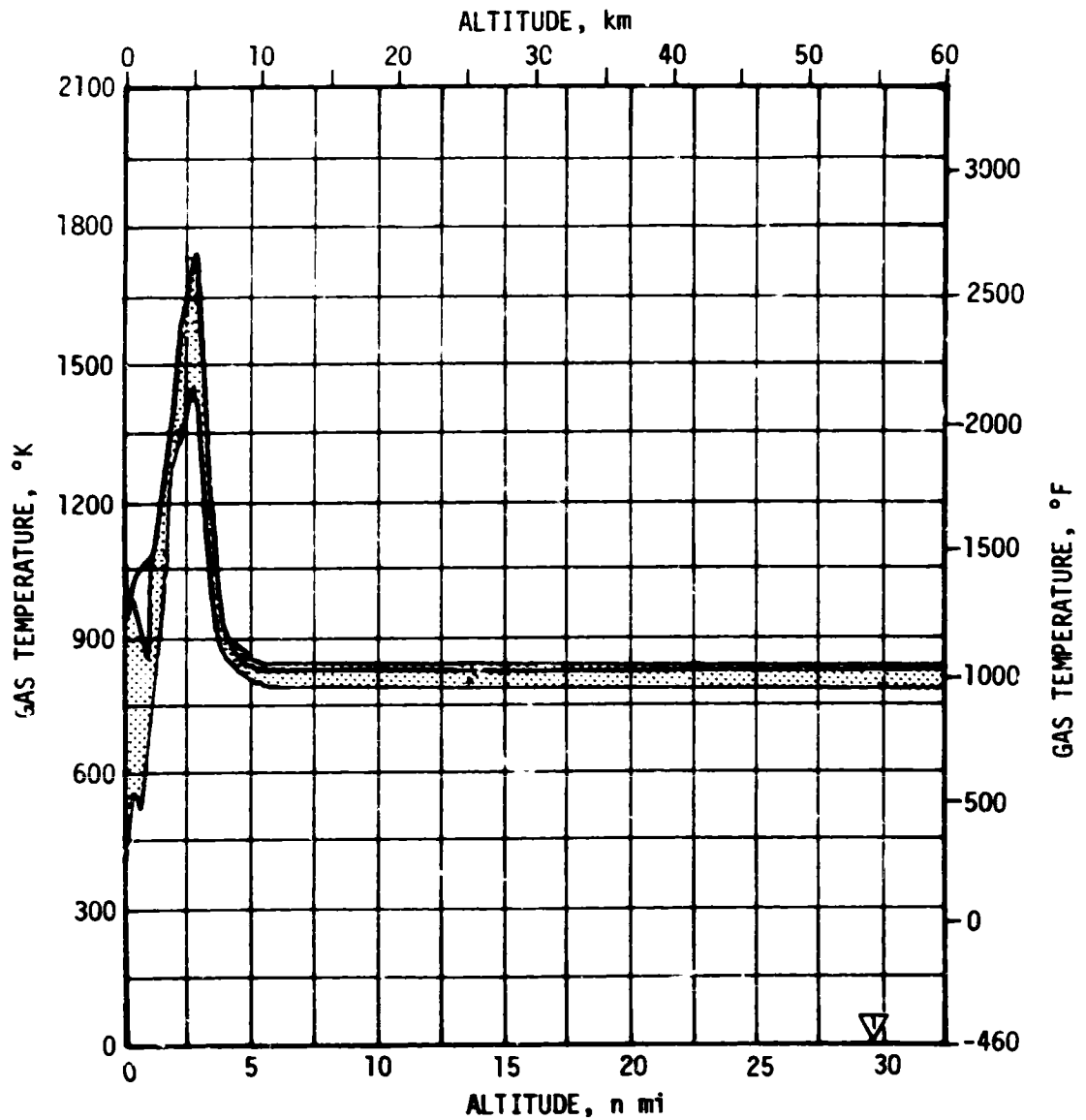
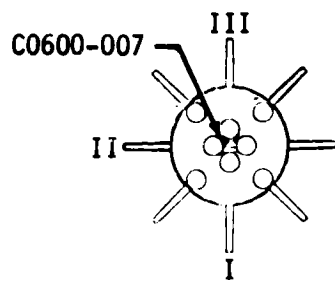


Figure 13-6. S-IB Stage Flame Shield Gas Temperature.

SA-203 THRU SA-206 DATA BAND  
 SA-207 DATA  
 IECG

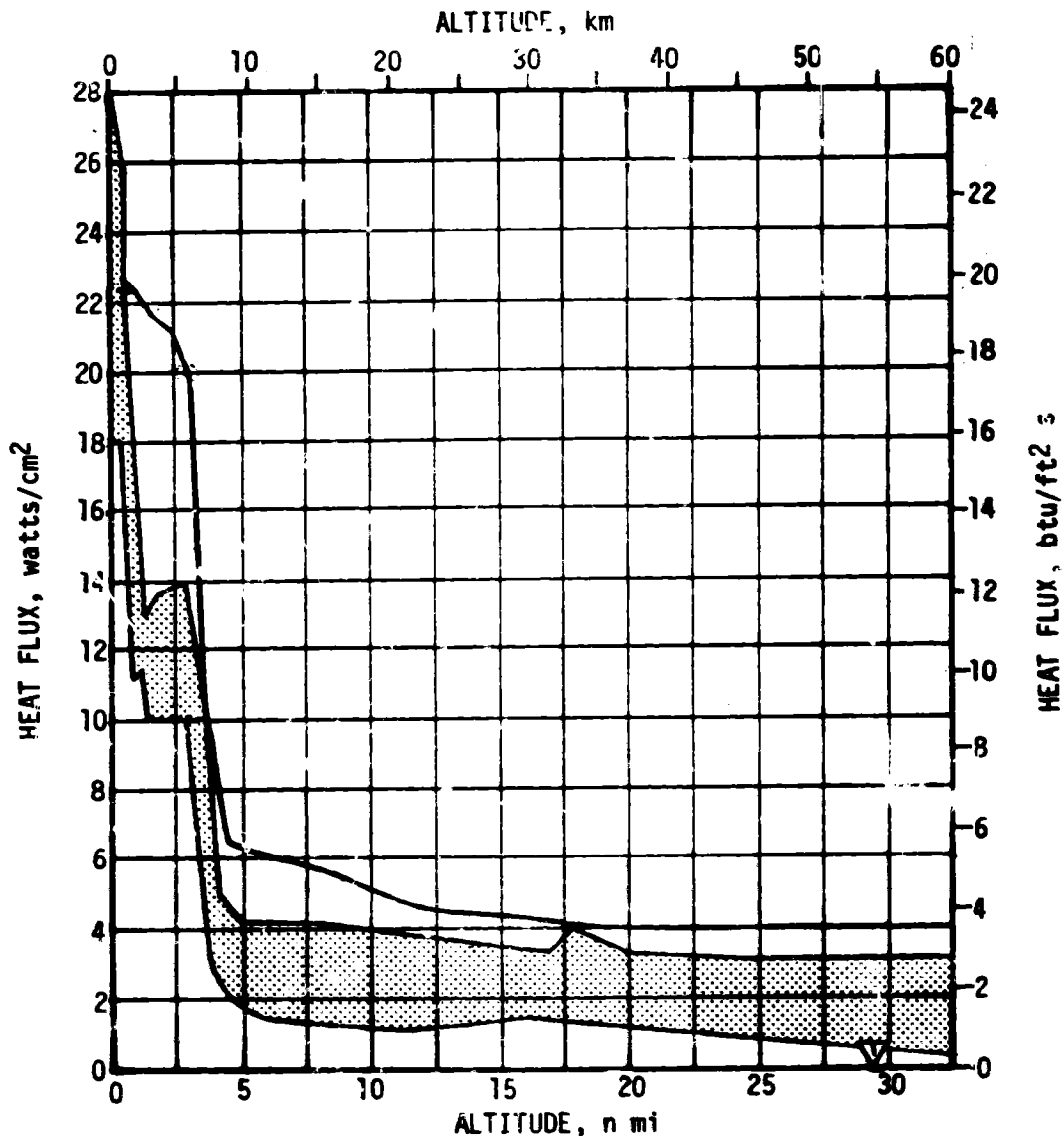
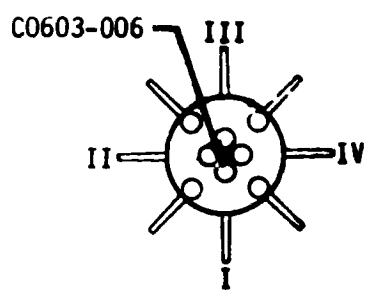


Figure 13-7. S-IB Stage Flame Shield Radiation Heating Rate

The flame shield radiation heating environment, as recorded by measurement C0603-C06, is presented in Figure 13-7. As shown, there is an appreciable deviation in the trend of the SA-207 radiant environment in comparison with the previous data band. It should be noted, however, that the magnitude of these data remained well below the flame shield design level. This deviation occurred from an altitude of 0.2 n mi until the aspiration of air into the area was terminated with the intersection of inboard engine exhaust plumes and subsequent exhaust gas reversal (approximately 2.7 n mi). Following this reversal the radiant environment returned to near nominal remaining 1 to 2 watts/cm<sup>2</sup> above the previous data band.

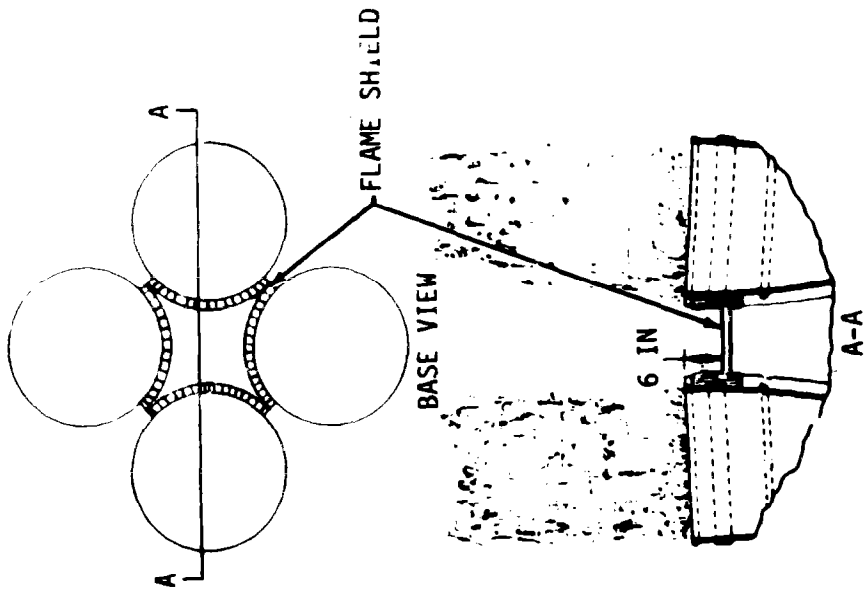
The flame shield thermal design is based on the much higher environments recorded prior to the configuration change that was effective on SA-203. Prior to SA-203 the inboard engine turbine exhaust gases were ducted overboard and the flame shield was recessed approximately 6 inches above the inboard engine nozzle exit plane. This is shown schematically by Section AA in Figure 13-8. Effective on SA-203 the inboard turbine exhaust gases were rerouted such that they were dumped through the flame shield on the inboard side of the engines (Section BB, Figure 13-8), and the flame shield was moved aft 6 inches.

The overall impact of this configuration change on the flame shield thermal environment is shown in Figures 13-9, 13-10 and 13-11. These figures compare the data envelopes from the Saturn I, Block II vehicles and the Saturn IB vehicles since SA-203. Also shown are the SA-207 data traces along with the S-IB flame shield radiant and total heating design levels. As shown by these comparisons the rerouted turbine exhaust design resulted in a significant reduction in the severity of the flame shield thermal environment. The gases that are now dumped into this region are very opaque and prevent much of the radiation from the hot exhaust plumes from reaching the flame shield. The comparison in Figure 13-9 also shows that the aforementioned deviation in the trend of the SA 207 radiant environment remained well below the flame shield thermal design capability.

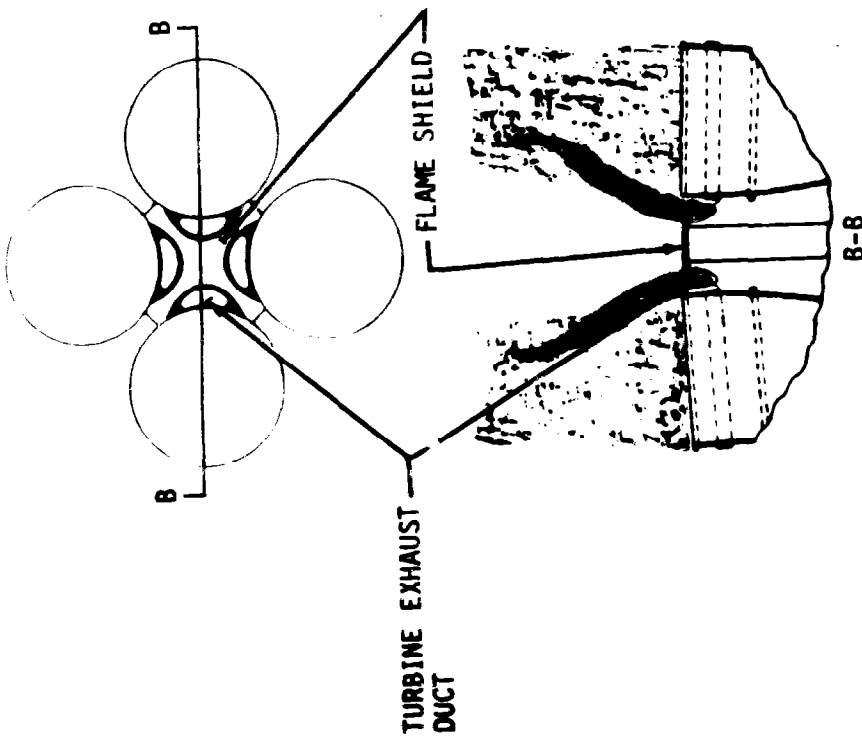
The cause of the increased radiant heating is unknown; however, several possible causes have been investigated. The data trend does not indicate erroneous measurements. The data trace is smooth, with no irregularities, and decays to zero after OEEO in a normal manner. None of the data indicate a deviation in either engine or turbine performance.

There are two possible causes which would allow more radiation from the engine exhaust plume to reach the flame shield radiometer:

- a. A reduction in opaqueness of the turbine exhaust gas would allow more radiation to be detected. However, because a comparable deviation was not detected by the total calorimeter, it would be necessary for such a reduction to have been localized; producing a much greater effect in the vicinity of the radiation calorimeter.



SATURN I AND IB VEHICLES THROUGH SA-202



SATURN IB VEHICLES STARTING WITH SA-203

Figure 13-8. S-1B Stage Flame Shield Configurations

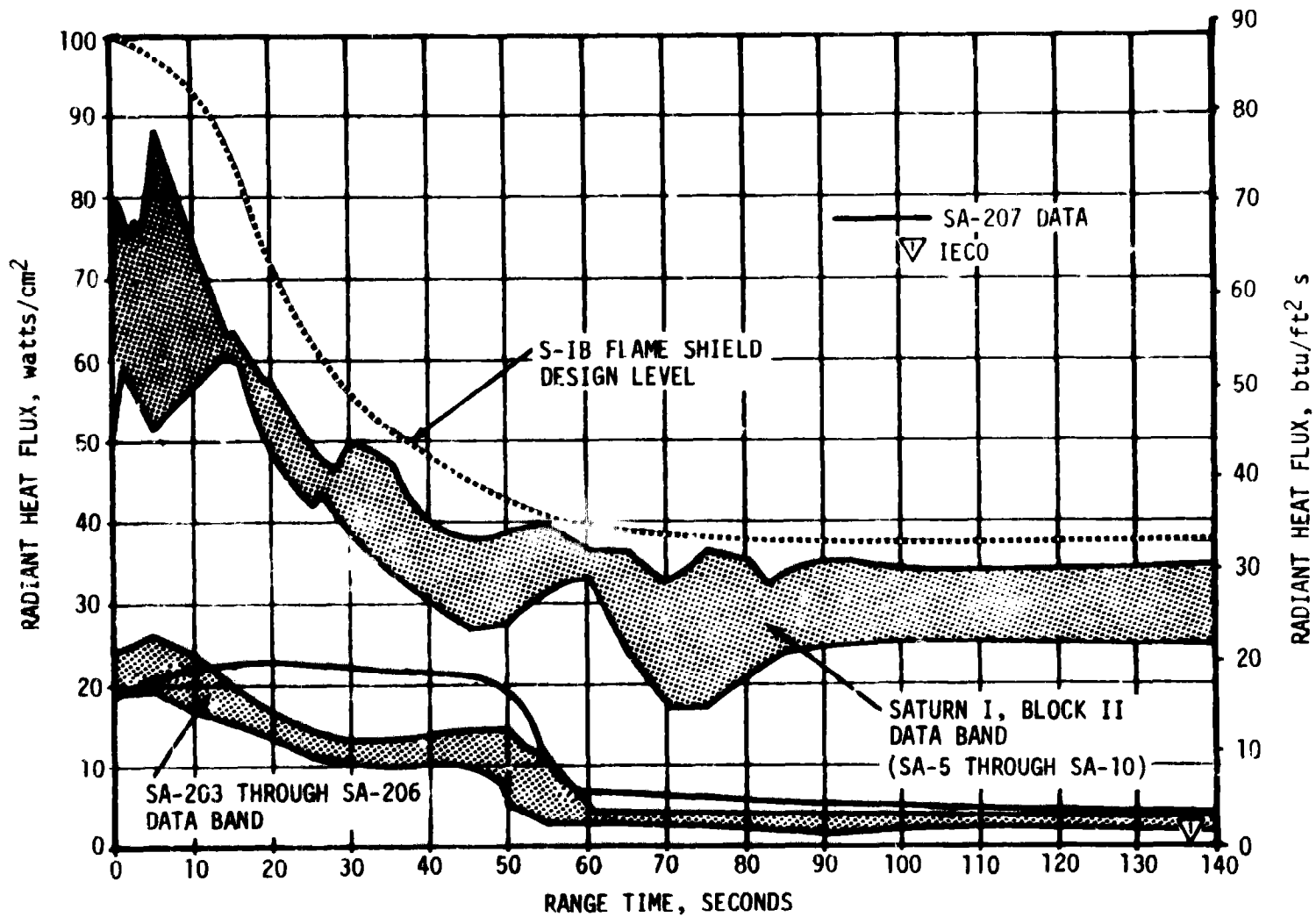


Figure 13-9. Comparison of S-IB Stage Flame Shield Radiant Heating Data with Design Level

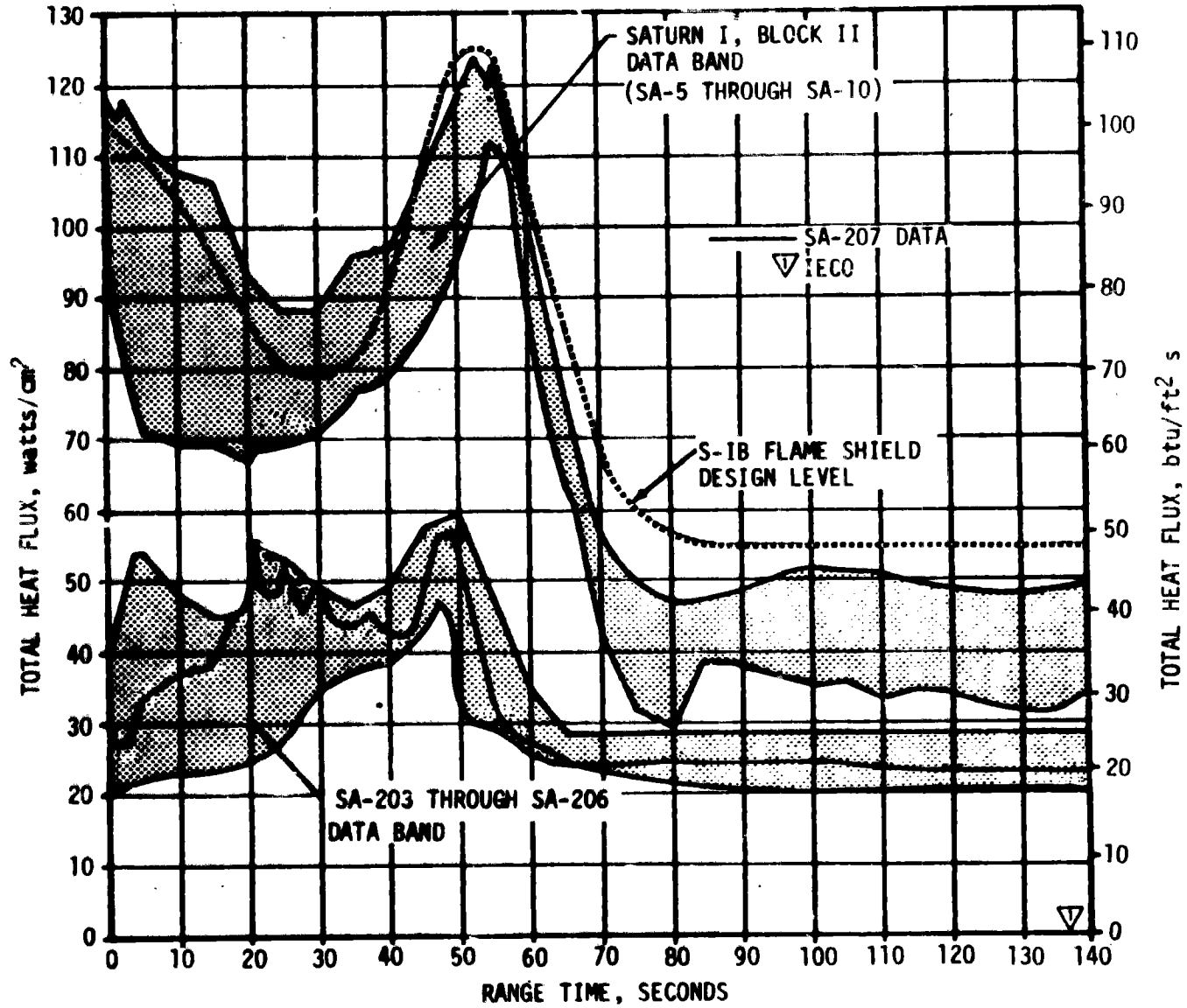


Figure 13-10. Comparison of S-IB Stage Flame Shield Total Heating Data with Design Level

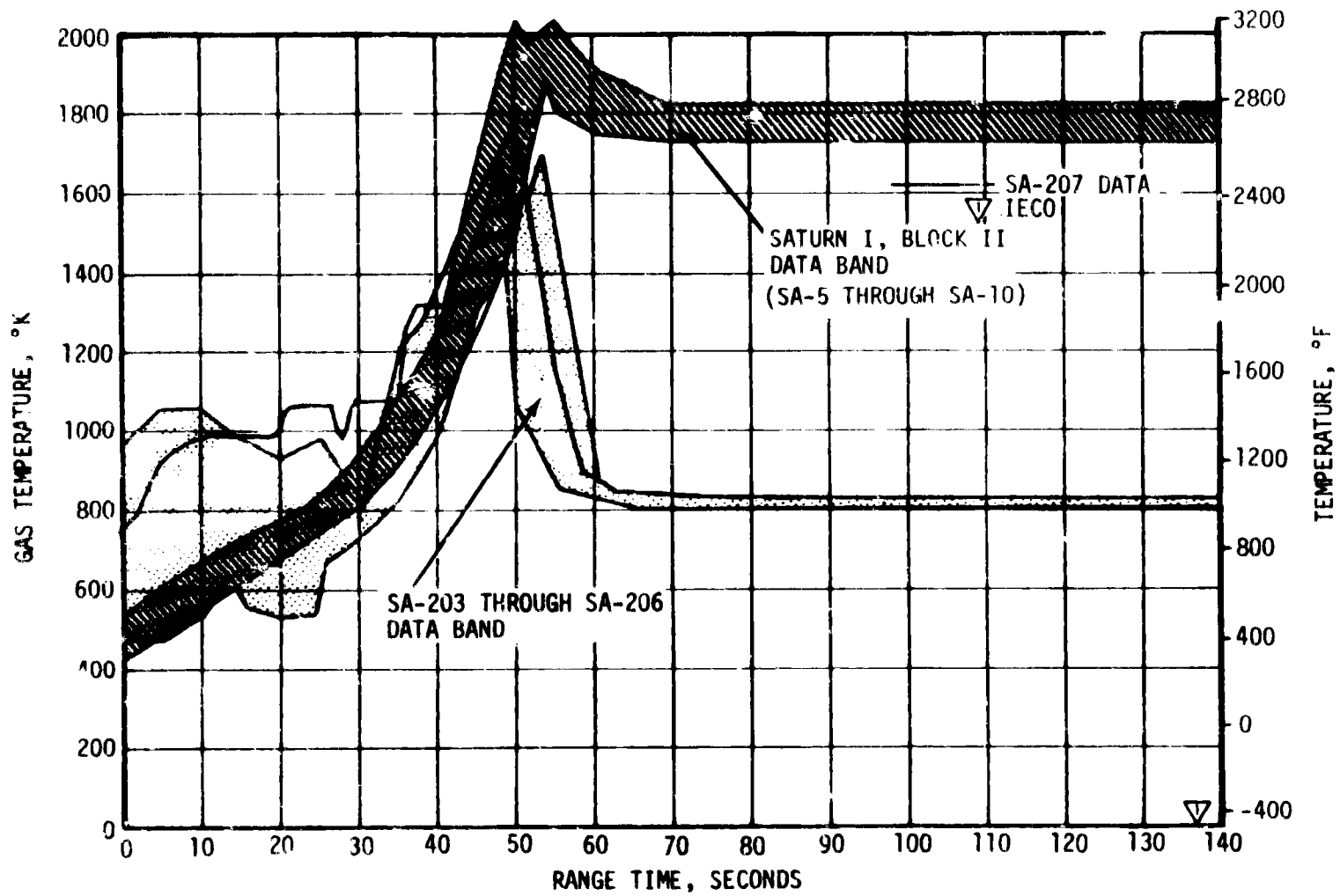


Figure 13-11. Comparison of S-1B Stage Flame Shield Gas Temperature Data

This could have been induced by a slight alteration in the flow pattern from one of the turbine exhaust ducts. A small window in the turbine exhaust of Engine No. 5 or 6 could allow the radiation calorimeter to view a relatively constant emission source until exhaust gas reversal was realized. The position of this window could be such that the total calorimeter did not view the emission source and hence, did not experience a comparable deviation.

- b. Sustained local afterburning of the turbine exhaust gases could also cause an increase in the reading of the radiation calorimeter. Combustion analyses and films verify that the turbine exhaust gases can be ignited if mixed with sufficient air. However, except under controlled conditions, the flame from this ignition is of low infrared intensity and remains shrouded by soot. In the flame shield area it is questionable if a combustible mixture could be maintained by the air supply that is being drawn into the region during aspiration. Furthermore if a combustible mixture did exist something would have to serve as a flame holder in order to sustain local burning. Otherwise, the flame, and the combustible mixture, would be drawn downstream by the action of the engine exhaust plumes. It is difficult to conceive of any deformation or flow disruption in this region that would serve as a viable flame holder.

The SA-207 flame shield and turbine exhaust duct configurations were unchanged from previous vehicles since SA-203. Only two notable deviations were found as a result of reviewing manufacturing records and work order sheets. One was that Engine No. 5 was replaced on SA-207 after static tests. However, all flight performance data from this engine appeared normal. The second was an Unsatisfactory Condition Report (UCR) that was filed concerning Engine Position 6 turbine exhaust duct warpage. The position in response to this UCR was that "--the exhaust duct warpage was within tolerances expected following an engine hot-firing." As related to the subject deviation, such a warpage may or may not have been sufficient to cause a disruption in the normal exit flow pattern of the turbine exhaust gases.

Neither of these explanations is completely satisfactory, but reduced local opaqueness is more probable. The SA-207 thermal environment was well below the thermal design capability, and neither the deviation nor its cause is of continuing concern.

## SECTION 14

### ENVIRONMENTAL CONTROL SYSTEMS

#### 14.1 SUMMARY

The S-IB stage engine compartment and instrument compartment require environmental control during prelaunch operations, but are not actively controlled during S-IB boost. The desired temperatures were maintained in both compartments during the prelaunch operation.

The Instrument Unit (IU) stage Environmental Control System (ECS) exhibited satisfactory performance for the duration of the IU mission. Coolant temperatures, pressures, and flowrates were continuously maintained within the required ranges and design limits.

#### 14.2 S-IB ENVIRONMENTAL CONTROL

The S-IB engine compartment temperature was maintained at approximately 63°F for 7 hours prior to liftoff. Data from this measurement are monitored during prelaunch activities to assess ECS flow and supply temperature requirements for maintaining engine compartment temperature within the specified limits of 53 and 75°F. In maintaining the 63°F engine temperature, the ECS delivery was nominal, with GN<sub>2</sub> being supplied to the S-IB stage aft compartment at the average rate of approximately 300 lbm/min, with an interface temperature of approximately 139°F.

The S-IB instrument compartment environmental conditioning system also performed satisfactorily during countdown. This was evidenced by the D20 and D10 battery case temperatures. Battery temperatures remained at approximately 76°F throughout the countdown. This temperature range was maintained after LOX load by a GN<sub>2</sub> conditioning flow of 44 lbm/min at a temperature of 78°F.

It was concluded that the critical components in the engine and instrument compartments were well within their qualification limits.

#### 14.3 IU ENVIRONMENTAL CONTROL

The IU ECS exhibited normal performance for the duration of the IU mission including initiation of deorbit. Coolant temperatures, pressures, and flowrates were continuously maintained within the required ranges and design limits.

### 14.3.1 Thermal Conditioning System (TCS)

The TCS performance was satisfactory throughout the IU mission. The temperature of the coolant supplied to the IU thermal conditioning panels, IU internally cooled components, and the S-IVB was continuously maintained within the required limits of 45 to 68°F for the IU lifetime.

Sublimator performance parameters for the initial cycle are presented in Figure 14-1. The water supply valve opened as programmed at approximately 180 seconds, allowing water to flow to the sublimator. Significant cooling by the sublimator was evident at approximately 230 seconds at which time the temperature of the coolant began to decrease rapidly. At the first thermal switch sampling (480 seconds), the coolant temperature was below the thermal switch actuation point; hence the water supply valve closed.

Figure 14-2 shows temperature control parameters over the total mission. Sublimator cooling was normal and the coolant control temperature was maintained within the required limits of 45 to 68°F.

Hydraulic performance of the TCS was nominal as indicated by the parameters shown in Figure 14-3. System flowrates and pressures were relatively constant throughout the mission.

The TCS GN<sub>2</sub> supply sphere pressure decay, which is indicative of the GN<sub>2</sub> usage rate, was nominal as reflected by Figure 14-4.

### 14.3.2 Gas Bearing System (GBS)

The GBS performance was nominal throughout the IU mission. Figure 14-5 depicts the platform pressure differential and platform internal pressure.

The GBS GN<sub>2</sub> supply sphere pressure decay was nominal as shown in Figure 14-6.

### 14.3.3 Component Temperatures

Low emissivity surfaces were installed on SA-207, S-IVB stage, between the forward skirt cold plates and stage structure to insure that IU component temperatures remain above minimum operating temperatures.

All internally cooled component temperatures were normal throughout the mission as shown in Figures 14-7 and 14-8.

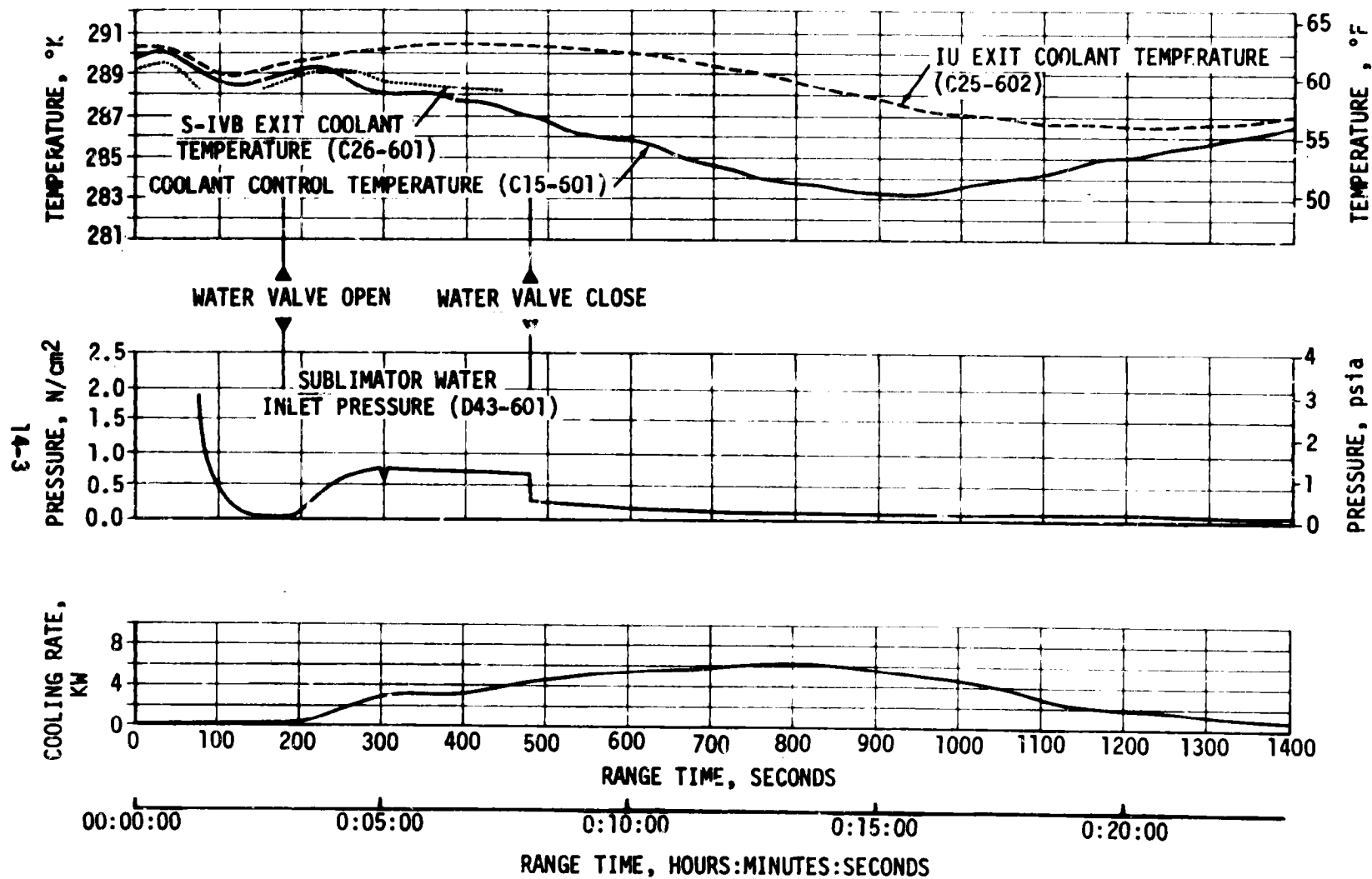


Figure 14-1. IU Sublimator Start Up Parameters for Initial Cycle

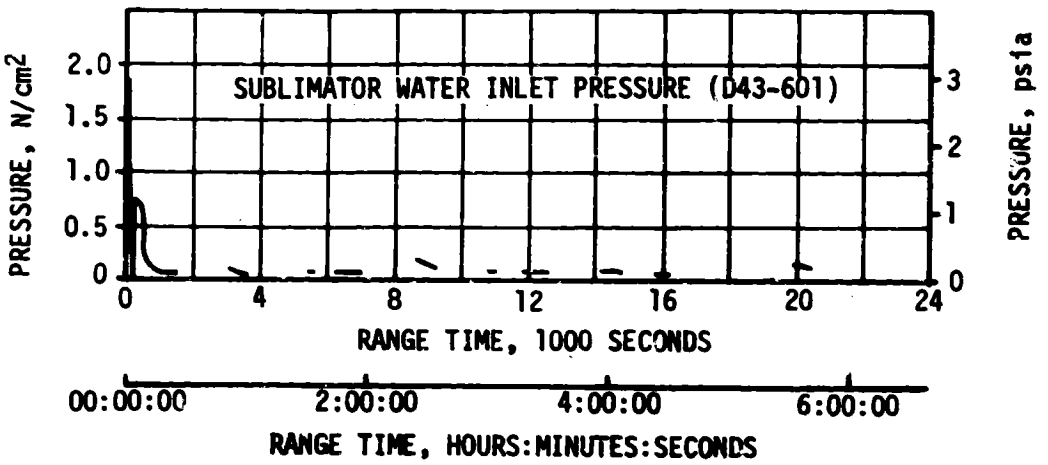
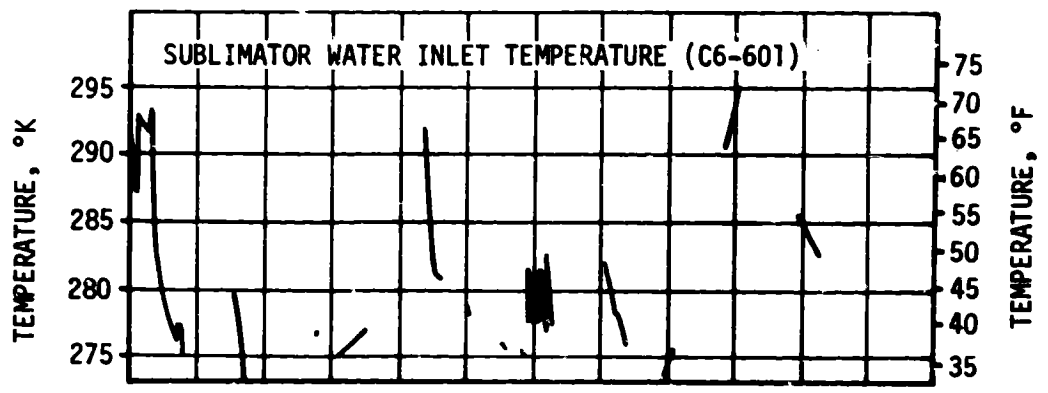
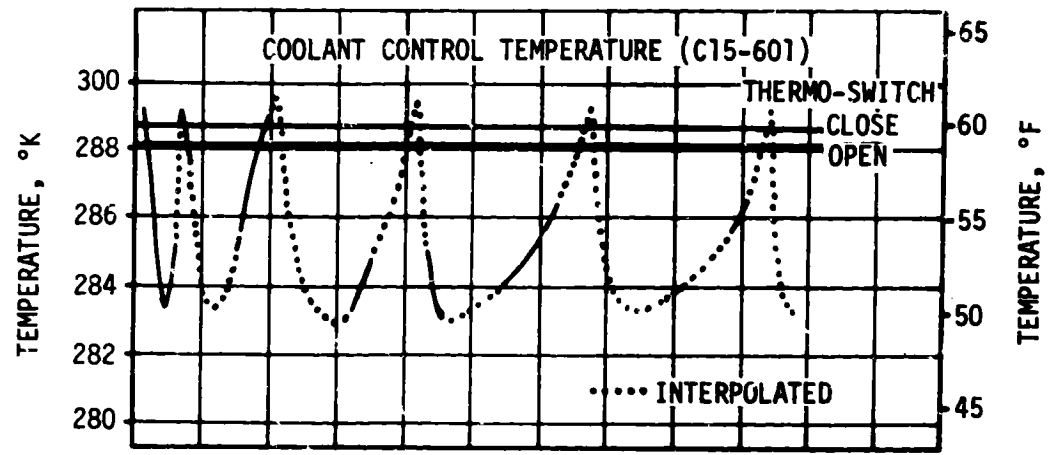


Figure 14-2. IU TCS Coolant Control Parameters

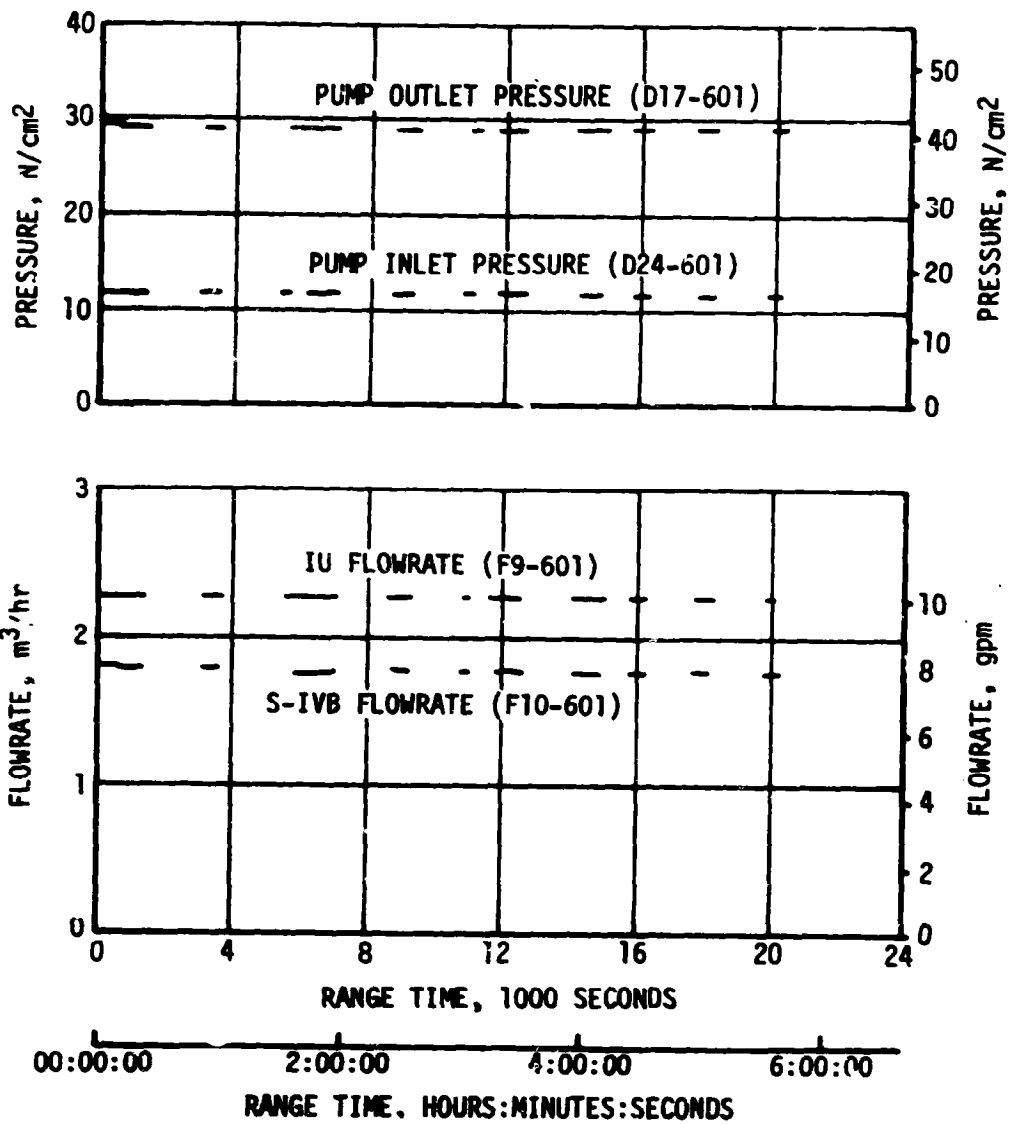


Figure 14-3. IU TCS Hydraulic Performance

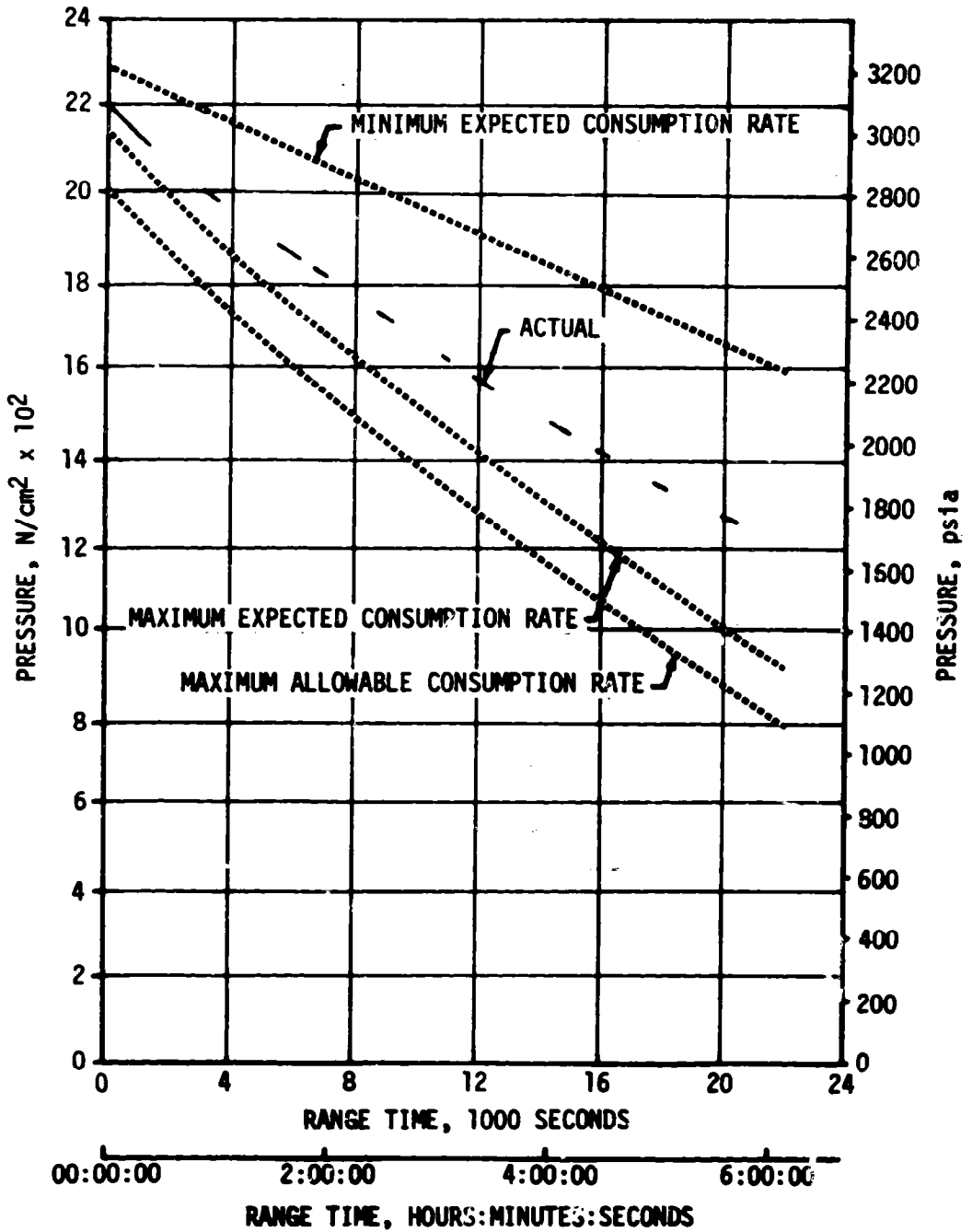


Figure 14-4. IU TCS GN<sub>2</sub> Sphere Pressure (D25-601)

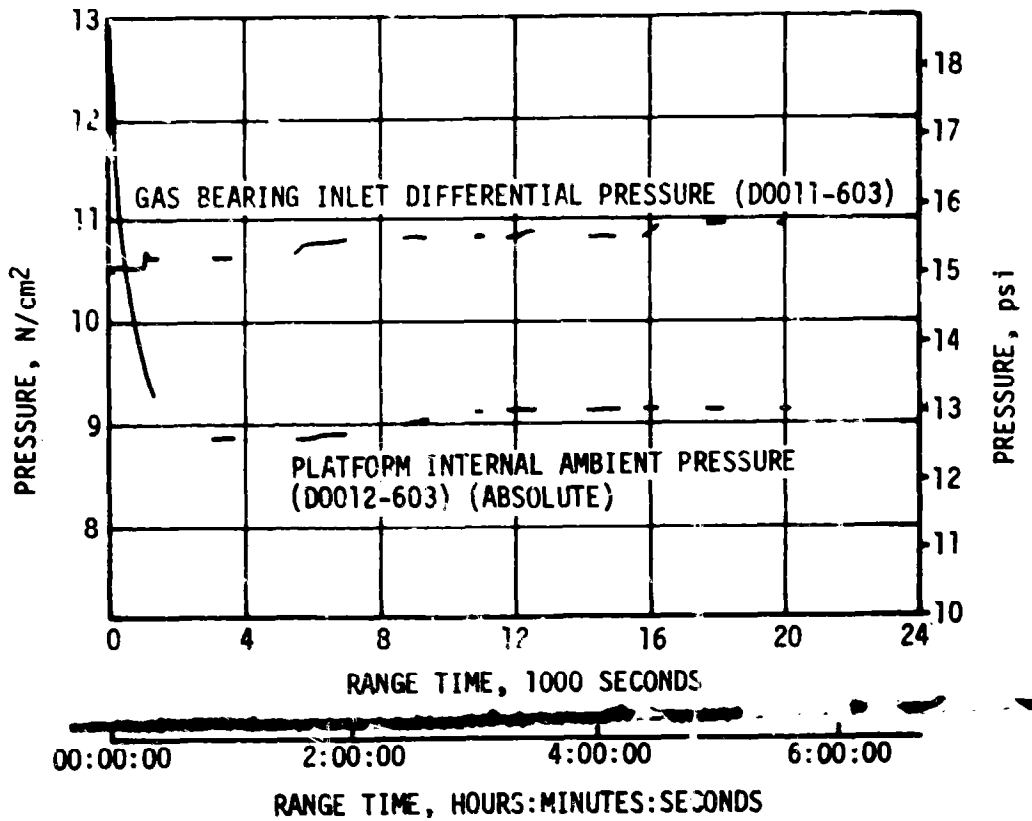


Figure 14-5. IU Platform Internal Gas Bearing  $GN_2$  Pressures

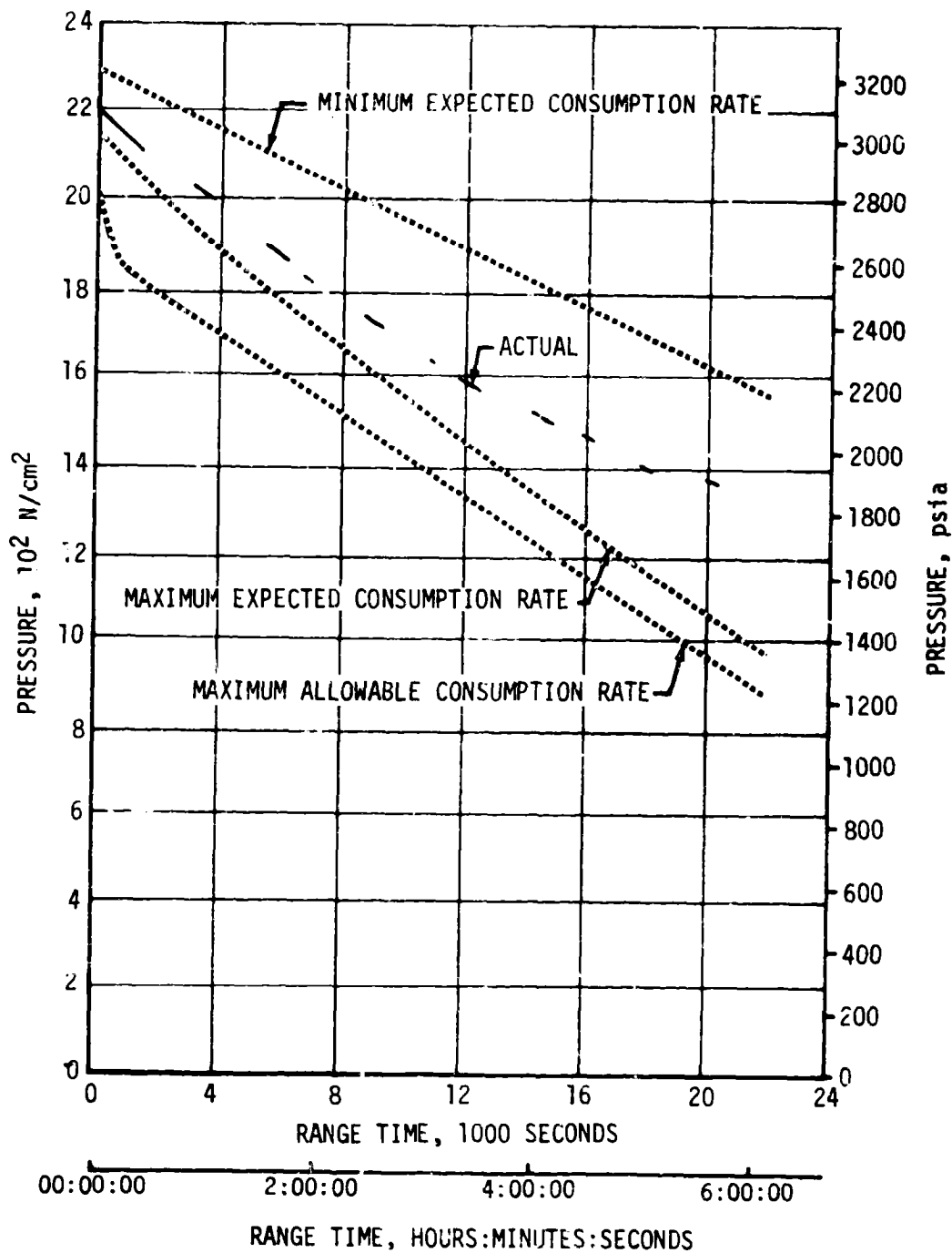


Figure 14-6. IU GBS GN<sub>2</sub> Sphere Pressure (D10-603)

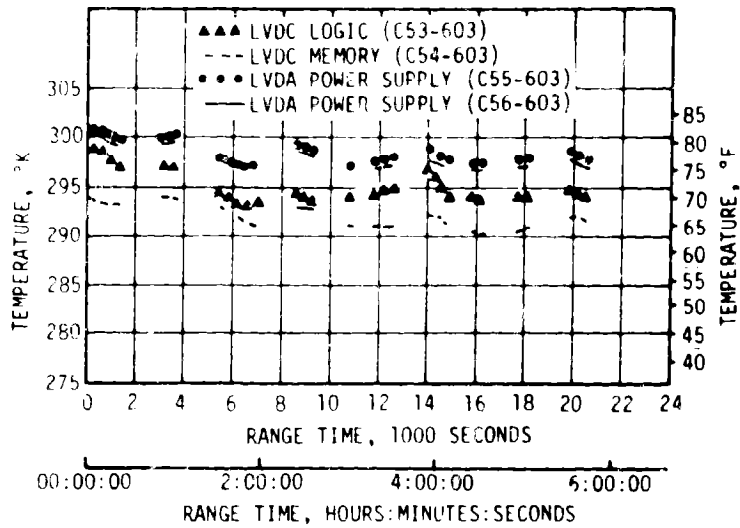


Figure 14-7. Selected IU Component Temperatures

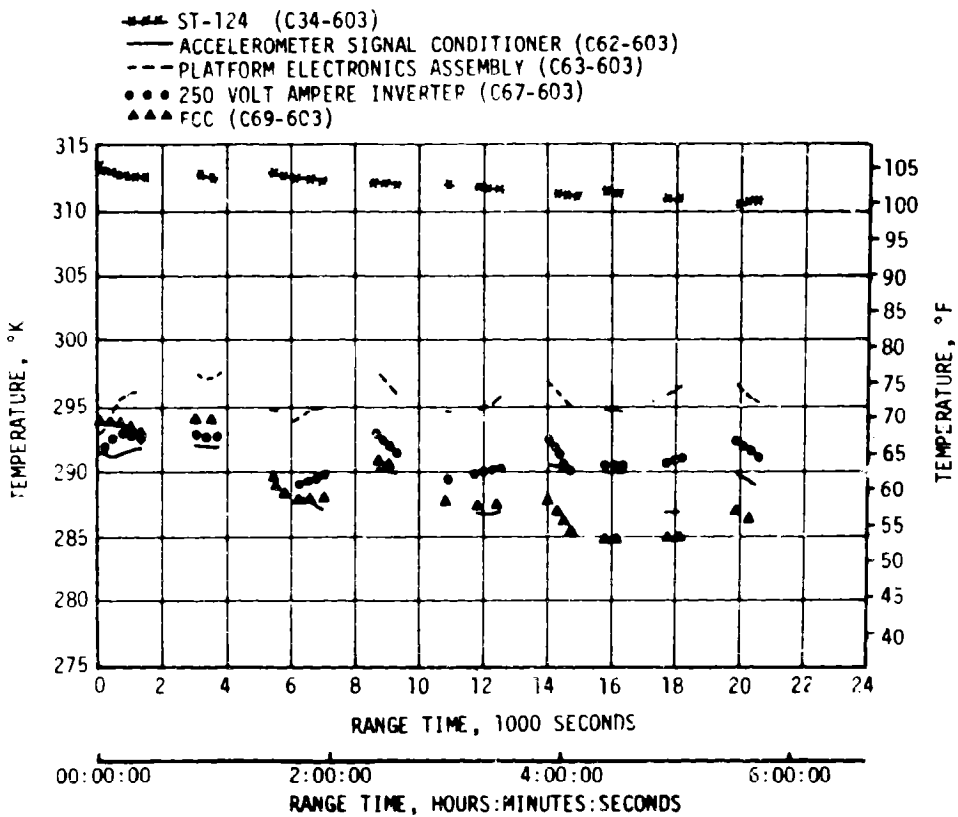


Figure 14-8. Selected IU Component Temperatures

## SECTION 15

### DATA SYSTEMS

#### 15.1 SUMMARY

The SA-207 vehicle data systems performed satisfactorily except for a failure in the S-IVB telemetry system. This failure resulted in the loss of three S-IVB measurements, but had no impact on vehicle performance or postflight analysis. The overall measurement system reliability was 99.6 percent. The usual telemetry interference due to flame effects and staging were experienced. Usable telemetry data were received until 20,500 seconds (5:41:40). Good tracking data were received from the C-Band radar, with Kwajalein (KWJ) indicating final Loss of Signal (LOS) at 21,175 seconds (5:52:55). The Secure Range Safety Command Systems on the S-IB and S-IVB stages were ready to perform their functions properly, on command, if flight conditions during launch phase had required destruct. The Digital Command System (DCS) performed satisfactorily from liftoff through deorbit. Instrument Unit (IU) telemetry data needed for real time support of deorbit operations were not available at Mission Control Center-Houston (MCC-H) during the third orbital revolution pass over the Hawaii (HAW) ground station because of improper implementation of ground procedures at HAW and Johnson Space Center (JSC). In general, ground engineering camera coverage was fair being somewhat below the standard set by previous launches. Three S-150 experiment data dumps were satisfactorily accomplished.

#### 15.2 VEHICLE MEASUREMENT EVALUATION

The SA-207 launch vehicle had 821 measurements scheduled for flight; one measurement was waived prior to start of the automatic countdown sequence leaving 820 measurements active for flight. Three measurements failed during flight, resulting in an overall measurement system reliability of 99.6 percent. A summary of measurement reliability is presented in Table 15-1 for the total vehicle and for each stage. The waived measurements and partially failed measurements are listed by stage in Tables 15-2 and 15-3. These measurement problems had no significant impact on postflight evaluation.

#### 15.3 AIRBORNE TELEMETRY SYSTEM EVALUATION

The stage telemetry systems provided good data from liftoff until each stage exceeded each subsystem's range limitations. A failure in the S-IVB telemetry subsystem at approximately 142 seconds resulted in the loss of three measurements. This failure is discussed in detail in paragraph 15.3.1. Procedural errors at HAW and JSC caused some real time data display problems during the third orbital revolution pass over HAW. This anomaly is discussed in paragraph 15.3.2. The five

Table 15-1. SA-207 Measurement Summary

MEASUREMENT CATEGORY	S-IB STAGE	S-IVB STAGE	INSTRUMENT UNIT	TOTAL VEHICLE
Scheduled	266	239	316	821
Waived	0	1	0	1
Failed	0	3	0	3
Partial Failed	0	0	0	0
Questionable	0	0	0	0
Reliability Percent	100%	98.7%	100%	99.6%

telemetry links performed satisfactorily although data dropouts, as indicated in Table 15-4, were experienced at various times. These dropouts are similar to those on previous flights and are not indicative of flight hardware problems. The S-IB telemetry dropout is attributed to widely varying signal strength and to bursts of electrical noise. These effects are normally sensed at the ground station during the first 10 seconds of flight. A dropout caused by S-IB/S-IVB separation (S-IB retro motors) occurred at Central Instrumentation Facility (CIF) from 142.1 seconds to 145.0 seconds. A dropout in the DP-1 link occurred over the Canary Island (CYI) ground station because of a vehicle antenna null resulting from vehicle attitude. The effect of the dropout on command histories is discussed in paragraph 15.6. All inflight calibrations occurred as programmed and were within specifications. The last telemetry signal was received at approximately 20,500 seconds (5:41:40) by the Honeysuckle (HSK) ground station. A summary of IU and S-IVB telemetry coverage showing Acquisition of Signal (AOS) and LOS for each station is shown in Figure 15-1.

Three S-150 experiment Auxiliary Storage and Playback (ASAP) data dumps were satisfactory. Times of commanded switchover between normal IU Pulse Code Modulated (PCM) data and S-150 ASAP data are shown in Table 15-5. The normal data dump duration is approximately 300 seconds and contains data recorded during the previous 5400 seconds. The first and third data dumps were as expected. The second data dump, however, had been started rather late in the pass over Goldstone (GDS) and had not been completed before the signal to noise ratio became so low, just prior to

Table 15-2. SA-207 Flight Measurements Waived Prior to Flight

MEASUREMENT NUMBER	MEASUREMENT TITLE	NATURE OF FAILURE	REMARKS
S-IVB STAGE			
D0160-403	Press-Helium (Ambient) Sphere	Shifted upward 2% when DP-1 transmitter turned on, then drifted gradually up 9%.	Transducer was RFI sensitive. Backup measurement D0255-403, not RFI sensitive, was used to monitor redline parameter.

Table 15-3. SA-207 Measurement Malfunctions

MEASUREMENT NUMBER	MEASUREMENT TITLE	NATURE OF FAILURE	TIME OF FAILURE (RANGE TIME)	DURATION OF SATISFACTORY OPERATION	REMARKS
MEASUREMENT FAILURES, S-IVB STAGE					
K0124-401	Event-Oxid Turbine Bypass Valve - Open	Measurements lost because of failure in the telemetry system. (See paragraph 15.3.)	Approximately 142 secs.	No satisfactory data obtained.	System performance analysis verified that the basic events properly occurred.
K0125-401	Event-Oxid Turbine Bypass Valve - Closed				
K0216-404	Event-Engine Start on Backup				
<b>NOTE: There were no partial failures.</b>					

Table 15-4. SA-207 Launch Vehicle Telemetry Links Performance Summary

LINK	FREQUENCY (MHZ)	MODULATION	STAGE	FLIGHT PERIOD (RANGE TIME, SEC)	DATA DROPOUTS	
					RANGE TIME (SEC)	DURATION (SEC)
GF-1	240.2	FM/FM	S-IB	0 to 386	2.25	.25
GP-1	256.2	PCM/FM	S-IB	0 to 386	2.25	.25
CP-1	258.5	PCM/FM	S-IVB	0 to 20,459	142.1	2.3
DF-1	250.7	FM/FM	IU	0 to 20,500	142.5 17,992.9	2.5 .9
DP-1	255.1	PCM/FM	IU	0 to 20,500	142.5 17,992.9	2.5 .9

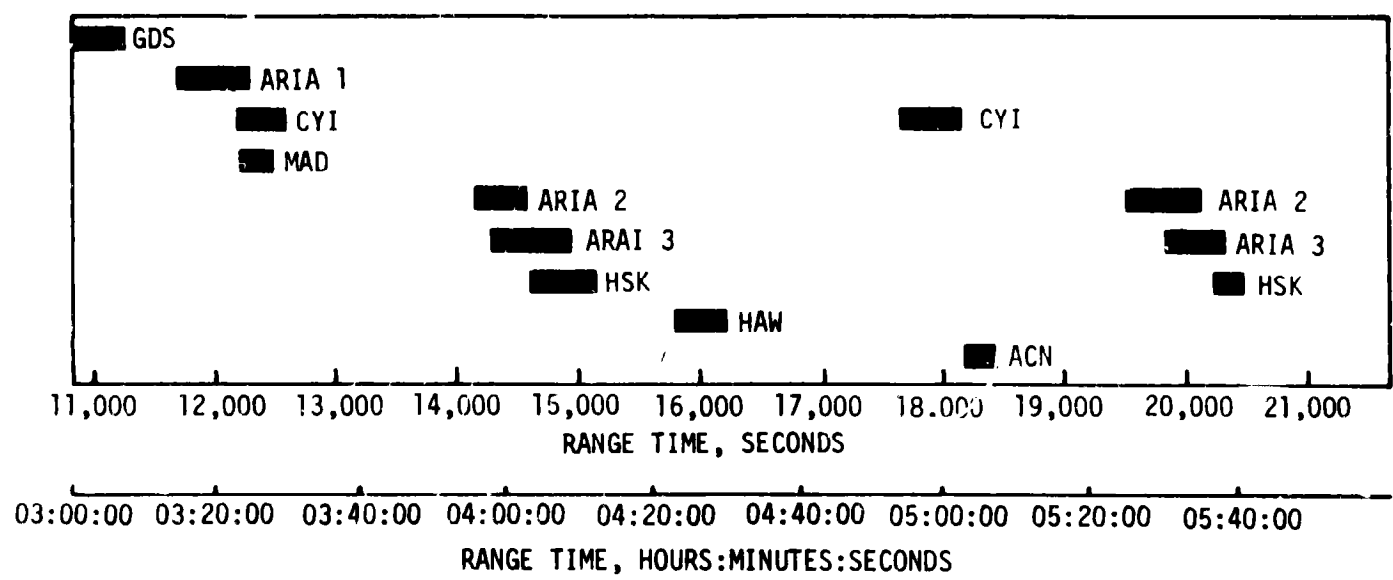
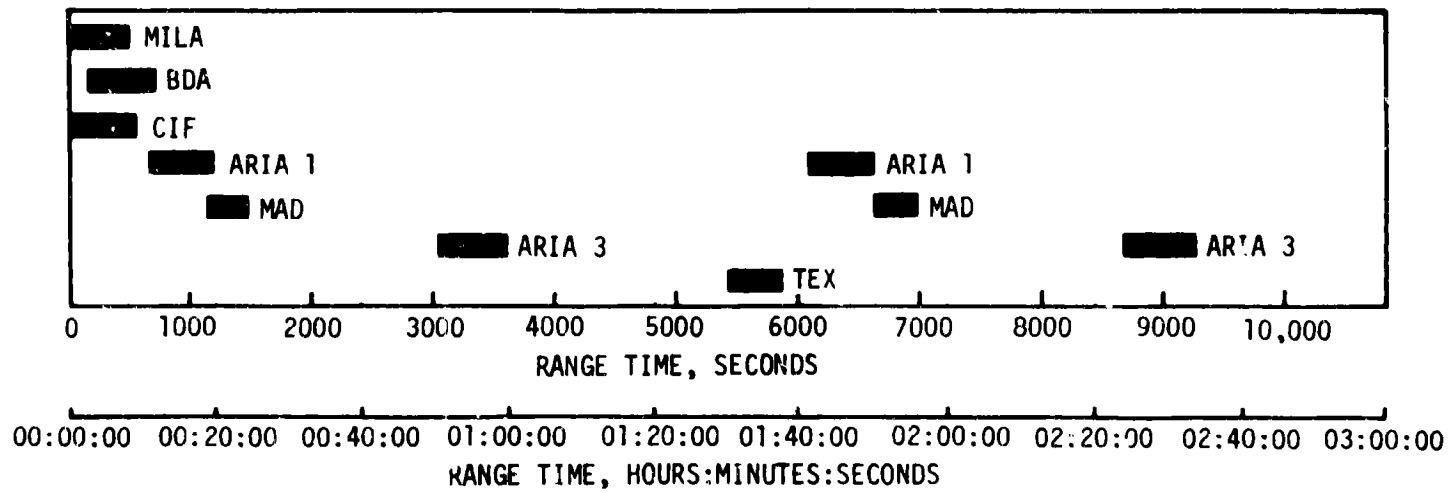


Figure 15-1. SA-207 Telemetry Ground Station Coverage

Table 15-5. SA-207 S-150 Experiment ASAP Data Dumps

COMMAND TIME (SEC)	DUMP START (SEC)	DUMP END (SEC)	GROUND STATION
5552.3	5555.5	5856.4	TEX
10,948.3	10,952.5	During LOS	GDS
14,756.4	14,758.8	15,061.2	HSK

LOS, that the data was unreadable. As a result, the data dump end time at GDS could not be determined. The data contained in the last part of this dump was recovered during the third S-150 ASAP data dump which occurred over HSK. This happened because the ASAP tape recorder, having a capacity of 5400 seconds, had been recording for approximately 3500 seconds following the data dump at GDS which left approximately 1900 seconds of data recorded prior to the data dump at GDS.

#### 15.3.1 S-IVB Remote Digital Sub-Multiplexer Failure

Six S-IVB PCM flight measurements were not transmitted after S-IB/S-IVB separation, approximately 142 seconds, because of component failure in the Remote Digital Sub-Multiplexer (RDSM). Three of the six measurements were cross-strapped to the IU DP-1 link and were successfully transmitted and received. The other three measurements were lost. The six flight measurements were located in PCM telemetry format time slot channel 9B, word 4 and were processed by one of ten digital gate Printed Wiring Assemblies (PWA) in the RDSM. There are nine components on the digital gate PWA and two components on the decoder PWA that could cause the observed failure. The exact failure mode cannot be determined from the flight data but it is suspected that one of these eleven components did fail resulting in an inability of the PWA to properly handle data. There has been no previous RDSM flight failure of this type. However, five similar failures have occurred during ground tests. Each failure was traced to a different one of the components. Failure analysis indicated that these failures were random and no corrective action was required.

Analysis of S-IVB engine performance shows that the events associated with the three lost measurements did, in fact, occur as expected. Because approximately 650 of these digital gate cards have been flown on Saturn vehicles with no similar failures, this failure is considered to be of a random nature. Therefore no corrective action will be taken.

### 15.3.2 Loss of Operational Data Display During Revolution No. 3

IU telemetry data needed for real time support of deorbit operations were not available for display at MCC-H during the third orbital revolution pass over the HAW ground station. Display of the commanded Launch Vehicle Digital Computer (LVDC) memory dump on measurement H60-603 (Guidance Computer Operation) was not obtained and, as a result, verification of the S-IVB/IU deorbit command was delayed until the pass over the CYI ground station. After this verification there was not enough time remaining for the scheduled third LVDC compressed data dump and fourth S-150 experiment ASAP data dump prior to LOS at CYI. Failure to obtain the third LVDC compressed data dump slightly reduced confidence in the conclusions derived from evaluation of the attitude disturbance anomaly discussed in paragraph 10.3.2. Loss of the S-150 experiment data dump resulted in loss of spectral data collected by the star sensor, however, the primary X-Ray portion of the experiment was not affected because the X-Ray sensor was inoperative due to the problem discussed in Section 18.

Postflight review of data, including ground station tape recordings, has shown that the vehicle telemetry system and command system performed satisfactorily. The failure to obtain real time display data resulted from improper implementation of ground procedures at HAW and JSC. This problem has been identified to JSC for appropriate action.

### 15.4 C-BAND RADAR SYSTEM EVALUATION

The C-Band radar performed satisfactorily during flight. A summary of C-band radar coverage time from AOS to LOS for each station is shown in Figure 15-2. As on previous missions, phase front disturbances were observed at Merritt Island Launch Area (MILA) and Bermuda (BDA) during the boost phase. These phase front disturbances result from severe antenna nulls or distorted beacon returns and cause momentary tracking errors at the ground stations.

A dropout at BDA from 545 to 573 seconds was attributed on the operator's log to beacon dropout. However, MILA was tracking during this same time period and experienced no problem, indicating that the dropout at BDA was caused by a ground station tracking problem rather than an onboard problem. No problems were reported by the ground stations tracking the transponder after orbital insertion.

The last station to interrogate the transponder was KWJ. KWJ tracked the transponder until vehicle break up at 21,175 seconds (5:52:55).

### 15.5 SECURE RANGE SAFETY COMMAND SYSTEMS EVALUATION

Telemetered data indicated that the command antennas, receivers/decoders,

15-8

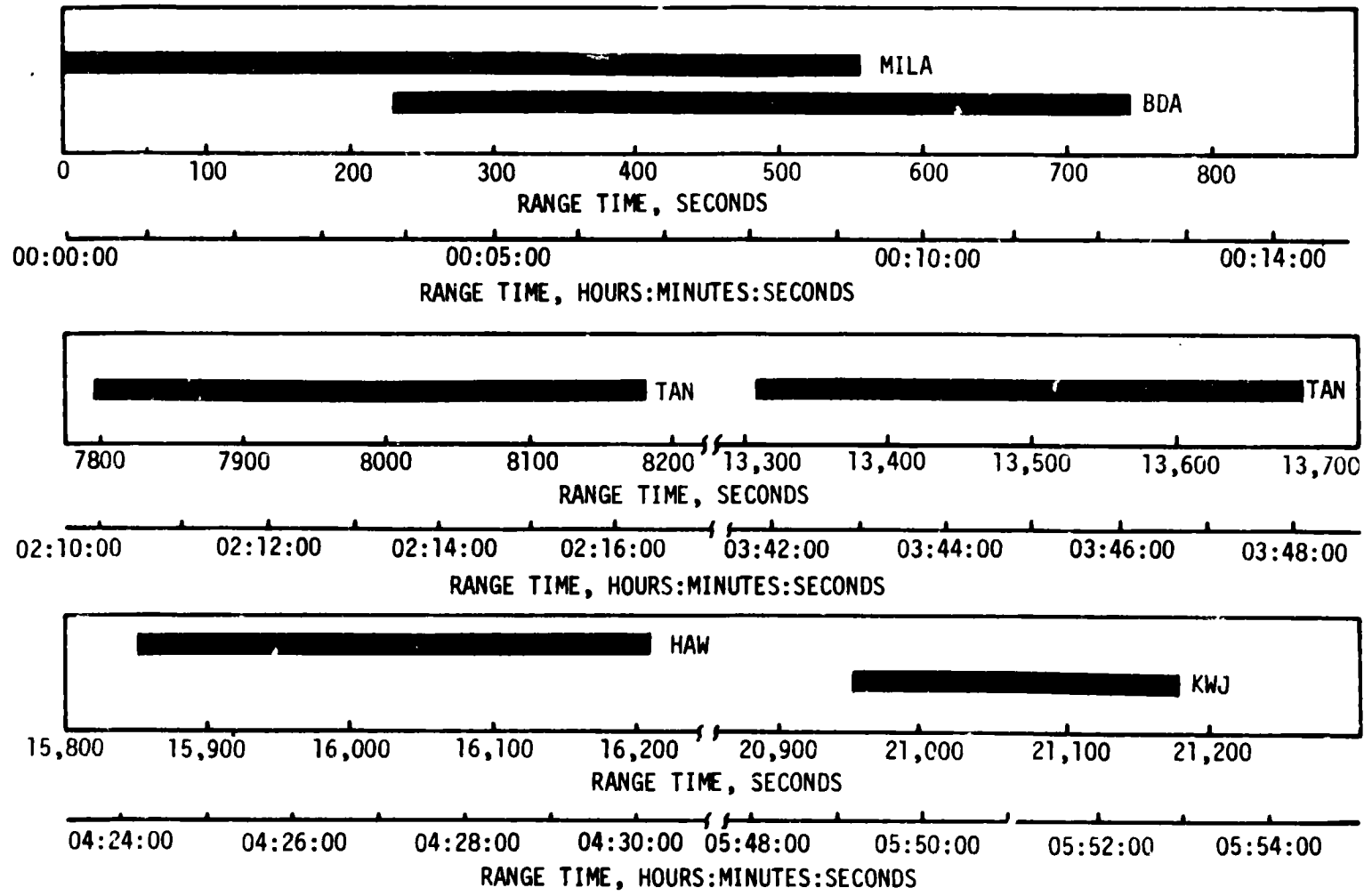


Figure 15-2. SA-207 C-Band Acquisition and Loss Times

Exploding Bridge Wire networks, and destruct controllers on each powered stage functioned properly during flight. They were in the required state-of-readiness if flight conditions during the launch had required vehicle destruct. Since no arm/cutoff or destruct commands were required, all data except receiver signal strength remained unchanged during the flight. Power to the S-IVB stage range safety command systems was cut off at 607.2 seconds by ground command, thereby deactivating (safing) the systems.

#### 15.6 DIGITAL COMMAND SYSTEM EVALUATION

The DCS performed satisfactorily throughout this mission. Fifteen commands were initiated by MCC-H and all but one were accepted by the onboard equipment. Table 15-6 lists the commands transmitted to the IU.

The deorbit dump command transmitted from HAW at 15,906 seconds (4:25:06) did not produce the desired memory data display at MCC-H and the same command was retransmitted at 16,049 seconds (4:27:29). The second transmission also failed to produce the desired display although telemetry data indicated the command was accepted by the DCS. It was later discovered that the ground station was not relaying the memory data to MCC-H (see paragraph 15.3.2). The deorbit dump command was reinitialized by MCC-H when the vehicle was over CYI at 17,993 seconds (4:59:53). The look angles from CYI at this time were such that numerous antenna nulls were being encountered. The command mode word was transmitted and accepted onboard. A telemetry dropout occurred which prevented the ground station from receiving the verification pulses. The mode word was retransmitted three times. However, the onboard computer was waiting for the first data word in the command and rejected the retransmitted mode word. A terminate command was then transmitted to clear the computer and the deorbit dump command was reinitialized at 18,010 seconds (5:00:10). No problems were encountered during this last transmission.

#### 15.7 GROUND ENGINEERING CAMERAS

Ground camera coverage was fair, being somewhat below the standards established on previous launches. Forty-nine items (43 from fixed cameras and 6 from tracking cameras) were received from Kennedy Space Center for evaluation. Data loss was experienced on 16 items. One camera failed to operate, one jammed, one had erratic timing, one had an incorrect field of view, four had their field of view obscured by falling frost and ice, three had severely overexposed film, and five had severely underexposed film. The three long range cameras are included in the five having underexposed film. The three short range cameras contained usable data although it was somewhat degraded due to underexposure. The underexposed film is attributed to lower than expected light levels resulting from overcast skies and fog. The overexposures resulted from high levels of engine plume light reflected from the ground fog, falling frost,

Table 15-6. SA-207 IU Commands

RANGE TIME		TRANS. STATION	COMMAND (NO. OF WORDS IN COMMAND)	NO. OF WORDS TRANS	REMARKS
SECONDS	HRS:MIN:SEC				
1271	0:21:11	MAD	S-150 Maneuver Change (21)	21	Accepted
1278	0:21:18	MAD	Memory Dump (7)	7	Accepted
1338	0:22:18	MAD	S-150 Return to Time Line (6)	6	Accepted
1340	0:22:20	MAD	Memory Dump (7)	7	Accepted
5552	1:32:32	TEX	S-150 ASAP Dump (6)	6	Accepted
6715	1:51:55	MAD	Compressed Data Dump (1)	1	Accepted
10,950	3:02:30	GDS	S-150 ASAP Dump (6)	6	Accepted
12,473	3:27:53	CYI	Compressed Data Dump (1)	1	Accepted
14,756	4:05:56	HSK	S-150 ASAP Dump (6)	6	Accepted
15,886	4:24:46	HAW	Deorbit (7)	7	Accepted
15,906	4:25:06	HAW	Deorbit Dump (7)	7	Accepted
16,049	4:27:29	HAW	Deorbit Dump (7)	7	Accepted
17,993	4:59:53	CYI	Deorbit Dump (7)	4*	Not verified
18,004	5:00:04	CYI	Terminate (1)	1	Accepted
18,010	5:00:10	CYI	Deorbit Dump (7)	7	Accepted

\*The first word of this command was accepted onboard; but was not verified at the ground station due to a telemetry dropout. The first word was then retransmitted three (3) times.

and falling ice. The incorrect field of view resulted when the camera mount allowed the camera to rotate forward at about 1 second. Equipment age and usage is suspected as a prime contributor to the field of view shift. As a result of the 16 failures, system efficiency was 67%.

## SECTION 16

### MASS CHARACTERISTICS

#### 16.1 SUMMARY

Total vehicle mass, determined from post-flight analysis, was within 0.21 percent of predicted from ground ignition through S-IVB/spacecraft separation. Hardware weights, propellant loads and propellant utilization were close to predicted values during flight.

#### 16.2 MASS EVALUATION

Post-flight mass properties are compared with final predicted mass properties (MSFC Memorandum S&E-ASTN-SAE-73-59) and the operational trajectory (MSFC Memorandum S&E-AERO-MFP-100-73).

The post-flight mass properties were determined from an analysis of all available actual and reconstructed data from S-IB ignition through S-IVB cutoff. Dry weights of the launch vehicle are based on actual weighings and evaluation of the weight and balance log books (MSFC Form 998). Propellant loading and utilization was evaluated by stage contractors from propulsion system performance reconstructions. Spacecraft data were obtained from the Johnson Space Center (JSC).

Differences between predicted and actual dry weights of the inert stages and the loaded spacecraft were all within 1.2 percent of predicted, which is within acceptable limits.

During S-IB burn phase, the total vehicle mass was greater than predicted by 738 kilograms (1628 lbm) (0.12 percent) at ignition, and greater than predicted by 172 kilograms (379 lbm) (0.09 percent) at physical separation. These small differences may be attributed to a larger than predicted fuel loading and a larger than predicted upper stage weight.

S-IB burn phase total vehicle mass is shown in Tables 16-1 and 16-2.

During S-IVB burn phase, the total vehicle mass was more than predicted by 265 kilograms (584 lbm) (0.19 percent) at ignition, and less than predicted by 67 kilograms (147 lbm) (0.21 percent) at S-IVB stage cutoff signal. These differences are due primarily to a greater than predicted spacecraft weight and a less than expected residual. Total vehicle mass for the S-IVB burn phase is shown in Tables 16-3 and 16-4.

A summary of mass utilization and loss, both actual and predicted, from S-IB stage ignition through spacecraft separation is presented in Table 16-5. A comparison of actual and predicted mass, center of gravity, and moment of inertia is shown in Table 16-6.

Table 16-1. SA-207 Total Vehicle Masses (Kilograms)

EVENT	GROUND IGNITION		FIRST MOTION		INBOARD ENGINE CUTOFF SIGNAL		OUTBOARD ENGINE CUTOFF SIGNAL		SEPARATION SIGNAL	
	PRED	ACTUAL	PRED	ACTUAL	PRED	ACTUAL	PRED	ACTUAL	PRED	ACTUAL
RANGE TIME (SEC)	33.00	33.13	33.3	33	136.60	137.4	139.63	140.73	140.93	142.03
S-IB STG DRY	38214.	38211.	38214.	38211.	38214.	38211.	38214.	38211.	38214.	38211.
LOX IN TANKS	283158.	283124.	277595.	277552.	1094.	1264.	0.	0.	0.	0.
LOX BELOW TANKS	3518.	3518.	3722.	3722.	3673.	3673.	1502.	1342.	1248.	1140.
LOX ULLAGE	13.	13.	35.	35.	1174.	1174.	1189.	1189.	1190.	1190.
RPI IN TANKS	124410.	124877.	122491.	122358.	2090.	2317.	360.	432.	0.	52.
RPI BELOW TANKS	2145.	2145.	2566.	2566.	2566.	2566.	2355.	2355.	2218.	2260.
RPI ULLAGE	2.	2.	3.	3.	26.	26.	26.	26.	26.	26.
HELIUM SUPPLY	35.	35.	44.	44.	11.	11.	11.	11.	10.	10.
NITROGEN	6.	6.	6.	6.	4.	4.	4.	4.	4.	4.
HYDRAULIC OIL	12.	12.	12.	12.	12.	12.	12.	12.	12.	12.
ORONITE	14.	14.	14.	14.	2.	2.	2.	2.	2.	2.
FRGST	453.	453.	453.	453.						
TOTAL S-IB STAGE	451936.	452417.	445453.	445333.	48871.	49266.	43680.	43569.	42929.	42917.
S-IB/S-IVB DRY	2612.	2609.	2612.	2609.	2612.	2609.	2612.	2609.	2612.	2609.
RETRO PROPELLANT	481.	481.	481.	481.	481.	481.	481.	481.	481.	481.
TOTAL FIRST STG	455080.	455508.	448545.	448974.	51965.	52357.	46774.	46680.	46023.	46003.
TOTAL S-IVB STG	116505.	116572.	116505.	116572.	116460.	116481.	116460.	116481.	116460.	116481.
INSTRUMENT UNIT	2072.	2094.	2072.	2094.	2072.	2094.	2072.	2094.	2072.	2094.
SPACECRAFT	19902.	20123.	19902.	20123.	19902.	20123.	19902.	20123.	19902.	20123.
TOTAL VEHICLE	593560.	594299.	587027.	587753.	190400.	191057.	185209.	185380.	184458.	184704.

Table 16-2. SA-207 Total Vehicle Masses (Pounds)

EVENT	GROUND IGNITION		FIRST MOTION		INBOARD ENGINE CUTOFF SIGNAL		OUTBOARD ENGINE CUTOFF SIGNAL		SEPARATION SIGNAL	
	PRED	ACTUAL	PRED	ACTUAL	PRED	ACTUAL	PRED	ACTUAL	PRED	ACTUAL
RANGE TIME (SEC)	-3.00	-3.10	0.30	.30	136.60	137.4	139.60	140.73	140.90	142.00
S-IB STG DRY	84248.	84242.	84248.	84242.	84248.	84242.	84248.	84242.	84248.	84242.
LOX IN TANKS	624259.	624183.	612658.	612582.	2413.	2758.	0.	0.	0.	0.
LOX BELOW TANKS	7757.	7757.	8206.	8206.	8099.	8099.	5511.	2960.	2753.	2514.
LOX ULLAGE	30.	30.	79.	79.	2590.	2590.	2623.	2623.	2625.	2625.
RP1 IN TANKS	274278.	275309.	270047.	271078.	4607.	5109.	795.	952.	0.	116.
RP1 BELOW TANKS	4729.	4729.	5658.	5658.	5658.	5658.	5193.	5193.	4891.	4982.
RP1 ULLAGE	5.	5.	8.	8.	58.	58.	58.	58.	59.	59.
HELIUM SUPPLY	78.	78.	75.	75.	24.	24.	24.	24.	24.	24.
NITROGEN	15.	15.	15.	15.	9.	9.	9.	9.	9.	9.
HYDRAULIC OIL	28.	28.	28.	28.	28.	28.	28.	28.	28.	28.
ORONITE	33.	33.	33.	33.	6.	6.	6.	6.	6.	6.
FROST	1000.	1000.	1000.	1000.						
TOTAL S-IB STAGE	996461.	997410.	982056.	983005.	107743.	108614.	96298.	98093.	94644.	94606.
S-IB/S-IVB DRY	5759.	5753.	5759.	5753.	5759.	5753.	5759.	5753.	5759.	5753.
RETRO PROPELLANT	1062.	1062.	1062.	1062.	1062.	1062.	1062.	1052.	1062.	1062.
TOTAL FIRST STG	1003282.	1004225.	988877.	989820.	114564.	115429.	103119.	102910.	101465.	101421.
TOTAL S-IVB STG	256851.	256999.	256851.	256999.	256751.	256799.	256751.	256799.	256751.	256799.
INSTRUMENT UNIT	4568.	4618.	4568.	4618.	4568.	4618.	4568.	4618.	4568.	4618.
SPACECRAFT	43878.	44365.	43878.	44365.	43878.	44365.	43878.	44365.	43878.	44365.
TOTAL VEHICLE	1308579.	1310207.	1294174.	1295802.	419761.	421211.	408316.	408695.	406662.	407203.

Table 16-3. SA-207 Upper Stages and Payload Vehicle Masses (Kilograms)

	S-IVB STAGE GROUND IGNITION		J-2 ENGINE START COMMAND		MAINSTAGE		J-2 ENGINE CUTOFF COMMAND		ORBITAL INSERTION	
	PRED	ACTUAL	PRED	ACTUAL	PRED	ACTUAL	PRED	ACTUAL	PRED	ACTUAL
RANGE TIME (SEC)	43.00	43.10	142.30	143.40	145.70	146.80	576.17	572.93	606.07	602.93
S-IVB STAGE DRY	10057.	10055.	10041.	10040.	10041.	10040.	10041.	10040.	10041.	10040.
ULL ROCKET CASES	97.	98.	97.	98.	97.	98.				
ULL ROCKET GRAIN	79.	79.	47.	46.						
LOX IN TANK	88421.	88347.	88421.	88347.	88299.	88241.	1377.	990.	1348.	960.
LOX BELOW TANK	180.	180.	180.	180.	180.	180.	180.	180.	186.	186.
LOX ULLAGE	11.	11.	11.	11.	14.	15.	165.	134.	165.	134.
LH2 IN TANK	17315.	17379.	17315.	17379.	17264.	17333.	912.	1036.	902.	1026.
LH2 BELOW TANK	26.	23.	26.	23.	26.	23.	26.	23.	21.	19.
H2 ULLAGE	72.	59.	72.	59.	72.	59.	412.	144.	242.	144.
HELIUM-LOX PRESS	114.	114.	114.	114.	114.	113.	43.	34.	43.	34.
APS PROPELLANT	59.	57.	59.	57.	59.	57.	57.	54.	57.	54.
G-2/START TANK	2.	2.	2.	2.	0.	0.	0.	0.	0.	0.
HYDRAULIC OIL	6.	6.	6.	6.	6.	6.	6.	6.	6.	6.
N2-H2O RESERVOIR	1.	1.	1.	1.	1.	1.	1.	1.	1.	1.
ENVIRONMENTAL FLUID	6.	12.	6.	12.	6.	12.	6.	12.	6.	12.
HELIUM-APS	1.	1.	1.	1.	1.	1.	1.	1.	1.	1.
HELIUM PNEUMATIC	5.	5.	5.	5.	5.	5.	5.	5.	5.	5.
FROST	45.	136.	0.	45.	0.	45.	0.	45.	0.	45.
TOTAL S-IVB STG	116505.	116572.	116411.	116492.	116192.	116230.	13030.	12710.	12900.	12656.
INSTRUMENT UNIT	2072.	2094.	2072.	2094.	2072.	2094.	2072.	2094.	2072.	2094.
SPACECRAFT	19902.	20123.	19902.	20123.	19902.	20123.	19701.	19900.	19701.	19900.
TOTAL VEHICLE	138480.	138791.	138386.	138661.	138167.	138424.	30840.	30770.	30701.	30717.

REPRODUCIBILITY OF THE ORIGINAL PAGE IS POOR

Table 16-4. SA-207 Upper Stages and Payload Vehicle Masses (Pounds)

	S-IB STAGE		J-2 ENGINE		MAIN STAGE		J-2 ENGINE		URGITAN	
	GROUND IGNITION	START COMMAND	PRED	ACTUAL	PRED	ACTUAL	PRED	ACTUAL	PRED	ACTUAL
RANGE TIME (SEC)	-3.00	-3.10	142.20	143.40	145.70	146.80	396.07	392.93	606.07	602.93
S-IVB STAGE DRY	22173.	22169.	22137.	22135.	22137.	22135.	22137.	22135.	22137.	22135.
ULL ROCKET CASES	214.	217.	214.	217.	214.	217.				
ULL ROCKET GRAIN	176.	176.	103.	102.						
LOX IN TANK	194937.	194773.	194937.	194773.	194667.	194540.	3035.	2184.	2972.	2124.
LOX BELOW TANK	397.	397.	397.	397.	397.	397.	397.	397.	367.	367.
LOX ULLAGE	25.	26.	25.	26.	32.	34.	364.	297.	364.	297.
LH2 IN TANK	38174.	38315.	38174.	38315.	38062.	38213.	2011.	2204.	1989.	2262.
LH2 BELOW TANK	58.	52.	58.	52.	58.	52.	58.	52.	48.	42.
H2 ULLAGE	160.	131.	160.	131.	160.	131.	467.	318.	467.	318.
HELIUM-LOX PRESS	253.	252.	253.	252.	251.	251.	77.	77.	96.	76.
APS PROPELLANT	132.	126.	132.	126.	132.	126.	126.	126.	126.	126.
GH2/START TANK	5.	5.	5.	5.	1.	1.	1.	1.	1.	1.
HYDRAULIC OIL	15.	15.	15.	15.	15.	15.	15.	15.	15.	15.
N2-HYD RESERVOIR	3.	3.	3.	3.	3.	3.	3.	3.	3.	3.
ENVY CONT FLUID	14.	27.	14.	27.	14.	27.	14.	14.	14.	27.
HELIUM-APS	3.	3.	3.	3.	3.	3.	3.	3.	3.	3.
HELIUM PNEUMATIC	12.	12.	12.	12.	12.	12.	12.	12.	12.	12.
FROST	100.	300.	0.	100.	0.	100.	0.	100.	0.	100.
TOTAL S-IVB STG	256851.	256999.	256644.	256691.	256160.	256257.	28741.	28025.	28616.	27902.
INSTRUMENT UNIT	4568.	4618.	4568.	4618.	4568.	4618.	4568.	4618.	4568.	4618.
SPACECRAFT	43878.	44365.	43878.	44365.	43878.	44365.	34682.	35201.	34682.	35201.
TOTAL VEHICLE	305297.	305982.	305090.	305674.	304606.	305240.	67991.	67844.	67866.	67721.

Table 16-5. SA-207 Flight Sequence Mass Summary

	ACTUAL		PREDICTED	
	KG	LBW	KG	LBW
S-IB STAGE AT GROUND IGNITION (G.I.)	452417.	997410.	451986.	996461.
S-IB/S-IVB INTERSTAGE AT G.I.	-3091.	5515.	3093.	6821.
S-IVB STAGE AT G.I.	116572.	256995.	116505.	256851.
INSTRUMENT UNIT AT G.I.	2094.	4610.	2072.	4560.
CSM*SLA*LES	20123.	44365.	19902.	43570.
FIRST FLIGHT STAGE AT G.I.	594299.	1310207.	593950.	1308979.
THRUST BUILDUP PROP	-6533.	-14404.	-6533.	-14404.
FIRST FLIGHT STAGE AT FIRST MOTION	587765.	1295002.	587027.	1294174.
MAIN STAGE PROP	-400516.	-882907.	-399994.	-881030.
FRUST	-453.	-1000.	-453.	-1000.
SEAL PURGE (N2)	-2.	-6.	-2.	-6.
GEAR BOX CONSUMPTION (RP-1)	-317.	-699.	-317.	-699.
FULL ADDITIVE (TORONITE)	-12.	-27.	-12.	-27.
I.E.T.O. PROP	-992.	-2187.	-992.	-2187.
S-IVB FRUST	-90.	-200.	-95.	-100.
FIRST FLIGHT STAGE AT O.E.C.O.S.	185380.	405695.	185209.	405310.
OFTD TO SEP PROP	-659.	-1519.	-762.	-1661.
FIRST FLIGHT STAGE AT SEPARATION (PHYSICAL)	184691.	407175.	184445.	406039.
S-IB STAGE AT SEPARATION	-42900.	-94579.	-42517.	-94517.
S-IB/S-IVB INTERSTAGE	-3091.	-5515.	-3093.	-6821.
S-IVB AFT FRAME	-14.	-31.	-14.	-31.
S-IVB ULLAGE ROCKET PROPELLANT	-33.	-74.	-32.	-71.
S-IVB DETONATION PACKAGE	-1.	-3.	-2.	-5.
SECOND FLIGHT STAGE AT IGNITION (ESC)	138651.	305674.	138350.	305095.
THRUST BUILDUP PROP	-140.	-327.	-159.	-374.
ULLAGE ROCKET PROPELLANT	-45.	-102.	-47.	-105.
GRZ START GUN	-1.	-4.	-1.	-4.
SECOND FLIGHT STAGE AT 95 PERCENT THRUST	138504.	305245.	138167.	304500.

Table 16-5. SA-207 Flight Sequence Mass Summary (Continued)

	ACTUAL		PREDICTED	
	KG	LBM	KG	LBM
SECOND FLIGHT STAGE AT 90 PERCENT THRUST	138454.	305240.	138167.	304636.
AUX-PROP. POWER ROLL	-2.	-6.	-2.	-6.
MAINSTAGE	-103423.	-228009.	-103055.	-227477.
ULLAGE ROCKET CASES	-98.	-217.	-97.	-214.
LES	-4156.	-9164.	-4171.	-9195.
SECOND FLIGHT STAGE AT ECC	30773.	67844.	30840.	67971.
THRUST DECAY PROP	-37.	-82.	-38.	-85.
PROP BELOW VALVE	-18.	-40.	-18.	-43.
SECOND FLIGHT STAGE AT ETD	30717.	67721.	30783.	67866.
CSM	-14167.	-31234.	-13932.	-30715.
SLA PANELS ROTATED	0.	0.	0.	0.
VENT	-187.	-414.	-97.	-213.
CSM SEPARATED	16362.	36073.	16754.	36937.
S-IVB STAGE	-12458.	-27488.	-12083.	-26402.
V.I.U.	-2094.	-4618.	-2072.	-4563.
SLA	-1799.	-3967.	-1799.	-3967.

Table 16-6. SA-207 Mass Characteristics Comparison

EVENT	MASS		LONGITUDINAL CG, (X STAB)	RADIUS INCHES	RADIUS METERS	DELTA AL-6	DELTA AL-6	ROLL MOMENT OF INERTIA	PITCH MOMENT OF INERTIA	YAW MOMENT OF INERTIA
	KG	LB								
S-IV STAGE DRY	PRED	3821.4	3885	0.0152	0.0597	0.0000	0.0000	0.223	2.592	2.561
	ACTUAL	3821.2	3885	0.0152	0.0597	0.0000	0.0000	0.223	2.592	2.561
S-IVS-1V9 INTER-STAGES TOTAL	PRED	3094	3094	0.0559	26.706	0.0000	0.0000	0.033	0.023	0.024
	ACTUAL	3091	3094	0.0559	26.708	0.0000	0.0000	0.033	0.023	0.024
S-IVB STAGE DRY AT G-1	PRED	10155	13006	0.2145	33.035	0.0000	0.0000	0.075	0.271	0.271
	ACTUAL	10155	13006	0.2145	33.035	0.0000	0.0000	0.075	0.271	0.271
INSTRUMENT UNIT TOTAL	PRED	2072	4568	0.4192	22.796	0.0000	0.0000	0.019	0.011	0.009
	ACTUAL	2093	4618	0.4192	22.796	0.0000	0.0000	0.020	0.011	0.009
SPACECRAFT TOTAL	PRED	19923	22009	0.727	55.902	0.0000	0.0000	0.038	0.533	0.534
	ACTUAL	19923	22009	0.727	55.902	0.0000	0.0000	0.038	0.533	0.534
1ST FLIGHT STAGE AT IGNITION	PRED	59350	7465	0.067	18.989	0.0000	0.0000	2.150	76.349	76.307
	ACTUAL	59350	7465	0.067	18.984	0.0000	0.0000	2.201	76.349	76.307
1ST FLIGHT STAGE AT FIRST MOTION	PRED	59702	7465	0.067	18.911	0.0000	0.0000	2.121	76.416	76.412
	ACTUAL	59766	7465	0.067	18.926	0.0000	0.0000	2.166	76.416	76.412

Table 16-6. SA-207 Mass Characteristics Comparison (Continued)

EVENT	MASS		LONGITUDINAL C.G. (X STA.)		RADIAL C.G.		ROLL MOMENT OF INERTIA		PITCH MOMENT OF INERTIA		YAW MOMENT OF INERTIA	
	KILO POUNDS	O/O DEV.	VETERS INCHES	DELTA INCHES	METERS INCHES	DELTA INCHES	KG-M2 O/O DEV.	X10-6 DEV.	KG-M2 O/O DEV.	X10-6 DEV.	KG-M2 O/O DEV.	X10-6 DEV.
1ST FLIGHT STAGE AT OUTBOARD ENGINE CUTOFF SIGNAL	PRED		29.087		0.0217							
	ACTUAL		1145.1		0.0570		0.428		38.650			38.648
1ST FLIGHT STAGE AT SEPARATION (PHYSICAL)	PRED		29.122		0.035							
	ACTUAL		1146.5		0.0670		0.473		41.664		7.80	41.662
2ND FLIGHT STAGE AT IGNITION (ESC)	PRED		29.186		0.0218							
	ACTUAL		1149.0		0.0550		0.424		38.208			38.206
2ND FLIGHT STAGE AT 90 PERCENT THRUST	PRED		29.222		0.035							
	ACTUAL		1150.4		0.0650		0.469		41.220		7.80	41.218
2ND FLIGHT STAGE AT CUTOFF SIGNAL	PRED		35.693		0.0241							
	ACTUAL		1405.2		0.0507		0.137		10.995			10.994
2ND FLIGHT STAGE AT 90 PERCENT THRUST	PRED		35.729		0.035							
	ACTUAL		1406.6		0.0671		0.138		11.080		0.77	11.079
2ND FLIGHT STAGE AT CUTOFF SIGNAL	PRED		35.694		0.0241							
	ACTUAL		1738.2		0.0507		0.136		10.992			10.991
2ND FLIGHT STAGE AT ETD	PRED		35.729		0.035							
	ACTUAL		1747.7		0.0671		0.137		11.077		0.77	11.076
2ND FLIGHT STAGE AT 90 PERCENT THRUST	PRED		44.151		0.1020							
	ACTUAL		1738.2		0.0507		0.134		3.762			3.760
2ND FLIGHT STAGE AT 90 PERCENT THRUST	PRED		44.392		0.241							
	ACTUAL		1747.7		0.0671		0.134		3.713		-1.24	3.711
2ND FLIGHT STAGE AT ETD	PRED		44.178		0.1020							
	ACTUAL		1739.3		0.0507		0.133		3.749			3.747
2ND FLIGHT STAGE AT ETD	PRED		44.420		0.241							
	ACTUAL		1749.8		0.0671		0.134		3.700		-1.20	3.698
SPACECRAFT SEPARATED	PRED		35.345		0.1388							
	ACTUAL		1391.5		0.0571		0.130		0.764			0.761
SPACECRAFT SEPARATED	PRED		35.494		0.149							
	ACTUAL		1397.4		0.0671		0.131		0.751		-1.20	0.749

## SECTION 17

### SPACECRAFT SUMMARY

The SA-207/Skylab-3 space vehicle was launched at 11:10:50 Universal Time (UT) (7:10:50 a.m. Eastern Daylight Time) on July 28, 1973, (first visit day) from Launch Complex 39B at the Kennedy Space Center, Florida. This vehicle, the second to visit the Saturn Work Shop, was manned by Captain Alan L. Bean, Commander; Owen K. Garriott, Science Pilot; and Major Jack R. Lousma, Pilot.

The space vehicle, consisting of a modified Apollo command and service module payload on a Saturn IB launch vehicle, was inserted into earth orbit approximately 10 minutes after liftoff. The orbit achieved was 226.29 by 149.87 kilometers.

Rendezvous maneuvers were performed as planned during the first five revolutions after insertion. During this time, a leak was detected in the command and service module reaction control system engine B3 of quad B (one of four reaction control system modules) and determined to be caused by an oxidizer valve which was stuck in the open position. The quad was isolated and the mission continued. Stationkeeping with the Saturn Work Shop began approximately 8 hours after liftoff. Docking occurred approximately 8 1/2 hours into the mission.

All three crewmen experienced motion sickness during the first three mission days, with the result that the Saturn Work Shop activation and experiment implementation activities were curtailed. By adjusting the crew's diet and maintaining a low work load, the crew was able to complete the adjustment to space flight by visit day 5, and the flight activities were increased to the preflight planned levels.

The service module reaction control system quad D (opposite quad B) engines were inhibited and the isolation valves closed after an oxidizer leak developed on mission day 6. Acceptable control modes and procedures were defined consistent with the constraints imposed by the two reaction control system problems.

The first extravehicular activity was delayed to visit day 10 because of the crew's motion sickness. The extravehicular activity lasted almost 8 hours during which time the crew changed the Apollo Telescope Mount film, deployed the twin-pole sun shield, inspected and performed repair work on the S-055 (Ultraviolet Spectrometer) experiment and deployed the S-149 (Particle Collection) experiment.

The second extravehicular activity was performed on visit day 28 at which time the Apollo Telescope Mount film was replaced and a gyro package was installed.

Final activities consisted of workshop closeout, suit donning and checkout, undocking, deorbit, and entry. There was no workshop fly-around maneuver following command and service module undocking. Tunnel hatch installation was completed on September 25, 1973 at 14:30 UT, and command and service module undocking occurred at 19:48 UT. Separation occurred at 19:50 UT, followed by a service propulsion system firing at 21:38 UT. The single firing deorbit maneuver resulted in spacecraft splashdown approximately 250 miles southwest of San Diego, California, at 22:20 UT. The spacecraft assumed a stable attitude and crew recovery followed approximately 43 minutes after splashdown.

## SECTION 18

### MSFC INFLIGHT EXPERIMENT

#### 18.1 SUMMARY

Skylab Experiment S-150, Galactic X-Ray Mapping Experiment, was performed during the flight of SA-207. The object of the experiment was to map the X-Ray flux intensity of galactic space. The experiment, which had a planned operating time of 265 minutes, collected X-Ray data for only 110 minutes before the experiment high voltage switched off because of low gas pressure in the X-Ray sensor. Even though the operating time of the X-Ray experiment was less than planned, it was greater than the accumulative time of all preceding similar experiments. The associated spectral data continued to be collected by the experiment star sensors, however, these data are of use principally in determining experiment pointing direction. The lack of one Auxiliary Storage and Playback (ASAP) cycle discussed in Section 15 resulted in loss of this spectral data for the third revolution.

#### 18.2 EXPERIMENT ANOMALY

During the second revolution of S-IVB/IU orbital flight, abnormally low readings in measurements D71-602, P-10 gas supply low pressure, and D73-603, collimator pressure, were reported by the Goldstone ground station. The experiment was designed to be fully operational when the internal experiment sensor P-10 gas (90% argon, 10% methane) pressure reached 14.5 psia with an operational pressure range of 14.5 psia to 15.1 psia. The experiment will operate at a minimum pressure of 12.0 psia; however, sensing capability for the lower energy X-Ray (200 EV to 1 KEV) is lost at pressures below 14.5 psia. When the pressure drops below 12.0 psia, the experiment high voltage power is automatically switched off, but spectral data continues to be collected by the star sensor.

At approximately 31 minutes range time the experiment was fully operational (P-10 gas to minimum operational pressure). The experiment operated normally for one revolution (92 minutes per revolution) plus 18 minutes out of a planned operating time of two revolutions plus 81 minutes. At approximately 2 hours 20 minutes the experiment high voltage automatically switched off when the pressure dropped below 12.0 psia and no further X-Ray data were received. Star sensor data received through the last IU/S-150 ASAP data dump (total star sensor data 2 revolutions plus 32 minutes) were not affected by the P-10 pressure loss. However, star sensor data were lost because of a revolution 3 data display problem (see Section 15).

### 18.2.1 Gas System Description

A schematic of the P-10 Supply System is shown in Figure 18-1. In the normal flight operation mode, P-10 gas is supplied from a high pressure storage sphere through a combination of two regulators wherein the pressure is reduced and controlled to the level required by the S-150 Experiment counter package. The orifice regulator consists of two fixed orifices in series through which gas is continuously vented to space at a nominal rate of about 0.000142 Standard Cubic Meters per Second (SCMS) [0.26 Standard Cubic Feet per Minute (SCFM)]. The pressure across the upstream orifice is maintained at a nominal  $8.96 \text{ N/cm}^2$  (13.0 psid) by the pressure regulator. The pressure between the two orifices is supplied to the experiment interface at a nominal level of  $20.68 \text{ N/cm}^2$  (30 psia).

The functional interface between the S-150 and the P-10 supply system for the operational (flight) mode is a normally closed solenoid valve B (Figure 18-1) at the counter package inlet. A control system internal to the experiment counter package is designed to maintain a constant density of P-10 gas through frequency modulation of this solenoid valve. The valve is cycled (opened and closed) at a frequency required to replenish gas leaked from the counter package through the thin film (0.3 mil Kimfoil) X-Ray incident window. The maximum gas consumption rate by the S-150 experiment in this mode of operation is 0.000020 SCMS (0.038 SCFM, reference Interface Control Document 13M07394). The P-10 supply system was designed to provide gas to the experiment interface at a pressure of  $20.68 + 3.45 \text{ N/cm}^2$  ( $30 \pm 5$  psia) for consumption rates not to exceed this value.

The gas supply system is inactive until initiation of the experiment subsequent to completion of the primary, SA-207 mission. After Command Service Module separation but prior to the deployment of the experiment package, the normally closed shut-off valve at the storage sphere outlet is opened by switch selector command, permitting gas to flow to the regulators.

### 18.2.2 Gas System Performance

System operation was initiated at 0:23:35 when programmed switch selector commands opened the high pressure supply solenoid valve A and powered on the S-150 sensor. The S-150 control valve B opened fully at this time and the counter package began filling with gas. Deployment of the experiment sensor was initiated with firing of the pyrotechnic devices at approximately 0:24:14. At approximately 0:24:22, the sensor was fully deployed against its mechanical stop. Filling of the control package continued at the predicted rate, and at approximately 0:29:44, the experiment counter collimator pressure D73-603 approached the desired operating pressure, and the S-150 control valve B went from full open to cyclic mode of operation. By 0:31:30 the supply pressure at the S-150 interface (measurement D71-602) had reached operating pressure.

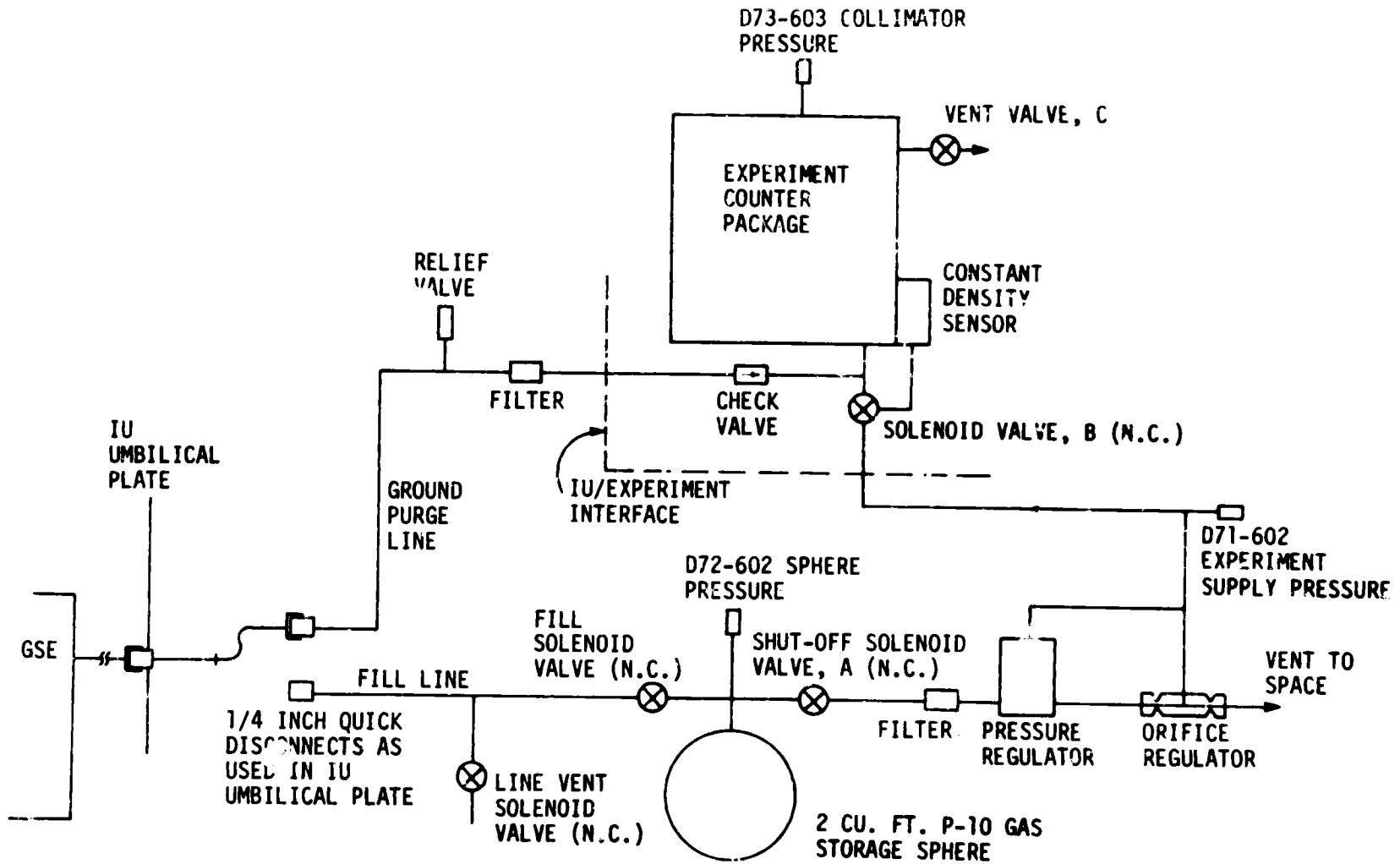


Figure 18-1. P-10 Gas Supply System Schematic

At this time the S-150 and P-10 supply systems stabilized into the as-designed operational mode with all performance parameters nominal. The frequency of cycling of the S-150 control valve B was constant at about one cycle every three seconds. This period of nominal operation continued through the first revolution until just beyond two hours of flight time when the P-10 supply pressure, followed by the collimator pressure, decayed below allowable limits.

Pertinent data for the anomalous period is shown in Figure 18-2. At about 2:04:56, the frequency of cycling of the S-150 control solenoid valve began to decrease, indicating less demand for P-10 gas. This was coincident with the start of an increase in S-150 counter package temperature (C148-603) which had been stable prior to this time. The heating up of the counter package is thought to have been brought on by exposure to solar radiation. As the temperature did increase, the response of the S-150 control system was a decrease in the gas demand. Valve B eventually closed altogether and remained closed for about 100 seconds beginning at 2:08:06.

During this period the supply pressure to the valve drifted upward slightly and stabilized at about  $22.89 \text{ N/cm}^2$  (33.2 psia), a natural response of the regulation system to the decreasing consumption. The counter internal pressure remained constant at  $10.14 \text{ N/cm}^2$  (14.7 psia).

As shown in Figure 18-2, the control valve B began cycling again at about 2:09:51 but at a much higher rate than previously observed. Operation was erratic with frequency alternately increasing and then decreasing until the valve went to the full open position near 2:12:50 where it remained for the duration of the missile. The demand for gas by the S-150 counter package was higher than the P-10 supply system was able to provide at the nominal pressure level and thus the supply pressure began to decline. As the valve cycle frequency momentarily slowed about 2:11:21, the rate of decay of the supply pressure was decreased markedly as the regulation system attempted to recover. It is also significant to note that the counter pressure was maintained constant at its nominal  $10.14 \text{ N/cm}^2$  (14.7 psia), through rapid cycling of the valve, until the supply pressure had decayed to less than one psi above the counter pressure. Only then did the valve go full open and the counter pressure begin to decrease. When the counter pressure reached  $8.27 \text{ N/cm}^2$  (12 psia) the sensor high voltage was switched off by the experiment sensor, as designed, thus ending the X-Ray experiment at 2:20:25.

### 18.2.3 Gas Consumption

Calculation of total gas consumption through use of the storage sphere bleed down data, and the vent flowrate using the proven orifice regulator flow relationship, results in the following values:

18-5

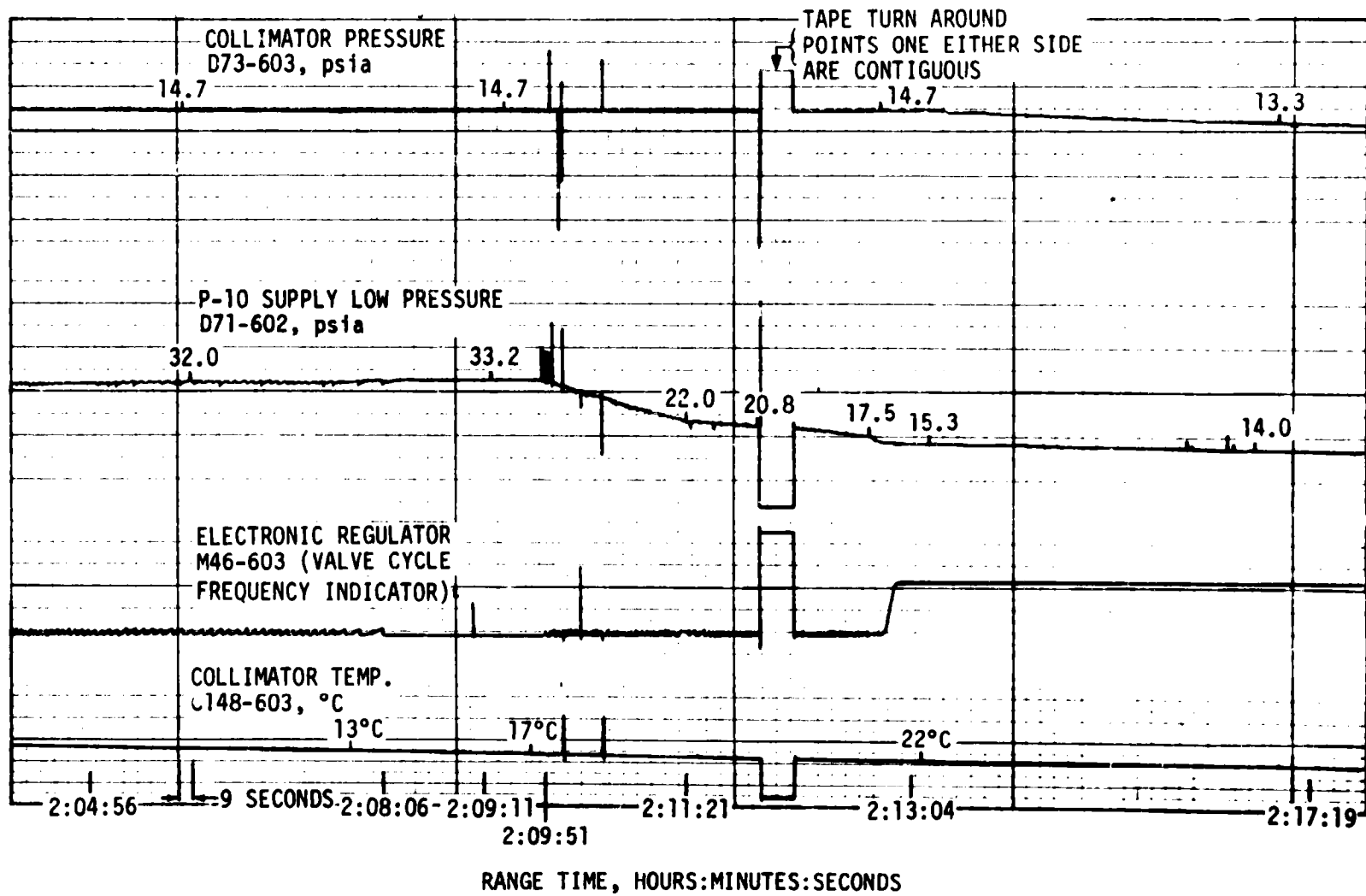


Figure 18-2. S-150 Environmental Parameter History

	<u>Period of Nominal Operation (00:32-2:10)</u>	<u>Period Following Anomaly (2:10-5:00)</u>
Total Flow	0.000179 SCMS (0.336 SCFM)	0.000107 SCMS (0.201 SCFM)
Vent Flow	0.000160 SCMS (0.304 SCFM)	0.000064 SCMS (0.120 SCFM)
Experiment Flow	0.000018 SCMS (0.034 SCFM)	0.00043 SCMS (0.081 SCFM)

The P-10 gas supply system was designed to maintain a minimum pressure of 17.24 N/cm<sup>2</sup> (25 psia) at the experiment interface for a maximum experiment consumption rate of 0.042 SCFM. The loss of positive pressure control of the S-150 experiment counter package was due to excessive consumption of P-10 gas by the experiment - over twice the specification value and beyond that for which the system was designed and capable of providing.

The most probable cause of the pressure loss is increased gas leakage through the X-Ray incident window. This window is a porous "Kimfoil" film approximately 0.3 mil thick which is age and temperature sensitive. A slight deterioration was noted in the window two weeks prior to launch but the leakage rate at that time was considered acceptable. Replacement of the existing window very well could have resulted in a window with a higher leakage rate. The most immediate cause of accelerated deterioration and failure was exposure to direct sunlight. The times and durations of these exposures were normal and predicted, but the effects on the integrity of the sensor were underestimated.

Since the S-150 experiment was unique to the Skylab-3 flight, no corrective action is required. However, if the experiment is flown again, the "Kimfoil" window film thickness will be increased to 0.5 mil and the operating band of the pressure regulator will be broadened to reduce sensitivity to this recognized failure mode.

## APPENDIX A

### ATMOSPHERE

#### A.1 SUMMARY

This appendix presents a summary of the atmospheric environment at launch time of the SA-207/SL-3. The format of these data is similar to that presented on previous launches of Saturn Vehicles to permit comparisons. Surface and upper level winds, and thermodynamic data near launch time are given.

#### A.2 GENERAL ATMOSPHERIC CONDITIONS AT LAUNCH TIME

During the early morning launch of Skylab 3, the Cape Kennedy launch area was experiencing cloudiness, fog, mild temperatures and gentle surface winds. All frontal activity was located in the middle and northern regions of the United States as is shown in the surface synoptic weather map of Figure A-1. Numerous thunderstorms occurred over the state on the previous afternoon (July 27) with rather extensive cloud cover remaining during the night and through launch. Surface winds in the Cape Kennedy area were light and southwesterly as shown in Table A-1. Wind flow aloft is shown in Figure A-2 (500 millibar level). The maximum wind belt was located north of Florida, giving less intense wind flow aloft over the Cape Kennedy area.

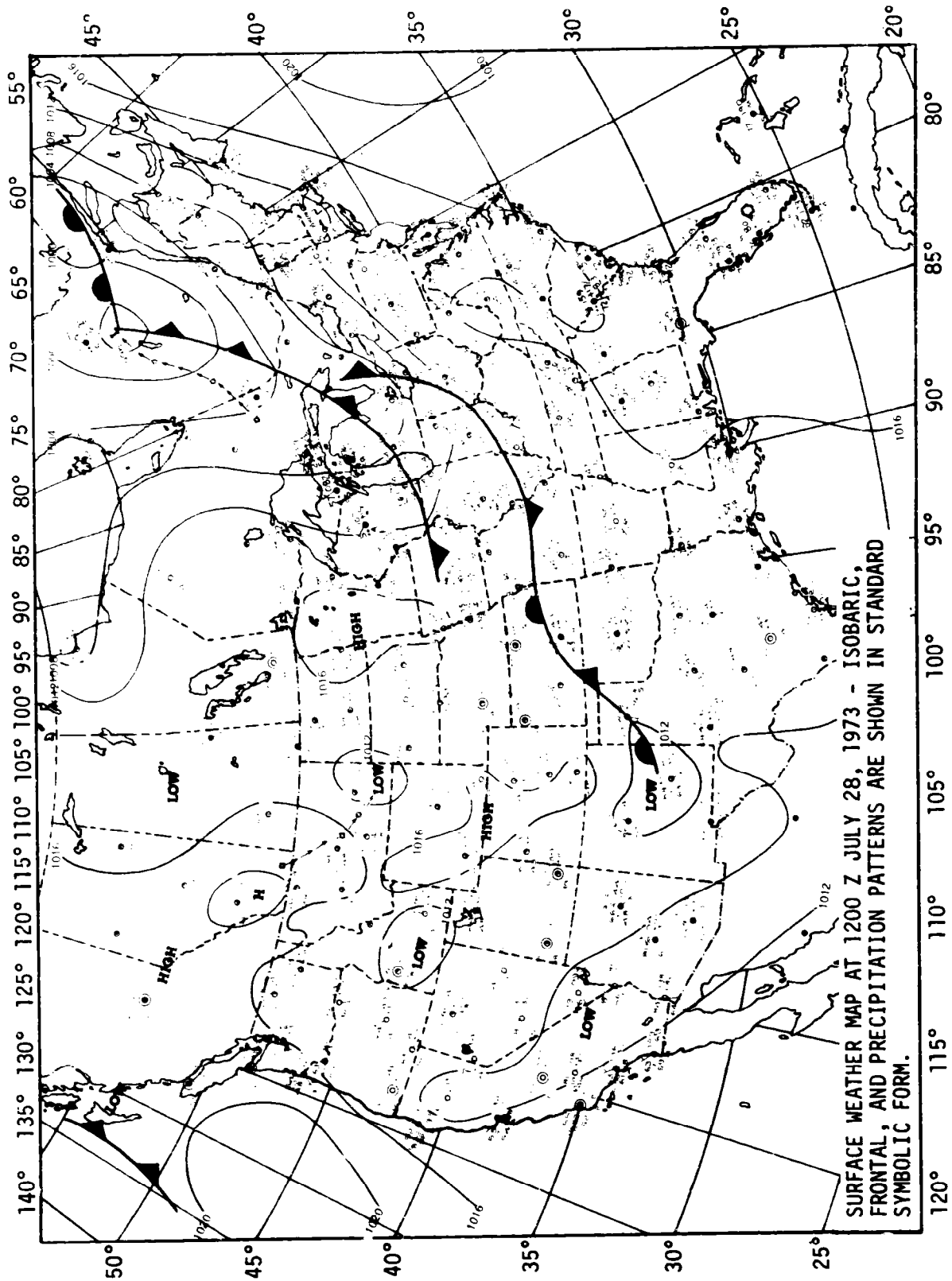
#### A.3 SURFACE OBSERVATIONS AT LAUNCH TIME

At launch time, total sky cover was 10/10, consisting of broken alto-cumulus at 4.6 kilometers (15,000 ft), with cirrus clouds observed at 6.4 kilometers (21,000 ft) altitude. Visibility was limited to 3 miles due to the formation of early morning ground fog. The fog was approximately 600 feet thick in spots. Neither precipitation nor lightning were observed at launch time.

Surface ambient temperature was 296°K (74.0°F) with 93% relative humidity. During ascent the vehicle did pass through the cloud layers. All surface observations at launch time are summarized in Table A-1. Solar radiation data for the day of launch is not available, due to miscalibration of the instruments.

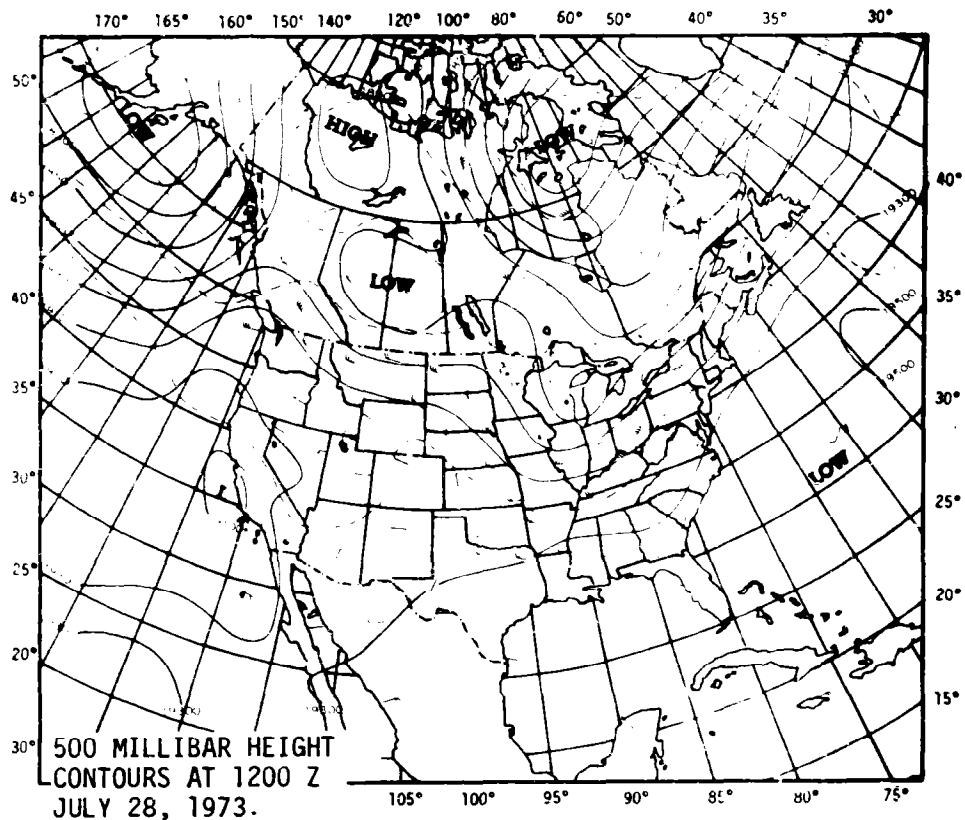
#### A.4 UPPER AIR MEASUREMENTS

Data were used from three of the upper air wind systems to compile the final meteorological tape. Table A-2 summarizes the wind data systems used. Only the Rawinsonde and the Loki Dart meteorological rocket data were used in the upper level atmospheric thermodynamic analyses.



SURFACE WEATHER MAP AT 1200 Z JULY 28, 1973 - ISOBARIC, FRONTAL, AND PRECIPITATION PATTERNS ARE SHOWN IN STANDARD SYMBOLIC FORM.

Figure A-1. Surface Weather Map Approximately 49 Minutes After Launch of SA-207/SL-3



CONTINUOUS LINES INDICATE HEIGHT CONTOURS IN FEET ABOVE SEA LEVEL. DASHED LINES ARE ISO-THERMS IN DEGREES CENTIGRADE. ARROWS SHOW WIND DIRECTION AND SPEED AT THE 500 MB LEVEL. (ARROWS SAME AS ON SURFACE MAP.)

Figure A-2. 500 Millibar Map Approximately 49 Minutes After Launch of SA-207/SL-3

Table A-1. Surface Observations at SA-207 Launch Time

LOCATION	TIME AFTER T-0 (MIN)	PRES-SURE N/CM <sup>2</sup> (PSIA)	TEM-PERATURE °K (°F)	DEW POINT °K (°F)	RELATIVE HUMIDITY (%)	VISI-BILITY KM (STAT MI)	SKY COVER			WIND*	
							CLOUD AMOUNT (TENTHS)	CLOUD TYPE	HEIGHT OF BASE METERS (FEET)	SPEED M/S (KNOTS)	DIR DEG
NASA 150 m Ground Wind Tower Winds measured at 10 m (32.8 ft)**	0	10.162 (14.74)	297.0 (75.0)	295.9 (73.0)	93	4.8 GF (3)	9  5  10###	Alto-cumulus Cirrus	4570 (15,000) 6400 (21,000)	1.3# (2.5)	271#
Cape Kennedy AFS*** Surface Measurements	10	10.169 (14.75)	296.3 (73.6)	296.0 (73.0)	98	--	--	--	--	1.0## (1.9)	200##
Pad 39B Lightpole NW 18.3 m (60.0 ft)**	0	--	--	--	--	--	--	--	--	2.6 (5.1)	264
Pad 39B LUT W 161.5 m (530 ft)**	0	--	--	--	--	--	--	--	--	6.9 (13.5)	274
Pad 39B Camera Site #3 - SE	0	10.165 (14.74)	297.0 (75.0)	296.5 (74.0)	97	--	--	--	--	--	--

\* Instantaneous readings at T-0, unless otherwise noted.  
 \*\* Above natural grade.  
 # 10 minute average about T-0.  
 \*\*\* Balloon release site.  
 ## 1 minute average.  
 ### Total Sky cover.

A-4

Table A-2. Systems Used to Measure Upper Air Wind Data for SA-207

TYPE OF DATA	RELEASE TIME		PORTION OF DATA USED			
	TIME (UT) HOURS:MIN	TIME AFTER T-0 (MIN)	START		END	
			ALTITUDE M (FT)	TIME AFTER T-0 (MIN)	ALTITUDE M (FT)	TIME AFTER T-0 (MIN)
FPS-16 Jimsphere	11:25	14	100 (328)	14	14,975 (49,130)	65
Rawinsonde	11:21	10	15,000 (49,212)	59	25,250 (82,840)	93
Loki Dart	12:44	93	61,750 (202,590)	93	25,500 (83,660)	118

#### A.4.1 Wind Speed

Wind speeds were light, being 1.0 m/s (1.9 knots) at the surface and increasing to a peak of 13.2 m/s (25.7 knots) at 13.83 kilometers (45,357 ft). The winds decreased slightly above this altitude, and then became stronger again as shown in Figure A-3. The overall maximum speed was 59.0 m/s (114.7 knots) at 47.50 kilometers (155,838 ft) altitude. Maximum dynamic pressure occurred at 15.30 kilometers (50,200 ft). At max Q altitude, the wind speed and direction was 6.8 m/s (13.2 knots), from 33 degrees. SL-3 pad 39B wind data is available in MSFC memorandum, S&E-AERO-YT-28-73.

#### A.4.2 Wind Direction

At launch time, the surface wind direction was from 200 degrees. The wind directions had a westerly component throughout the troposphere, switching northerly by 10 kilometers (32,808 ft) and becoming easterly above 17 kilometers (55,774 ft) altitude. Figure A-4 shows the complete wind direction versus altitude profile. As shown in Figure A-4, wind directions were quite variable at altitudes with low wind speeds.

#### A.4.3 Pitch Wind Component

The pitch wind velocity component (component parallel to the horizontal projection of the flight path) at the surface was a tailwind of 0.9 m/s (1.8 knots). The maximum wind, in the altitude range of 8 to 16 kilometers (26,247 to 52,493 ft), was a head wind of 11.7 m/s (22.7 knots) observed at 12.43 kilometers (40,764 ft) altitude. See Figure A-5.

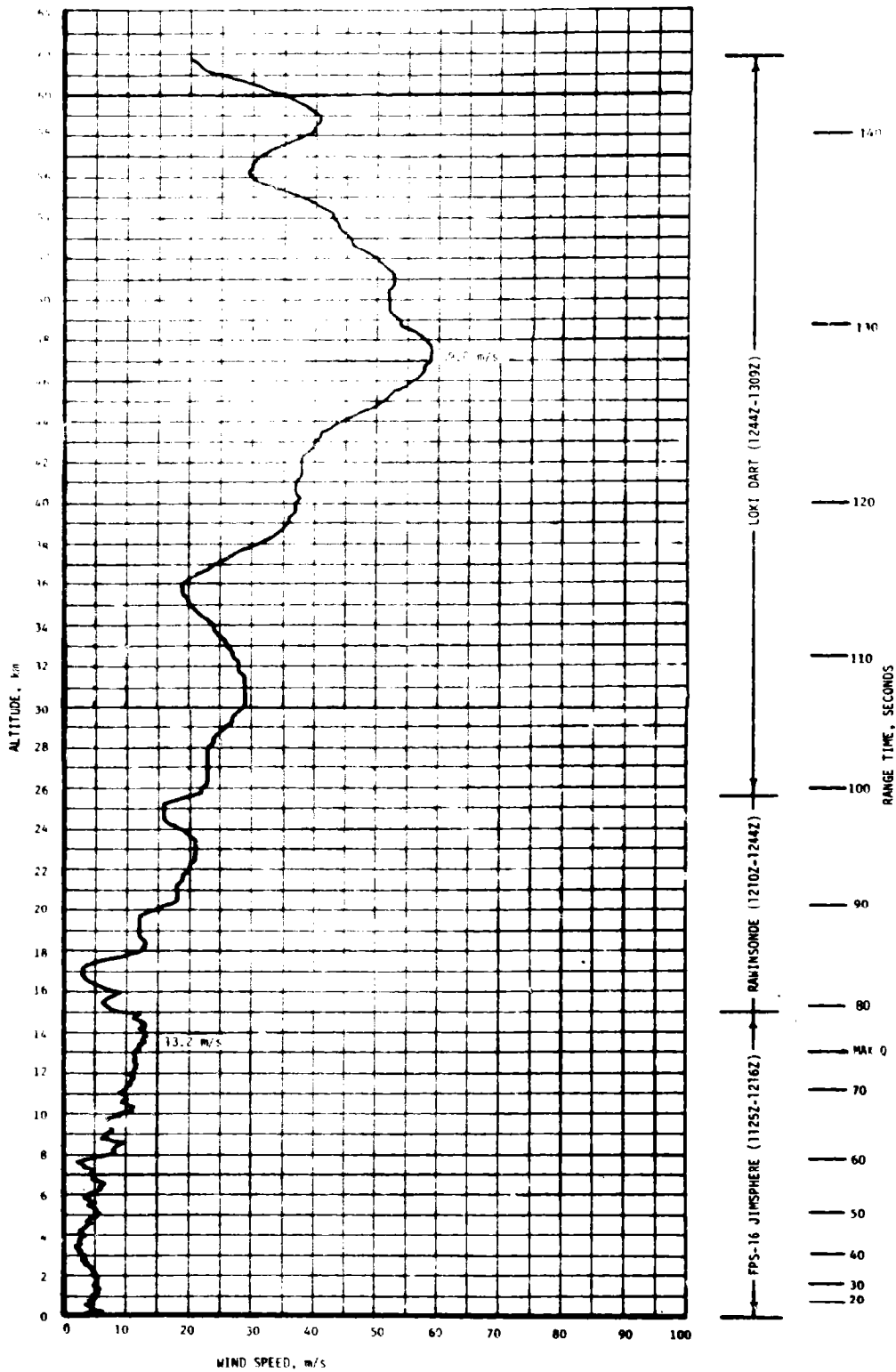


Figure A-3. Scalar Wind Speed at Launch Time of SA-207/SL-3

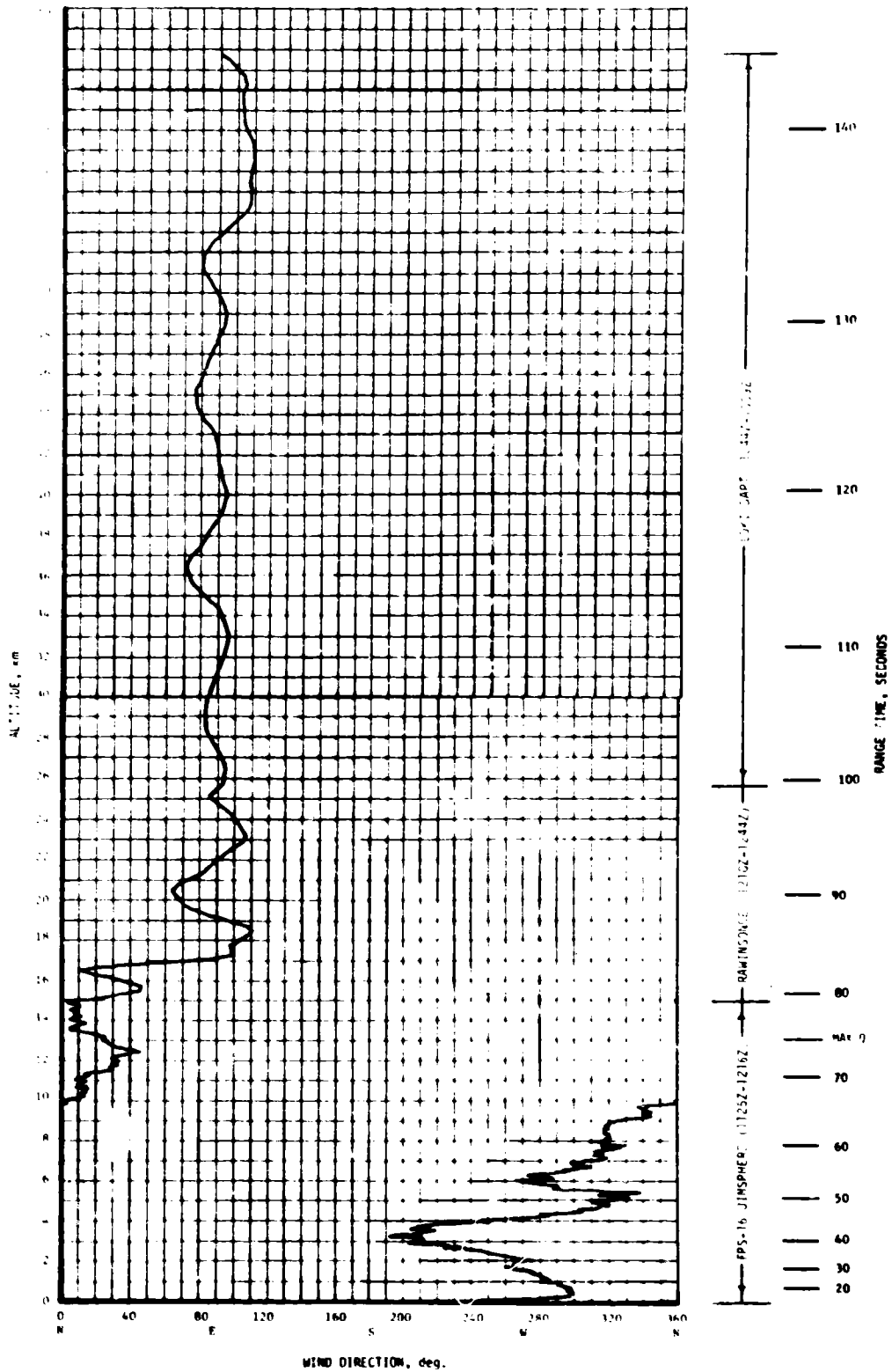


Figure A-4. Wind Direction at Launch Time of SA-207/SL-3

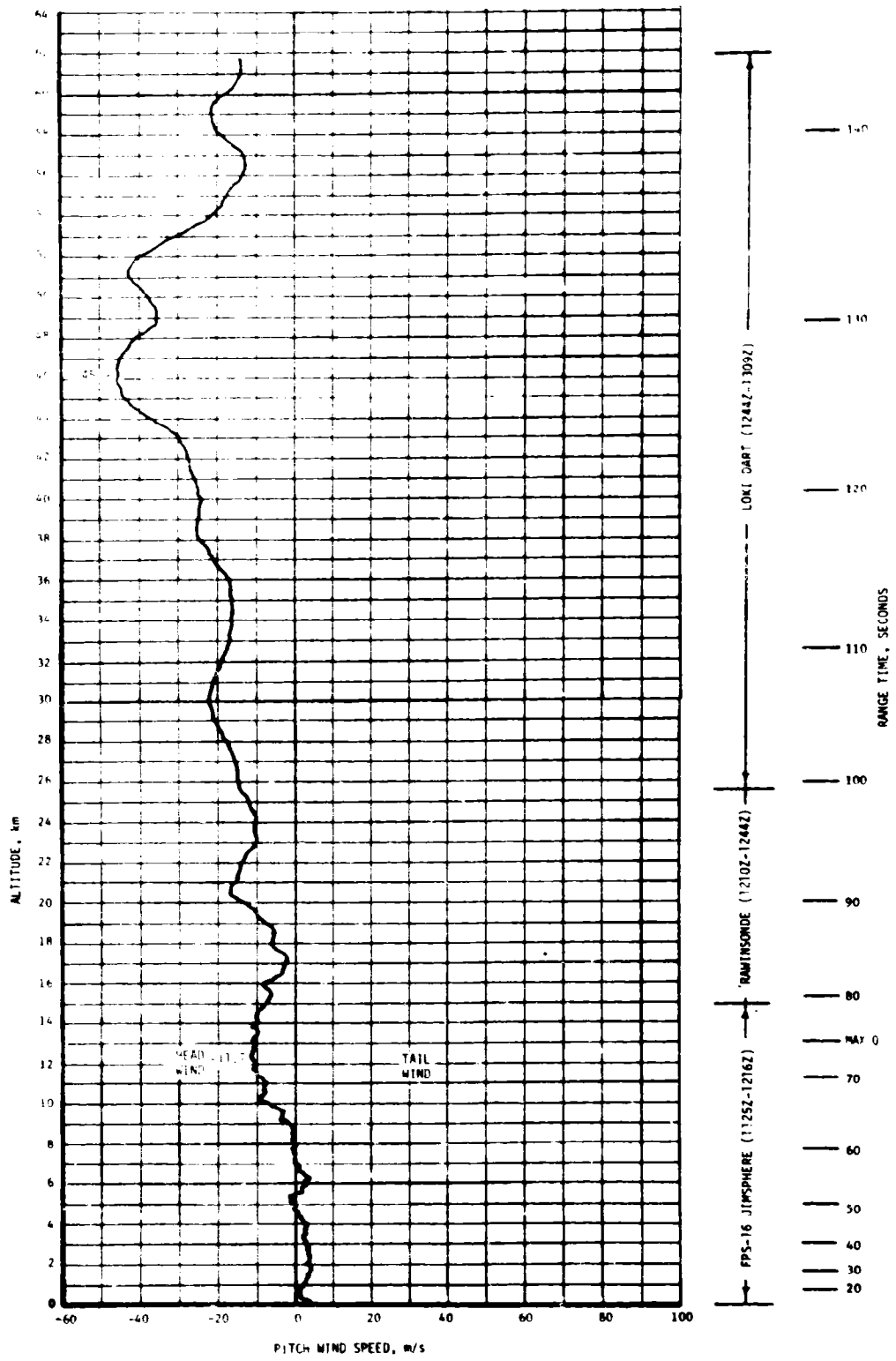


Figure A-5. Pitch Wind Velocity Component ( $w_x$ ) at Launch Time of SA-207/SL-3

#### A.4.4 Yaw Wind Component

The yaw wind velocity component (cross range wind component) at the surface was a wind from the right of 0.4 m/s (0.8 knots). The peak yaw wind velocity in the high dynamic pressure region was from the left of 9.6 m/s (18.6 knots) at 8.60 kilometers (28,215 ft). See Figure A-6.

#### A.4.5 Component Wind Shears

The largest component wind shear ( $\Delta h = 1000$  m) in the max Q region was a pitch shear of  $0.0063 \text{ sec}^{-1}$  at 10.15 kilometers (33,300 ft). The largest yaw wind shear, at these lower levels, was  $0.0083 \text{ sec}^{-1}$  at 15.50 kilometers (50,852 ft). See Figure A-7.

#### A.4.6 Extreme Wind Data in the High Dynamic Region

A summary of the maximum wind speeds and wind components is given in Table A-3. A summary of the extreme wind shear values ( $\Delta h = 1000$  meters) is given in Table A-4.

### A.5 THERMODYNAMIC DATA

Comparisons of the thermodynamic data taken at SA-207 launch time with the annual Patrick Reference Atmosphere, 1963 (PRA-63) for temperature, pressure, density, and Optical Index of Refraction are shown in Figures A-8 and A-9, and are discussed in the following paragraphs.

#### A.5.1 Atmospheric Temperature

Atmospheric temperature differences were small, deviating less than 3 percent from the PRA-63 below 62 kilometers (203,410 ft) altitude. In the max Q region, temperatures did deviate to +2.31 percent of the PRA-63 value at 9.75 km (31,988 ft). Air temperatures were generally warmer than the PRA-63, over the entire profile, as shown in Figure A-8.

#### A.5.2 Atmospheric Pressure

Atmospheric pressure deviations were small in the lower levels of the atmosphere. Deviations were less than 3 percent of the PRA-63 below 18 kilometers (59,054 ft) altitude. See Figure A-8, which shows the entire pressure profile with altitude.

#### A.5.3 Atmospheric Density

Atmospheric density deviations were small, generally being within 4 percent of the PRA-63 below 28 kilometers (91,862 ft) altitude. The density deviation reached a maximum of 4.28 percent greater than the PRA-63 value at 14.75 kilometers (48,392 ft) as shown in Figure A-9.

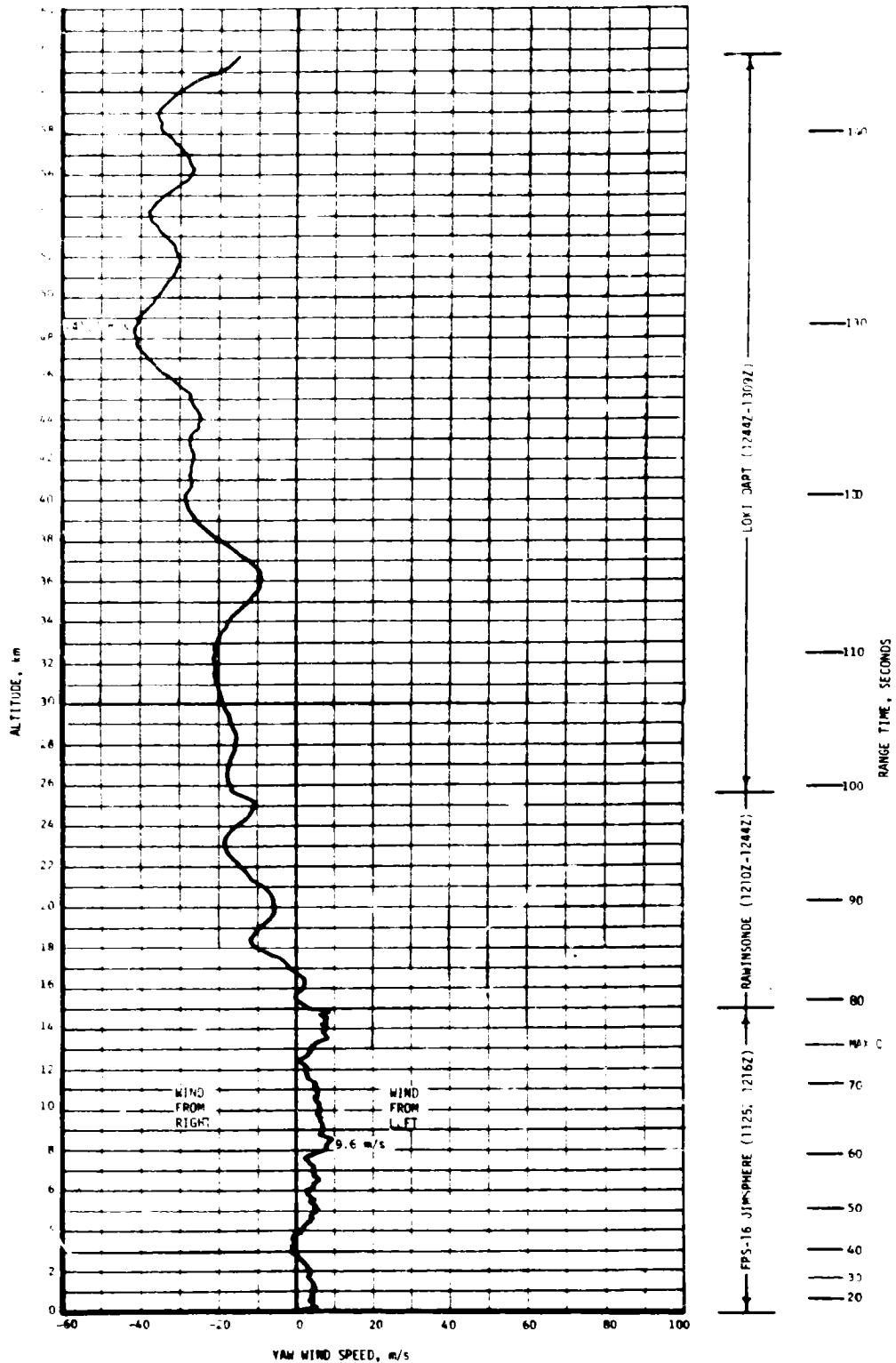


Figure A-6. Yaw Wind Velocity Component ( $W_z$ ) at Launch Time of SA-207/SL-3

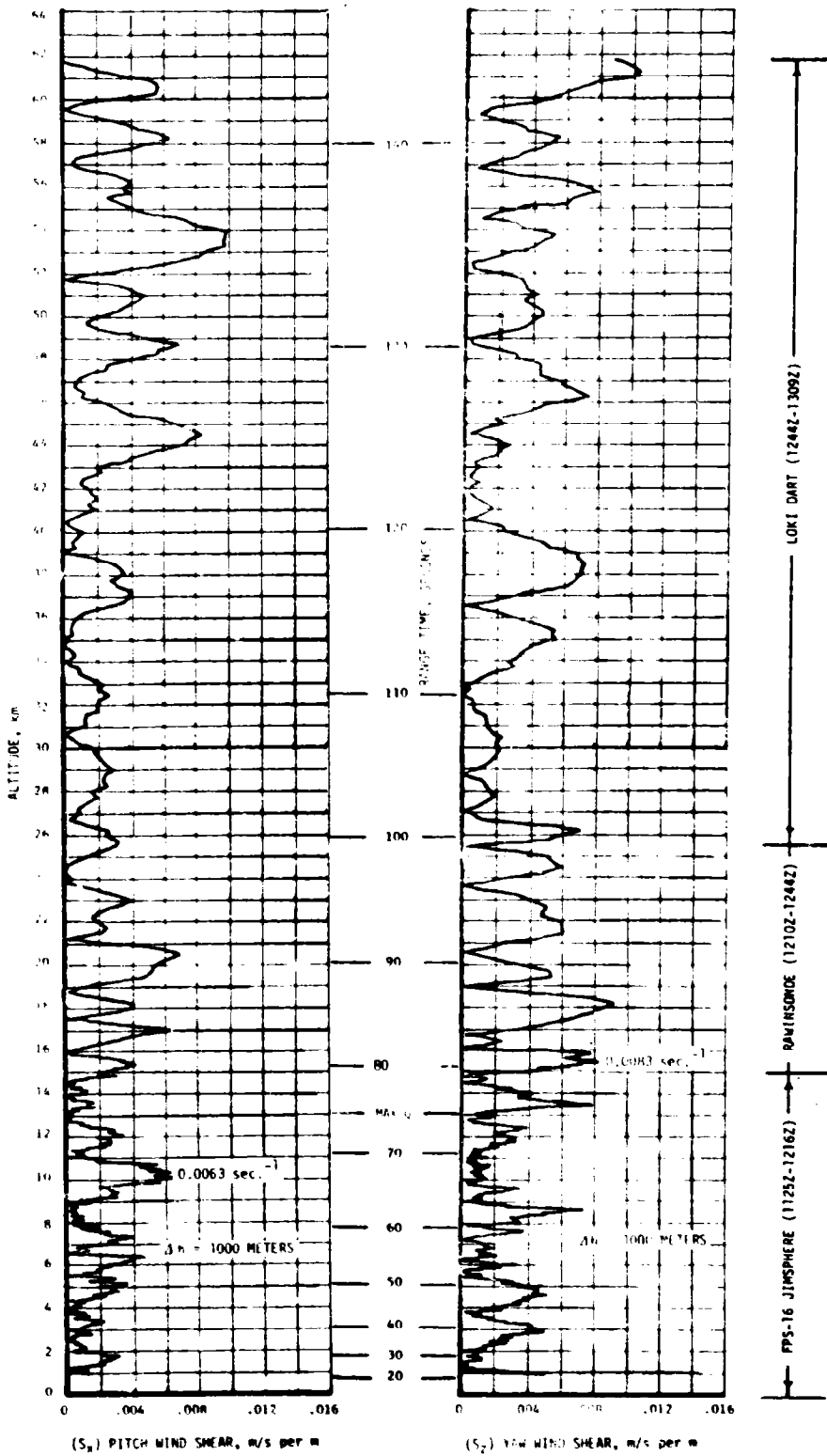


Figure A-7. Pitch ( $S_x$ ) and Yaw ( $S_y$ ) Component Wind Shears at Launch Time of SA-207/SL-3

Table A-3. Maximum Wind Speed in High Dynamic Pressure Region for Saturn Launch Vehicles 201 through 207

VEHICLE NUMBER	MAXIMUM WIND			MAXIMUM WIND COMPONENTS			
	SPEED M/S (KNOTS)	DIR (DEG)	ALT KM (FT)	PITCH ( $w_x$ ) M/S (KNOTS)	ALT KM (FT)	YAW ( $w_z$ ) M/S (KNOTS)	ALT KM (FT)
SA-201	70.0 (136.1)	250	13.75 (45,100)	57.3 (111.4)	13.75 (45,100)	-43.3 (-84.2)	13.25 (43,500)
SA-203	18.0 (35.0)	312	13.00 (42,600)	11.1 (21.6)	12.50 (41,000)	16.6 (32.3)	13.25 (43,500)
SA-202	16.0 (31.1)	231	12.00 (39,400)	10.7 (20.8)	12.50 (41,000)	-15.4 (-29.9)	10.25 (33,600)
SA-204	35.0 (68.0)	288	12.00 (39,400)	32.7 (63.6)	15.25 (50,000)	20.6 (40.0)	12.00 (39,400)
SA-205	15.6 (30.3)	309	14.60 (44,500)	15.8 (30.7)	12.08 (36,800)	15.7 (30.5)	15.78 (47,500)
SA-206	42.0 (81.7)	286	13.38 (43,881)	27.9 (54.2)	14.93 (48,966)	36.3 (70.6)	13.35 (43,799)
SA-207	13.2 (25.7)	014	13.83 (45,357)	-11.7 (-22.7)	12.43 (40,764)	9.6 (18.6)	8.60 (28,215)

Table A-4. Extreme Wind Shear Values in the High Dynamic Pressure Region for Saturn Launch Vehicles 201 through 207

VEHICLE NUMBER	$(\Delta h = 1000 \text{ m})$			
	PITCH PLANE		YAW PLANE	
	SHEAR (SEC <sup>-1</sup> )	ALTITUDE KM (FT)	SHEAR (SEC <sup>-1</sup> )	ALTITUDE KM (FT)
SA-201	0.0206	16.00 (52,500)	0.0205	12.00 (39,400)
SA-203	0.0104	14.75 (48,400)	0.0079	14.25 (46,800)
SA-202	0.0083	13.50 (44,300)	0.0054	13.25 (43,500)
SA-204	0.0118	16.75 (55,000)	0.0116	14.00 (45,900)
SA-205	0.0113	15.78 (48,100)	0.0085	15.25 (46,500)
SA-206	0.0145	14.93 (48,966)	0.0141	14.33 (47,162)
SA-207	0.0063	10.15 (33,300)	0.0083	15.50 (50,852)

#### A.5.4 Optical Index of Refraction

The Optical Index of Refraction at the surface was  $7.01 \times 10^{-6}$  units lower than the corresponding value of the PRA-63. The maximum negative deviation of  $-9.22 \times 10^{-6}$  occurred at 250 meters (820 ft). The deviation then became less negative with altitude, and approximated the PRA-63 at high altitudes, as is shown in Figure A-9. The maximum value of the Optical Index of Refraction was  $2.18 \times 10^{-6}$  units greater than the PRA-63 at 14.57 kilometers (47,818 ft).

#### A.6 COMPARISON OF SELECTED ATMOSPHERIC DATA FOR SATURN IB LAUNCHES

A summary of the atmospheric data for each Saturn IB launch is shown in Table A-5.

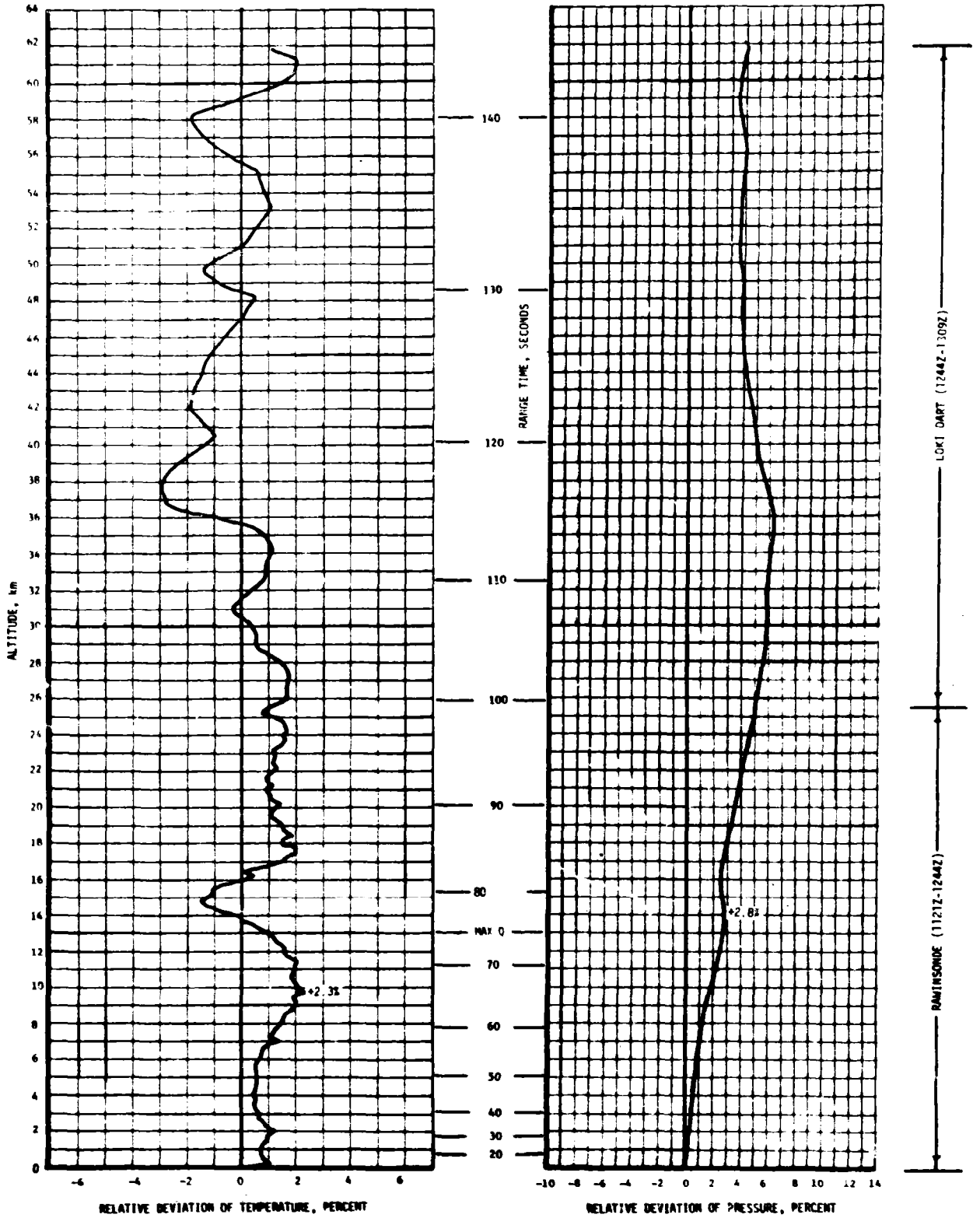


Figure A-8. Relative Deviation of Temperature and Pressure from the PRA-63 Reference Atmosphere, SA-207/SL-3

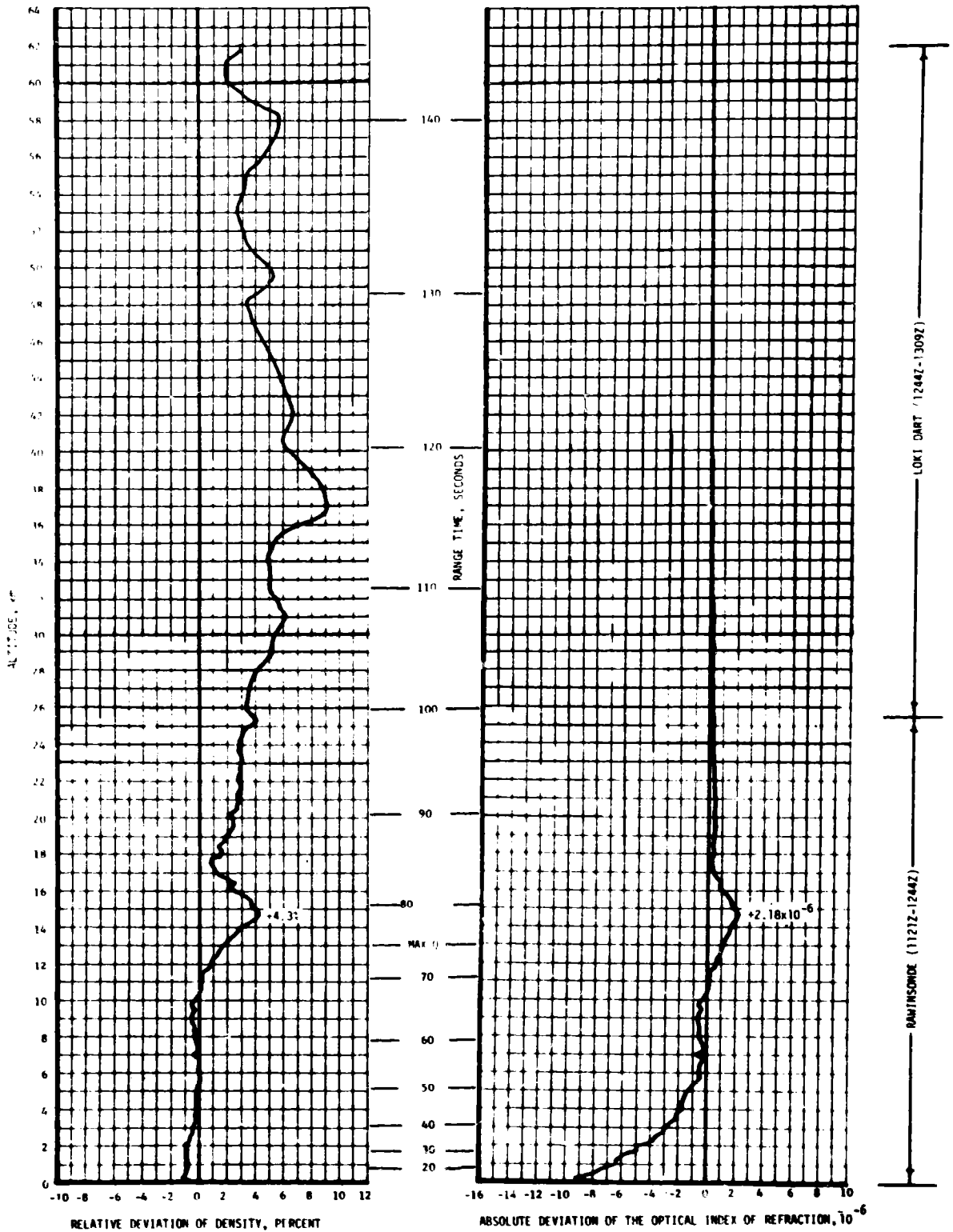


Figure A-9. Relative Deviation of Density and Absolute Deviation of the Index of Refraction From the PRA-63 Reference Atmosphere, SA-207/SL-3

Table A-5. Selected Atmospheric Observations for Saturn Launch Vehicles 201 through 207 at Kennedy Space Center, Florida

VEHICLE NUMBER	VEHICLE DATA			SURFACE DATA						INFLIGHT CONDITION		
	DATE	TIME NEAREST MINUTE	LAUNCH COMPLEX	PRESSURE N/cm <sup>2</sup>	TEMPERATURE °C	RELATIVE HUMIDITY PERCENT	WIND*		CLOUDS	MAXIMUM WIND IN 8-16 KM LAYER		
							SPEED m/s	DIR DEG		ALTITUDE km	SPEED m/s	DIRECTION DEG
SA-201	26 Feb 66	1112 EST	34	10.217	16.1	48	6.5	330	Clear	13.75	70.0	250
SA-203	5 Jul 66	0953 EST	37B	10.166	30.2	69	6.3	242	1/10 Cumulus 1/10 Altocumulus 1/10 Cirrus	13.00	18.0	312
SA-202	25 Aug 66	1216 EST	34	10.173	30.0	70	4.1	160	8/10 Cumulus 1/10 Cirrus	12.00	16.0	231
SA-204	22 Jan 68	1748 EST	37B	10.186	16.1	93	4.2	45	3/10 Cumulus	12.00	35.0	288
SA-205	11 Oct 68	1103 EDT	34	10.180	28.3	65	10.2	90	3/10 Cumulonimbus	14.60	15.6	309
SA-206	25 May 73	0900 EDT	39B	10.105	26.1	85	5.5 6.1	212 224	5/10 Fractocumulus 5/10 Altocumulus 1/10 Cirrus	13.38	42.0	286
SA-207	28 Jul 73	0711 EDT	39B	10.162	23.9	93	2.6 6.9	264 274	9/10 Altocumulus 5/10 Cirrus	13.83	13.2	014

\* Instantaneous readings from charts at T-0 (unless otherwise noted) from anemometers on launch pad light poles at the following levels: Pad 34 at 19.5 m (59.4 ft), Pad 37B at 20.7 m (63.1 ft), and Pad 39B at 18.3 m (60.0 ft). Beginning with SA-206, wind measurements were required at the 161.5 m (530 ft) level from anemometer charts on the LUT. These instantaneous LUT winds are given directly under the listed pad light pole winds. Heights of anemometers are above natural grade.

## APPENDIX B

### SA-207 SIGNIFICANT CONFIGURATION CHANGES

#### B.1 INTRODUCTION

The SA-207 launch vehicle configuration was essentially the same as the SA-206 configuration with significant exceptions shown in Tables B-1 through B-3. The basic vehicle description is presented in Appendix B of the Saturn IB Launch Vehicle Flight Evaluation Report SA-206, Skylab-2, MPR-SAT-FE-73-3.

Table B-1. S-IB Significant Configuration Changes

SYSTEM	CHANGE	REASON
Electrical	<p>The stage premature ignition detection circuit was modified so that the two Gas Generator auto igniter links on each engine are wired in parallel, instead of series, thus requiring both links to open in order to actuate the ground detection circuit.</p> <p>Design change to provide additional shielding on Remote Digital Sub-multiplexer (RDSM) input wires.</p>	<p>Decrease possibility of receiving a false premature ignition signal.</p> <p>To reduce electromagnetic interference pickup on data inputs to RDSM.</p>

Table B-2. S-IVB Significant Configuration Changes

SYSTEM	CHANGE	REASON
Stage	Modifications to extend the coast capability of S-IVB-207 were implemented. These modifications bring S-IVB-207 to the same configuration as S-IVB-206 and S-IVB-208.	Modifications extend the stage orbital coast capability from 4.5 to 7.5 hours.
Propulsion	Increased size of purge control valve vent line from 1/4 inch to 3/8 inch.	Eliminate potential valve instability during an emergency accumulator shutdown.
Environmental Control	Installed low emissivity surfaces between forward skirt cold plates and stage structure.	To insure that IU electrical components do not go below minimum operating temperatures.
Electrical	Delete measurement C0017-411 temperature - Propellant Utilization (PU) system internal	Spare PU electronics assembly utilized on S-IVB-207 does not contain measurement C0017-411.



Table B-3. IU Significant Configuration Changes (Continued)

SYSTEM	CHANGE	REASON
<p>Flight Program (Continued)</p> <p>Discrete Inputs</p> <p>S-150 Galactic X-Ray Experiment</p>	<p>Stop checking for DI 9 at T4<sub>a</sub> or T5.</p> <p>DI 6 added.</p> <p>Mode Code 27</p> <ul style="list-style-type: none"> <li>o Bit 6 indicates T4<sub>a</sub> initiated.</li> </ul> <p>May be activated after T4<sub>a</sub>GRD by:</p> <ul style="list-style-type: none"> <li>o DCS command</li> <li>o DI 6</li> </ul> <p>Sequencing</p> <ul style="list-style-type: none"> <li>o Alternate sequence T4<sub>a</sub> activates the experiment</li> <li>o Alternate sequence T4<sub>b</sub> will initiate a dump of experiment data stored on auxiliary storage and playback recorder eac. time it is requested by DCS command after T4<sub>b</sub>GRD and before T5.</li> <li>o Time correlation alternate sequence issued at T4<sub>a</sub> +2096.6 and every 1800 seconds thereafter until T5.</li> <li>o Calibrate command alternate sequence issued at T4<sub>a</sub> +2096.6 and every 1800 seconds thereafter until T5.</li> <li>o Redefine class 4 alternate sequence logic to give internal priority to experiment sequences and to allow multiple class 4 sequence to be pending.</li> </ul> <p>Orbital Guidance</p> <ul style="list-style-type: none"> <li>o Maneuver the S-IVB/IU to the attitudes required to perform the experiment.</li> </ul> <p>Data Compression</p> <ul style="list-style-type: none"> <li>o Table 1 added (Process Input-Output's 3034, 3035, and 3031).</li> <li>o Compress gimbal angle data and associated time every 4 seconds.</li> <li>o Minimum capability of 1500 samples.</li> </ul>	<p>To eliminate single point failure as a result of erroneous DI 9 after spacecraft separation.</p> <p>Indicates spacecraft separation and activate T4<sub>a</sub>.</p> <p>Required for S-150 experiment.</p>

APPROVAL

SATURN IB LAUNCH VEHICLE FLIGHT EVALUATION REPORT

SA-207, SKYLAB-3

By Saturn Flight Evaluation Working Group

The information in this report has been reviewed for security classification. Review of any information concerning Department of Defense or Atomic Energy Commission programs has been made by the MSFC Security Classification Officer. The highest classification has been determined to be unclassified.

*Stanley L. Fragge*

Stanley L. Fragge  
Security Classification Officer

This report has been reviewed and approved for technical accuracy.

*George H. McKay, Jr.*

George H. McKay, Jr.  
Chairman, Saturn Flight Evaluation Working Group

*Herman K. Weidner*

Herman K. Weidner  
Director, Science and Engineering

*Richard G. Smith*

Richard G. Smith  
Saturn Program Manager

**END**

**DATE**

**FILMED**

DEC 14 1973